Review Article

Axel Schulz* and Jonas Surkau

Main group cyanides: from hydrogen cyanide to cyanido-complexes

https://doi.org/10.1515/revic-2021-0044
Received December 23, 2021; accepted April 25, 2022;
published online September 21, 2022

Abstract: Homoleptic cyanide compounds exist of almost all main group elements. While the alkali metals and alkaline earth metals form cyanide salts, the cyanides of the lighter main group elements occur mainly as covalent compounds. This review gives an overview of the status quo of main group element cyanides and cyanido complexes. Information about syntheses are included as well as applications, special substance properties, bond lengths, spectroscopic characteristics and computations. Cyanide chemistry is presented mainly from the field of inorganic chemistry, but aspects of chemical biology and astrophysics are also discussed in relation to cyano compounds.

Keywords: analytics; computations; homoleptic cyanide compounds; hydrogen cyanide; main group cyanides; syntheses.

Units of measurement

In this review the units of measurement are used in accordance to the International System of Units (SI). All derived units and their expression in terms of the SI base units are given below.

Dimension	Unit	Notation	Conversion to SI-units
Energy	H	Hartree	1 H = 4.3597×10^{-18} J
	eV	Electronvolt	1 eV = 1.602×10^{-19} J
Frequency	MHz	Megahertz	1 MHz = 1×10^{6} s^{-1}
	Hz	Hertz	1 Hz = 1 s^{-1}
Heat quantity	kJ	Kilojoule	1 kJ = 1×10^{3} kg m^2 s^{-2}
	kcal	Large calorie	1 kcal = 4.1868 kJ
Length	Å	Ångström	1 Å = 1×10^{-10} m = 0.1890 B
Pressure	Pa	Pascal	1 Pa = 1×10^{-5} bar
Temperature	K	Kelvin	$\vartheta/°C = T/K - 273.15$
Time	h	Hour	1 h = 3.6×10^{3} s
	min	Minute	1 min = 60 s
Wave number	cm^{-1}	Reciprocal centimetre	1 cm^{-1} = 100 m^{-1}

Introduction

Historical review

Centaurea cyanus is the Latin name for cornflower, which is famous for its intense blue color (Figure 1), but the origin of the color has nothing to do with cyanides. The name was derived from the Greek word for deep blue κυανός (*kyanos*). However, the accidental discovery of a new blue pigment at the beginning of the eighteenth century can be regarded as the beginning of the cyanide chemistry (Figure 2).

As early as 1706 J. Diesbach and J. Dippel accidentally discovered Prussian blue (originally named in German *Berliner Blau*) (Unknown, 1710; Roth, 2003), a blue dye in the reaction of iron salts (e.g. *Eisenvitrol* = $FeSO_4$) with lime potash (*Kalilauge* German for KOH) containing hexacyanoferrate(III) salts (Prussiate salts, in German *Blutlaugensalze*), which were formed in the repeated treatment of Dippel's *Tieröl* (oil isolated from a dry distillation of remains of animals, mostly blood) with potash. With an excess of $FeSO_4$ an insoluble intense blue pigment was obtained (eqs. 1, 2, Figure 1, Scheme 1). The first publication appeared in 1710 anonymously in the journal *Miscellanea Berolinensia* (Kraft, 2011; Unknown, 1710). Ever since Prussian blue became a great economic success as dye (Figure 1) (Andreas, 2017).

***Corresponding author: Axel Schulz**, Chemie, Universität Rostock, Albert-Einstein-Straße 3a, 18059 Rostock, Mecklenburg-Vorpommern, Germany, E-mail: axel.schulz@uni-rostock.de. https://orcid.org/0000-0001-9060-7065
Jonas Surkau, Chemie, Universität Rostock, Albert-Einstein-Straße 3a, 18059 Rostock, Mecklenburg-Vorpommern, Germany. https://orcid.org/0000-0001-8729-9807

Figure 1: *Centaurea cyanus*.

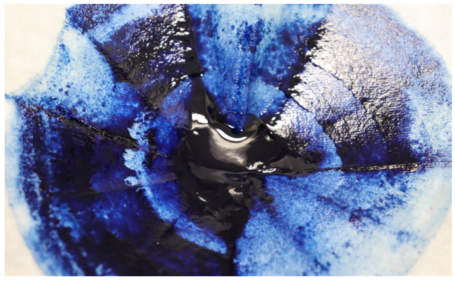

Figure 2: Filtered Prussian blue.

Only in 1973, A. Ludi et al. succeeded in elucidating the structure of pure Prussian blue: "The results of the chemical analyses clearly demonstrate that all of our samples have a composition close to the ideal formula $Fe^{III}_4[Fe^{II}(CN)_6]_3 \cdot 15\,H_2O$" (Buser et al., 1977) displaying Fe^{2+} and Fe^{3+} bridged by $[CN]^-$ ions.

With the recipe for the generation of Prussian blue in hand, many alchemists/chemists studied its properties and chemistry. In 1782, the German-Swedish alchemist Karl Wilhelm Scheele obtained the volatile *Berlinerblausäure* (= Berlin blue acid, HCN, eq. (3)) during experiments with Prussian blue and yellow Prussiate by treatment with aqueous sulfuric acid. Ever since Scheele's discovery of HCN, the German name *Berlinerblausäure* was used, however, often shortened to *Blausäure* (= blue acid = prussic acid) which is still used for HCN in the German language to date (von Ittner, 1809). It was Joseph Louis Gay-Lussac in 1815 who introduced the French term *cyanogène* (derived from the Greek word for blue – see above – and γεννάω, I create) for the radical $[CN]^{\cdot}$, which he figured out to be the central moiety in prussic acid in accordance with C.-L. Berthollet's work (Berthollet, 1787; Ladenburg, 1907; von Ittner, 1809). Hence, he renamed prussic acid into *l'acide hydrocyanique* (HCN, hydrogen cyanide; other common names for HCN: hydrocyanic acid, prussic acid). Moreover, J. L. Gay-Lussac observed the formation of gaseous dicyan, NC–CN, on thermal treatment of mercury dicyanide (eq. (4), Scheme 1).

Both HCN and its salts have attracted increasing attention in the past centuries as an important product of the primitive earth atmosphere as well as a reaction intermediate in the formation of important biological molecules such as amino acids, and of course in industry as valuable starting material for a plethora of pharmaceutical and chemical products or for the mining of gold (Abelson, 1966; Loew, 1971; Moffat and Tang, 1976; Park, 2014; Soto-Blanco, 2013).

Cyanide, a classic pseudohalide

With the preparation of HCN by K. W. Scheele in 1782, the first pseudohalogen compounds were isolated, although this term was introduced more than 100 years later (von Ittner, 1809). The pseudohalogen concept was introduced by Lothar Birckenbach and Karl Kellermann in 1925 and further established and justified in a series of experimental reports (Birckenbach and Huttner, 1929; Birckenbach and Kellermann, 1925a; Birckenbach and Linhard, 1929, 1930; Birckenbach et al., 1929a) as well as applied and further developed by others (Brand et al., 2005a, 2007; Hering et al., 2014; Schulz and Klapötke, 1992; Stopenko et al., 1986). Interestingly, the term was introduced by L. Birckenbach and K. Kellermann "to avoid the controversial term ***radical***" (Birckenbach and Kellermann, 1925a), therefore proposed the term ***pseudoelement*** in the free state. Since

(1) $Fe^{3\oplus} + K_4[Fe(CN)_6] \longrightarrow 3\,K^{\oplus} + K[Fe^{III}Fe^{II}(CN)_6]$

(2) exc. $Fe^{3\oplus} + 3\,K[Fe^{III}Fe^{II}(CN)_6] \xrightarrow{n\,H_2O} 3\,K^{\oplus}_{(aq.)} + 3\,Fe^{III}_4[Fe^{II}(CN)_6]_3 \cdot n\,H_2O$

(3) $6\,H^{\oplus}_{(aq.)} + K_4[Fe(CN)_6] \longrightarrow 6\,HCN_{(g)} + 4\,K^{\oplus} + Fe^{2\oplus}$

(4) $Hg(CN)_2 \longrightarrow Hg + NC{-}CN_{(g)}$

Scheme 1: Historic reactions that led to the development of CN chemistry.

the $[CN]^{\cdot}$ radical behaves chemically like a halogen, they therefore called it a ***pseudohalogen***. As all pseudohalides, the cyanide ion represents a monovalent resonance stabilized mono-anion. The diatomic $[CN]^-$ ion is the simplest of all pseudohalides (such as $[N_3]^-$, $[OCN]^-$, $[SCN]^-$, $[CNO]^-$, etc.). Due to the larger number of atoms forming the pseudohalide, usually larger ionic radii and different steric properties are observed compared to the halides. Moreover, unlike the halides, the cyanide with its ambidentate character with respect to bonding can form dative bonds either via the nitrogen or the carbon atom or even via both in a 1,2-bridging coordination mode. The bridging mode is also known from halides (Corain, 1982; Stopenko et al., 1986). Nevertheless, there are a number of chemical properties that are very similar to those of the halogens (Scheme 2). For example, the cyanide fulfills the following criteria with respect to a halogen-like chemical behavior: It forms (i) a strongly bound univalent $[CN]^{\bullet}$ radical (eq. 5), (ii) a singly charged anion ($[CN]^-$, eq. 6), (iii) a hydrogen acid (HCN, hydrocyanic acid, eq. 7), (iv) salts of the type $M(CN)_n$ with silver, lead and mercuric salts, which exhibit a low solubility (eq. 8), (v) a neutral dipseudohalogen compound (NC–CN, eq. 9), which disproportionates in water (into $[CN]^-$ and $[OCN]^-$, eq. 10) and can be added to double bonds (which is not the case for NC–CN but for HCN), and (vi) interpseudohalogen species (Arulsamy et al., 1999; Brand et al., 2005b; Brupbacher et al., 1997; Chow and Britton, 1974; Grundmann and Fulton, 1964; Guo et al., 1996; Hvastijová et al., 1999; Köhler and Lux, 1968; Maier and Teles, 1987a, 1987b; Maier et al., 1996a, 1996b, 1997a, 1997b; McGibbon et al., 1992; Middleton et al., 1958; Pasinszki, 2008; Robles et al., 2011; Schulz and Klapötke, 1996; Vörös et al., 2012, 2015) (e.g. NC–CNO, eq. 11) (Maier and Teles, 1987a) as well as halogen-pseudohalogen compounds (X–CN (Berlinerblau, 1884; Coleman et al., 2007; Corain, 1982; Gail et al., 2004; Geier and Willner, 2008; Hartman and Dreger, 1931; Ho et al., 2006; Kichigina et al., 1998; Mayer, 1969a; Rubo et al., 2006; Slotta, 1934; Wu et al., 1998), X = halogen, eq. 12) (Brand et al., 2005a, 2007; Stopenko et al., 1986). Recently, it was shown that this concept can be extended by the criterion that a pseudohalogen should also form a pseudohalonium ion, e.g. in case of CN of the type $[TMS–CN–TMS]^+$ (eq. 13) (Schulz and Villinger, 2010). Furthermore, the cyano radical is – like the halogen radicals – a strongly electronegative molecule, its electron affinity being measured to be (3.862 ± 0.004) eV (Bradforth et al., 1993).

Characteristic of cyanides

The term cyanide refers to any compound containing the cyanide ion ($[CN]^-$) with one carbon atom triple bonded to a nitrogen atom. Experimentally, it has been shown that gaseous HCN is partially polymerized at pressures beyond 1.3 GPa (Sinosaki and Hara, 1929). Hydrogen cyanide (HCN) is a colorless gas (T_B = 298.8 K) with a faint bitter almond odor, while sodium cyanide (NaCN) and potassium cyanide

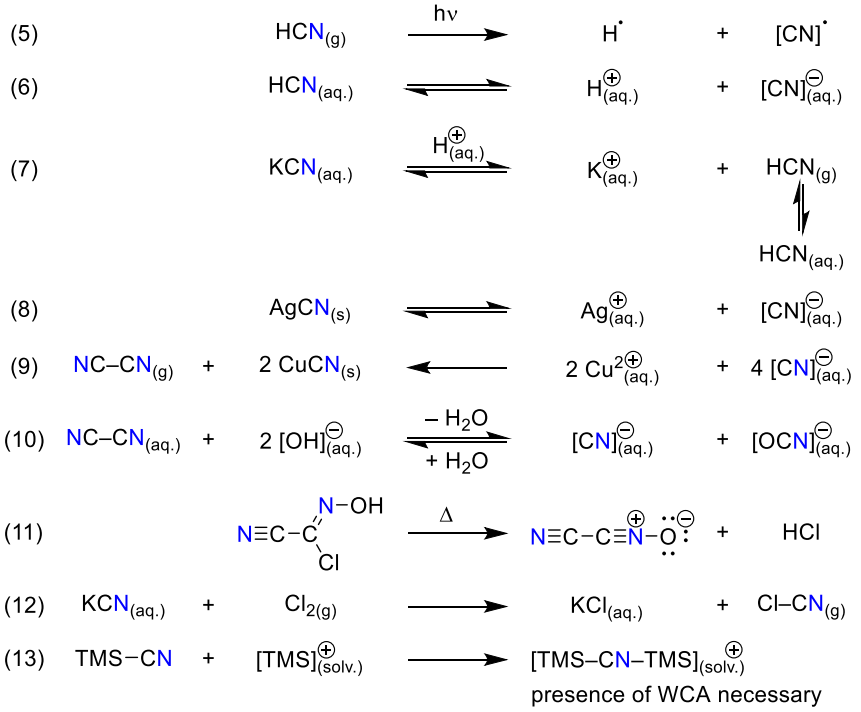

Scheme 2: Overview of cyano-pseudohalogen-chemistry.

(KCN) are white crystalline powders. HCN is a weak acid with a pK_a of 9.2 (Ambient Water Quality, 1980); therefore, HCN and $[CN]^-$ can be transformed into each other depending on pH and temperature. In water at pH = 7, most of the HCN is in the undissociated form. The simple cyanide salts KCN and NaCN are very soluble in water. Besides hydrogen cyanide, cyanides and cyanogen are the most prominent representatives of cyano-compounds. Table 1 summarizes some computed spectroscopic and physical data of these species, while Figure 3 displays the occupied molecular orbitals. The smallest species, the formal monopseudohalogen $[CN]^{\cdot}$, is a radical that is formed when hydrogen cyanide or cyanogen is irradiated (Scheme 2, eq. 5). The $[CN]^{\cdot}$ radical is probably one of the most extensively studied spectroscopic species since it was one of the first detected molecules in the interstellar space (Adams, 1941; Black and van Dishoeck, 1991; Cerny et al., 1978; Cook and Levy, 1973; Forthomme et al., 2014; Lee, 1992; Li et al., 1984; Liszt and Lucas, 2001; Paul and Dalby, 1962; Penzias et al., 1974; Poletto and Rigutti, 1965; Radford and Broida, 1962; Skatrud et al., 1983; Shi et al., 2011; Weinberg et al., 1967; Wootten et al., 1982; Yang et al., 1992). Commonly, $[CN]^{\cdot}$ radicals are detected in mixtures with HCN or NC–CN as it is easily formed by irradiation of these species. The spin density is located mainly at the carbon atom (0.92e vs. 0.08e at the nitrogen atom) (Cochran et al., 1962; Easley and Weltner, 1970; Milligan and Jacox, 1967a, 1967b; Sorensen and England, 2002). So it is not surprising that recombination of two $[CN]^{\cdot}$ radicals form C–C bound cyanogen, NC–CN. Cyanogen (Brotherton and Lynn, 1959) is a linear molecule ($D_{\infty h}$ symmetry) that has no dipole moment but a quadrupole moment (Dagg et al., 1986). Due to the delocalization of the CN triple bond also across the C–C bond (hyperconjugation, see Figure 3), the experimental C–C distance of 1.3768(3) Å is very short and thus has partial double bond character (Torrie and Powell, 1989). This also results in a

Table 1: Computed spectroscopic data of some basic CN species (PBE0/aug-cc-pVDZ; dipole moment in Debye, lengths in Å, charges in e, zpe in kcal mol^{-1}, unscaled wave numbers in cm^{-1}) (Schulz, 2021).

parameter	$[CN]^{\cdot}$	$[CN]^-$	HCN	NC–CN
Ground state	$^2\Sigma^+$	$^1\Sigma_g$	$^1\Sigma_g$	$^1\Sigma_g$
Dipole	1.48	0.62	3.05	0.00
r_{C-N}	1.171	1.182	1.156	1.161
q(C)	0.43	−0.21	0.09	0.19
q(N)	−0.43	−0.79	−0.33	−0.19
λ[a]	0.80	1.01	0.82	0.78
zpe	3.11	3.06	10.25	10.35
ν_{CN}	2173	2173	2211	2467/2282[b]

[a]sp^{λ} hybride for the nitrogen lone pair. [b]In-phase (Σ_g) and out-of-phase (Σ_u) vibration.

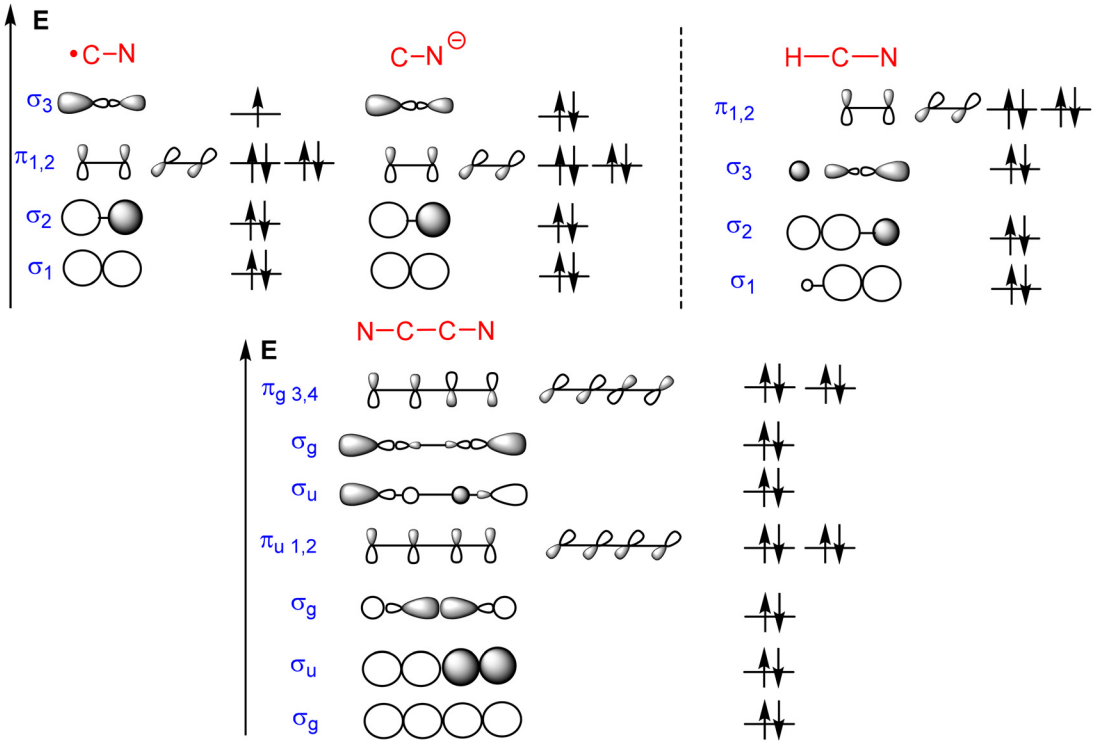

Figure 3: Qualitative MO description of $[CN]^{\cdot}$, $[CN]^-$, HCN, and NC–CN.

large dissociation energy of 135.14 kcal mol^{-1} (Feller et al., 2008). Cyanogen polymerizes at temperatures above 573 K to form polycyanogen.

Like HCN, cyanogen is a colorless, flammable, and toxic gas. It is formed not only during the thermal decomposition of transition metal cyanides, but also during the blast furnace process according to $2C + N_2 \rightarrow NC–CN + 309$ kJ mol^{-1} (Chase et al., 1974). Formally, cyanogen is the anhydride of ammonium oxalate, $[NH_4]_2[C_2O_4] = NC–CN \cdot 4H_2O$, i.e. it can also be generated by dehydration of ammonium oxalate (Stopenko et al., 1986).

Selected cyanide reactions

In the field of organic as well as inorganic chemistry there are a number of different reactions with HCN or CN sources (mostly metal cyanides or cyanides of weakly coordinating cations (WCC)). Although in the following chapters on the main group cyanides the specific synthetic pathways are discussed for each cyanide class, the most important general cyanide reactions are listed in equations (14)–(24) (Scheme 3). Especially in the field of organic cyanide chemistry, many articles, books and reviews about nitriles (R–CN, organic cyanides) have already been published (Beyer and Walter, 1991; Livinghouse, 1981; Glöcklhofer et al., 2015; Gröger and Asano, 2020; Krüss, 1884; Letts, 1872; Mowry, 1948; Nauth and Opatz, 2019; Plumet and Roscales, 2019; van Epps and Reid, 1916; Yan et al., 2017), so that we have focused here mainly on cyanide reactions in the field of inorganic chemistry (Arlt et al., 2021; Harloff et al., 2019a, 2020a; Stopenko et al., 1986).

HCN sources, toxicology, treatment, and mode of action (Newhouse and Chiu, 2010)

When K. W. Scheele discovered HCN in 1782, he was unaware of its toxicity. The fact that he died of hydrogen

salt metathesis

(14) with metal salts:

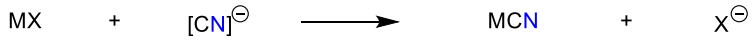

(15) with redox reaction:

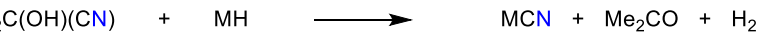

(16) with cyanido complex formation:

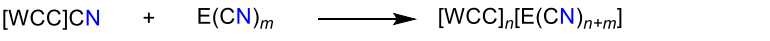

(17) without solvent, in the melt:

neutralisation

(18) with metal hydroxide:

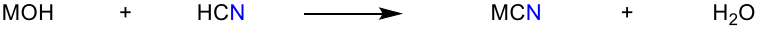

(19) with metal amides:

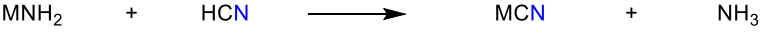

(20) with a decomposable cation:

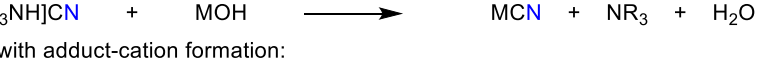

(21) with adduct-cation formation:

substitution

(22) with alkyl halide:

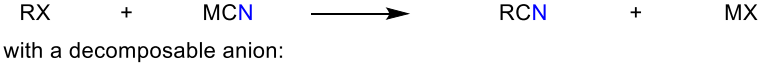

(23) with a decomposable anion:

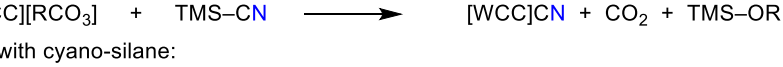

(24) with cyano-silane:

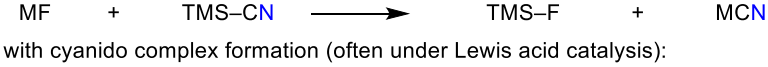

(25) with cyanido complex formation (often under Lewis acid catalysis):

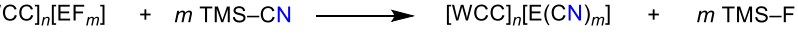

Scheme 3: Overview of several types of reaction (additional reference to 25: Bläsing et al., 2016a).

cyanide poisoning is probably only a rumor, even if he died relatively early at the age of 44, however after a long illness (Walden, 1943). Nevertheless, the fact that cyanides are highly toxic has been known for a long time and was used as a poison to murder people. Hence, it is not surprising that cyanides are very often even the subject of detective novels such as Agatha Christie's "Sparkling Cyanide" from 1944 (Christie, 1945).

HCN sources

Cyanides are found both in nature and in everyday life. In nature, HCN – bound in non-toxic cyanogenic glycosides – occurs in some plants. Mostly their fruit kernels contain cyanide. The best-known example are bitter almonds, but small amounts of cyanides are also found in plums, blackthorn, apricots, peaches, etc., in legumes, spurges such as manioc, sweet grasses, flax and columbine. Therefore, the columbine, for example, is avoided by grazing cattle. Cyanogenic glycosides [R^1R^2C(O–sugar)CN] themselves have no toxic effect, only enzymatic cleavage of the cyanogenic glycoside molecule leads to the release of HCN, which is the actual toxic substance. Cyanides are also released in industry, e.g. agriculture (herbicide), metal industry (metal extraction, leaching of precious metal), chemical industry (waste water). Furthermore, cyanides are also formed during pyrolysis of coal and during fires (of plastics e.g. polyurethanes), so that flue gas mostly contains HCN (up to 1/3) (Newhouse and Chiu, 2010). HCN is also released from biomass burning and volcanoes.

Cyanides are also used in the food industry. For example, cyano-complexes such as alkali ferrocyanide (E 535/E 536, $Na_4[Fe^{II}(CN)_6]/K_4[Fe^{II}(CN)_6]$) and calcium ferrocyanide (E 538, $Ca_2[Fe^{II}(CN)_6]$) are used as a food additive. These salts are permitted in small quantities as artificial anti-caking agents, release agents and stabilizers for table salt and table salt substitutes. They are considered harmless, as the HCN cannot be released by the stomach acid.

HCN is also present in cigarette smoke. A smoker ingests 10–400 µg HCN per cigarette through smoke. Even passive smokers still absorb 0.06–108 µg HCN. Compared with a nonsmoker, serum and urine levels of thiocyanate ($[SCN]^-$), the primary metabolite of HCN, are two to five times greater in smokers, clearly demonstrating the markedly increased intake of HCN from cigarette smoke (Newhouse and Chiu, 2010).

Toxicology

Cyanide salts and HCN are very toxic. Inhalation of hydrogen cyanide is more toxic than ingestion of the cyanide salts because they can be detoxified by the first-pass effect in the liver and absorption is slower. Orally ingested alkali cyanide reacts immediately with gastric acid in the stomach to form HCN ($[CN]^-_{(aq)} + H^+_{(aq)} \rightarrow HCN_{(aq)}$). It should be noted that cyanide is also readily absorbed through the skin. In the course of poisoning, headache, dizziness, nausea, feeling of suffocation, metabolic acidosis, hyperventilation, saturation of venous blood (pink skin color), convulsions, unconsciousness, respiratory arrest, and dilated pupils occur. The cause of death is usually central respiratory paralysis due to inhibition of cytochrome *c* oxidase. The lethal oral dose of KCN and NaCN for humans ranges from 0.5 to 3.5 mg kg^{-1} body weight (bw) (Newhouse and Chiu, 2010). After inhalation, the distribution of HCN in the body is almost complete after about 5 min. For example, in the bodies of people who died from HCN poisoning, cyanides were found in the blood as well as in the lungs, kidneys, brain, and heart (Gettler and Baine, 1938). The organism has a natural enzymatic detoxification capacity (enzyme rhodanase) of about 0.1 mg kg^{-1} bw h^{-1}: The enzyme is present in the mitochondria of the liver and kidney and detoxifies cyanide ions by transformation into non-toxic rhodanide ($[CN]^- + S \rightarrow [SCN]^-$). This is the reason why a large part of the cyanide is excreted in the urine as thiocyanates. Only a small part is exhaled as HCN gas. Cyanide binds to Fe^{3+} ions of the cytochrome *c* oxidase, whereas binding to Fe^{2+} ions of hemoglobin is comparatively low. Cyanide binding primarily impairs O_2 utilization in the mitochondria. The time course of cyanide poisoning is as follows: unconsciousness sets in after 30 s, respiratory arrest after 3–5 min, and ultimately death after 5–8 min. Even if cardiac arrest does not occur immediately (5–8 min) after inhalation, death can still occur after hours if the clinical picture progresses. A complete cure is only possible with early therapy immediately after poisoning. Depending on the duration of exposure, the level of cyanide concentration ingested, and the type of exposure by inhalation, absorption, or ingestion, the severity of the effect varies. A distinction is made between different degrees of severity of cyanide poisoning: (i) mild form: dizziness, confused state, mild respiratory problems; (ii) acute form: headache with severe dizziness, loss of consciousness, breathing difficulties and convulsions; coma – often with cardiovascular complications such as collapse, pulmonary edema or cardiac arrest; (iii) fulminant form: all of the above symptoms occur very rapidly and can lead to death within minutes. Interestingly, in 75% of all fire deaths (smoke inhalation), pure cyanide poisoning or mixed intoxication with CO is the cause. Even if someone survives cyanide poising, it can lead to long-term

neurological damage (Berger, 1997; Gettler and Baine, 1938; Hartwig, 1972; Newhouse and Chiu, 2010).

Treatment of cyanide poisoning

As an antidote in cyanide poisoning after smoke inhalation it is recommended to use hydroxocobalamin (1st choice), in cases of proven and suspected cyanide poisoning, especially in the case of mixed intoxication with CO (e.g. flue gas). Hydroxocobalamin exchanges the $[OH]^-$ group for $[CN]^-$, forming the non-toxic cyanocobalamin, or vitamin B_{12} for short. It is not suitable for oral cyanide poisoning, as the cyanide dose is usually too high. As a 2nd alternative, 4-DMAP (dimethylaminophenol, acts as met-hemoglobin former, Met-Hb) can be utilized when complexing agents such as hydroxocobalamin are not available. This antidote (like $NaNO_2$) oxidizes the divalent iron Fe^{2+} in hemoglobin to trivalent Fe^{3+} iron. This then forms a bond with the cyanides. Both agents have similar side effects. First, the hemoglobin in the Met-Hb is no longer available for oxygen transport. On the other hand, both agents cause vasodilation and hypotonias. Finally, sodium thiosulfate, $Na_2S_2O_3$, which acts as a sulfur donor (sulfur donor: $[S_2O_3]^{2-} \rightarrow$ "S" + $[SO_3]^{2-}$), is administered for sequential use with other cyanide antidotes (Anseeuw et al., 2013; Baskin et al., 1992; Bebarta et al., 2012, 2017; Beelitz et al., 2017; Borron et al., 2007; Gracia and Shepherd, 2004; Hall et al., 2007; Henretig et al., 2019; Thompson and Marrs, 2012).

For oral ingestion 4-DMAP should be given, which oxidizes hemoglobin to Met-Hb. Met-Hb in turn binds cyanide. Therapeutic dosage is 3–4 mg 4-DMAP kg^{-1} bw (about 250 mg). This can bind about 16 mmol cyanide (corresponding to 1000 mg potassium cyanide). Since cyanide is only bound to Met-Hb, but is not eliminated, and there is a risk that it will be released again from the Met-Hb complex, then administration of sodium thiosulfate is useful. If 4-DMAP is not available then immediately infuse sodium nitrite intravenously as countermeasure. Subsequently, $Na_2[S_2O_3]$ solution should be infused. The nitrite like 4-DMAP forms met-hemoglobin, Met-Hb, which reacts with the cyanide in the tissues and renders it harmless. The sodium thiosulfate provides sulfur, which is needed for the natural breakdown of cyanide in the body by enzymes (rhodinase, vide supra). The metabolic inactivation of the cyanide occurs mainly (approx. 80%) via the production of thiocyanate, which is catalyzed by the rhodanese of the liver. Lactacidosis (pH > 7.2) caused by cyanide poisoning requires the administration of $NaHCO_3$ (Anseeuw et al., 2013; Baskin et al., 1992; Bebarta et al., 2012, 2017; Beelitz et al., 2017; Borron et al., 2007; Gracia and Shepherd, 2004; Hall et al., 2007; Henretig et al., 2019; Thompson and Marrs, 2012).

Cyanide poisoning – mechanism of action

Simply put: cyanide blocks cellular respiration in the cells. In the case of poisoning, the cells can no longer utilize the vital oxygen. Therefore, cyanide is considered chemically asphyxiant because it interferes with aerobic metabolism without affecting tissue oxygenation. Since cyanide has a high affinity for iron (III), it results in the formation of a strong bond to tissue cytochrome *c* oxidase (see above). This in turn leads to inactivation of tissue cytochrome *c* oxidase. Because cytochrome *c* oxidase normally takes up oxygen from the blood and functions as an electron acceptor in cellular energy production, this inactivation inhibits cellular respiration (Newhouse and Chiu, 2010). That is, the strong $Fe^{(III)}$–CN bond inhibits the enzyme and blocks the last step in oxidative phosphorylation. The result is a deficiency of mitochondrial ATP and cell death (Berger, 1997). This leads to an increased anaerobic metabolism. Therefore, blood levels of pyruvic acid, lactic acid, and NADPH increase, while the ATP/ADP ratio consistently decreases. Thus, the first symptoms of acute cyanide poisoning occur in organs with high aerobic energy demands, especially the brain and heart. Inhibition of cellular oxygen consumption results in the presence of oxyhemoglobin in venous blood, which is why the skin turns bright red. All acute effects of cyanide poisoning are closely related to the disruption of aerobic metabolism and the release of secondary neurotransmitters and catecholamines. Acute cyanide poisoning effects include altered respiration, nausea, vomiting, and weakness. Eventually, severe convulsions, coma and death occur. In addition to cytochrome *c* oxidase, cyanide also binds to other metalloproteins and other cellular molecules, and also contributes to the symptoms of acute cyanide toxicity (Berger, 1997; Gettler and Baine, 1938; Hartwig, 1972; Newhouse and Chiu, 2010).

The deadly HCN probably wrote its worst chapter in the National Socialist concentration camps (extermination camps) during the Second World War. In the Holocaust, millions of Jews were poisoned by the gas "Zyklon B". "Zyklon B" consisted of liquid HCN, which was dripped onto absorbent carrier materials, e.g. diatomaceous earth, during production. "Zyklon B" was developed to make HCN (boiling point 298.8 K) safe to handle by lowering its vapor pressure.

Safety precautions while working with HCN

Appropriate safety precautions (HCN detector, gas mask, low temperatures, basic solutions, small amounts, pressure and temperatures control, use of powerful fume hoods) should be taken. *Note:* Some people cannot detect the typical odor (bitter almond oil) of hydrogen cyanide. Therefore, the use of an HCN detector is strongly recommended. *Caution!* HCN is not only highly toxic but can also decompose explosively under various conditions! Without stabilizer, pure HCN polymerizes very rapidly and exothermically, e.g. under basic conditions (or by autocatalysis) and the resultant HCN polymer subsequently decomposes violently (>373 K).

Scope of this review

Homoleptic cyanide compounds exist of almost all main group elements. While the alkali and alkaline earth metals form cyanide salts, the cyanides of the lighter main group elements occur mainly as covalent compounds. There are already a large number of review articles in the field of organic synthetic chemistry (nitriles) (Beyer and Walter, 1991; Glöcklhofer et al., 2015; Gröger and Asano, 2020; Krüss, 1884; Letts, 1872; Livinghouse, 1981; Mowry, 1948; Nauth and Opatz, 2019; van Epps and Reid, 1916; Yan et al., 2017; Plumet and Roscales, 2019), on E–CN bond formation (Yu et al., 2017), CN-coordination chemistry (Stopenko et al., 1986; Corain, 1982), as well as cyanide salts and compounds (Gail et al., 2004; Rubo et al., 2006). This review presents an overall view of the status quo of main group element cyanides and cyanido complexes. Mainly, only ternary compounds of the formal type $E_x(CN)_y$ with E = main group element are considered. They can be neutral as well as positively or negatively charged. In some cases, we have also included corresponding CN adducts in the discussion if they show certain properties or stabilize interesting CN fragments. With regard to the alkaline and alkaline earth metals, this review is limited to the pure metal cyanide compounds. Due to the fact that the cyanide anion belongs to the group of pseudohalides, the properties of the cyanide compounds considered are quite similar to those of alkali and earth alkaline halides. Especially at higher temperatures, the cyanide anion starts to rotate and forms a spherical rotor increasing the geometrical similarity to the spherical halides. A significant difference of metal cyanides and metal halides is the existence of various solid-state modifications of the metal cyanides mainly caused by different orientations of the cyanide group at low temperatures and a steric hindrance of its rotation. Due to many similarities of these cyanide compounds, the syntheses and crystal structures of 1st and 2nd main group compounds will be discussed in general. This review also compiles reports on compounds consisting exclusively of one element of the main groups 3–8 paired with at least one cyanide group to provide a summary.

In general, this review focuses on information about syntheses, bond lengths, spectroscopic characteristics, applications, special substance properties and computations. Accordingly, all fields of chemistry, but also biology and astrophysics are engaged. On this way, the report includes experimental findings from the nineteenth century as well as modern quantum mechanistic calculations and sophisticated gas phase experiments.

Hydrogen cyanide

Since HCN occupies a central role in the cyanide chemistry of the main group elements and, moreover, its chemical physical properties are markedly different from those of the alkali cyanides, HCN will be discussed here separately from them. Some important points concerning its history, bonding, and toxicity have been deliberately written into the introduction to emphasize the aspect of its central role.

Similar to hydrogen halides this compound consists of a polar covalent bond between H–CN (see pseudohalide concept in chapter 1.2), which is able to dissociate in aqueous solution to form the rather week acid, hydrocyanic acid (prussic acid), $pK_a = 9.2$ (Ambient Water Quality, 1980; Cotton et al., 1967). Pure hydrogen cyanide is a colorless volatile liquid ($T_B = 298.75$ K) with a characteristic smell of bitter almonds (Cotton et al., 1967). The compound is very poisonous, because it prevents the oxygen uptake in the respiratory chain of the human body (see chapter 1.5.2) (Meredith et al., 1993).

On pure HCN, there are a large number of theoretical (Johansson et al., 1972; Jucks and Miller, 1988; Karpfen, 1996; King and Weinhold, 1995; Kurnig et al., 1990; Moffat and Tang, 1976; Pacansky, 1977; Ramos et al., 1988) and experimental (Al-Azmi et al., 2003; Anex et al., 1988; Beichert et al., 1995; Brown et al., 1981; Earnshawb and Ireland, 1995; Fowler et al., 1994; Giauque and Ruehrwein, 1939; Gutowsky et al., 1992; Jucks and Miller, 1988; Knözinger, 1986; Kurnig et al., 1990; Legon et al., 1977; Meot-Ner and Speller, 1989; Nauta et al., 1999; Wofford et al., 1986; Völker, 1960; Schrems et al., 1987; Sun et al., 2000) studies on its clusters $(HCN)_n$ in the gas phase (microwave rotational spectroscopy, IR or matrix IR). These studies show that HCN forms linear H-bonded chains in all its

phases. The crystal structure of HCN in the solid phase showed "infinite" parallel linear H-bridged chains (see 2.2 Crystal structure) (Dulmage and Lipscomb, 1951), while a linear structure consisting of three formula units was experimentally derived for the liquid phase (Tyuzyo, 1957). Density and heat capacity measurements of HCN in the gas phase proved the presence of $(HCN)_n$ oligomers, especially di- and trimers at 298 K and 1 atm (Felsing and Drake, 1936; Giauque and Ruehrwein, 1939; Sinosaki and Hara, 1929). Using rotational spectroscopy, the HCN dimer and trimer could be characterized without doubt as H-bonded linear species in the gas phase (Brown et al., 1981; Buxton et al., 1981; Ruoff et al., 1988).

It was shown that the formation of very strong hydrogen bonds is mainly responsible for the formation of aggregates in the condensed phase. The energy of the hydrogen bond in gas phase increases from 3.28 to 8.72 kcal mol^{-1} by addition of a third hydrogen cyanide molecule. Comparing the gaseous and liquid state the energy of the hydrogen bond increases to 4.6 kcal mol^{-1} due to dimer formation (Pauling, 1968).

Monomeric HCN adducts can be formed with Lewis acids, e.g. HCN–BF_3, HCN–$NbCl_5$, or HCN–AsF_5) (Burns and Leopold, 1993; Chavant et al., 1975; Davydova et al., 2010; Haiges et al., 2004; Reeve et al., 1993; Saal et al., 2019; Tornieporth-Oetting et al., 1992). The only experimental study of an HCN···HCN adduct in the gas phase was described by K. R. Leopold et al. who investigated HCN···HCN–SO_3 in the gas phase using rotational spectroscopy (Fiacco et al., 2000). A. Schulz and co-workers succeeded in stabilizing an HCN dimer in the solid state by a strong Lewis acid, such as $B(C_6F_5)_3$, and investigating the influence of different solvents (HCN, CH_2Cl_2 and aromatic hydrocarbons, such as benzene, toluene) on the crystallization process. Dimer formation was observed (Figure 4, Scheme 4) when HCN or CH_2Cl_2 were used as solvents, whereas the use of aromatic hydrocarbons led to the formation of monomeric aryl···HCN–$B(C_6F_5)_3$ adducts (Figure 4), which are stabilized via η^6-coordination of the aromatic ring system and thus resemble the well-known half-sandwich complexes (Bläsing et al., 2018).

Hydrogen cyanide is widely used in industrial processes as an intermediate to mainly produce plastics, for example polymethacrylate or polyamides, drugs, insecticides, iron cyanide pigments, organic pigments and also pesticides (Henderson and Cullinan, 2007). A significant amount is also converted into cyanides, which are used in the cyanide process, the surface hardening of metals, in ore dressing and electroplating. Hydrogen cyanide, which is marked by the radioactive carbon isotope $H^{14}CN$, is used in biochemical research to synthesize traced amino acids (Koschel et al., 1971).

A natural source of hydrocyanic acid is the glycoside amygdaline ($C_{20}H_{27}NO_{11}$), which is contained in the kernel of apricots, apples and almonds. It is obtained by hydrolysis of the amygdaline and other glycosides in presence of the enzyme β-glycosidase leading to glucose and benzaldehyde (Scheme 5) (Williams, 1915).

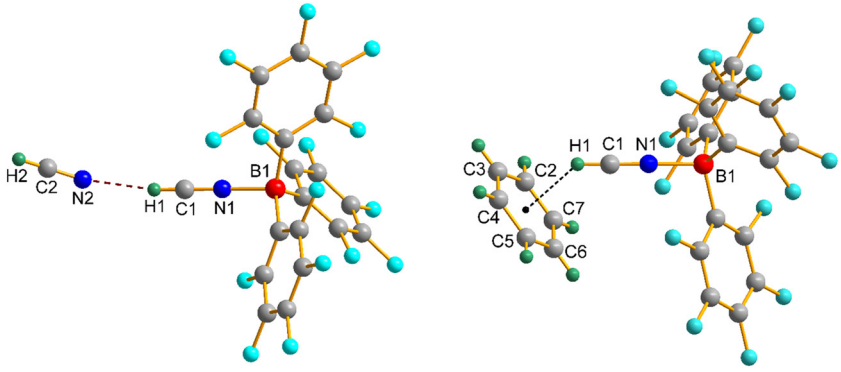

Figure 4: Molecular structure of a Lewis acid stabilized dimer (left) and η^6-coordination of the benzene adduct (right) (Bläsing et al., 2018).

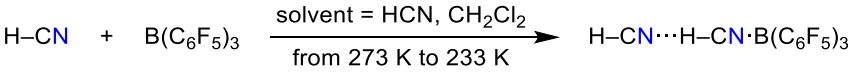

Scheme 4: Synthesis of an HCN dimer stabilized as $B(C_6F_5)_3$ adduct (Bläsing et al., 2018).

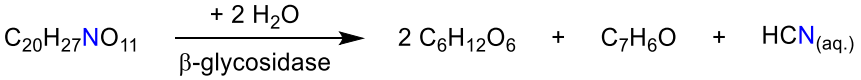

Scheme 5: Hydrolysis of the glycoside amygdaline leading to hydrocyanic acid (Williams, 1915).

Synthesis

In 1782 Karl Wilhelm Scheele obtained HCN by treating a solution of dried blood and potash (containing the potassium ferrocyanide, Prussian blue) with dilute acid (Böhland et al., 1978). He also described a synthesis by distillation of ferro cyanide in acid. The observed products of decomposition are merely CO_2 and N_2. But 30 years later, Joseph Louis Gay-Lussac could provide proof by isolation in a pure state (Williams, 1915).

Today many synthetic routes of hydrogen cyanide are known using different sources of nitrogen (NH_3, N_2, organic nitrogen compounds) and carbon (coal, CO, CH_4). An important industrial process is the catalytical combustion of a gas mixture containing NH_3 and CH_4, which is an extremely exothermic reaction $\Delta_R H = -949.6$ kJ (Scheme 6) (Andrussow, 1926, 1955; Böhland et al., 1978).

The two most famous industrial processes including this reaction are called Andrussow and Degussa process involving a platinum catalyst. The Andrussow process is carried out at temperatures of about 1273 K. The Degussa process requires higher temperatures of about 1473 K and oxygen free conditions (Andrussow, 1926; Andrussow, 1935; Krause, 1965). Yields of 90% can be achieved by fast reaction process and separation of the product (Greenwood et al., 1988).

Another simple approach to isolate hydrogen cyanide is the reaction of cyanide containing salts, for example NaCN, KCN or $K_4[Fe(CN)_6]$, with acids (Slotta, 1934; Thaulow, 1844; Williams, 1948; Ziegler, 1921). This kind of synthesis is often used in laboratories because of the high stability of the salts and the nearly quantitative conversion. It is also reported a complete reaction of moist CO_2 and KCN to hydrogen cyanide (Henninger, 1876).

In the laboratory, if one wishes to produce anhydrous, pure HCN, HCN can be elegantly produced by the solvent-free reaction of NaCN and stearic acid (T_M = 342 K) at 353–373 K in vacuo as a gas, which can be immediately condensed into the appropriate reaction vessel (Scheme 7, Figure 5) (Günther et al., 1935; Labbow et al., 2016).

Hydrogen cyanide undergoes fast decomposition, which can be retarded by addition of mineral acids or up to 20% of glycerine (Williams, 1948). Also an adsorption of hydrogen cyanide on appropriate surfaces is possible. A reaction of HCN with NaOH returns to the sodium salt NaCN, which can be stored and converted to hydrogen cyanide easily (Koschel et al., 1971). The decomposition of hydrogen cyanide is mainly a kind of a polymerization reaction. Higher temperatures increase the polymerization and finally lead to the formation of ammonia and ammonium cyanide (Völker, 1960). Polymeric hydrogen cyanide, usually referred to as polymeric hydrocyanic acid or

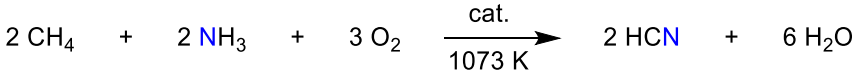

Scheme 6: Industrial synthesis of HCN by catalytical combustion of CH_4 and NH_3 (Andrussow, 1926; Andrussow, 1955; Böhland et al., 1978).

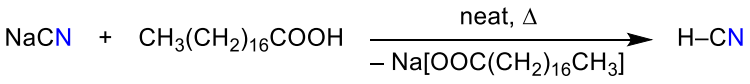

Scheme 7: Lab-synthesis of pure dry HCN (Figure 5) (Labbow et al., 2016).

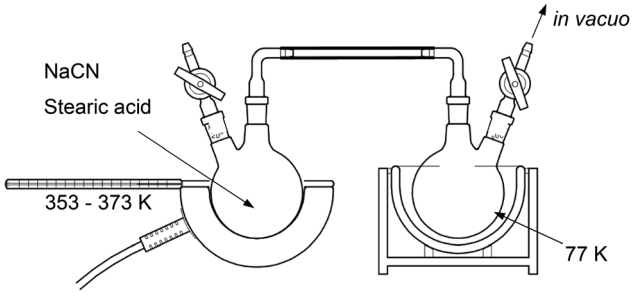

Figure 5: Apparatus for the synthesis of pure HCN with stearic acid and important spectroscopic data: HCN (27.03 g mol^{-1}): T_M = 260 K. **^{1}H NMR** (298 K, CD_2Cl_2, 250.1 MHz): δ = 4.00 (s, 1H, *H*CN, $^1J(^1H\text{-}^{13}C)$ = 266 Hz). **$^{13}C\{^1H\}$ NMR** (298 K, CD_2Cl_2, 62.9 MHz): δ = 110.1 (s, H*C*N). **$^{14}N\{^1H\}$ NMR** (298 K, CD_2Cl_2, 36.1 MHz): δ = –125.0 (s, HC*N*, $\Delta\nu_{1/2}$ = 50 Hz). **Raman** (632 nm, 6 mW, 20 s, 20 acc., 233 K, cm^{-1}): 819 (1), 1611 (1), 2163 (1), 2197 (10), 3151 (1) (Labbow et al., 2016).

azulminic acid, is formed by anionic polymerization of HCN in aqueous solution. The reaction proceeds via dimeric hydrocyanic acid (iminoacetonitrile). At the same time, ring closure takes place between γ-positioned nitrile groups, which stabilizes the polymer (Marín-Yaseli et al., 2017; Ruiz-Bermejo et al., 2013; Völker, 1960).

As already mentioned, HCN also plays/played a major role in the formation of H/C/N compounds on earth as well as on other celestial bodies, e.g. Titan (Carrasco et al., 2009; Coll et al., 1998; Hörst et al., 2012; Israël et al., 2005; Kaiser and Mebel, 2012; Maillard et al., 2021; Thompson et al., 1994; Rüger et al., 2019; Selliez et al., 2020; Somogyi et al., 2016; Szopa et al., 2006; Vuitton et al., 2010). Titan, the second largest moon in our Solar System, has a dense atmosphere consisting mainly of nitrogen and a few percent methane. Nitrogen radicals are formed in this gaseous environment, for example by the UV radiation of the sun (Kaiser and Mebel, 2012). Their reaction with methane leads to the formation of a dense haze. Because of this formation, the study of this nebula represents a major interest for prebiotic chemistry and planetary sciences (Hörst et al., 2012; Kaiser and Mebel, 2012; Maillard et al., 2021; Sagan and Khare, 1979; Selliez et al., 2020; Somogyi et al., 2016; Rüger et al., 2019). Mainly NH_3 and HCN serve as precursors for the formation of more complex nitrogen-containing matter systems. In connection with the atmosphere of Titan, which is often tried to be reproduced in laboratory experiments, the production of so-called *tholins* (derived from Greek for muddy) plays a major role (Sagan and Khare, 1979). The term coined by C. Sagan describes a mixture of organic substances observed after irradiation of gas mixtures analogous to the atmosphere of Titan. Tholins are thought to be a very complex mixture of different compounds (Sagan and Khare, 1979).

Crystal structure

The calculated molar heat capacities indicate a reversible phase transition of hydrogen cyanide at 170.35 K (Giauque and Ruehrwein, 1939). The experimental determination of two different crystal structures by W. J. Dulmage and W. N. Lipscomb confirmed this result in 1951. Besides an orthorhombic modification, they reported a tetragonal form of hydrogen cyanide for temperatures higher than the temperature of phase transition (Table 2) (Dulmage and Lipscomb, 1951).

Both lattices consist of linear molecule chains parallel to the *c*-axis of the lattice (Figure 6) and are surrounded by four more chains, which are displaced by half of a lattice parameter to the main chain (Dulmage and Lipscomb, 1951; Langel et al., 1989). Each chain is composed of HCN molecules that are linked by NC–H···N hydrogen bonds. The reported structural parameters are identical (r_{C-N} = 1.19 Å; r_{H-C} = 1.07 Å). The hydrogen bond with a computed distance of $r_{NC-H\cdots N}$ = 2.08 Å can be considered very strong. For comparison, the gas phase data of HCN are r_{C-N} = 1.15525 Å and r_{H-C} = 1.06666 Å as well as r_{H1-C1} = 1.06728 Å, r_{C1-N1} = 1.15361 Å, $r_{N1\cdots H2}$ = 2.21186 Å, r_{H2-C2} = 1.07300 Å and r_{C2-N2} = 1.15588 Å for the linear hydrogen bonded dimer $H^1C^1N^1\cdots H^2C^2N^2$ (at the CCSD(T)-F12b/aug-cc-pVQZ level of theory, optimized geometries with $C_{\infty v}$ symmetry) (Mihrin et al., 2018).

Table 2: Crystallographic data of the tetragonal high temperature modification and orthorhombic low temperature modification of hydrogen cyanide (temperatures in K; lengths in Å; angles in °; volumes in Å^3) (Dulmage and Lipscomb, 1951).

Parameter	HCN tetragonal	HCN orthorhombic
T	>170	<170
Space group	*I*4*mm*	*Imm*2
a	4.63	4.13
b	4.63	4.85
c	4.34	4.34
α	90.00	90.00
β	90.00	90.00
γ	90.00	90.00
V	92.9	86.8
Z	2	2

In contrast, the low-temperature modification is characterized by an orthorhombic form, which is quite similar to the tetragonal form (Figure 6) (Dulmage and Lipscomb, 1951). Because of parallel molecular and crystal axes a dielectric anisotropy weakens the hydrogen bonds, which leads to slightly stretched intermolecular distances (Baglin et al., 1970).

Due to the polarity of hydrogen cyanide, two models are reported to describe the primitive cell of the low-temperature modification. The polar crystal structure of the first model is based on an arrangement of parallel dipole moments in accordance with W. J. Dumlage and W. N. Lipscomb (space group *I*4*mm*). In contrast, the anti-parallel hydrogen-bonded HCN chains and their anti-parallel dipole moments of the second model (space group *P*4/*nmm*) leads to a non-polar crystal structure (Figure 7) (Cummins et al., 1988; Panas, 1992).

Furthermore, more modifications of hydrogen cyanide including different electric conductivities are expected at high pressures of more than 73 GPa. Due to calculations they propose a transition from the orthorhombic to the tetragonal and from the tetragonal to the triclinic modification. The

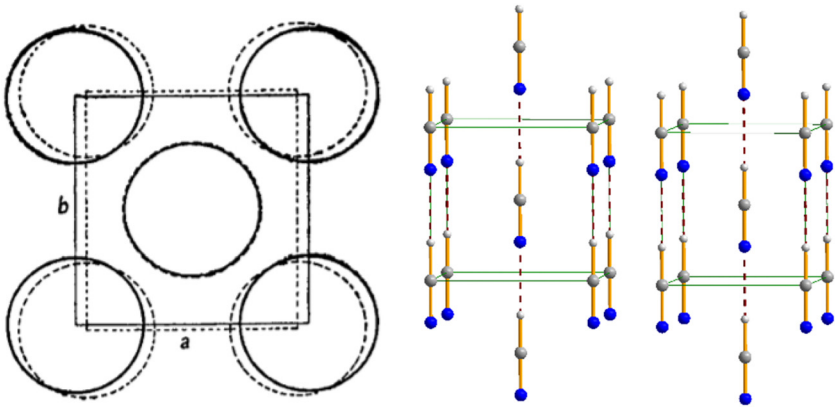

Figure 6: Left: unit cells of the high-temperature (full lines) and the low-temperature modification (broken lines) of hydrogen cyanide (representation taken from W. J. Dulmage and W. N. Lipscomb), middle: unit cell of the tetragonal and right: of the orthorhombic form (view along *a*-axis) (Dulmage and Lipscomb, 1951).

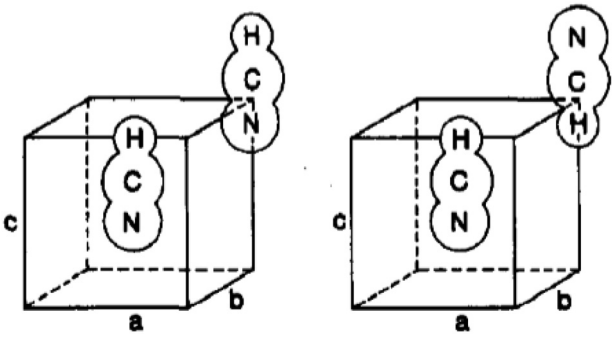

Figure 7: Polar and non-polar crystal structures of hydrogen cyanide in low-temperature modification (representation taken from Cummins et al., 1988).

phase transition depends on the pressure and the presence of polar or non-polar phase inside the orthorhombic cell (Khazaei et al., 2011).

HCN/HNC-isomerization

The HNC species is a metastable isomer of hydrogen cyanide, which is mainly detectable in the interstellar matter. Isomeric pairs of small molecular entities such as HCN/HNC are prevalent in the interstellar medium. Previous observations of the HNC/HCN abundance ratio show that the ratio decreases with increasing temperature. It was shown that chemical gas phase reactions affect the HNC/HCN ratio and can thus contribute to the observed dependence, e.g. H + HNC → HCN + H or C + HNC → HCN + C (Graninger et al., 2014). The origin and the mechanism of formation of the isocyanide species is not completely resolved. It is known that the ratio of hydrogen cyanide and hydrogen isocyanide depends on the temperature (Ferus et al., 2011; Wang et al., 2007).

The first infrared spectroscopic (IR) evidence of HNC in laboratory was found by D. E. Milligan and M. E. Jacox during the photolytic decomposition of methyl azide (Milligan and Jacox, 1967a, 1967b). D. E. Milligan could confirm his proposal by studies on the photolysis of HCN in vacuum under ultraviolet light at 14 K (Milligan and Jacox, 1967a, 1967b). The IR data of HNC are presented in Table 3.

The isocyanide species is an important system of theoretical calculations because its simplicity allows also complex calculations and the results are able to be adopted to more complex systems (Burkholder et al., 1987; Pearson et al., 1975). C. Glidewell and C. Thomson also carried out many calculations using different basis sets to characterize both compounds and their transition state discussing differences of selected methods (Glidewell and Thomson, 1984). The H–C and C–N distances of the T-shaped transition state are quite similar to the distances of the HCN and HNC species, but the N–H distance of the transition state is elongated. An HCN angle of 70°–80° is found for the transition state (HCN → CNH) (Vichietti and Haiduke, 2014). The experimentally observed CN bond in HCN is slightly shorter than in NCH, while the CH bond is slightly longer (Table 4) (Costain, 1958; Okabayashi and Tanimoto, 1993).

P. K. Pearson and H. F. Schaefer reported a transition state structure with HCN/HNC angle of both isomers at 73.7°, so the transition state resembles more the structure of the hydrogen cyanide. The HCN isomer is energetically

Table 3: IR data of HNC compounds after photolysis of methyl azide in argon matrix at 4 K and after photolysis of HCN in argon matrix at 14 K (wave numbers in cm^{-1}) (Milligan and Jacox, 1967a, 1967b).

Compound	ν_1	ν_2	ν_3	Compound	ν_1	ν_2	ν_3
$H^{14}N^{12}C$	2032	535	3583	$H^{14}N^{12}C$	2029	477	3620
$D^{14}N^{12}C$	1940	413	2733	$D^{14}N^{12}C$	1940	374	2769
$H^{15}N^{12}C$	2005	–	3571	$H^{15}N^{12}C$	2004	475	3610
$D^{15}N^{12}C$	1923	–	2710	–	–	–	–
$H^{14}N^{13}C$	1990	–	3583	$H^{14}N^{13}C$	1987	477	3620

Table 4: Structural data of the isomers HCN and HNC using different basis sets (bond lengths in Å; angles in °) (Gleiter et al., 1995; Pople et al., 1978; Vichietti and Haiduke, 2014).

Compound	Method + basis set	r_{A-B}	$r_{H-A/B}$	<(H–A–B)
HCN	MP2/6-31G*	1.177	1.069	180.0
	HF/6-31G*	1.133	1.059	180.0
	B3LYP/aug-cc-pVQZ	1.1451	1.0655	–
	MPW1K/aug-cc-pVQZ	1.1358	1.0621	–
	Experimental (Costain, 1958)	1.154(1)	1.063(3)	–
HNC	MP2/6-31G*	1.187	1.003	180.0
	HF/6-31G*	1.154	0.985	180.0
	B3LYP/aug-cc-pVQZ	1.1632	0.9964	–
	MPW1K/aug-cc-pVQZ	1.1543	0.9895	–
	Experimental (Okabayashi and Tanimoto, 1993)	1.16835(2)	0.996064(3)	–

Table 5: Raman data of HCN at different temperatures (temperatures in K; wave numbers in cm^{-1}).

Publication	State	T	ν_1	ν_2	ν_3
Douglas and Sharma (1953)	Gaseous	–	2095.5	–	–
Pézolet and Savoie (1969)	Liquid	292	2096	3215	794
		261	2097	3207	798
	Solid	183	2098, 2104	3145, 3180	819
		78	2098, 2104	3129, 3150	827, 840

Table 6: IR data of HCN at different temperatures (temperatures in K; wave numbers in cm^{-1}).

Publication	State	T	ν_1	ν_2	ν_3
Hoffmann and Hornig (1949)	Gaseous	–	2089	3312	712
	Solid	93	2097	3132	828, 838
Kozirovski and Folman (1966)	On NaCl	77	2095	3145	745, 800

favoured over the HNC species by ca. 60–80 kJ mol^{-1} (Pearson et al., 1975; Pople et al., 1978; Redmon et al., 1980; Vazquez and Gouyet, 1981) depending on the used basis sets and method (Komornicki et al., 1977; Loew and Chang, 1971; Pople et al., 1978). W. J. Hehre et al. could confirm the difference of energies between both isomers by experimental measurements ((62.0 ± 8.3) kJ mol^{-1}) whereas A. G. Maki and R. L. Sams reported an energy difference of (43.12 ± 4.61) kJ mol^{-1} by IR spectroscopic observation (Maki and Sams, 1981; Pau and Hehre, 1982). The activation barriers are computed to lie between 198 and 202 kJ mol^{-1} for HCN → HNC and 137–141 kJ mol^{-1} for the reverse process HNC → HCN (Khalouf-Rivera et al., 2019). R. M. Vichietti et al. computed activation enthalpies of 184 kJ mol^{-1} for the forward and 121 kJ mol^{-1} for the reverse reaction (Vichietti and Haiduke, 2014).

Spectroscopic data

Vibrational data of solid, liquid and gaseous hydrogen cyanide are listed in Tables 5 and 6. Spectroscopic data of IR and Raman spectra of two different isotopically substituted compounds were discussed in detail by Chadwick and Edwards (1973). Furthermore, Walsh et al. (1978) carried out detailed studies on HCN- and DCN-monomers and dimers in different matrices, e.g. noble gas and N_2.

HCN and adducts of HCN species were studied by means of ^1H, ^{13}C, ^{14}N NMR experiments in CD_2Cl_2 (Table 7) (Alkorta and Elguero, 1998; Arp et al., 2000; Bläsing et al., 2018, 2020; Corain, 1982; Emri and Györi, 1994; Harloff et al., 2019a, 2020b; Klapötke et al., 1996; Mai and Patil, 1986; Mamajanov and Herzfeld, 2009; Nagy et al., 2005; Olsson et al., 1995; Provasi et al., 2005; Saal et al., 2019; Schulz and Klapötke, 1992; Tornieporth-Oetting et al., 1992). It should be noted that in case of adducts such as $B(C_6F_5)_3$ or its dimer HCN–HCN–$B(C_6F_5)_3$, all resonances (in the ^1H, ^{13}C, ^{14}N and ^{11}B NMR spectra) are very broad but still detectable at 253 K indicating a highly dynamic system (Bläsing et al., 2018). For example, even the nitrogen atoms of HCN–HCN–$B(C_6F_5)_3$ can be observed in the ^{14}N NMR experiment at –128 and –192 ppm with half widths of 960 and 2250 Hz (*cf.* HCN: –125 ppm and $\Delta\nu_{1/2}$ = 50 Hz). As expected, upon borane adduct formation (Table 7), the resonance of the proton is shifted to lower field by ca. 2 ppm (*cf.* HCN 4.00 vs. 6.42 in the dimer adduct) displaying an increase of the acidity. A broad resonance formally assigned to the loosely bound second HCN molecule of HCN–HCN–$B(C_6F_5)_3$ is detected at 4.02 ppm, indicating

Table 7: Selected NMR data of HCN, HCN-$B(C_6F_5)_3$, and HCN-HCN-$B(C_6F_5)_3$ [δ scale] (Bläsing et al., 2018).

Compound	^1H	^{11}B	$^{13}C\{^1H\}$	$^{14}N\{^1H\}$
HCN	4.00	–	110.1	–125.0
HCN–$B(C_6F_5)_3$	6.19	–14.7	103.8	–188.8
HCN–HCN–$B(C_6F_5)_3$	4.02	–10.9	106.9	–128.1
	6.42	–	106.9	–192.2

dynamic exchange between loosely bound and free HCN species (Bläsing et al., 2018). The ^{1}H NMR spectrum of HC^{15}N shows a sharp doublet at 3.60 ppm, which was directly taken after preparation. The proceeding oligomerization inducing fast intermolecular proton exchanges leads to disappearance of the splitting of the proton resonance and a sharp single signal, while the color turns to yellow (Binsch and Roberts, 1968).

$[HCN]^{\cdot-}$ radical anion

After a treatment of cyanide doped alkali halide crystals by γ-irradiation or UV photolysis at low temperatures between 21 and 77 K and followed by tempering to 100 K the $[HCN]^{\cdot-}$ radical anion could be detected EPR-spectroscopically. The formation and decomposition of this $[HCN]^{\cdot-}$ species has been investigated at different temperatures in detail (Adrian et al., 1969; Beuermann and Hausmann, 1967; Hausmann, 1966; Root et al., 1966). The radical anion could be detected also in potassium cyanide irradiated by UV light at 77 K and in the gas phase during mass spectrometric measurements of methyl and ethyl cyanides (von der Weid et al., 1979; Tsuda et al., 1971).

The stretching mode of the C–N bond is observed in IR spectroscopic measurements at 1758 cm^{-1} showing partial C≡N bond character (Pacansky et al., 1978). It corresponds to a much weaker C–H bond of lower energy than in the HCN. The EPR measurements support this explanation as they feature a quite high spin density value of $\rho_H = 0.27$ for the unpaired electron density on the hydrogen atom ($\rho_C = 0.32$ and $\rho_N = 0.41$) (Adrian et al., 1969). Furthermore, SCF computations of the orbital containing the unpaired electron indicate a significant hydrogen character and the bond angle decreases from linear structure of HCN to 122°–131° on forming the radical anion. In summary, the $[HCN]^{\cdot-}$ radical anion is isoelectronic to the $HCO^{\cdot}$ radical showing quite similar properties (Pacansky et al., 1978; Pedersen, 1970) (Table 8).

Table 8: Structural data of the $[HCN]^{\cdot-}$ radical anion (bond lengths in Å; angles in °).

Publication	Exp./calc.	r_{H-C}	r_{C-N}	< (H–C–N)
Douglas and Sharma (1953)	Exp. – IR	1.153	1.066	–
	Exp. – EPR	–	–	131
Adrian et al. (1969)				
Thomson (1970)	INDO	1.23	1.18	133
Pedersen (1970)	INDO	1.256	1.164	129
Pacansky et al. (1978)	SCF/CGTO	1.233	1.122	121.7

$[HCN]^{\cdot+}$ cation

The formation of the cationic $[HCN]^{+}$ species is mostly observed during excitation in microwave discharge and in high-energy systems (Forney et al., 1992). The first ionization energy of hydrogen cyanide is determined to about 13.60 eV by photoionization and photoelectron spectroscopy (Dibeler and Liston, 1968; Fridh and Åsbrink, 1975). Furthermore, theoretical calculations indicate that the isocyanide cation species $[HNC]^{+}$ is more stable than the cyanide cation species $[HCN]^{+}$, which means a reversion of stability in contrast to the neutral hydrogen cyanide (Murrell and Derzi, 1980). The ground state of $[HNC]^{+}$ ($^{2}\Sigma^{+}$) is decreased by 75–125 kJ mol^{-1} compared to the ground state of $[HCN]^{+}$ ($^{2}\Pi$) (Forney et al., 1992). G. Frenking and H. Schwarz suggest that the change of electron density causes a reversion of stability (Table 9) (Frenking and Schwarz, 1982). J. N. Murrell and A. A. Derzi suggested that the unpaired electron in $[CN]^{+}$ is predominantly on the nitrogen atom and hence they expected the $^{2}\Sigma^{+}$ state resulting from interaction with the hydrogen to be more stable for the isomer $[HNC]^{+}$ as is found (Table 10) (Murrell and Derzi, 1980). Also kinetic studies on a mixture of hydrogen cyanide and hydrogen isocyanide cations indicate a difference of reactivity of both isomers (Petrie et al., 1990).

$[HCNH]^{+}$ cation and the $[H(HCN)_n]^{+}$ cluster ion series

The $[HCNH]^{+}$ cation, the first representative of the cationic cluster series $[H(HCN)_n]^{+}$, has been observed in interstellar

Table 9: Total energy, energy of repulsion ($\Delta E_{rep.}$) and total energy of electrons ($\Delta E_{elec.}$) of HCN, HNC and their cations (ΔE in kJ mol^{-1}; HF/4-31G) (Frenking and Schwarz, 1982).

Compound	$\Delta E_{tot.}$	$\Delta E_{rep.}$	$\Delta E_{elec.}$
HCN	0	0	433.2
HNC	39.8	473.9	0
$[HCN]^{+}$	128.1	0	1702.4
$[HNC]^{+}$	0	1574.2	0

Table 10: Structural data of cationic hydrogen cyanide species (bond length in Å; calculations using the SCF/cc-pVDZ level of theory) (Murrell and Derzi, 1980).

Compound	State	r_{A-B}	r_{H-A}
$[HCN]^{+}$	$^{2}\Pi$	1.190	1.091
$[HCN]^{+}$	$^{2}\Sigma^{+}$	1.114	1.072
$[HNC]^{+}$	$^{2}\Pi$	1.225	1.021
$[HNC]^{+}$	$^{2}\Sigma^{+}$	1.116	1.013

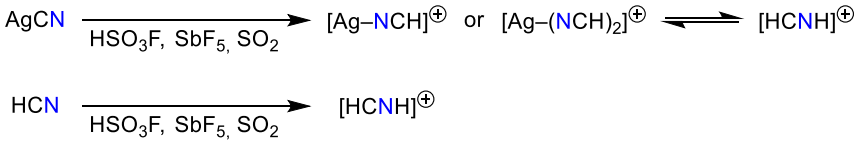

Scheme 8: Synthetic routes of $[HCNH]^+$ (Olah and Kiovsky, 1968).

matter and is a significant part of the ionosphere of Titan, a moon of Saturn (Cravens et al., 2006; Fox and Yelle, 1997; Herbst and Klemperer, 1973; Keller et al., 1998). Because of the cation's supposed key role in chemistry of interstellar matter, many studies are carried out to determine its structure, fundamentals and transition frequencies (Amano and Tanaka, 1986).

The first synthesis of the $[HCNH]^+$ cation has been carried out 1968. NMR spectroscopic measurements could prove the formation of the cation in a mixture of fluorosulfuric acid HSO_3F and antimony pentafluoride SbF_5 (1:1) in a solution of HCN and SO_2. The first IR measurement of the cation has been published by Altman et al. (1984a). Also in 1968 G. A. Olah and T. E. Kiovsky published another synthetic route of the cation starting with silver cyanide in a solution of HSO_3F, SbF_5 and SO_2 also studied by NMR spectroscopy (Scheme 8, Table 11) (Olah and Kiovsky, 1968).

The cation is discussed as possible precursor of HCN and HNC in the interstellar matter. The proposed dissociative recombination reaction leads to the normal hydrogen cyanide and metastable isocyanide in relation of 1:1 (Scheme 9) (Kalescky et al., 2013; Ngassam et al., 2005; Pearson and Schaefer, 1974; Talbi and Ellinger, 1998).

But radio astronomic studies indicate a temperature depending ratio of both isomers and also the position of the isomers inside the molecular cloud is important (Irvine and Schloerb, 1984; Schilke et al., 1992). Further reactions influencing this relation are the equilibrium reaction and ion-neutral reactions, which also occur in interstellar matter (Conrad and Schaefer, 1978; Herbst, 1995; Talbi, 1999; Talbi and Herbst, 1998). Furthermore, the singlet $[HCNH]^+$ in a low-lying vibrational state produces HCN whereas the triplet mostly leads to HNC caused by a smaller bond-dissociation energy of the C–H bond in contrast to the N–H bond in the exited state (Allen et al., 1980; Jursic, 1999). But it will require further studies to permit detailed information about the unexpectedly high ratio of HNC in interstellar matter.

In literature three different singlet isomers of $[HCNH]^+$ are discussed (Figure 8). The linear form, which is the low-lying structure, is isoelectronic to acetylene and two three-bonded forms, in which $[H_2CN]^+$ is the energetic most unfavoured one with low isomerization barrier to the linear form (Table 12) (Allen et al., 1980; Conrad and Schaefer, 1978; Jursic, 1999).

During a period of about 20 years spectroscopic data of the $[HCNH]^+$ cation have been measured several times using different methods, which partially lead to big differences (Table 13).

Table 11: Selected NMR data of $[HCNH]^+$ (chemical shifts in ppm; coupling constants in Hz) (Olah and Kiovsky, 1968; Olah and White, 1969).

Spectrum	δ	J
^{1}H NMR	−7.50	8.5
$^{13}C\{^1H\}$ NMR	−95.7	320.0

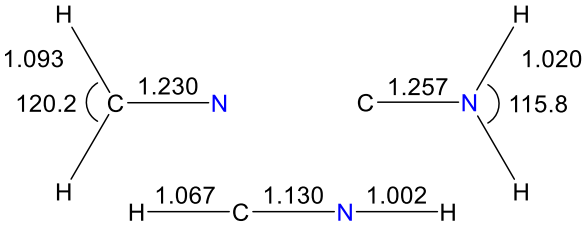

Figure 8: Structural data of the $[HCNH]^+$ isomers in ground state (bond length in Å; angles in °; DZ SCF method) (Conrad and Schaefer, 1978).

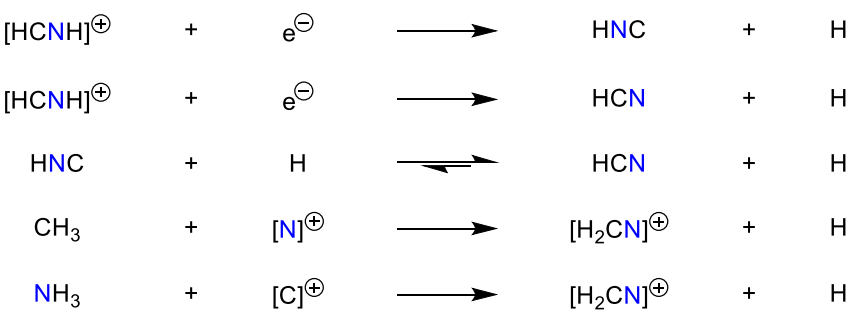

Scheme 9: Possible reaction pathways to generate HCN and HNC (Kalescky et al., 2013; Ngassam et al., 2005; Pearson and Schaefer, 1974; Talbi and Ellinger, 1998).

Table 12: Relative energies of the $[HCNH]^+$ isomers (in kJ mol^{-1}) calculated with different methods (Conrad and Schaefer, 1978).

Compound	SCF/DZ	CI/DZ	SCF/DZ + P	CI/DZ + P
$[HCNH]^+$	0.0	0.0	0.0	0.0
$[H_2CN]^+$	292.7	239.9	273.8	299.8
$[H_2NC]^+$	173.3	131.5	167.5	192.6

Moreover, experimental data of the $[H(HCN)_n]^+$ (n = 1–4) aggregates in the gas phase were published by M. Moet-Ner utilizing a pulsed high-pressure mass spectrometric technique to determine thermochemistry data of these species (Meot-Ner, 1978).

The $[CN(HCN)_n]^-$ cluster ion series

M. Moet-Ner, S. Scheiner, and J. F. Liebman reported on thermochemical measurements and computations of HCN-cyanide-aggregates, $[CN(HCN)_n]^-$, in the gas phase utilizing a pulsed high-pressure mass spectrometric technique (Meot-Ner et al., 1988). It was found that the aggregate series $[CN(HCN)_n]^-$ (n = 1–7) is formed exothermically for each HCN addition step ($\Delta H°$ between –20.7 and –7.6 kcal mol^{-1}). The hydrogen bond energy in $[CN(HCN)]^-$ was also determined from ion cyclotron resonance $[CN]^-$/HCN-exchange equilibria measurements (Larson and McMahon, 1984).

The synthesis of salts bearing the $[CN(HCN)_n]^-$ cluster ions (Bläsing et al., 2020), was also attempted. For this purpose, pure cyanides of the type [WCC]CN ($[WCC]^+$ = weakly coordinating cation = $[Et_3NMe]^+$, $[^nPr_3NMe]^+$, $[Ph_3PMe]^+$) (Price et al., 2009), were treated with an excess of liquid HCN (generated from NaCN and stearic acid (T_M = 342 K) at 353–373 K under vacuum) (Bläsing et al., 2018; Günther et al., 1935; Labbow et al., 2016). However, this synthetic approach did not work since almost instantaneous polymerization was observed affording a deep brown highly viscous oil. To avoid fast polymerization, $[Ph_4P]CN$ and $[Ph_3PNPPh_3]CN$ (= [PNP]CN), containing bulkier and more symmetrical cations, were used. Indeed, this reaction of $[Ph_4P]CN$/[PNP]CN with liquid HCN (at low temperatures of 263–273 K) finally yielded crystals. X-ray studies revealed unequivocally the presence of hydrogen-bridged linear $[CN(HCN)_2]^-$ ions in case of the $[Ph_4P]^+$ salt, while Y-shaped $[CN(HCN)_3]^-$ anions were found with the $[PNP]^+$ as counterion (Figures 9 and 10) (Arlt et al., 2021).

The stepwise formation of the HCN solvates $[CN(HCN)_n]^-$ were computed to be exothermic and exergonic for n = 1–3, however, the larger n the values for $\Delta_nH°_{298}/\Delta_nG°_{298}$ become less negative ($\Delta_nH°_{298}$ = –23.6, –18.7, and –13.0 kcal mol^{-1}; $\Delta_nG°_{298}$ = –15.9, –11.1, and –7.0 kcal mol^{-1}; cf. from mass spectroscopy: $\Delta_1H°_{298}$ = –20.1 ± 1.6 (Chacko et al., 2006) and –20.7 kcal mol^{-1}, as well as $\Delta_2H°_{298}$ = –16.4 kcal mol^{-1} and $\Delta_3H°_{298}$ = –12.6 kcal mol^{-1}) (Meot-Ner et al., 1988).

Owing to the hydrogen bonding within the cluster anions, these species may be regarded as fragments of the solid structure of HCN upon (partial) deprotonation. In accord with computations, linear $[CN(HCN)_2]^-$ can be regarded as a cyanide ion stabilized by two hydrogen-bonded HCN molecules, while Y-shaped $[CN(HCN)_3]^-$ is energetically slightly preferred over an analogous linear isomer. There is always only little change of stability when $[CN]^-$ and HCN do not form a linear complex, indicating a highly dynamic system at ambient temperatures as proven by computed rather flat rotational potentials either within a linear or Y-shaped HCN framework (Figure 11). Moreover, pseudohalide HCN aggregate ions of the type $[N_3(HCN)_3]^-$, $[OCN(HCN)_3]^-$, $[SCN(HCN)_2]^-$ and $[P(CN{\cdot}HCN)_2]^-$ with similar strong hydrogen bonds and structural motifs have also been isolated and fully characterized (Arlt et al., 2021; Bläsing et al., 2020; Harloff et al., 2020b).

Table 13: Spectroscopic data of $[HCNH]^+$ using different methods (wave numbers in cm^{-1}).

Publication	Exp./calc.	ν_{NH}	ν_{CH}	ν_{CN}	δ_{HCN}	δ_{HNC}
Pearson and Schaefer (1974)	SCF/DZ	4300	3507	2354	1023	922
Lee and Schaefer (1984)	SCF/DZ + P	3869	3501	2434	937	799
	CI/DZ + P	3754	3423	2283	836	700
Altman et al. (1984a) (1984b)	Exp. – IR	3483	3188	–	–	–
DeFrees and McLean (1985)	MP2/6-31G*	3675	3397	2164	822	659
	HF/6-31G*	3465	3147	2177	866	699
Ho et al. (1987)	Exp. – IR	–	–	–	–	646
Peterson et al. (1995)	HF/4-31G	3445	3176	2088	901	762
	HF/6-31G*	3534	3213	2100	849	685

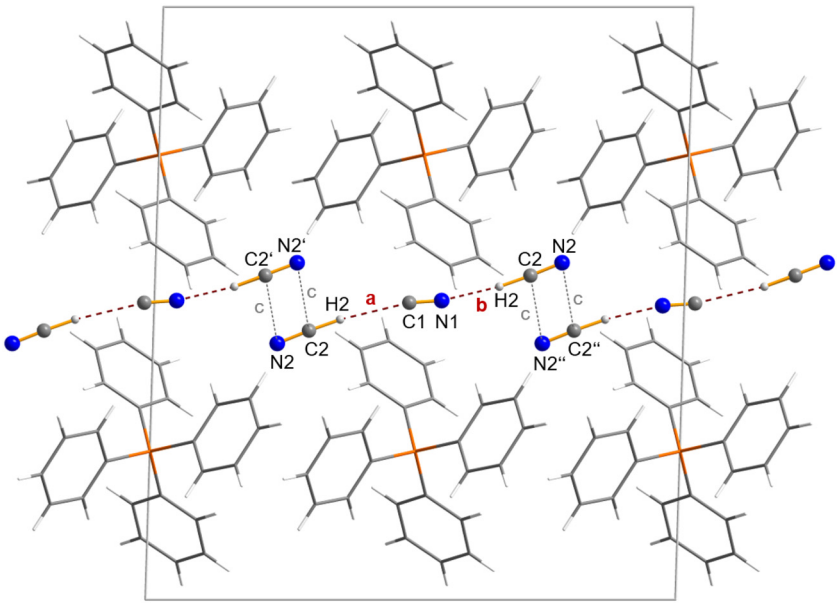

Figure 9: Ball-and-stick (anions) and wireframe (cations) representations of the molecular structure of $[Ph_4P][CN(HCN)_2]$ in the crystal. View along *[010]*. The linear molecular anion is formed by two hydrogen bridges (**a** and **b**). A chain is formed when short contacts (**c**) are considered. A section of such a chain is shown (Pézolet and Savoie, 1969).

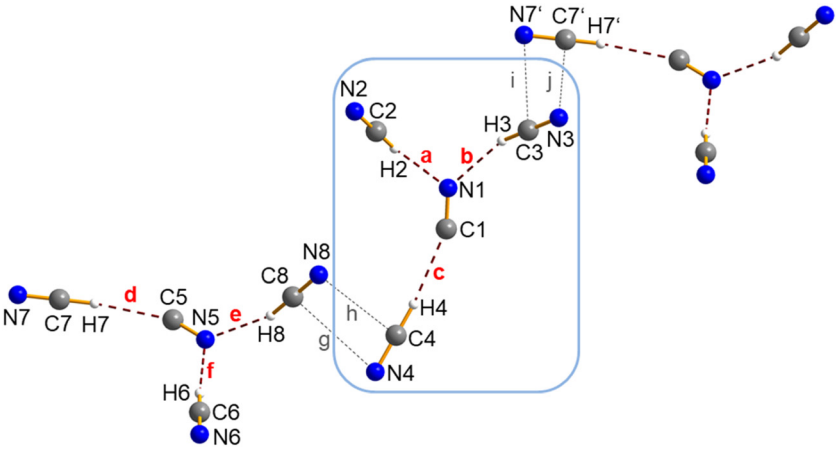

Figure 10: Ball-and-stick representation of the $[CN(HCN)_3]^-$ ion in a crystal of [PNP] $[CN(HCN)_3]$. The Y-shaped molecular anion is formed by three hydrogen bridges (**a**–**c** and **d**–**f**). A chain is formed when short contacts (**g**–**j**) are considered. A section of such a chain is shown, while the cations are omitted for clarity (Arlt et al., 2021).

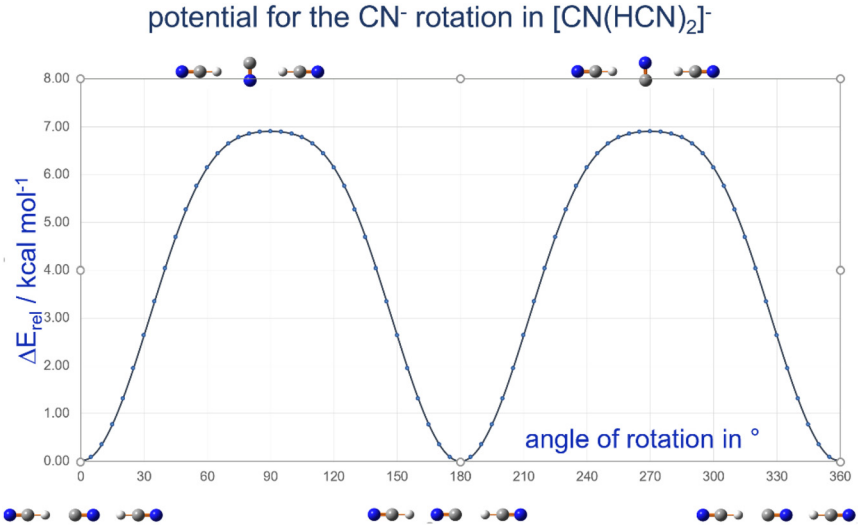

Figure 11: Rotational potential for the rotation of a $[CN]^-$ ion within the frame of two HCN molecules (Pézolet and Savoie, 1969).

1st Main group – alkali cyanides

The alkali cyanides are extensively investigated especially focusing on the compounds of lithium, potassium and sodium. All alkali cyanides are well water-soluble, sodium cyanide is also soluble in alcoholic solutions. Sodium and potassium cyanide can be received by evaporating their aqueous solution, whereas the synthesis of the lithium, rubidium and cesium compound is more difficult due to their fast decomposition on air. Important properties are listed in Table 14.

A review article of A. Rubo et al. also provides further detailed information of properties and also production, uses, e.g. gold mining or electroplating and hardening of metals, or economic aspects (Rubo et al., 2006).

The alkali cyanides are one of the smallest ionic systems having strong rotational-translation coupling in solid phases (Klein et al., 1981). The crystals of alkali cyanides combine properties of ionic and also molecular crystals, so called ionic-molecular crystals, because of the pseudohalogen properties of the cyanide anion (Henriques and von der Weid, 1985). So alkali cyanides are typical alkaline pseudohalogen compounds and their optical, structural and thermic properties are effected by the polyatomic character of the anion. Furthermore, under exclusion from air these compounds are stable against gentle heating and do not decompose.

The spectroscopic data of the alkali cyanides are quite similar, only the ν_1 and ν_2 frequencies are showing bigger differences in relation to the size of the cation, which pushes the band to smaller energies (Tables 15 and 16) (do Carmo et al., 1981). A. Loupy and J. Corset also reported the independence of the stretching mode ν_1 of LiCN, NaCN and KCN from the concentration of the salt. Only the intensities are changing. If the concentration of the salt decreases, the band at lower frequencies increases and that one of higher frequencies declines.

Table 15: Raman data of different alkali cyanides (wave numbers in cm^{-1}).

Compound	ν_{CN}	Comments
LiCN (Loupy and Corset, 1976)	2079	In aqueous solution
NaCN	2079 (Loupy and Corset, 1976)	In aqueous solution
	2086.7 ± 2.7 (Glockler and Baker, 1942)	–
KCN (Loupy and Corset, 1976)	2079	In aqueous solution

Synthesis

Until the 1960s, the Castner–Kellner process was the common synthetic route of NaCN using sodium, which was heated by charcoal in an atmosphere of ammonia. The received sodium amide reacts with the charcoal to sodium cyanamide. After a second reaction with one equivalent of charcoal sodium cyanide is obtained (Scheme 10) (Derry and Williams, 1993).

The quite similar Beilby process was often used to synthesize potassium cyanide, but nowadays this synthetic route has no importance (Scheme 11) (Martin and Barbour, 1915).

The most common synthesis of alkali cyanides is the acid base neutralization reaction using hydrogen cyanide

Table 14: Some substance-specific properties of alkali cyanides (temperatures in K, densities in g cm^{-3}).

Compound	T_M	T_B	ρ at 298 K	Relative hygroscopicity (DeLong and Rosenberger, 1986)
HCN	259.8 (Henderson and Cullinan, 2007)	298.8 (Henderson and Cullinan, 2007)	0.69* (Williams, 1948)	Miscible with water
LiCN	433 (Lely and Bijvoet, 1942)	–	1.08 (DeLong and Rosenberger, 1986)	Extreme
NaCN	837(1) (DeLong and Rosenberger, 1986)	1773(10) (Ingold, 1923)	1.60 (DeLong and Rosenberger, 1986)	Considerable
KCN	907.7 (DeLong and Rosenberger, 1986)	–	1.52 (DeLong and Rosenberger, 1986)	Little
RbCN	872.2 (Kondo et al., 1979)	–	2.32 (DeLong and Rosenberger, 1986)	Little
CsCN	801(2) (DeLong and Rosenberger, 1986)	–	3.41 (DeLong and Rosenberger, 1986)	High

Table 16: IR data of different alkali cyanides in varying media (wave numbers in cm^{-1}).

Compound	ν_{CN}	ν^2_{CN}	ν_{MC}	Comments
LiCN	2080.4 (Ismail et al., 1972)	–	680.5 (Ismail et al., 1972)	In neon matrix
	2084.5 (Ismail et al., 1972)	–	646.4 (Ismail et al., 1972)	In argon matrix
	2079 (Loupy and Corset, 1976)	–	–	In aqueous solution
	2070, 2086, 2100, 2116 (Loupy and Corset, 1976)	–	–	In DMF
NaCN	2080 (Miller and Wilkins, 1952)	3330 (Miller and Wilkins, 1952)	–	–
	2090 (do Carmo et al., 1981)	4156 (do Carmo et al., 1981)	–	–
	2060, 2076 (Loupy and Corset, 1976)	–	–	In DMF
	2060, 2076 (Loupy and Corset, 1976)	–	–	In DMSO
KCN	2077 (do Carmo et al., 1981)	4131 (do Carmo et al., 1981)	–	–
	2079 (Loupy and Corset, 1976)	–	–	In aqueous solution
	2054, 2064, 2070 (Loupy and Corset, 1976)	–	–	In DMSO
RbCN (do Carmo et al., 1981)	2071	4121	–	–
CsCN (do Carmo et al., 1981)	2063	4103	–	–

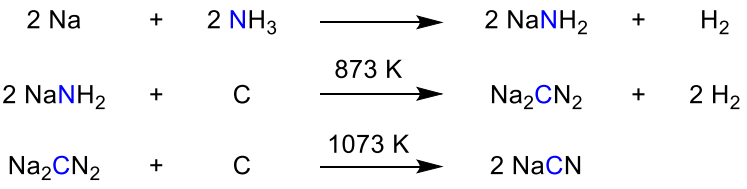

Scheme 10: Castner–Kellner process to synthesize sodium cyanide (Derry and Williams, 1993).

and an aqueous solution of alkaline hydroxide (Scheme 12) with yields as high as 98–99% (Guernsey and Sherman, 1926; Meyer, 1921; Reifsig, 1863; Sugisaki et al., 1968).

Because of a fast hydrolysis of alkali cyanides, they are often used as a solution of alcohol and small amounts of water. Especially, the lithium and cesium cyanide are very hygroscopic, which leads to less efficient synthesis of LiCN starting with LiOH and necessitate another synthetic approach. In this context, it is also possible to synthesize most of the alkaline cyanides using dried hydrogen cyanide and the pure alkali metal, which is dissolved in ethanol, ammonia or other non-aqueous solvents (Scheme 13) (DeLong and Rosenberger, 1986; Meyer, 1921). The purification of the salts is often carried out by recrystallization. The solids are suspended in liquid ammonia or

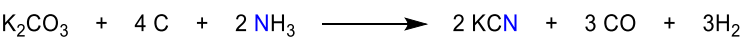

Scheme 11: Beilby process to synthesize potassium cyanide (Martin and Barbour, 1915).

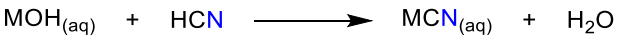

Scheme 12: Neutralization reaction to synthesize alkali cyanides (M = Li^+, Na^+, K^+, Rb^+, Cs^+) (Guernsey and Sherman, 1926; Meyer, 1921; Reifsig, 1863; Sugisaki et al., 1968).

ethanol to avoid hydrolysis and less soluble carbonates and cyanates are removed by filtration (Thompson, 1931). Vacuum distillation is reported to be inefficient (Hackspill and Grandadam, 1925).

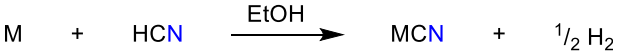

Scheme 13: Synthesis of alkali cyanides using dried HCN and the alkali metal (M = Li^+, Na^+, K^+, Cs^+) (DeLong and Rosenberger, 1986; Meyer, 1921).

T. J. Neubert and S. Susman reported another process of purification of NaCN and KCN. After melting the solid in vacuum and increasing the temperature from ambient temperature to 473 K and then to 938 K the alkaline cyanide is zone refined and also filtrated using a frit made of quartz. Single crystals containing 10 ppm Na and very small quantities of $[OCN]^-$ can be obtained and are suitable for polarized-light experiments (Neubert and Susman, 1964). LiCN can also be purified by recrystallization in THF. The solvent is removed in vacuum, but one mol percent remains (Rossmanith, 1965). In 1963 I. B. Johns and H. R. DiPietro carried out a reaction of liquid, anhydrous hydrogen cyanide and *n*-butyllithium in *n*-hexane under nitrogen atmosphere. The LiCN precipitates immediately in quantitative yield (Scheme 14) (Johns and DiPietro, 1964).

The decomposition of hydrogen cyanide is one of the main causes of impurities. Several synthetic routes avoiding the use of HCN are published. One of the first is the reaction of alkali metals and silver cyanide in THF and in presence of naphthalene (Scheme 15). The LiCN also crystallizes as its colorless solvate, which is dried *in vacuo*, and is obtained in yields of 79.6% (Rossmanith, 1965).

In 1997 T. J. Markley et al. reported a metathesis reaction of lithium chloride and sodium cyanide at ambient temperature (Scheme 16). The product could be obtained in a yield of 94.9% after a reaction time of four days. Single crystals were obtained using a mixture of DMF and DMAc (2:1). The solvent can not be removed completely, so the crystals still contain 0.6 mol DMF and 0.4 mol DMAc per equivalent of LiCN (Markley et al., 1997).

During researches on the synthesis of $Ca(CN)_2$ in 1912, H. Sulzer carried out a reaction of calcium cyanamide and charcoal, which required high temperatures to melt the mixture minimizing the yield of the reaction because of the preferred reverse reaction. By the addition of fluxing agents, e.g. NaCl or Na_2CO_3, the reaction temperature could be decreased and H. Sulzer also observed a reaction of the cyanamide and alkali metal salts (Scheme 17) (Sulzer, 1912).

The ratio of anhydrous calcium cyanamide, charcoal and sodium chloride is optimized to 10:2.0–2.5:18–20 and the reaction is carried out in an iron crucible with lid to avoid air. In the case of sodium carbonate, its ratio is decreased to 7.5–9.0 and because of the higher melting point the reaction temperature has to be increased. But this reaction is preferred due to improved separation of alkali cyanide and insoluble alkaline earth carbonates in the melt. In contrast, the use of NaCl leads to soluble alkaline earth chlorides, which can not be separated easily (Sulzer, 1912).

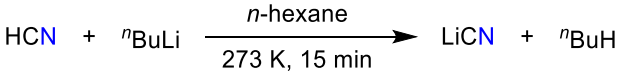

Scheme 14: Synthesis of LiCN by Johns and DiPietro (1964).

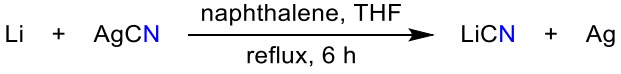

Scheme 15: Synthesis of LiCN without HCN (Rossmanith, 1965).

Scheme 16: Synthesis of LiCN without HCN by Markley et al. (1997).

Hydrolysis of alkali cyanides

Hydrolysis of basic alkali metal cyanide begins with dissociation upon addition of water molecules. The autoprotolysis of water provides protons to form hydrogen cyanide. The cyanide ion acts here as a base which grabs the proton. The formation of alkali formate and ammonia is also possible due to hydrolysis of alkali cyanides, while the increasing concentration of ammonia enhances the hydroxide concentration (Scheme 18).

Both types of reaction are prevalently observed at temperatures of more than 288 K, but the formation of hydrogen cyanide dominates at temperatures under 323 K. Higher temperatures of more than 353 K abet the generation of alkaline formate. In the subsequent step, the formed formates can also react with alkali hydroxides to form carbonates (Scheme 19).

Furthermore, cyanates and carbon will be formed, if the cyanides are heated to their melting point. This process is facilitated by an oxygen atmosphere, but an inert

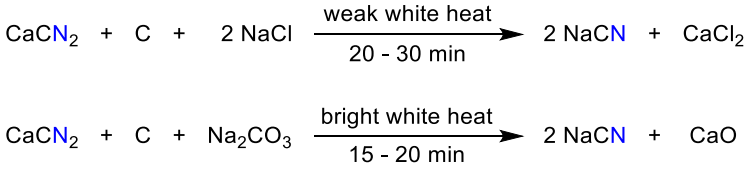

Scheme 17: Syntheses of NaCN using $CaCN_2$ as starting material (Sulzer, 1912).

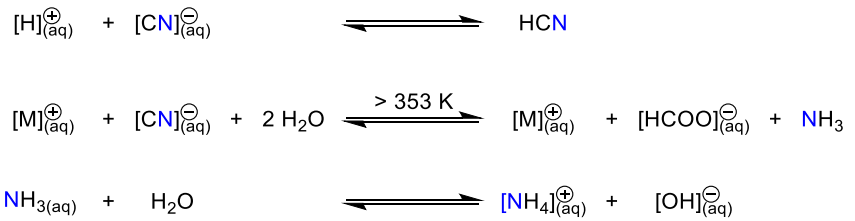

Scheme 18: Possible reactions due to hydrolysis of alkali cyanides (M = Na^+, K^+) (Hinks et al., 1972).

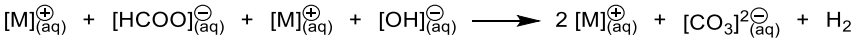

Scheme 19: Formation of carbonates (Hinks et al., 1972).

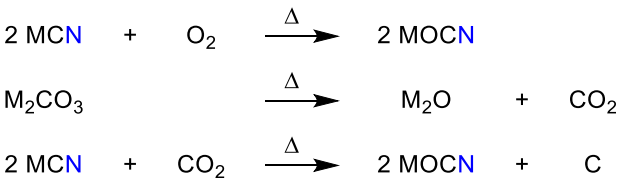

Scheme 20: Formation of cyanates due to decomposition of cyanides (Hinks et al., 1972).

atmosphere can not prevent this reaction because the formation of carbonates also permits the generation of cyanates (Scheme 20) (Hinks et al., 1972).

Crystal structures

The alkali metal cyanides correspond to the general composition MXY (M = cation of Na, K, Rb; XY = diatomic anion) and are characterized by the pseudocubic NaCl-type structure just below the melting point. They show similar properties as the alkaline halides, e.g. orientational disorder or rapid rotation of the linear $[CN]^-$ anion, because of the pseudohalide character of the cyanide anion (see 1.2 Cyanide, a classic pseudohalide) (Atoji, 1971; Kondo et al., 1979).

Lithium cyanide is an exception, since a NaCl-like structure could not be observed, although it should be theoretically possible, and the structures of cesium cyanide are also divergent. However, the difficulty in forming these cyanide compounds makes it difficult to study their crystal structures, resulting in only a few publications that deal with solid state structural studies on these salts. Structural data of various cyanide compounds are listed in Table 17. Further information on crystal data of cyanide compounds and their modifications are given in Table 18.

Table 17: Structural data of alkali metal cyanides.

Compound	Exp./calc.	r_{C-N}	r_{M-C}	r_{M-N}
HCN	MW	1.157 (Greenwood et al., 1988; Simmons et al., 1950)	1.061 (Greenwood et al., 1988; Simmons et al., 1950)	–
	MW	1.1538(10) (Costain, 1958)	1.0630(30) (Costain, 1958)	–
	MW	1.15321(5) (Glidewell and Thomson, 1984)	1.0655(2) (Glidewell and Thomson, 1984)	–
HNC	MW	1.172 (Glidewell and Thomson, 1984)	–	0.986 (Glidewell and Thomson, 1984)
	SCF	1.159 (Schmiedekamp et al., 1980)	–	0.982 (Schmiedekamp et al., 1980)
$[HCN]^-$	MW	1.1530 (Douglas and Sharma, 1953)	1.0657 (Douglas and Sharma, 1953)	–
LiCN	XRD	1.15(2) (Lely and Bijvoet, 1942)	2.11 (Lely and Bijvoet, 1942)	2.06 (Lely and Bijvoet, 1942)
	SCF	1.154 (Schmiedekamp et al., 1980)	1.930 (Schmiedekamp et al., 1980)	–
LiNC	SCF	1.169 (Schmiedekamp et al., 1980)	–	1.780 (Schmiedekamp et al., 1980)
NaCN	MW	1.170(4) (van Vaals et al., 1984a)	2.379(15) (van Vaals et al., 1984a)	2.233(15) (van Vaals et al., 1984a)
$NaCN \cdot 2H_2O$	XRD	1.07 (Le Bihan, 1958)	2.95 (Le Bihan, 1958)	3.10 (Le Bihan, 1958)
KCN	XRD	1.15 (Bozorth, 1922)	3.0 (Bozorth, 1922)	3.0 (Bozorth, 1922)

Table 18: Crystallographic data of lithium, sodium, rubidium cyanide and different modifications of potassium cyanide (temperature in K, pressure in MPa, lengths in Å; angles in °; volumes in Å^3).

Parameter	LiCN (Lely and Bijvoet, 1942) orthorhombic	NaCN (Swanson and Tatge, 1953) cubic	NaCN (Swanson and Tatge, 1953) orthorhombic	NaCN (Fontaine, 1975) orthorhombic	NaCN·2H_2O (Le Bihan, 1958) monoclinic	RbCN (Yoshimura et al., 1996)cubic	RbCN (Yoshimura et al., 1996) monoclinic	RbCN (Yoshimura et al., 1996) triclinic	RbCN (Rowe et al., 1984) monoclinic
T	–	299	279.6	171.9	–	295	85	85	4
Space group	*Pmcn*	*P23*	*Imm*	*Pmmn*	$P2_1/a$	*Fm3m*	*A2/m*	$P\bar{1}$	*Cc*
a	3.73	5.893	3.774	3.63	6.54(1)	6.83(1)	4.81(1)	9.79(1)	7.800(1)
b	6.52	5.893	4.719	5.45	10.66(1)	6.83(1)	4.87(1)	4.62(1)	4.876(1)
c	8.73	5.893	5.640	4.85	6.08(1)	6.83(1)	7.92(1)	4.88(1)	9.527(1)
α	90.00	90.00	90.00	90.00	90.00	90.00	90.00	121.1(1)	90.00
β	90.00	90.00	90.00	90.00	103.0(3)	90.00	122.7(1)	119.4(1)	122.25(1)
γ	90.00	90.00	90.00	90.00	90.00	90.00	90.00	90.0(1)	90.00
V	212.31	204.65	100.45	95.95	413.01	318.6	156.1	154.9	306.44
Z	4	4	2	2	4	4	2	2	4

Parameter	KCN (Rowe et al., 1983) monoclinic	KCN (Yoshimura, 1989)cubic	KCN[a] (Pople et al., 1978) monoclinic	KCN (Pople et al., 1978) orthorhombic	KCN (Stokes et al., 1993) monoclinic	KCN (Stokes et al., 1993) triclinic	KCN (Decker et al., 1974) monoclinic	KCN (Decker et al., 1974) cubic
T	170	298	163	163	150	110	298	347
p	0.101	0.101	0.101	0.101	365	365	2500	2200
Space group	*Cc*	*Fm3m*	*A2/m*	*Immm*	*C2/c*	$P\bar{1}$	*Cm*	*Pm3m*
a	7.96(1)	6.54(1)	4.61(1)	4.23(1)	7.441(1)	15.882(1)	5.531(2)	3.808(3)
b	4.59(1)	6.54(1)	4.58(1)	5.24(1)	4.595(1)	4.493(1)	5.209(1)	3.808(3)
c	9.18(1)	6.54(1)	7.58(1)	6.15(1)	9.115(1)	9.476(1)	3.743(1)	3.808(3)
α	90.00	90.00	90.00	90.00	90.00	120.55(1)	90.00	90.00
β	125.3(1)	90.00	122.2(1)	90.00	122.14(1)	125.25(1)	85.58	90.00
γ	90.00	90.00	90.00	90.00	90.00	28.37(3)	90.00	90.00
V	273.74	279.73	135.43	136.32	263.89	262.39	107.52	55.22
Z	4	4	2	2	4	4	2	1

[a]Metastable compound.

Crystal structure of lithium cyanide

The crystal structure of LiCN has to be discussed separately because its orthorhombic structure (cell dimensions: a = 3.73 Å; b = 6.52 Å; c = 8.73 Å; space group *Pmcn*) (Lely and Bijvoet, 1942) at ambient temperature and normal pressure is not comparable to the structures of other alkaline cyanides. The unit cell of LiCN contains four molecules. The electron densities of each atom is determined to Li 2.2, C 5.9 and *N* 7.9 which were derived from the electron map, so the lithium atom is ionized as expected and its missing electron is mainly located to the nitrogen atom (Lely and Bijvoet, 1942). In contrast to the eightfold coordination of CsCN and sixfold coordination of NaCN, KCN and RbCN, the lithium atom is fourfold coordinated (Bijvoet and Lely, 2010; Lely and Bijvoet, 1942; Verweel and Bijvoet, 1939). In detail, one carbon atom and three nitrogen atoms, which are located in the corners of an irregular tetrahedron, surround the lithium atom. J. A. Lely and J. M. Bijvoet report that the transition of the coordination can be described by the different sizes of the involved ions. Furthermore, the special polarizability of the anion due to the lithium ion is also important to the asymmetric surrounding of the cyanide group. The weak coordination of the lithium atom and the asymmetric surrounding also cause holes and channels leading to a small density and an unusual low melting point (Table 14) (Greenwood et al., 1988; Lely and Bijvoet, 1942).

Similarities of crystal structures of MCN (M = Na^+, K^+, Rb^+)

At ambient temperature and normal pressure the crystal structure of sodium, potassium and rubidium cyanide is similar to the pseudocubic unit cell of the NaCl-type structure (type I). The position of the aspherical cyanide ions on the positions of the chloride is described by two theories. The dynamic description was first published by P. A. Cooper, supported by quantum mechanical studies of L. Pauling in 1930 and is predicated on free rotation of the cyanide ions (Pauling, 1930). These ions possess no orientation on their lattice site and because of their high molecular movement they are characterized as a spherical rotor with radius of about r = 1.93 Å (Camargo and von der Weid, 1982; Morris, 1961; Sequeira, 1965). The cyanide anion is consequently very similar to the bromide corresponding to many shared properties of alkali metal halides and alkali metal cyanides. But due to the elliptic shape of the cyanide ion, the influence of temperature and pressure to the rotation of the cyanide ion is stronger and the phase diagram is consequently more complex than those of alkali metal bromides (Heckathorn et al., 1999).

The second model of description was established by R. M. Bozorth in 1922 and further discussed by J. Frenkel in 1935 (Bozorth, 1922; Sequeira, 1965). According to this theory, the cyanide anions are statistically spread on the (111)-axis of the lattice. Therefore, free rotation of the $[CN]^-$ seems to be unrealistic due to steric considerations (Durand et al., 1980; Isetti and Neubert, 1957; Yang and Luty, 1989).

In spite of several X-ray structure analyses, neutron diffraction experiments, thermodynamic studies, Raman spectra and NMR spectroscopic measurements a final correlation of the crystal structures to the different models of description is not possible (Atoji, 1971; Bijvoet and Lely, 2010; Coogan and Gutowsky, 1964; Elliott and Hastings, 1961; Messer et al., 1941; Sequeira, 1965; Shimada et al., 1986; Suga et al., 1965; Sugisaki et al., 1968; Verweel and Bijvoet, 1939). M. Atoji carried out several X-ray structure analyses and reported that the cyanide anions are spread on the (111)-axis at temperatures directly above the transition temperature according to the model of J. Frenkel. The deflection turns into the (110)-plane and then into the (100) by increasing temperatures. At the melting point of the compound free rotation is observed, which corresponds to the Pauling model (Atoji, 1971).

The cyanide ion of sodium and potassium cyanide reaches its energetical most favored position on the (100)-axis. Computational studies also indicate a decrease of energy differences as a result of increasing size of the cation, e.g. the energy difference between the [110] and [110] alignment: 22.6 kJ mol^{-1} (NaCN), 10.5 kJ mol^{-1} (KCN) and 5.9 kJ mol^{-1} (RbCN) (LeSar and Gordon, 1982). Theoretical studies of M. Ferrario et al. support the assumption that the degree of [111] orientation raises in correlation to increasing cation radii (Ferrario et al., 1986).

A first order phase transition is observed at temperatures of 288 K (NaCN), 168 K (KCN) and 132 K (RbCN) under normal pressure depending on the size of the cation (Bijvoet and Lely, 2010; Kondo et al., 1979; Shimada et al., 1986; Suga et al., 1965). The cyanides of sodium and potassium are showing [110] orientation in this phase and their dipole moments are still disordered corresponding to changes of entropy during measurements of heat capacities (Matsuo et al., 1968; Suga et al., 1965; Sugisaki et al., 1968). The structural change causes a contraction of one side converting the cubic cell into an orthorhombic cell and ferroelastic order (type A, space group *Immm*) (Suga et al., 1965; Yang and Luty, 1989).

X-ray structure analysis of RbCN indicates a [111] orientation of the cyanide anions in a monoclinic structure and antiferroelastic order (Bourson et al., 1992; Kondo

et al., 1979; Parry, 1962). This structure is also reported in studies of KCN, but in KCN it requires higher pressures or addition of alkali metal halides (Dultz and Krause, 1978; Dultz et al., 1981; Yang and Luty, 1989). In contrast, theoretical studies of R. Le Sar and R. G. Gordon indicates that an orthorhombic structure is energetically preferred by 11.7 kJ mol^{-1}. But due to this small energy difference they do not negate a higher stability of the monoclinic cell at certain temperatures (LeSar and Gordon, 1982). It was shown that a cycle of several heating and cooling of KCN led to a special phenomenon. During such a cycle this compound also shows a monoclinic phase just below the phase transition temperature. Furthermore, this phase occurs in pure form at higher pressures and is similar to the structure of RbCN. But the monoclinic phase can be observed only during the cooling process and not in the heating step (Ortiz-Lopez and Luty, 1988; Parry, 1962; Schmidt et al., 1992). Regarding the first phase transition of NaCN, KCN and RbCN, the phase transition temperature shows linear correlation to the cation size (Scheme 21).

This underlines the similarity of alkali metal cyanides and halides, which are also characterized by strong correlation of crystalline structure and ratio of ion radii r_{cation}: r_{anion} (Biltz, 1935; Kondo et al., 1979). An increase of this coefficient correlates to an enlarged coordination sphere of an eightfold coordination instead of four in both types of alkali metal salts. NaCN and KCN also undergo a second order phase transformation under normal pressure at 172 K (NaCN) respectively 83 K (KCN) (Table 18). This antiferroelastic structure (type B) is characterized by ordered dipoles of cyanide anions and space group *Pmmn* (Kondo et al., 1979; Rowe et al., 1977a, 1977b; Suga et al., 1965; Wasylishen and Jeffrey, 1983). The phase transition temperatures are not determined completely, so the correlation to the cation radius is uncertain.

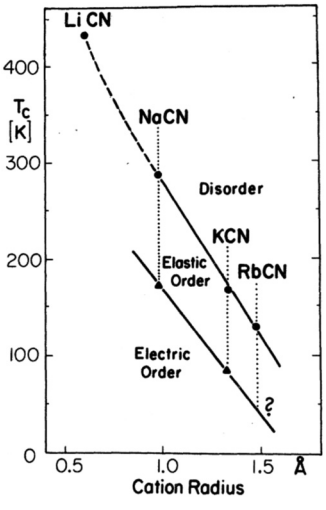

Scheme 21: Temperature of first order phase transition of alkali metal cyanides as a function of cation size (representation taken from Kondo et al., 1979).

The above Scheme 21 also illustrates the missing disordered structure of LiCN. This structure probably occurs at temperatures of about 400 K expecting a continuously linear correlation. But this temperature is very close to the melting point of about 433 K (Table 14), which is completely different from the melting point of other alkali metal cyanides. But this value perfectly fits to the correlation of the second order phase transition of NaCN and KCN (Kondo et al., 1979; Lely and Bijvoet, 1942). In this context Y. Kondo et al. mentioned that the rotation of the cyanide anions of NaCN, KCN and RbCN during the order-disorder transition is similar to the rotation in liquid phase, but their translation resembles a pseudocubic solid structure. In LiCN, the rotation is similar to the sodium, potassium and rubidium compound, but due to strong coupling to the small lithium cation it also shows translational movement, which destabilizes the pseudocubic structure and leads to melting instead of a phase transition (Mokross and Pirc, 1978; Rehwald et al., 1977).

The changes of the crystal structures of NaCN and KCN are represented in Figure 12. The properties are proved by computational calculations, Raman spectra, NMR spectroscopic measurements and neutron diffraction analyses to study the coupling of translation and rotation (Coogan and Gutowsky, 1964; Decker et al., 1974; Durand et al., 1980; Ehrhardt et al., 1980; Elliott and Hastings, 1961; Kondo et al., 1979; Messer et al., 1941; Loidl et al., 1980a; Wasylishen and Jeffrey, 1983).

The neutron diffraction also indicates that the cyanide dipoles of the modification type B (low temperature structure) are ordered parallel in the *a*,*c*-plane and are described by alternative inversion in respect to the *b*-axis (Figure 12) (Rowe et al., 1977b). However, the determination of the carbon and nitrogen positions faces several challenges due to quite similar atomic form factors (in contrast to those of the alkali metal).

Measurements of the heat capacity at temperatures till 14 K and the missing Curie-Weiß behavior reveal no second phase transition of RbCN and CsCN at normal pressure and low temperatures leading to orientation of the cyanide dipoles, which is caused by a “frozen-in state” (Sugisaki et al., 1968). These low temperatures inhibit the collective electric dipole order of induced dipole interaction and fix the orientation of the cyanide groups (Kondo et al., 1979; Sugisaki et al., 1968).

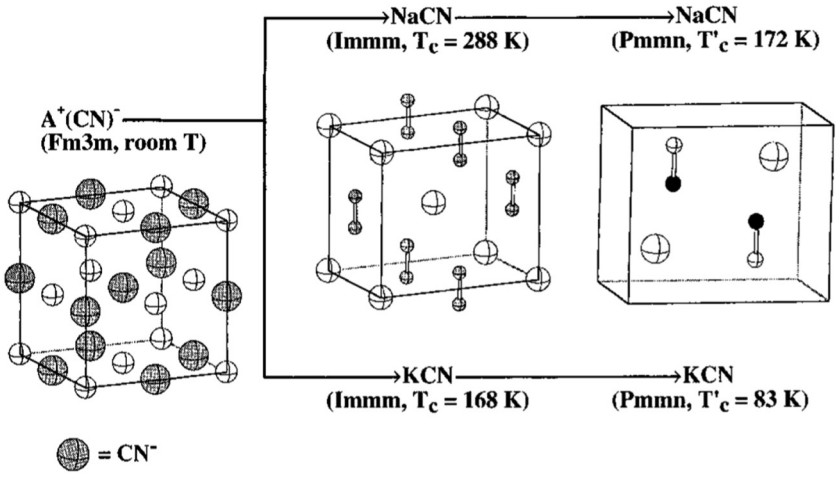

Figure 12: Crystal structures of NaCN and KCN in three different phases (representation taken from Buljan et al., 1997).

Further solid phases of alkali metal cyanides

In addition to already described solid state phases further modifications of alkali metal cyanides appear as a function of temperature and pressure shown in the following phase diagrams. Especially, the phase diagram of KCN is very complex showing many different phases (Figure 13) (Stokes et al., 1993).

The potassium cyanide has a slightly distorted, monoclinic, ferroelectric structure, which is similar to the CsCl-type, with the space group *Cm* at ambient temperature and high pressures (phase IV) (Decker et al., 1974). The cyanide anions are limited in their rotation and the relative volume is decreased of about 10% causing an increase of the coordination sphere to an eightfold coordination of the cation (Strössner et al., 1985). An additional increase of temperature leads to the phase III characterized by a cubic unit cell and space group $Pm\bar{3}m$. The cyanide anions are disordered in respect to reorientation with nearly spherical symmetry and coordinated eightfold. Phase C is supposed to be monoclinic ($C2/c$) and similar to phase A, the cyanide anions are ordered in relation to the direction of the C–N bond, but disordered head to tail (Stokes et al., 1993). Due to a shear strain of the *b*-axis one part of the crystal shows a tilt in one direction, the other part in the opposite direction, which, however, leads to a monoclinic structure in average. The decrease of temperature causes another phase transition to D, in which the cyanide anions are collocated in mirror planes and disordered with respect to the position of carbon and nitrogen atom. In contrast to the transition of phase A to B, the reorientation of the cyanide anions is hindered. As in phase C, a shear strain is also observed in phase D, but both parts are not equal, which leads to a monoclinic structure with space group $C2/m$ of phase D containing a triclinic fraction (Stokes et al., 1993).

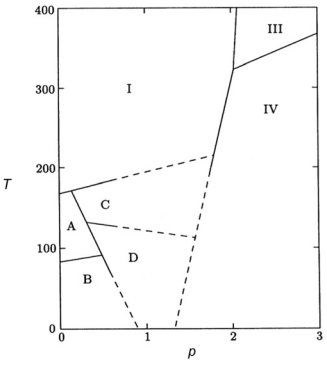

Figure 13: Phase diagram of KCN (*p* in GPa, *T* in K, representation taken from Stokes et al., 1993).

The phase diagram of NaCN also reveals a high-pressure structure IVa, which is quite similar to phase IV of KCN but with space group *Pm* (Figure 14). The decrease of pressure also leads to an antiferroelectric ordered phase B. The characterization of the coexistent region D between the ferroelectric ordered phase IVa and the phase B is as difficult as in KCN (Strössner et al., 1985).

The increase of pressure leads to a further phase transition of RbCN from the pseudocubic NaCl structure (phase I) to phase III, which is similar to the CsCl-type, causing a decrease of the volume of about 10% to the eightfold coordination. At pressures of about 1.8 GPa a second phase transition takes place. The observed monoclinic phase IV is quite similar to that phase of KCN (Strössner et al., 1985).

Crystal structure of cesium cyanide

At ambient temperatures cesium cyanide crystallizes in the pseudocubic CsCl-type structure (phase III), which is only

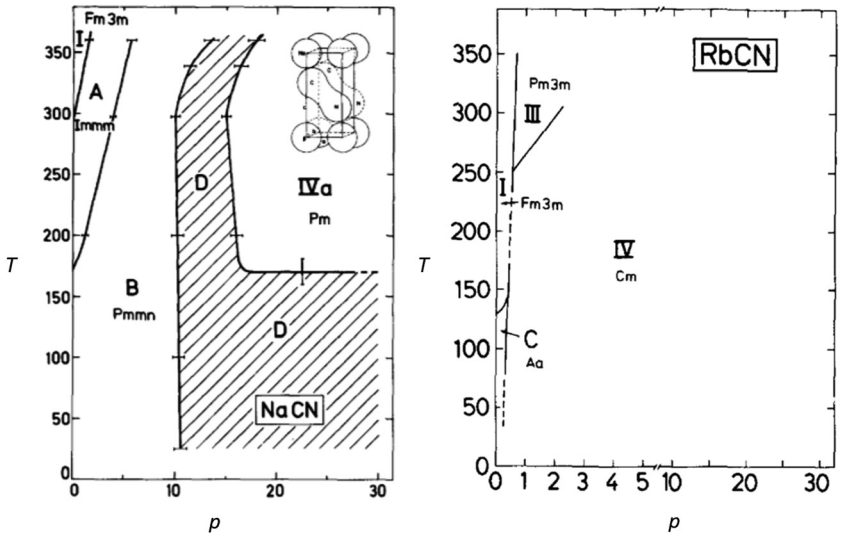

Figure 14: Phase diagram of NaCN and RbCN (*T* in K; *p* in GPa; representation taken from Strössner et al., 1985).

formed by other alkali metal cyanides at high pressures (Figure 15). The cyanide anions are orientationally disordered. At about 186 K a phase transition to the rhombohedral structure (phase VII) takes place and each unit cell contains one molecule (Daubert et al., 1976; Knopp et al., 1983; Sugisaki et al., 1968). The axes of the cyanide anions are aligned to the cubic (Borron et al., 2007) direction extending this axis (Loidl et al., 1980b, 1983; Sugisaki et al., 1968). The phase transition from III to VII is not connected to a decrease of the volume and the eightfold coordination is preserved (Strössner et al., 1985).

In summary, the alkali metal cyanides have many similar crystalline phases as a function of temperature and pressure. The phase boundaries differ due to the increasing size of the cation, e.g. the phase boundary is moved to lower pressure by increasing radii. After all, W. Dultz and H. Krause and also K. Strössner et al. provided a phase diagram including all shared phases (Figure 16) (Dultz and Krause, 1978; Strössner et al., 1985).

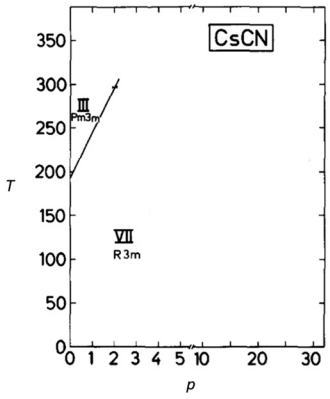

Figure 15: Phase diagram of CsCN (*T* in K, *p* in GPa, representation taken from Strössner et al., 1985).

M–CN/M–NC-isomerization – gas phase structure

The alkali metal cyanides are among the best studied metal cyanides. Experimental data and *ab initio* calculations reveal consistently high ionic character and a low potential energy surface causing simple transformations of these compounds. Overall, three different isomers of metal cyanides are discussed: the linear cyanide structure M–CN, the linear isocyanide structure M–NC and a T-shaped form M[CN] (dihapto, η^2). In contrast to the mono-coordinated (monohapto, η^1) metal cation of the first two structures, the cation of the T-shaped structure features bi-coordination (Figure 17) (Lee et al., 2007). In the solid state, of course due to a higher coordination number, both M–CN as well as M–NC coordination are found, e.g. in an M–CN–M arrangement, and all isomers were studied in the gas phase.

With the exception of LiCN, all other alkali metal cyanides feature the triangular η^2-bonded isomer as the lowest lying species in the gas phase (Table 19) (Bak et al., 1970; Clementi et al., 1973; Essers et al., 1982; Lee et al., 2007; Makarewicz and Ha, 1995; Redmon et al., 1980; Schmiedekamp et al., 1980; van Vaals et al., 1983). In the triangular complexes, the M–N distance is much shorter than the M–C distance. The potential barrier connecting the triangular form and the linear cyanide form decreases along the series Li → Fr. As shown in Table 19, these results highly depend on the chosen methods and the basis sets,

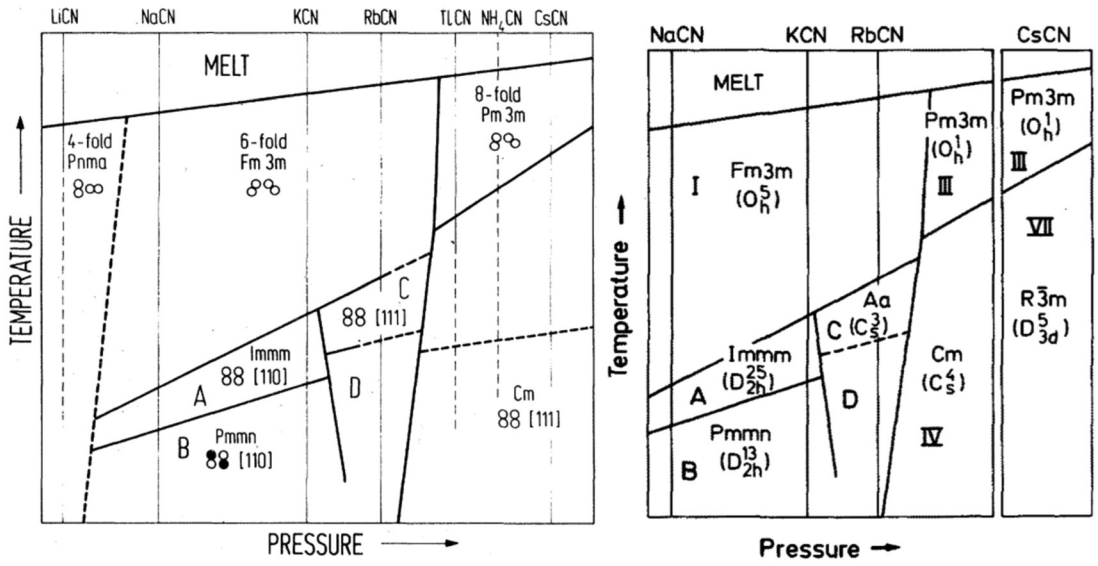

Figure 16: Phase diagrams of alkali metal cyanides (representations taken from Dultz and Krause, 1978; Strössner et al., 1985).

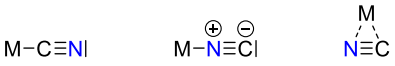

Figure 17: Different isomers of alkali metal cyanides: Linear cyanide, linear isocyanide and T-shaped structure.

Table 19: Computed relative energies of MCN isomers and their transition states (TS) (in kJ mol^{-1}) (Lee et al., 2007).

Atom	Method	MCN (linear)	TS1	M[CN] (η^2)	TS2	MNC (linear)
Li	HF	25.3	39.2	–	–	0
	CCSD	10.4	22.9	0.4	3.4	0
	CCSD(T)	8.8	20.6	0.1	2.9	0
	MRCI-1	4.5	–	–	–	0
	MRCI-2	1.3	–	0	–	3.2[a]
	MP2-4	6.9	–	1.2	–	0
Na	HF	16.8	22.5	0	2.5	2.2
	CCSD(T)	10.1	15.8	0	11.2	11.1
	MRCI	6.7	–	0	–	11.5
K	HF	21.6	22.7	0	–	4.1[a]
	CCSD(T)	18.3	19.3	0	–	13.0[a]
Rb	HF	21.6	22.2	0	–	22.2[a]
	CCSD(T)	18.3	18.8	0	–	12.5[a]
Cs	HF	22.0	22.1	0	–	3.9[a]
	CCSD(T)	18.6	18.8	0	–	11.3[a]
Fr	HF	21.4	21.5	0	–	4.1[a]
	CCSD(T)	18.5	18.5	0	–	11.9[a]

[a]Saddle point.

respectively (Bak et al., 1970; Clementi et al., 1973; Essers et al., 1982; Lee et al., 2007; Makarewicz and Ha, 1995; Redmon et al., 1980; Schmiedekamp et al., 1980; van Vaals et al., 1983). In the crystal structure the lithium favours the coordination to the nitrogen (ratio 3:1) supporting the higher stability of the isocyanide structure. Also experimental rotational and hyperfine spectra from J. J. van Vaals et al. and IR spectra from Z. K. Ismail et al. show the best agreement to the isocyanide structure (Ismail et al., 1972; van Vaals et al., 1983).

Including the effects of correlation in calculations the energy difference of the cyanide and isocyanide structure decreases due to higher stabilisation of the cyanide by correlation (Redmon et al., 1980). While this long-range energy in regard to Coulomb's law prefers the cyanide structure, the triangular structure is favoured by short range repulsion, which leads to the isocyanide structure as a compromise (Essers et al., 1982). The migration of the lithium cation from the carbon to the nitrogen end of the cyanide anion is correlated to a small energy barrier of about 10.6–14.3 kJ mol^{-1} due to high electron affinity of the cyanide anion and small ionization potential of the alkali metal leading to a ionic structure with dominating Coulomb force, which is isotropic and facilitates the shift of the lithium (Essers et al., 1982; Rao et al., 1996). This circling motion around the anion is also called "polytopic" (Rao et al., 1996). Due to low energy barriers, the isomerization of all alkali metal cyanides reveals polytopic character (van Vaals et al., 1984b).

In contrast P. v. R. Schleyer et al. prefer a T-shaped structure of LiCN as the most stable based on MP2/6-31G* computations (von Ragué Schleyer et al., 1986). Therefore, B. S. Jursic carried out several studies on suitable basis sets

indicating that the T-shaped configuration is slightly more unstable than the isocyanide one, but more stable than the structure of lithium cyanide (Jursic, 1998). The experimental proof of the T-shaped structure is still missing, which could be caused by the small dipole moment of 7.3 D. It should also lead to a hindered detection using rotational and hyperfine spectra. In contrast, the dipole moment of lithium isocyanide is 8.9 D and the dipole moment of lithium cyanide is 9.8 D (von Ragué Schleyer et al., 1986).

In contrast to the lithium compound, the minimum of the T-shaped configuration of NaCN and KCN can be located easily on the potential energy surface due to strong exchange interactions and a negative charge, which is mainly located in an s-type orbital of the cyanide anion (Essers et al., 1982; Greetham and Ellis, 2000; Lee et al., 2007). But the relative energies of different alkali metal cyanide isomers and their transition states also confirm, that the isocyanide structures of potassium and heavier alkali metals are just transition states and that the M–CN bond energy decreases from Li to K (Table 19) (Lee et al., 2006; Wormer and Tennyson, 1981).

Furthermore, the correlation effect leads to an increase of the M–N and C–N bond lengths and a contraction of the M–C bond of triangular isomers (Table 20). On the other hand, it causes an increase of the C–N bond length and a decrease of the M–C bond length of linear MCN isomers (Table 21). One reason might be a decrease of steric repulsion from the nonbonding electron pair of the carbon atom due to the electron correlation (Lee et al., 2007).

Table 20: Experimental and computational structural data of triangular (η^2) M[CN] compounds (bond lengths in Å) (Lee et al., 2007).

Atom	Method	r_{M-C}	r_{M-N}	r_{C-N}
Li	CCSD(T)	2.13	1.85	1.18
	MRCI-2	2.09	1.86	1.17
	Exp.[a] (van Vaals et al., 1983)	–	1.760	1.168
Na	CCSD(T)	2.39	2.23	1.18
	MRCI	2.72	2.26	1.17
	Exp. (van Vaals et al., 1984a)	2.38	2.23	1.17
K	CCSD(T)	2.73	2.55	1.18
	MRCI	2.86	2.59	1.17
	Exp. (van Vaals et al., 1984b)	2.72	2.55	1.17
Rb	CCSD(T)	2.86	2.68	1.18
Cs	CCSD(T)	3.03	2.82	1.18
Fr	CCSD(T)	3.09	2.89	1.18

[a]Supposedly LiNC linear.

Table 21: Computed structural data of linear (η^1) MCN compounds (bond lengths in Å) (Lee et al., 2007).

Atom	Method	r_{M-C}	r_{C-N}
Li	CCSD(T)	1.92	1.17
	MRCI	1.92	1.17
Na	CCSD(T)	2.25	1.17
	MRCI	2.91	1.17
K	CCSD(T)	2.60	1.17
Rb	CCSD(T)	2.73	1.17
Cs	CCSD(T)	2.88	1.17
Fr	CCSD(T)	2.94	1.17

$[M(CN)_2]^-$ anions

Super(pseudo)halogen anions $[M(CN)_2]^-$ ($M = Na^+, Li^+$)

The term "superhalogen" was established by G. L. Gutsev and A. I. Boldyrev in 1981 and names complexes of the structure $[MX_{k+1}]^-$ containing a metal M and electronegative fragments X of normal valence (Gutsev and Boldyrev, 1981). The index k indicates the normal valence of the metal atom, e.g. $[BF_4]^-$ and $[AlF_4]^-$. The electron affinity of these complexes of about 5.0 eV is higher than the electron affinity of chlorine (Behera and Jena, 2012; Sidorov, 1977). Only recently, a superhalogen $F@C_{20}(CN)_{20}$ with electron affinity of 10.8 eV was designed (Kulsha and Sharapa, 2019). Usually, a superhalogen is a molecule with high electron affinity, which forms a stable anion, and have low proton affinities leading to superacids.

The lithium and sodium compounds of the structure $[M(CN)_2]^-$ were studied by S. Smuczyńska and P. Skurski using *ab initio* methods (MP2/6-311 + G(d)). Their main goal was the utilization of pseudohalides to form novel superhalogen anions. In addition to the calculation of the dicyanide anion $[M(CN)_2]^-$, they compared this structure to the isocyanide form $[M(NC)_2]^-$. All compounds feature $D_{\infty h}$ symmetry and the bond length of the carbon and nitrogen atoms are in a range of 1.188–1.192 Å. For all species, a bond between the metal atom and the cyanide respectively isocyanide group was found (Behera and Jena, 2012; Smuczyńska and Skurski, 2009).

Calculations of the vertical electron detachment energy (VDE) also reveal a stronger bond of the lithium to the isocyanide group $[Li(NC)_2]^-$ (VDE = 7.434 eV) than to the cyanide group (VDE = 7.233 eV), which correlates to the bond length of 1.900 Å for the Li–N bond, respectively 2.043 Å for the Li–C bond. Although, the VDE of the sodium isomers are considerably smaller ($[Na(CN)_2]^-$: 7.090 eV,

$[Na(CN)_2]^-$: 5.871 eV) they are also called superhalogen anions (Smuczyńska and Skurski, 2009).

To continue the studies of the superhalogens with cyanide ligands and their properties, S. Behera and P. Jena carried out calculations of the electron affinity as a function of the number of bonded cyanide ligands and neutral or single and double negative charged complexes, e.g. $[Na(CN)_n]^{x-}$ with $n \leq 3$ and $x \leq 2$. Focusing on neutral species, they report the NaNC to be the most stable one, while $Na(CN)_2$ and $Na(CN)_3$ tend to form cyanogen $(CN)_2$ by dimerization of two cyanide anions (Figure 18). Due to the fact that the negative charge of superhalogens is mainly located at the electronegative ligand, they named sodium complexes of the type $[Na(CN)_n]$ (with $n = 2$) super(pseudo) halogens (Behera and Jena, 2012).

2nd Main group

For a long period of time the scientific interest mainly focussed on hydrogen cyanide and the well-known alkali metal cyanides. However, since the observation of alkaline earth cyanides in interstellar matter the increasing interest in these compounds caused several recent studies focusing on computations to analyse experimental spectra. Furthermore, the synthesis of pure alkaline earth cyanides is quite difficult compared to the alkaline mono cyanides, e.g. the crystallization of the barium and strontium compound using an aqueous solution is difficult and the isolation of the magnesium and calcium compound by re-crystallization from heated aqueous solutions is not possible. In contrast to alkali cyanides, which are part of several applications, the salts of alkaline earth cyanides tend to fast decomposition and formation of hydrogen cyanide due to displacement of the weak acid by carbon dioxide or weak organic acids from their solution (Williams, 1915). But they are mostly stable in presence of an inert gas atmosphere or ammonia solution (Franck and Freitag, 1926). As a consequence of these problems (decomposition and difficult isolation), the physical properties of these compounds are still mainly unknown. Only a very broad melting point of calcium cyanide $Ca(CN)_2$ at about (913 ± 30) K by extrapolation and incipient decomposition at temperatures above 623 K are reported (Petersen and Franck, 1938). Moreover, also the number of reported IR spectroscopic data is highly limited (Table 22).

Table 22: IR data of different alkaline earth dicyanides (wave numbers in cm^{-1}).

Compound	ν_{CN}	ν_{MC}
$Be(CN)_2$ (Williams et al., 2001)	2233	756
$Mg(CN)_2$ (Williams et al., 2001)	2197	492
$Ca(CN)_2$ (Loupy and Corset, 1976)	2068, 2084[a]	–
$Ba(CN)_2$	2058, 2075, 2088[a] (Loupy and Corset, 1976)	461, 610, 645 (Miller et al., 1960)

[a]Measurement in DMF.

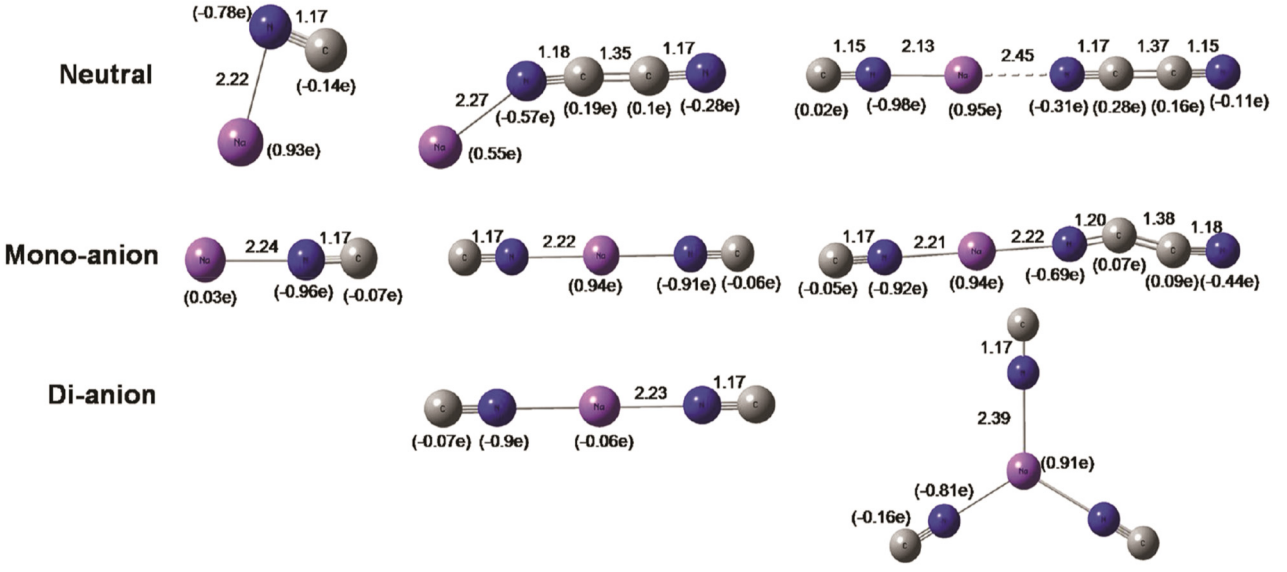

Figure 18: Optimized structures of neutral, single negative and double negative charged $Na(CN)_n/Na(NC)_n$ complexes (B3LYP/6–311++G(3df); Na – purple; N – blue; C – grey; partial charges in parentheses; representation taken from Behera and Jena, 2012).

Alkaline earth monocyanides MCN

The first spectroscopic observation of monocyanides was reported by L. Pasternack and P. J. Dagdigian in 1976. Laser-induced fluorescence measurements of reactions of cyanogen bromide and metals M = Ca^{2+}, Sr^{2+}, and Ba^{2+} led to very broad bands, which were very similar to the fundamentals of monohalogens and could be allocated to the monocyanides (Pasternack and Dagdigian, 1976). In 1984, additional computations of MCN, where M = Be^{2+}, Mg^{2+}, Ca^{2+}, and Ba^{2+}, carried out by C. W. Bauschlicher and S. R. Langhoff, indicated that L. Pasternack and P. J. Dagdigian observed the isocyanide instead of the cyanide isomers. In contrast to the alkali cyanides, the alkaline earth cyanides mainly prefer a linear isocyanide structure in the $^2\Sigma^+$ ground state lying 0.3 – 0.5 eV below the energy of the cyanide isomer, which enables a differentiation of both isomers (Table 23). The interconversion barrier from MNC to MCN decreases, e.g. the BeNC and MgNC have a barrier of 0.71 and 0.23 eV, respectively, CaCN and BaCN have no barrier at all, as a consequence of an increased ionic character of the compounds (Bauschlicher et al., 1985; Lanzisera and Andrews, 1997a; Mikhailov et al., 2003).

In a reaction of laser-ablated beryllium with hydrogen cyanide, different cyanide and isocyanide compounds of beryllium could be observed and matrix IR spectra were compared to calculated fundamentals using DFT computations (BP86/6-311G*). FTIR spectroscopic measurements of reactions of hydrogen cyanide and laser-ablated beryllium at 6–7 K support this suggestion. In the end, the beryllium isocyanide is the most stable isomer with the cyanide structure lying 15.5 kJ mol^{-1} higher in energy and no stable T-shaped structure (Lanzisera and Andrews, 1997a).

Further experimental and theoretical studies indicate that not only compounds in the electronic ground state show strong ionic bonding and a linear structure, but also MgNC and CaNC are linear in the energetic minimum of the excited state (Anderson et al., 1994; Steimle et al., 1992, 1994; Whitham et al., 1990). Supplementary molecular orbital calculations (ROHF/TZ2P and SDCI + Q/TZ2P) of the three atoms Mg, C and N were carried out by T. Hirano and co-workers identifying three stationary points: the two linear structures MgCN and MgNC and also a cyclic intermediate with Mg closer to the carbon atom, which is already known from alkali cyanides (Table 24, Figure 19) (Ishii et al., 1993, 1994). These calculations were carried out due to previous observations of the magnesium isocyanide in the circumstellar shell of IRC + 10,216 and were in accordance with experimental data from microwave spectroscopic (MW) measurements (Kawaguchi et al., 1993).

The properties of the molecular orbitals of the $[C{\equiv}N]^-$ anion are quite similar to those of the cyano radical (Figure 3) and the SOMO is similarly located at the magnesium atom (Ishii et al., 1993). Overall, the structure is described as an ionic molecule with an oriented $Mg^{\delta+}$ next to a cyano radical $[{\cdot}C{\equiv}N{:}]^{\delta-}$ leading to a very small isomerization barrier of 2170–2230 cm^{-1} (Ishii et al., 1994).

Removing one single electron from the magnesium leads to the $[MgCN]^+$ cation, which has also a cyclic, T-shaped isomer lying 7.5 kJ mol^{-1}, respectively 12.6 kJ mol^{-1} below the two linear isomers $[MgCN]^+$, respectively $[MgNC]^+$, displaying similarities to the isoelectronic structure of the NaCN (MP2/6-31G*) (Barrientos and Largo, 1995; Petrie, 1996). The stability of the cyclic structure is a consequence of orbital interaction. Three molecular orbitals are formed of the atomic orbitals of magnesium, carbon and nitrogen and only the lowest molecular orbital is completely occupied. In comparison to the neutral MgCN, the additional half occupied orbital causes an energetic preference of the linear structure (Barrientos and Largo, 1995).

Another T-shaped configuration, which is known from potassium and sodium cyanide, is not known of alkaline earth cyanides due to the strong Coulomb interaction of the metal cation and the cyanide anion, which achieves a maximum for a linear structure (Mikhailov et al., 2003). The same effect influences the structure of SrNC, which was

Table 23: Computed energies (in eV) of alkaline earth monocyanide isomers (calculations at SCF/TZ2P) (Bauschlicher et al., 1985).

Compound	MNC	[M(CN)]	MCN	Found
BeCN	4.10	3.17	3.62	4.46 ± 0.29
MgCN	3.36	3.00	3.07	4.21 ± 0.26
CaCN	4.12	3.88	3.78	4.46 ± 0.22
BaCN	4.34	4.17	4.02	4.87 ± 0.26

Table 24: Computed structural data of alkaline earth monocyanide isomers (bond lengths in Å; calculations at SCF/TZ2P, only SrCN at B3LYP/DGDZVP).

Compound	MCN		MNC	
	r_{M-N}	r_{C-N}	r_{M-C}	r_{C-N}
BeCN (Bauschlicher et al., 1985)	1.529	1.159	1.693	1.132
MgCN (Bauschlicher et al., 1985)	1.931	1.154	2.090	1.138
CaCN (Bauschlicher et al., 1985)	2.233	1.154	2.418	1.138
SrCN (Chan and Hamilton, 1998)	2.350	1.188	2.512	1.175
BaCN (Bauschlicher et al., 1985)	2.551	1.154	2.741	1.143

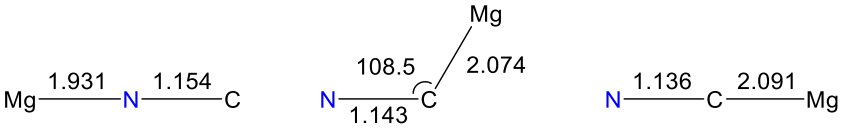

Figure 19: Computed structural data of the linear isocyanide and cyanide isomer and their intermediate (bond lengths in Å; angle in °, at ROHF/TZ2P) (Ishii et al., 1993).

studied using low-resolution laser excitation fluorescence spectroscopy (Douay and Bernath, 1990).

The reaction coordinate of the isomerization of CaNC and CaCN was calculated by T. Taketsugu and co-workers in 2003. Starting with the isocyanide isomer the activation barrier is 25.25 and 7.20 kJ mol^{-1} from the cyanide side (Figure 20) (Ishii et al., 2003).

Alkaline earth dicyanides $M(CN)_2$

Structure of alkaline earth dicyanides

In comparison to the cyanide compounds of the alkaline metals, the alkaline earth dicyanides are less investigated. P. v. R. Schleyer et al. calculated potential energy surfaces of different compounds of the type MC_2N_2 using the Hartree–Fock method and also the MP-perturbation theory (MP2) to analyse the global minima structures of $M(CN)_2$ with M = Be^{2+}, Mg^{2+}, Ca^{2+}, Sr^{2+}, and Ba^{2+} extending the calculations of J. Gardner et al. on magnesium species to all alkaline earth metals. In this context, the linear structure of some magnesium species could not be transferred to the later elements (Gardner et al., 1993; Kapp and Schleyer, 1996).

Starting with three different basic linear structures, the metal cation was coordinated by both carbon atoms (CC), by both nitrogen atoms (NN) or by one carbon and one nitrogen atom of the two different cyanide anions (Figure 21).

The considered linear structures of Ba and Sr are just second-order saddle points, but using HF methods the bent *end-on*-isomers (*CC-2*, *NN-2*, *CN-2*) are structural minima and using the MP2 level only structure *CC-2* is a minimum. In accordance to the other isomers *NN-2* and *CN-2*, the most stable structures are the side-on isomers *BB-4* and *CB-4*, but with small energy differences to the linear ones. P. v. R. Schleyer and J. Kapp summarized that compounds coordinated via nitrogen atoms are more stable than those coordinated via carbon atoms (energies of each favoured N coordination: BaC_2N_2 – 11.7 kJ mol^{-1} and SrC_2N_2 – 9.6 kJ mol^{-1}) and the most stable isomers are showing a *side-on* coordination of the cyanide anion. Calculating the potential energy surfaces of calcium and magnesium dicyanides using HF method and MP2 method, the minima structures are indeed linear isomers. Although bent structures are not existing (*NN-2*, *CN-2*, *CC-2*) with optimizations leading to the linear isomers, some *side-on* coordinated structures could be optimized by MP2, for example *BB-3* and *CB-3* are minimum structures with small energy

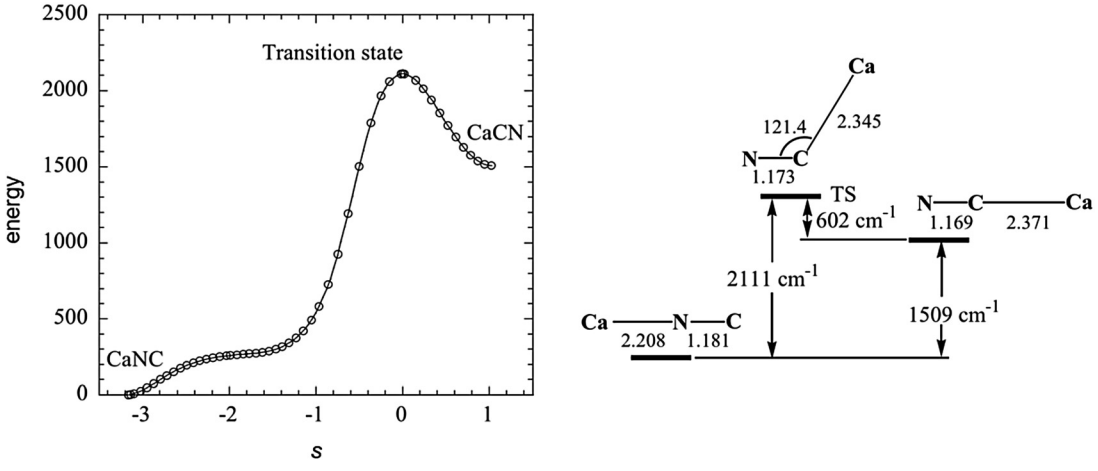

Figure 20: Energy profile of the isomerization reaction of CaCN (energy in cm^{-1}, reaction coordinate s in bohr $amu^{1/2}$) and activation barriers of the isomerization including bond lengths (in Å) and bond angles (in °) of the isomers (representations taken from Ishii et al., 2003).

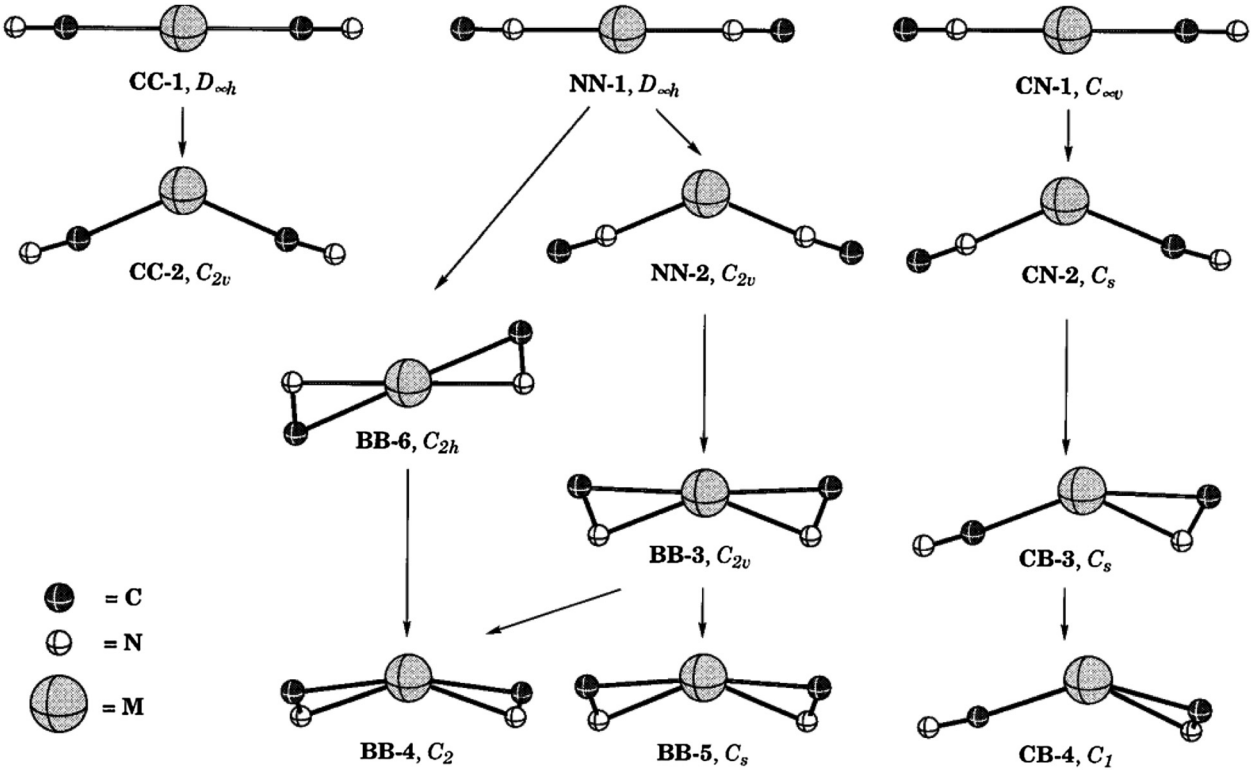

Figure 21: Considered geometries and connections of structures MC_2N_2 (representation taken from Kapp and Schleyer, 1996).

differences of the *side-on* isomers. Furthermore, the potential energy surface of the $Mg(CN)_2$ is very flat, so its behavior extremely depends on the basis set and chosen method (Gardner et al., 1993; Petrie, 1999a). For example, using the MP2(full)/6-31G* method the NC–Mg–CN dicyanide is a global minimum structure and the other linear structures are also identified as energetic minima, which are linked by π-complexes (Petrie, 1999a). On that method, these π-complexes are characterized as minima on the energy surface, but calculations on G2-or CBS-Q level suggest that these π-complexes are just transition states upon the potential energy surface and that the dicyanides coordinated via the nitrogen atom (CN–Mg–NC) is the most stable one. The difference of energy between this minimum structure and the highest transition state is only 30 kJ mol^{-1}. The calcium compound is very similar to the Sr and Ba compounds. The energy of the nitrogen dicoordinated isomer is smaller of about 8.8 kJ mol^{-1} for each cyanide anion than the other two linear isomers, but the structure *BB-3* of $Ca(CN)_2$ is most stable by about 18.4 kJ mol^{-1}. The minima of the energy surface of the smallest dicyanide BeC_2N_2 are only linear structures including the diisocyanide as the most stable one.

Synthesis of alkaline earth dicyanides

Synthesis of $M(CN)_2$ ($M = Be^{2+}$, Mg^{2+})

The beryllium dicyanide is formed by dimethylberyllium and an excess of hydrogen cyanide in benzene or other inert solvents. It is also reported that it is insoluble in solvents other than those which cause hydrolysis. The suggestion of a four times coordinated product was disproved by calculations, which were discussed in the chapter above (Coates and Mukherjee, 1963).

In anhydrous conditions, metal chloride and trimethylsilyl cyanide (TMS–CN) are used to synthesize beryllium and magnesium dicyanide. After addition of TMS–CN to the stirred solution of beryllium dichloride in butyl ether at 253 K the resulting solution is stirred at ambient temperatures for 18 h and additional 12 h at 373 K. The solid product is separated by filtration, dried *in vacuo* and tempered at 773 K for two days. The synthesis of the magnesium compound requires two steps. First, one equivalent of magnesium dichloride is mixed with two equivalents of TMS–CN at ambient temperature and heated under reflux for 18 h. The product is similarly separated by filtration and

dried *in vacuo*. Then two equivalents of TMS–CN are added and the mixture is heated to 473 K for 12 h under nitrogen atmosphere. After tempering the product for 4 h at 648 K, the dicyanide is obtained in a yield of 63% (Williams et al., 2001).

F. Fichter and R. Suter also described a synthesis of magnesium dicyanide using metallic magnesium and a solution of hydrogen cyanide (10–25%). The clear solution rapidly decomposes forming magnesium hydroxide (Fichter and Schölly, 1920; Fichter and Richard, 1922). Therefore, they question the synthesis of O. Schulz (1856a), who reported a high stability of magnesium dicyanide. And the reaction of dry magnesium hydroxide with etheric hydrocyanic acid to form magnesium dicyanide requires small amounts of water, which supports the rapid decomposition of the dicyanide to form the dihydroxide (Fichter and Richard, 1922).

Synthesis of $M(CN)_2$ ($M = Ca^{2+}$, Sr^{2+}, Ba^{2+})

The barium and calcium dicyanide are synthesized in a classic neutralization reaction using the metal hydroxide and hydrocyanic acid (Scheme 22) (Williams, 1915).

Although the solid product cannot be isolated from an aqueous solution due to fast decomposition and the solution can only be concentrated up to 35%, which also increases polymerization (Franck and Freitag, 1926). In 1915 H. E. Williams already remarked, that crystals of the magnesium and calcium dicyanides cannot be obtained by removing the solvent of the aqueous solutions (Williams, 1915). And the decomposition of dissolved dicyanides of concentrations higher than 15% is already very fast and depends on the concentration. Oligomers of hydrogen cyanide and ammonium cyanide are formed, which cause the brown color. But solutions of dicyanides are also sensitive to heat and decompose to hydrogen cyanide and metal hydroxide.

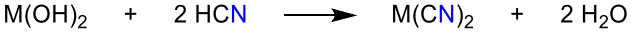

Scheme 22: Syntheses of barium and calcium dicyanide ($M = Ba^{2+}$, Ca^{2+}) (Williams, 1915).

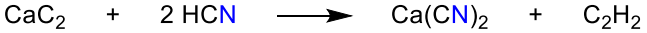

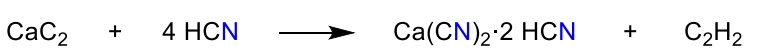

Scheme 23: Synthesis of the hydrogen cyanide adduct instead of the dicyanide (Metzger, 1926).

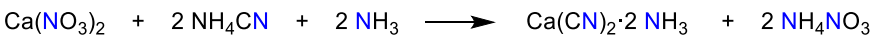

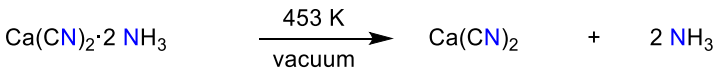

Scheme 24: Synthesis of calcium dicyanide using ammonia solvate complexes (Franck and Freitag, 1926).

The barium dicyanide is obtained as its dihydrate from aqueous solution. By drying at 348 and 373 K the water molecules can be removed (Joannis, 1882a).

In 1926 F. J. Metzger reported another synthesis starting with calcium carbide and addition of hydrogen cyanide under nearly anhydrous conditions. Due to the relatively slow reaction he reported an acceleration of the reaction by addition of 2% water to form the calcium hydroxide *in situ*, which should directly react with the added hydrogen cyanide. However, it was formed a hydrogen cyanide adduct $Ca(CN)_2 \cdot 2HCN$ he could not isolate (Scheme 23) (Metzger, 1926).

H. H. Franck and C. Freitag also reported that the product is a mixture of up to 55% $Ca(CN)_2$ and 25% hydrogen cyanide. Nevertheless, they tried to obtain pure calcium dicyanide from the colorless, powdery diammonia complex, which was synthesized using calcium and a solution of ammonium cyanide or salts of calcium, for example $Ca(NO_3)_2$, and cyanides as NH_4CN or AgCN. The ammonia can be removed by heating up to 453 K *in vacuo* leading to calcium cyanide in nearly quantitative yields (Scheme 24) (Franck and Freitag, 1926).

At temperatures higher than 623 K the kinetic stabilized calcium dicyanide decomposes to calcium cyanamide and carbon in an exothermic reaction. If the temperature is strongly increased, the equilibrium will be shifted towards the calcium dicyanide (Scheme 25) (Petersen and Franck, 1938).

So the calcium dicyanide can also be obtained by tempering of calcium cyanamide up to 1523 K and fast quenching of the equilibrium to about 573 K (Petersen and Franck, 1938). Such an equilibrium is also known of barium dicyanide, but the temperature range of 500–900 K is much smaller. This equilibrium is part of the reaction of barium carbide and nitrogen and leads to the formation of

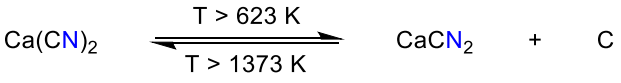

Scheme 25: Temperature depending equilibrium of calcium dicyanide and calcium cyanamide (Petersen and Franck, 1938).

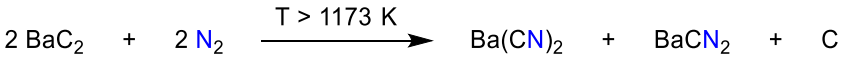

Scheme 26: Formation of barium cyanamide and dicyanide starting with barium carbide (Neubner, 1934; Petersen and Franck, 1938).

the cyanamide at lower temperatures of about 773 K and the formation of the dicyanide at higher temperatures (T > 1173 K) in yields of about 82.5% (Scheme 26) (Neubner, 1934; Petersen and Franck, 1938).

Another synthetic route of alkaline earth dicyanides starts with earth alkaline ferrocyanides. For example, the strontium cyanide is obtained after thermal treatment of strontium ferrocyanide under exclusion of air (Scheme 27) (Schulz, 1856b).

To obtain magnesium, calcium or barium dicyanides, it is also possible to start with an anhydrous double salt mixture of potassium ferrocyanide and calcium chloride or magnesia, which is heated to red heat to form the earth alkaline cyanide and then isolated. The stability of the formed earth alkaline cyanides decreases along $Mg(CN)_2 \rightarrow Ba(CN)_2$ and they cannot be stored in solid state for a long time.

Synthesis of $Ra(CN)_2$

Actually, there is no synthetic route reported to obtain pure radium dicyanide, but the free reaction enthalpy $\Delta_f H°_{298\ K}$ has been estimated to be about (–217 ± 62) kJ mol^{-1} on the basis of data of the other earth alkaline dicyanides (Wilcox and Bromley, 1963).

Established crystal structures of alkaline earth cyanides

Crystal structures of earth alkaline cyanides are merely known of beryllium and magnesium cyanide. Both structures show a cubic unit cell, further crystallographic data and some atomic distances are given in Table 25. The metal cations are coordinated tetrahedrally by four cyanide anions, which show strong disorder, and the tetrahedra are linked at their vertices (Williams et al., 2001). The literature also offers powder diffraction data of calcium dicyanide of the year 1938, but further analyses of its crystal structure are not published (Hanawalt et al., 1938). The data of strontium dicyanide are also rare. There is only one rudimentary description of its orthorhombic tetrahydrate by A. Joannis from 1882 (Joannis, 1882b).

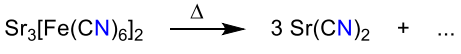

Scheme 27: Synthesis of strontium dicyanide starting with strontium ferrocyanide (Schulz, 1856b).

Table 25: Crystallographic data of beryllium and magnesium dicyanide (temperatures in K; lengths in Å; angles in °; volumes in Å^3, bond lengths in Å) (Williams et al., 2001).

Parameter	$Be(CN)_2$ cubic	$Mg(CN)_2$ cubic
T	298	298
Space group	$Pn\bar{3}m$	$Pn\bar{3}m$
a	5.339(1)	6.122(1)
α	90.00	90.00
V	151.2(1)	229.45(1)
Z	2	2
r_{C-N}	1.187(1)	1.085(7)
r_{M-CN}	1.718(1)	2.108(4)

Further cyanide compounds of the 2nd main group

Calcium monocyanide cation $[CaCN]^+$

The calcium cyanide cation is isoelectronic with potassium cyanide and displays some similar properties. For example, the T-shaped π-complexes T–$[MCN]^{n+}$ are global minima on the potential energy surface. The linear isomers $[CaCN]^+$ and $[CaNC]^+$ are also minima at the MP2(full)/6-31G* level and identified as second order saddle points by the G2(QCI) procedure. There are also similarities to the T-shaped structures NaCN and MgCN (Petrie, 1999b). The dissociation energy of this cation has been calculated by C. W. Bauschlicher and H. Patridge to be 228.2 kJ mol^{-1} on SCF(TZ2P) and 268.0 kJ mol^{-1} on MCPF(ANO) (Bauschlicher and Partridge, 1991).

Superhalides $[M(CN)_3]^-$ (M = Be^{2+}, Mg^{2+}, Ca^{2+})

The geometry of superhalides $[M(CN)_3]^-$ with M = Be^{2+}, Mg^{2+}, Ca^{2+} is trigonal-planar (D_{3h} symmetry). The VDEs were determined to be 8.12–8.24 eV of the cyanide and 6.96–8.41 eV of the isocyanide. Overall, the number of coordinated cyanide anions correlates with an increased electronic stability of the compounds due to the strong electron-withdrawing property of the anion (Smuczyńska and Skurski, 2009).

S. Behera and P. Jena also examined the correlation of the VDE and the number of coordinated cyanide anions. Therefore, they had a look on neutral and single or double negatively charged magnesium compounds of the type $[Mg(CN)_n]^{m-}$ with $0 < n < 4$ and $0 < m < 2$ (Figure 22). The energies of the isocyanide structures are slightly smaller due to the higher electronegativity of the nitrogen and the bond has a high ionic character. Furthermore, the neutral species $Mg(CN)_3$ can also be called a superhalogen (Behera and Jena, 2012).

3rd Main group

The general tendencies for compounds of the 3rd main group elements in terms of chemical bonding and the stability of the respective oxidation states are also evident in cyanide chemistry. While boron forms covalent bonds in the energetically favored oxidation state (III), the ionic character of the bonds between aluminum or gallium in the same oxidation state and cyanide units increases significantly. In contrast to these lighter elements, thallium is stabilized in the oxidation state (I) due to the inert pair effect. This results in an alkali metal-like chemical behavior of thallium. TlCN is the only monocyanide that is experimentally known for all elements in this main group. The remaining monocyanides have mainly been studied in theoretical investigations or experimentally by generating these molecules in low amounts in gas phase reactions. Compounds of the constitution $E(CN)_3$ (E = B, Al, In) are known for all elements except thallium. The anionic species $[E(CN)_4]^-$ are known for boron, gallium and thallium, whereas the anion of indium ($[In(CN)_4]^-$) has not been reported so far and regarding aluminium there is just one publication from 1951 reporting the synthesis of Li $[Al(CN)_4]$. The indium cyanide chemistry has not been

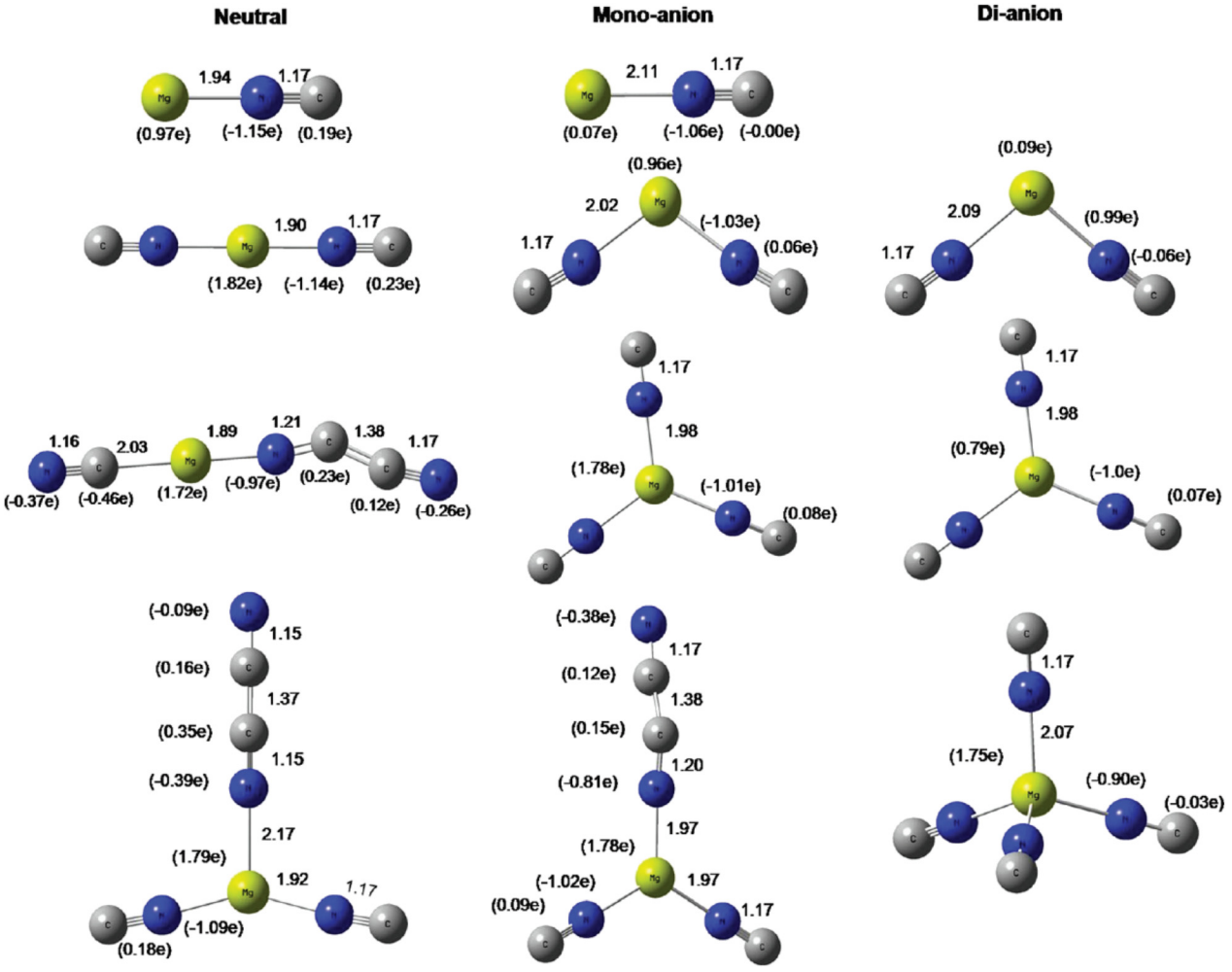

Figure 22: Optimized geometries (ground states, B3LYP/6–311++G(3df)) of different magnesium cyanide compounds with bond lengths (in Å) and NBO charges (representation taken from Behera and Jena, 2012).

investigated intensively, presumable reasoned by a missing application for these compounds. The anion $[B(CN)_4]^-$ is the most frequently applied compound of all reviewed species. There are no significant applications documented for the analogous aluminum or gallium compounds. The thallium monocyanide was utilized in organic syntheses although these procedures did not find a broad application range. As isostructural and isoelectronical to the tricyanomethanide, the tricyanoborate dianion constitutes a unique species in the 3rd main group.

Boron

The chemistry of boron cyanides $B(CN)_n$ is largely focused on the tetracyanidoborate anion $[B(CN)_4]^-$ (Bernhardt et al., 2000; Berkei et al., 2002; Koppe et al., 2007; Küppers et al., 2005). Experimentally known are also the tricyanoborate dianion $[B(CN)_3]^{2-}$ and the tricyanoborane $B(CN)_3$ in form of Lewis acid-base complexes (Bernhardt et al., 2011a; Chizmeshya et al., 2007; Williams et al., 2000). The boron monocyanide BCN is well studied by computations and has additionally been observed in gas phase experiments (Lanzisera et al., 1997).

Boron monocyanide BCN

So far, no successful synthesis of stoichiometric boron monocyanide BCN in significant amounts has been published. In 1997, L. Andrews et al. reported results of reactions of laser-ablated boron atoms with hydrogen cyanide while condensing in argon at low temperatures. The generated IR spectra included absorption bands matching the expectations from calculations and predicted absorption shift (Lanzisera et al., 1997). In the following years, several studies described the structure of BCN formed as thin layer on different surfaces (Qin et al., 2012; Shimada et al., 2006; Sugino et al., 2002; Ugarov et al., 1999). While the composition was usually determined by X-ray photoelectron spectroscopy (XPS), the connectivity of the elements was not verified. Furthermore, the specific B–C and C–N absorption bands were not observed in IR spectra.

The first computations of BCN were published by J. B. Moffat (1971). Additional studies suggest that the isocyanide structure BNC is the energetically favoured isomer compared to the BCN molecule. The ground state $^1\Sigma^+$ energies differ by (39.77 ± 2.09) kJ mol^{-1} (CASSCF/cc-pVQZ, CCSD(T)/cc-pVQZ) (Martin and Taylor, 1994). The results of different theoretical studies are listed in Table 26.

Table 26: Structural data of BCN based on computational investigations (bond lengths in Å; wave numbers in cm^{-1}).

Publication	Method + basis set	r_{B-C}	r_{C-N}	ν_{CN}
Moffat (1971)	SCF/GTO	1.588	1.157	–
Glidewell and Thomson (1984)	SCF/6-311G**	1.585	1.133	–
Martin and Taylor (1994)	CASSCF/cc-pVDZ	1.592	1.181	2210
Lanzisera et al. (1997)	B3LYP/D95	1.60	1.17	2262.5

Noteworthy to Table 26, J. B. Moffat did not optimize the structure using a software algorithm. Instead he varied the B–C distance in constant steps between 1.03 and 2.65 Å and calculated each system in order to find the energetically best structure. Although he stated the C–N distance as 1.157 Å, the results for the optimized structure fit well with later findings. In all cases, the molecule was simulated with a linear structure.

Tricyanoborane $B(CN)_3$

The initial reports regarding tricyanoborane $B(CN)_3$ from 1954 to 1956 have been replicated or verified by others. A reproducible synthesis for Lewis acid-base adduct of $B(CN)_3$ involving trimethylsilyl cyanide TMS–CN as cyanide source and several Lewis bases was published by D. Williams et al. in 2000 (Scheme 28) (Williams et al., 2000).

Several Lewis acid-base adducts were reported using different Lewis bases and in 2007 A. V. G. Chizmeshya et al. added results for a Lewis adduct with pyridine. All these adducts have one thing in common: they have a nitrogen atom as a donor atom, which forms a dative bond with $B(CN)_3$ via a free electron pair (Figure 23) (Chizmeshya et al., 2007; Williams et al., 2000).

To achive a quantitative conversion, the first step (as shown in Scheme 28) has to be carried out at higher temperatures of about 333 K. In contrast, the disubstituted product is observed, when the reaction is carried out at ambient temperature. The resulting TMS–CN·$B(CN)_3$ was heated to 523 K to receive $B(CN)_3$ following Scheme 29. Therefore, these Lewis adducts can be utilized as a $B(CN)_3$ precursor.

The adduct $Me_3N{\cdot}B(CN)_3$ was also obtained by treating the synthesized $B(CN)_3$ with trimethylamine. Some experimental results from single crystal X-ray diffraction (XRD) experiments and IR measurements are listed in Table 27 (Williams et al., 2000). The tetrahedral structure of the amine adduct exhibits a slight distortion (109.03(13)°–

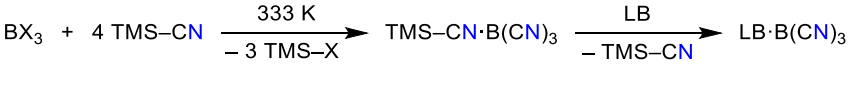

Scheme 28: Synthesis of the Lewis acid-base adduct by D. Williams et al. (X = SMe, LB = TMS–CN, NMe_3, C_5H_5N) (Chizmeshya et al., 2007; Williams et al., 2000).

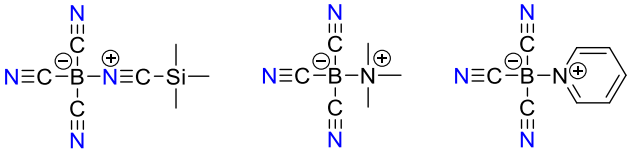

Figure 23: Reported Lewis acid-base adducts (Chizmeshya et al., 2007; Williams et al., 2000).

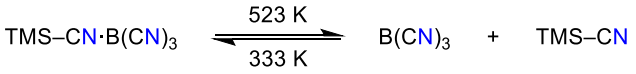

Scheme 29: Reversible formation of non-coordinated $B(CN)_3$ (Williams et al., 2000).

Table 27: Experimental data of some reported Lewis adducts of $B(CN)_3$ (bond lengths in Å; wave numbers in cm^{-1}).

Compound	r_{B-C}	r_{B-N}	r_{C-N}	ν_{CN}
$TMSCN{\cdot}B(CN)_3$ (Williams et al., 2000)	–	–	–	2310/2232
$Me_3N{\cdot}B(CN)_3$ (Williams et al., 2000)	1.594(4)/1.586(2)	1.596(3)	1.143(3)/1.146(2)	2225
$H_5C_5N{\cdot}B(CN)_3$ (Chizmeshya et al., 2007)	1.590/1.578/1.582	1.571	1.133/1.133/1.131	2227

109.6(12)°) and its unit cell is orthorhombic, while the crystals of the pyridine adduct show a monoclinic unit cell (Chizmeshya et al., 2007; Williams et al., 2000).

Tricyanidoborate dianion $[B(CN)_3]^{2-}$

Recently, E. Bernhardt, H. Willner et al. reported the successful synthesis of the tricyanidoborate dianion $[B(CN)_3]^{2-}$ by two different approaches. In case of the use of pure alkali metals like lithium, sodium or potassium, the preferred solvent is ammonia when $M[B(CN)_4]$ is treated with elemental alkali metals (Scheme 30).

When butyllithium is used, it is feasible to utilize other solvents than ammonia like THF for the synthesis of the lithium salt, but even at higher temperature of 373 K the solvent molecule cannot be removed from $Li_2[B(CN)_3]{\cdot}THF$ in vacuum (Scheme 31).

But in both cases, the strong base is necessary to form the product. Even under mild conditions, 233 K and liquid ammonia for example, the solvolysis occurs for all reported

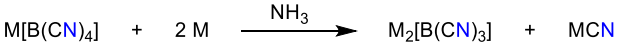

Scheme 30: Synthesis of the tricyanoborate dianion $[B(CN)_3]^{2-}$ using alkali metals (M = Li, Na, K) (Bernhardt et al., 2011a).

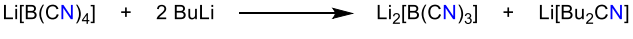

Scheme 31: Synthesis of the lithium tricyanoborate using butyllithium (Bernhardt et al., 2011a).

salts, proceeds fast for the lithium salt, much slower for the sodium and potassium salts and is kinetically hindered at low temperatures. The solvolysis products like $[HB(CN)_3]^-$, $[HB(CN)_2(C(NH)_2)]^{2-}$ and $[H_2B(CN)_2]^-$ are formed by polarity inversion of protons into hydridic hydrogen in the B–H bond. The more stable sodium and potassium salts start to decompose at 503 K. Some computational data of the tricyanoborate dianion and experimental data of two salts are compiled in Table 28 (Bernhardt et al., 2011a).

The potassium salt $K_2[B(CN)_3]$ could also by synthesized by J. Landmann et al. starting with $K[BH(CN)_3]$ and the non-nucleophilic base $K[N(SiMe_3)_2]$ leading to the dianion and $HN(SiMe_3)_2$ in yields of 97% (Landmann et al., 2017).

The dianion is described as a molecule with D_{3h} symmetry and a nucleophilic boron atom. It is discussed that the occupied boron p_z orbital donates electron density into the anti-bonding orbitals of the cyanide groups. This leads to elongated C–N distances and shortened B–C bond lengths compared to similar structures with an

Table 28: Computational data of the tricyanoborate dianion (B3LYP/6–311++G(d,p)) and experimental data of two salts (bond lengths in Å; wave numbers in cm^{-1}) (Bernhardt et al., 2011a).

Compound	r_{B-C}	r_{C-N}	$\nu^{as.}{}_{BC}$	$\nu^{sym.}{}_{CN}$	$\nu^{as.}{}_{CN}$
$[B(CN)_3]^{2-}$	1.526	1.181	1105[a]/1064[b]	2121	2057
$Na_2[B(CN)_3]\cdot 3NH_3$	1.512(4)	1.161(3)	–	–	–
$K_2[B(CN)_3]$	1.513	1.165	1137[a]/1083[b]	2098	2022

[a]The first wave number refers to ^{10}B. [b]The second wave number refers to ^{11}B.

electrophilic boron atom ($B(CN)_3$: Δr_{BC} = −0.075 Å, Δr_{CN} = 0.025 Å). Consequently, the negative charge is delocalized over all three cyanide groups illustrated in Figure 24.

Tetracyanidoborate anion $[B(CN)_4]^-$

The tetracyanidoborate (also known as tetracyanoborate) anion $[B(CN)_4]^-$ is the most intensively investigated $B(CN)_n$ species. The synthesized products, which were described in initial reports from 1951, 1967 and 1977, seem to differ from the expected experimental results for the $[B(CN)_4]^-$ anion, especially the spectroscopic data (Bessler, 1977; Bessler and Goubeau, 1967; Wittig and Raff, 1951). For example, in 1977, E. Bressler (Bessler, 1977) claimed to have synthesized $M[B(CN)_4]$ (M = Cu^+, Ag^+) starting from BCl_3 and MCN, however, it later turned out that the analytical data given in the publication did not correspond to the presumed product, so that it was assumed that the tetraisocyanidoborate anion ($[B(NC)_4]^-$) was obtained rather than the tetracyanidoborate. Therefore, the synthesis was presumably achieved for the first time by E. Bernhardt et al. for the tetrabutylammonium, silver and potassium salts in 2000 (Scheme 32) (Bernhardt et al., 2000).

Synthesis. The first reactions described in the literature to prepare $[B(CN)_4]^-$ date back to 1950 (Grundmann and Beyer, 1954; Wittig and Bille, 1951; Wittig and Raff, 1951). At that time, an attempt was made to react $Li[BH_4]$ with hydrocyanic acid. However, this reaction stopped at the $Li[BH_3(CN)]$ stage despite a large excess of HCN and temperatures of 373 K. The analogous reaction of $Li[AlH_4]$, on the other hand, leads to $Li[Al(CN)_4]$. Around 2000, E. Bernhardt et al. worked intensively on the synthesis of $[B(CN)_4]^-$ salts and developed several new synthetic routes. The reaction shown in eq. 1 (Scheme 32) can also be understood as the reaction of $[^nBu_4N][BX_3Br]$ with CN, where the X stands for Br or Cl, but not for F. In fact, when BF_3 was used, no complete conversion could be observed even up to 473 K. Disadvantages of this synthesis route are the long reaction time of 1–3 weeks, the reaction coming to a standstill if the KCN is not always ground up and the column chromatographic purification of the product (Bernhardt et al., 2000). The second synthesis method (Scheme 32, eq. 2) starts from alkali metal tetrafluoridoborates and TMS–CN, but again long reaction times are required for the synthesis of the cyanido(fluorido)borates. For the preparation of $M[BF(CN)_3]$, a month is required using KBF_4, for $LiBF_4$ 1–2 weeks (Bernhardt et al., 2003a). $M[B(CN)_4]$ (M = Li^+, K^+) could not be obtained via this reaction. A more efficient synthesis of the tetracyanidoborates on a larger scale, starting from the commercially available reagents KBF4, LiCl and KCN (Scheme 32, eq. 5), was published in 2003 in connection with investigations on the thermal behavior of the mixed cyanido(fluorido)borates

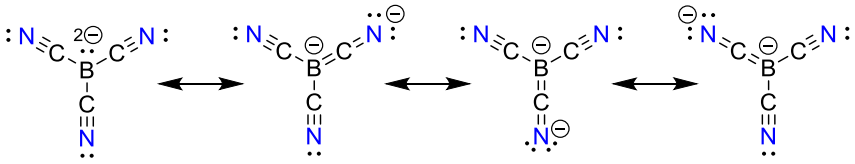

Figure 24: Lewis structures of the dianion featuring π-back bonding.

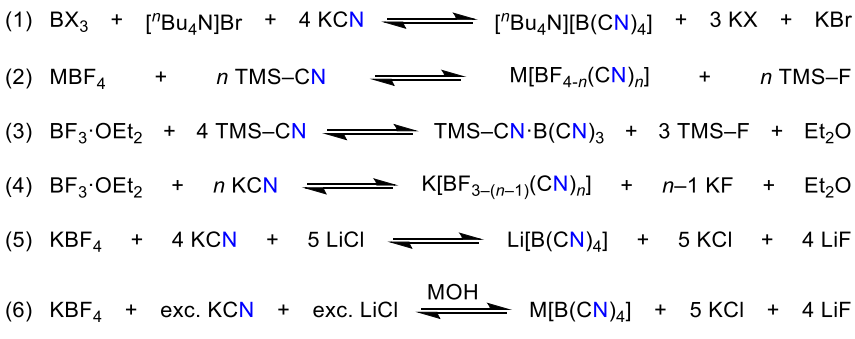

Scheme 32: Synthesis of the tetracyanidoborate anion by E. Bernhardt et al. (X = Cl^-, Br^-) (Bernhardt et al., 2000).

$K[BF_{4-n}(CN)_n]$ (n = 1 – 3) by the same working group (Bernhardt et al., 2003b). The reaction is a solid-state synthesis in which the salt mixture melts already at 280–563 K. After melting of the reactants, the exothermic reaction begins and temperatures of up to 823 K are reached for a short time. After 1 h of reaction time, $Li[B(CN)_4]$ is obtained in this way, which can be purified by a rather complex procedure and double re-salting. The yields of this reaction are between 60 and 65%. Simultaneously to our work, a publication by J. A. P. Sprenger et al. appeared in 2015, in which a more efficient synthesis of $M[BF(CN)_3]$ (M = Na^+, K^+) was presented (Sprenger et al., 2015). By addition of 10 mol% TMS–Cl, which seems to catalyze the reaction, the cyanidation with TMS–CN was already successful at 373 K after 6 h of reaction time (yields 80–90%). The silver and potassium salts were synthesized by salt metathesis reaction and the more complex salts listed in Table 30 are accessible via salt metathesis reaction based on the simple alkaline tetracyanidoborates (Bernhardt et al., 2000). Three years after the initial study, E. Bernhardt et al. reported an alternative synthetic route by a sinter process (Scheme 32, eqs. 5 and 6, M = Na^+, K^+) (Bernhardt et al., 2003b).

Table 29 lists some advantages and disadvantages of the different routes for the synthesis of $K[B(CN)_4]$. The main advantage of E. Bernhardt's sintering process(Scheme 32, eqs. 5 and 6) is the use of the less expensive KCN as a cyanide source compared to the autoclave and LA-catalyzed reaction (Scheme 33, eqs. 8 and 11), which uses the more expensive TMS–CN. However, E. Bernhardt's sintering process requires large amounts of LiCl, higher temperatures, more reaction steps and produces a large amount of waste product. In addition, the sintering process is not easy to carry out, as hot spots must be avoided and the purity of the starting materials plays an essential role in obtaining yields of up to 60%, which is, however, difficult to reproduce. The disadvantages of the autoclave reaction compared to the LA catalysis process are the salt metathesis step via silver salts (Scheme 33, eqs. 9 and 10) and the need to use autoclaves. The LA catalysis process represents a rapid, high-yield and easy-to-perform route not only to $K[B(CN)_4]$ but to almost all metal tetracyanidoborate salts. Furthermore, the number and amount of impurities (e.g. Cl^-, Li^+, CN^- or Ag^+) in the final products is significantly lower compared to the other methods (Bläsing et al., 2016a).

In 2016, however, the Schulz group reported a very simple synthesis possibility of tetracyanidoborates (Scheme 33) (Bläsing et al., 2016a; Ellinger et al., 2014; Ott et al., 2014a, 2014b). The reaction of $[BF_4]^-$ salts with TMS–CN was investigated at different temperatures and in the presence of several different Lewis acids, leading to the formation of the known $[BF_{4-n}(CN)_n]^-$ (n = 1–4) salts. Depending on the catalyst and the reaction conditions, it is shown that the whole series of $[BF_{4-n}(CN)_n]^-$ salts is now accessible under ambient conditions, avoiding long preparation times or excessive production of waste materials. The best synthesis of tetracyanidoborate salts at present is the reaction of $[R_3NH]BF_4$ with TMS–CN at 393 K with $GaCl_3$

Table 29: Reaction parameters of different routes to $K[B(CN)_4]$.

	Sinter process (Bernhardt et al., 2003b)	Autoclave (Bläsing et al., 2016a)	LA catalysis (Bläsing et al., 2016a)
Starting material	$K[BF_4]$	$[^nBu_4N][BF_4]$	$[^nPr_3NH][BF_4]$
Cyanide source	KCN	TMS–CN	TMS–CN
T	573 K	473 K	393 K
Reaction time	1 h	15 h	6 h
Product	$Li[B(CN)_4]$[b]	$[^nBu_4N][B(CN)_4]$	$[^nPr_3NH][B(CN)_4]$
Yield	–[b]	75%	70–80%
Metathese products	$[^nPr_3NH][B(CN)_4]$	$Ag[B(CN)_4]$	None
Steps	3	3	2
Overall time	20 h	25 h	10 h
Waste products	KCN, LiCl, LiF, KCl, $^nPr_3N$	$[^nBu_4N]NO_3$, AgBr	$^nPr_3N$
Solvents	CH_2Cl_2, THF	MeOH, CH_3CN	CH_2Cl_2
Yield $K[B(CN)_4]$	<60%[a]	60–70%	60 –80%

[a]It is very hard to achieve 60% yield at all, we never managed to obtain such yields as we only achieved isolated yields between 20 and 35% with the sinter method. However, we do want to stress that the overall yield strongly depends on the purity of the starting materials and avoiding of hot spots during the reaction. [b]The lithium salt is not isolated from the reaction mixture.

Table 30: (Selected) synthesized salts of $[B(CN)_4]^-$.

Publication	Cation
Bernhardt et al. (2000)	$[Bu_4N]^+$, Ag^+, K^+
Berkei et al. (2002)	Hg^{2+}, Hg_2^{2+}
Bernhardt et al. (2003b)	Li^+, Na^+, K^+, Cs^+, Cu^+, NH_4^+, $[Et_4N]^+$, $[(H_2N)_3C]^+$
Küppers et al. (2005)	Rb^+, Tl^+
Neukirch et al. (2006)	Zn^{2+}, Cu^{2+}
Küppers et al. (2007)	H^+, $[H_3O]^+$, $[H_5O_2]^+$
Koppe et al. (2007)	$[F_5C_6Xe]^+$
Nitschke and Köckerling (2009)	Co^{2+}
Flemming et al. (2010)	$[Ph_4P]^+$, $[^nBu_4P]^+$, $[EtPh_3P]^+$, $[^nBuPh_3P]^+$
Nitschke and Köckerling (2011)	Fe^{3+}, Fe^{2+}
Nitschke et al. (2014)	Mg^{2+}, Ca^{2+}

(7) $[^nBu_4N]BF_4$ + 3 TMS–CN $\xrightarrow[\text{exc. TMS–CN}]{\text{13 h, 423 K}}$ $[^nBu_4N][BF(CN)_3]$ + 3 TMS–F

(8) $[^nBu_4N]BF_4$ + 4 TMS–CN $\xrightarrow[\text{autoclave}]{\text{15 h, 473 K}}$ $[^nBu_4N][B(CN)_4]$ + 4 TMS–F

(9) $[^nBu_4N][B(CN)_4]$ + $AgNO_3$ ⟶ $Ag[B(CN)_4]$ + $[^nBu_4N]NO_3$

(10) $Ag[B(CN)_4]$ + KBr ⟶ $K[B(CN)_4]$ + AgBr

(11) $[^nPr_3NH]BF_4$ + 4 TMS–CN $\xrightarrow[5\ \text{mol\%}\ GaCl_3]{\text{6 h, 473 K}}$ $[^nPr_3NH][B(CN)_4]$ + 4 TMS–F

(12) $[^nPr_3NH][B(CN)_4]$ + KOH $\xrightarrow[-H_2O]{}$ $K[B(CN)_4]$ + $^nPr_3N$

Scheme 33: Synthesis of the $[B(CN)_4]^-$ according to A. Schulz and co-workers (X = Cl^-, Br^-) (Bläsing et al., 2016a; Ellinger et al., 2014; Ott et al., 2014a, 2014b).

as Lewis acidic catalyst (Scheme 33, eq. 11). This yields the ammonium salt in very good yields, which can be converted very elegantly with bases to the corresponding metal salts (Scheme 33, eq. 12) (Bläsing et al., 2016a).

Table 30 summarizes several synthesized salts, which can be mainly divided into ionic liquids (ILs), used as additive in dye-sensitized solar cells for example, and common inorganic salts applicable in different fields like fluorine free lithium batteries (Marszalek et al., 2011; Scheers et al., 2014). The tetracyanidoborate anion can also be employed as a starting material of more complex weakly coordinating anions (WCAs) like $[B\{CN{\cdot}B(C_6F_5)_3\}_4]^-$ or for other WCAs like $[B(CF_3)_4]^-$ (Figure 25) (Bernhardt et al., 2001, 2011b; Bernsdorf et al., 2009a).

Tetracyanoboronic acids $H[B(CN)_4]{\cdot}n\ H_2O$ (n = 0, 1, and 2) were synthesized by ion exchange (Küppers et al., 2007). These compounds can be again employed to generate several tetracyanidoborate salts by acid-base reaction (Bernsdorf and Köckerling, 2009; Nitschke and Köckerling, 2009, 2011). Furthermore, different magnesia salts are accessible by direct conversion due to the high reductive power of magnesia and the strong acidity of $HB(CN)_4$ (Nitschke et al., 2014). Ionic liquids containing

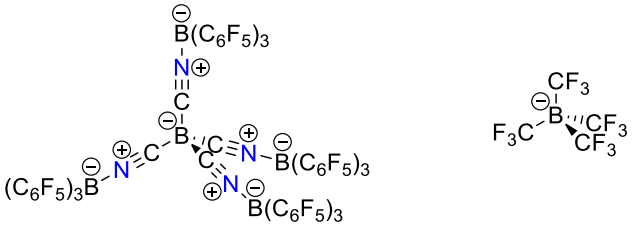

Figure 25: WCA based on $[B(CN)_4]^-{\cdot}4\ B(C_6F_5)_3$ adduct (= $[B\{CN{\cdot}B(C_6F_5)_3\}_4]^-$) in comparision to the $[B(CF_3)]_4^-$ ion.

the tetracyanidoborate anion as weakly coordinating anion were synthesized and extensively characterized in several approaches founding a great variety of tetracyanidoborate based ILs (Bläsing et al., 2016a). The tetracyanidoborate salts are stable at ambient temperature and their decomposition is not observed up to 383 K strongly depending on the cation, the alkali salts start to decompose at 773 K for example. Detailed information and additional data of bond lengths and spectroscopic data are represented in Table 31. The solubility also depends on the cation. The metal salts exhibit high hydrolysis stability, when they are exposed to boiling water or concentrated chlorine, and are also stable in dry hydrogen fluoride for over 1 h (Bernhardt et al., 2000).

The decomposition of tetracyanoboronic acid was investigated under inert conditions and observed by differential scanning calorimetry (DSC) and IR spectroscopy. The analysis led to a proposed decomposition process illustrated in Scheme 34 (Küppers et al., 2007).

The single crystal X-ray diffraction revealed a slightly compressed tetrahedral coordination of the boron atom in most cases. The silver(I), copper(I), lithium and sodium salts exhibit perfect tetrahedral symmetry for both the cation and the boron atom. A detailed analysis of the structural parameters and crystal systems was given by the groups of H. Willner and M. Köckerling in 2005 (Küppers et al., 2005). According to the initial report by E. Bernhardt et al., the $[Bu_4N]^+$ ion can be described as isolated due to the significant distances to the anion in the crystal structure corresponding to weak interactions between the cation and the anion, which also leads to a small melting point of T_M = 353 K (Bernhardt et al., 2000).

Table 31: Experimental data of some $[B(CN)_4]^-$ salts (bond lengths in Å; wave numbers in cm^{-1}; temperatures in K).

Cation	r_{B-C}	r_{C-N}	ν_{CN}	ν_{BC}	T_M	$T_{Dec.}$
$[H_5O_2]^+$ (Küppers et al., 2007)	1.593(1)	1.144(2)/1.143(2)/1.143(2)	2253	976/942	388	–
Na^+ (Bernhardt et al., 2003b; Küppers et al., 2005)	1.575(2)	1.130(3)	2252	–	793	813
K^+ (Bernhardt et al., 2003b; Küppers et al., 2005)	1.595(1)	1.142(1)	2233	–	703	783
Rb^+ (Küppers et al., 2005)	1.590(1)	1.136(2)	2232	–	703	783
Cs^+ (Bernhardt et al., 2003b; Küppers et al., 2005)	1.582(5)	1.127(7)	2230	–	693	783
Ag^+ (Bernhardt et al., 2000, 2003b)	1.589(2)	1.131(3)	2256	982/946	–	713
Cu^+ (Bernhardt et al., 2003b; Küppers et al., 2005)	1.588(2)	1.140(3)	2253	–	–	743
NH_4^+ (Bernhardt et al., 2003b; Küppers et al., 2005)	1.592(2)	1.133(2)	2233	–	–	573
$[Bu_4N]^+$ (Bernhardt et al., 2000, 2003b)	1.582(3)/1.590(3)	1.135(3)/1.141(3)	2222	967/937	353	623
$[Ph_4P]^+$ (Flemming et al., 2010)	1.596(2)/1.580(2)	1.141(2)/1.146(2)	2226	985/937	466	663
Cu^{2+} (Neukirch et al., 2006)	1.594(6)/1.591(3)/1.588(8)	1.131(4)/1.130(3)/1.132(6)	2234	979/946	–	623
Zn^{2+} (Neukirch et al., 2006)	1.595(2)/1.590(5)	1.139(2)/1.132(5)	2234	980/946	–	723
Hg^{2+} (Berkei et al., 2002)	1.60(1)/1.62(2)	1.12(1)/1.11(3)	2234	976/938	–	538
Hg_2^{2+} (Berkei et al., 2002)	1.63/1.57	1.12/1.14	2225	972/938	–	439

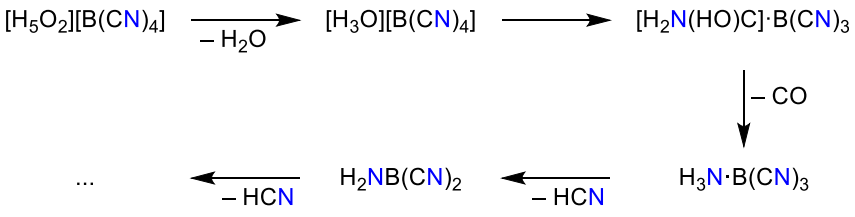

Scheme 34: Decomposition process of tetracyanoboronic acid (Küppers et al., 2007).

Aluminum

The properties of aluminum cyanide compounds $Al(CN)_n$ are comparable to those of $B(CN)_n$ chemistry even though this class is not as well investigated and applied. The compounds have been mainly investigated by theoretical approaches, while there are only a few experimental studies accessible.

Aluminum monocyanide AlCN

Aluminum monocyanide AlCN has been studied both theoretically and experimentally. The motivation of these investigations originates from a special interest since astrophysicists suspected the molecule AlCN and its isomer AlNC to be the source of some unidentified signals in the MW spectra of the carbon-rich mass-losing star IRC + 10,216 (Fukushima, 1998). Based on this incitement, the first theoretical report was published by B. Ma et al. in 1995. The calculations revealed that the isocyanide is the energetically favored isomer compared to the cyanide (ΔE = 23.0 kJ mol^{-1}, CCSD(T)/TZ2P + f) while both structures are linear molecules (Ma et al., 1995). These findings were confirmed by additional studies and demonstrate a similarity between the monocyanides of boron and aluminum (Jiang et al., 2002; Meloni and Gingerich, 1999; Petrie, 1996; Tokue and Nanbu, 2006, 2011). Furthermore, S. Petrie noted that the isomerization energy of the aluminum species is significantly larger compared to other theoretically investigated monocyanides like NaCN or MgCN (Petrie, 1996). The first experimental work was published by D. V. Lanzisera and L. Andrews operating with the same technique they successfully applied for the detection of BCN (Lanzisera and Andrews, 1997b). In 1999, I. Gerasimov et al. conducted photolysis experiments by laser fluorescence utilizing a supersonic beam containing trimethylaluminum and molecular nitrogen (Gerasimov et al., 1999). Some selected results are shown in Table 32 and a more detailed comparison including numerous results from several publications can be obtained from reports by I. Tokue and S. Nunbu (2011).

Aluminum tricyanide $Al(CN)_3$

The first hint for a synthesis of aluminum tricyanide was published in 1924 by F. W. Bergstrom when he treated $Hg(CN)_2$ with aluminum metal in liquid ammonia according to $2\,Al + 3\,Hg(CN)_2 \rightarrow 2\,Al(CN)_3 + 3\,Hg$ (Bergstrom, 1924). It was found that it is formed $Al(CN)_3{\cdot}5\,NH_3$. It is assumed that the number of ammonia molecules is much larger in

Table 32: Computational data of AlCN and its isomer (bond lengths in Å; wave numbers in cm^{-1}).

Publication	Method + basis set	Isomer	r_{Al-E}	r_{C-N}	ν_{CN}	ν_{AlE}
Ma et al. (1995)	SCF/TZ2P + f	AlCN	2.030	1.135	2479	472
		AlNC	1.842	1.158	2290	584
Lanzisera and Andrews (1997b)	BP86/6-311G* (LANL2DZ)	AlCN	2.09	1.17	2149.7	–
		AlNC	1.94	1.19	2024.4	–
Fukushima (1998)	QCISD(T)/6-311 + G(3df)	AlCN	2.0215	1.1712	2222.9	469.9
		AlNC	1.8639	1.1877	2105.2	554.2

NH_3 solution. $Al(CN)_3{\cdot}5\ NH_3$ is an effloresced white powder. By successive deammonation of the crystals of the composition $Al(CN)_3{\cdot}n\ NH_3$ with n = 13 or 14 at −33 °C the nona- and hexa-ammoniates are obtained as white solids. A substance of the composition $AI(CN)_3{\cdot}1.5\ NH_3$ can be obtained by heating the penta-ammoniate in vacuum (80 mm Hg). $Al(CN)_3{\cdot}5\ NH_3$ is decomposed by water, probably to form aluminum hydroxide, ammonia and ammonium cyanide. This is also the reason why $Al(CN)_3$ cannot be obtained from aqueous solution, as it immediately starts to hydrolyse.

The synthesis of pure $Al(CN)_3$ as the framework compound was achieved by a metathesis reaction according to Scheme 35 (Williams et al., 2001). Single crystal XRD experiments indicate that $Al(CN)_3$ crystallizes in a prussian blue-like octahedral structure. As mentioned before, strong absorption bands at 2220 and 530 cm^{-1} observed in the IR spectra indicate evidence of cyanide groups. The recorded ^{27}Al NMR spectrum exhibits seven signals. The authors assigned each signal to one of seven possible aluminum environments with varying ratios of surrounding carbon and nitrogen atoms due to C, N static disorder (Williams et al., 2001). G. Wittig and H. Bille described the formation of $Al(CN)_3$ in the reaction of AlH_3 with HCN, which crystallizes from the etheric solution as $Al(CN)_3{\cdot}O(C_2H_5)_2$ (Scheme 36) (Wittig and Bille, 1951).

Ternary Al–C–N compounds were observed in a thin film deposited using inductively coupled plasma (ICP) assisted DC magnetron sputtering (Jiang et al., 2002).

A comparison of calculated and observed data for the $Al(CN)_3$ framework was given by A. V. G. Chizmeshya et al. in 2007. The report included additional data on gallium and indium frameworks. The values of C–N bond lengths are reported as 1.164 Å for experimental and 1.158 Å for computational investigations (Chizmeshya et al., 2007).

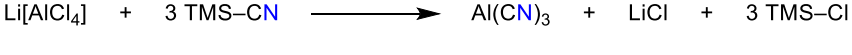

Scheme 35: Synthesis of $Al(CN)_3$ by J. Kouvetakis et al. (2001).

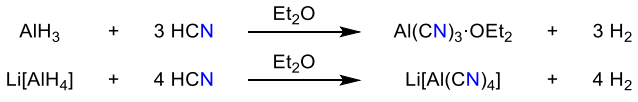

Scheme 36: Synthesis of $Al(CN)_3$ and $Li[Al(CN)_4]$ according to G. Wittig and H. Bille (Wittig and Bille, 1951).

Although the number of publications regarding the aluminum tricyanide $Al(CN)_3$ is small, this compound has been studied theoretically as a gas phase molecule and experimentally as a framework compound. In gas phase $Al(CN)_3$ is reported with a Al–C distance of 1.914 Å (SCF/LANL2DZP) and 1.912 Å (B3LYP/LANL2DZP) while the C–N bond length of the cyanide groups varies between 1.143 Å (SCF/LANL2DZP) and 1.170 Å (B3LYP/LANL2DZP), respectively. This constitutes the significant difference in calculated IR absorption bands of the C–N stretching mode of 2525 cm^{-1} (SCF/LANL2DZP) and 2276 cm^{-1} (B3LYP/LANL2DZP), respectively. A. Y. Timoshkin and H. F. Schaefer summarized that the results indicate the importance of the inclusion of electron correlation for such systems whereby the HF method is inadequate for a more precise description (Timoshkin and Schaefer, 2000). This is confirmed by IR measurements of the framework compound synthesized by A. V. G. Chizmeshya et al. which exhibits an absorption band at 2220 cm^{-1} assigned to the C–N stretching mode and therefore agrees more accurately with the results of the DFT calculations (Mikhailov et al., 2003).

Cyanidoaluminate anions $[Al(CN)_{6-n}]^{(3-n)-}$ (n = 0, 1, 2)

Interestingly, there is only one publication on the synthesis of cyanidoaluminates from 1951 by G. Wittig and H. Bille (Scheme 36) (Wittig and Bille, 1951). It describes the

reaction of $Li[AlH_4]$ with hydrocyanic acid, in the course of which hydrogen and $Li[Al(CN)_4]$ are formed. This complex salt precipitates from the ethereal solution as a colorless powder and was shown to be $Li[Al(CN)_4]$. It is decomposable even under exclusion of moisture and oxygen, as can be seen from the yellow coloration shortly after preparation and the decrease of the cyanide content. In water it decomposes to form aluminum hydroxide, lithium cyanide and prussic and hydrocyanic acid (Wittig and Bille, 1951).

The anionic species of aluminum cyanide compounds shown in Figure 26 have been recently studied by theoretical approaches. The initial work of S. Smuczyńska and P. Skurski on the $[AlCN]^-$ anion reported an Al–C distance of 1.975 Å and a C–N bond length of the cyanide group of 1.182 Å (MP2/6-311 + G(d)) (Smuczyńska and Skurski, 2009). Additional results by T. Sommerfeld and B. Bhattarai reported insignificantly longer bond lengths (Δr_{Al-C} = + 0.01 Å) in regard to the anion and an increase of the bond length from the anion to the dianion (Δr_{Al-C} = + 0.11 Å) and to the trianion (Δr_{Al-C} = + 0.17 Å) while the C–N bond length of the cyanide groups is insignificantly elongated (Δr_{C-N} = + 0.005 Å and Δr_{C-N} = + 0.008 Å, MP2/aug-cc-pVDZ). The authors added that the trianion $[Al(CN)_6]^{3-}$ is stable considering the VDEs (Sommerfeld and Bhattarai, 2011).

Generally, both structure optimizations used MP2 methods and were focused on the question of stability of the anions. S. Smuczyńska and P. Skurski noted that only one minimum energy structure was found on the potential energy surface (PES) of $[Al(CN)_4]^-$. The authors also investigated the VDEs of various $[M(CN)_n]^-$ species with M = Li^+, Na^+, Be^{2+}, Mg^{2+}, Ca^{2+}, B^{3+} and Al^{3+} and concluded that the electronic stability of the anion increases with an increasing number of cyanide ligands resulting in the highest VDE for $[Al(CN)_4]^-$ (Smuczyńska and Skurski, 2009). T. Sommerfeld et al. calculated two isomers of the aluminum cyanide trianion, $[Al(CN)_6]^{3-}$ and $[Al(NC)_6]^{3-}$, using ab initio methods (Sommerfeld and Bhattarai, 2011). These two isomers are predicted to be electronically stable and show significant barriers with respect to the dissociation of $[CN]^-$ ions.

Gallium

The cyanide-substituted gallium species are not as well investigated as the corresponding boron or aluminum species. Although computational studies are accessible as well, the part of experimental studies has increased compared to the first two elements of this main group, but the overall number of publications regarding gallium cyanide chemistry is smaller compared to boron and aluminum. Especially, the $Ga(CN)_3$ has been studied most intensively of all gallium cyanide species. Similarities of gallium and aluminum are existing in the tendency to form framework structures and in regard to the small number of studies investigating the anionic species of these elements.

Gallium monocyanide GaCN

Similar to the boron and aluminum analogues, the first successful synthesis of gallium monocyanide GaCN was reported by D. V. Lanzisera and L. Andrews in their analysis of the reaction of laser-ablated elements with hydrogen cyanide in 1997 (Lanzisera and Andrews, 1997b). Two years later this investigation was followed by an additional theoretical and experimental work of K. A. Walker et al. (2001). The results of these reports are listed comparatively in Table 33.

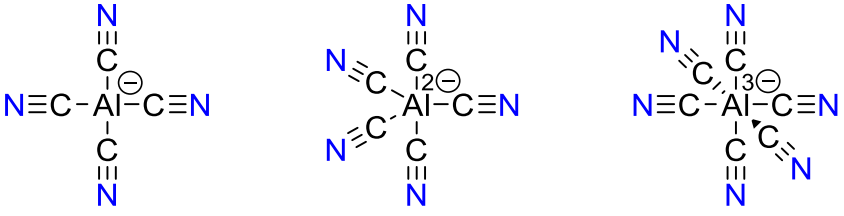

Figure 26: Anion, dianion and trianion of aluminum cyanide compounds.

Table 33: Computational data of GaCN (bond lengths in Å; wave number in cm^{-1}).

Publication	Method + basis set	Isomer	r_{Ga-E}	r_{C-N}	ν_{CN}	ν_{GaE}
Lanzisera and Andrews (1997b)	BP86/6-311G* (LANL2DZ)	GaCN	2.12	1.17	2147.0	339.3
		GaNC	1.97	1.19	2023.0	388.2
Petrie (1999a)	MP2(full)/6-31G*	GaCN	2.073	1.191	–	–
		GaNC	1.962	1.201	–	–
Walker et al. (2001)	B3LYP/aug-cc-pVTZ	GaCN	2.098	1.158	–	–
		GaNC	1.965	1.176	–	–

The question regarding the energetically preferred isomer depends on the employed computational method. The isocyanide isomer is the stable isomer at the DFT level calculated by D. V. Lanzisera and L. Andrews (1997b). At the G2 level, the gallium cyanide represents the global minimum on the PES and is therefore the favored isomer but not at G2[thaw(QCI)]. Due to the similar ground state energies and small isomerization barrier, S. Petrie concluded that the interaction between the gallium atom and the cyanide unit possesses mainly ionic character (Petrie, 1999a).

In 2010 K. Jacobs et al. suggested the intermediate formation of GaCN in a process resulting in GaN. The authors postulated an interaction of ammonia and graphite forming hydrogen cyanide, which reacts with gallium to form volatile GaCN in the second step. This mechanism is based on mass spectrometric findings and thermodynamic calculations (Jacobs et al., 2010).

Gallium tricyanide $Ga(CN)_3$

Gallium tricyanide, $Ga(CN)_3$, was initially reported by L. C. Brousseau et al. in 1997 as an anhydrous Prussian blue-like crystallizing compound (Figure 27). The synthesis was achieved by a reaction of azidodichlorogallane and trimethylsilyl cyanide TMS–CN (Scheme 37).

The compound is unstable in presence of air or at temperatures above 723 K. The IR spectrum revealed a strong absorption band at 2215 cm^{-1} for the CN group and 440 cm^{-1} assigned to the Ga–C stretching mode which is similar to related compounds like $GaMe_2CN$ (ν_{CN} = 2207 cm^{-1}, ν_{GaC} = 429 cm^{-1}). The bond lengths of r_{Ga-C} = 2.072 Å and r_{C-N} = 1.148 Å were determined by powder XRD and Rietveld analysis. The authors suggested that the high building tendency and stability of $Ga(CN)_3$ in contrast to otherwise substituted gallium species could originate from a metal ligand π-back bonding. A second synthetic route, starting from $GaCl_3$ and TMS–CN, was published to gain access to highly pure and crystalline $Ga(CN)_3$ (Scheme 38) (Brousseau et al., 1997).

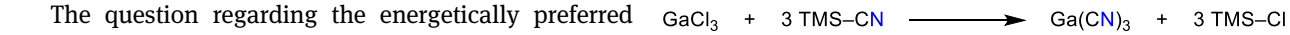

Scheme 38: Synthesis of highly pure $Ga(CN)_3$ (Brousseau et al., 1997).

Molecular $Ga(CN)_3$ was studied theoretically by A. Y. Timoshkin and H. F. Schaefer in 2000. Compared to values derived from HF calculations (r_{C-N} = 1.142 Å at SCF/LANL2DZP), the results from approaches utilizing DFT methods indicate an elongated C–N bond length (r_{C-N} = 1.169 Å at B3LYP/LANL2DZP) while both methods lead to similar Ga–C distances of r_{Ga-C} = 1.922 Å. The calculated IR absorption bands using DFT methods are in reasonable agreement with the observed bands from the $Ga(CN)_3$ framework (ν_{CN} = 2282 cm^{-1} at B3LYP/LANL2DZP, ν_{CN} = 2318 cm^{-1} at B3LYP/DZP), but HF methods would lead to significantly increased wave numbers (ν_{CN} = 2533 cm^{-1} at SCF/LANL2DZP). Questioning the energetic stability of both isomers, the results do not provide a final answer since different computational methods led to opposing data regarding the relative energies of the gallium cyanide and gallium isocyanide (Timoshkin and Schaefer, 2000).

Very little is known about molecular Lewis acid-base adducts of $Ga(CN)_3$. In 2007, A. V. G. Chizmeshya et al. analyzed $Ga(CN)_3{\cdot}2\ NC_5H_5$ revealing that the addition of $Ga(CN)_3$ (as coordination polymer) to pyridine leads to the formation of an adduct complex with two pyridine molecules ($Ga(CN)_3{\cdot}2\ NC_5H_5$) directly bound to the gallium center in contrast to the boron analogue where only one solvent molecule was attached. The average Ga–C bond length was documented as r_{Ga-C} = 2.027 Å and the average C–N bond length was determined to be r_{C-N} = 1.065 Å while the calculated bond lengths differed significantly (r_{Ga-C} = 1.946 Å and r_{C-N} = 1.161 Å at LDA). The difference of Ga–C distances was mainly caused by a computational method called local density approximation (LDA) which is known

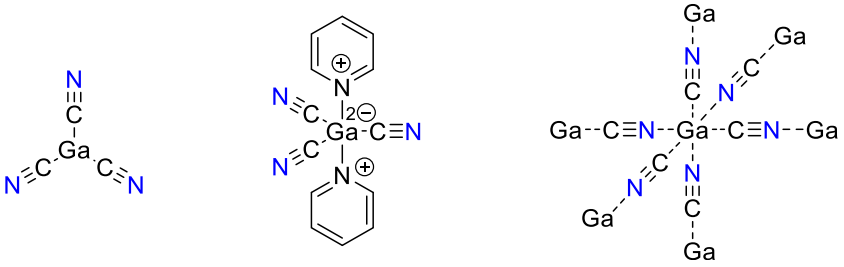

Figure 27: $Ga(CN)_3$ as a molecule, part of a Lewis acid-base adduct and part of a framework.

Scheme 37: Initial synthesis of $Ga(CN)_3$ (Brousseau et al., 1997).

for its tendency to underestimate bond lengths. Concerning the experimental data, the authors supposed that refinement artifacts in context of small scattering factors of carbon and nitrogen caused the disagreement. The recorded IR spectrum exhibited a strong absorption at 2180 and 436 cm^{-1} (Table 34) (Chizmeshya et al., 2007).

Tetracyanido gallide anion $[Ga(CN)_4]^-$

In their report on the $Ga(CN)_3$ coordination polymer, L. C. Brousseau et al. synthesized and analyzed lithium and copper tetracyanido gallide, $Li[Ga(CN)_4]$ and $Cu[Ga(CN)_4]$, as well. The substances are accessible by direct addition of the metal cyanide salt MCN to $Ga(CN)_3$ (Scheme 39, $M = Li^+, Cu^+$).

The cubic crystal system consists of MN_4 and GaC_4 tetrahedrons. Since it is not possible to distinguish between carbon and nitrogen, a general disorder could not be excluded. The Ga–E bond length is determined as r_{Ga-E} = 2.00(1) Å, the bond length of the cyanide group is reported as r_{C-N} = 1.07(1) Å and the cyanide stretching mode was found at ν_{CN} = 2227 cm^{-1} for the lithium salt. The compound $Zn(CN)_2$ crystallizes in the same structural type with a systematical disorder and shows an absorption band for the cyanide closely related to the lithium salt at 2218 cm^{-1} (Brousseau et al., 1997).

Indium

As discussed before, the tricyanido species of group 13 elements seem to be little studied in contrast to the corresponding halides. Indium tricyanide was reported a long time ago. In 1869, R. E. Mayer already described the reaction of indium acetate with aqueous hydrogen cyanide solution, which shows no precipitation, whereas the reaction with KCN leads to a white precipitate, which dissolves again in the excess of KCN (Meyer, 1869). The dissolving white precipitate was probably $K[In(CN)]_4$. On boiling, indium hydroxide is formed.

The indium cyanide chemistry is similar to the gallium chemistry, but has not been investigated intensively. In particular, the indium monocyanide is not as well theoretically studied as the gallium or aluminum analogue. Similar to other $E(CN)_3$ compounds with E = 3rd main group element, the framework structure has been analyzed in the late 1990s. Syntheses of defined $In(CN)_3$ Lewis base adducts failed in first attempts due to the formation of undefined mixtures (Chizmeshya et al., 2007). Reports of anionic species are not published so far.

Indium monocyanide InCN

Indium monocyanide InCN has been obtained experimentally by ablation of indium and the reaction of these ablated gas phase atoms with hydrogen cyanide (Lanzisera and Andrews, 1997b). Furthermore, computational calculations were conducted for comparison. The studies focused on vibration and rotation spectra (Chizmeshya et al., 2007; Walker et al., 2001). The DFT calculations by D. V. Lanzisera and L. Andrews resulted in an In–C distance of r_{In-C} = 2.28 Å and a C–N distance of r_{C-N} = 1.17 Å (BP86/6-311G*(LANL2DZ)) and the computational value of the cyanide absorption band is ν_{CN} = 2142 cm^{-1} compared to the experimental value of ν_{CN} = 2132.4 cm–1 (Lanzisera and Andrews, 1997b). These properties were also gained by applying the rigid bender model resulting in r_{In-C} = 2.268 Å and r_{C-N} = 1.143 Å, respectively (Walker et al., 2001).

Furthermore, D. V. Lanzisera and L. Andrews noted that the energy difference between both indium species InCN and InNC is small and interconversion between both isomers is facile reporting bond length of r_{In-N} = 2.14 Å and

Table 34: Experimental and computational data of different $Ga(CN)_3$ species (bond lengths in Å; wave numbers in cm^{-1}).

Compound	Exp./calc.	r_{Ga-C}	r_{C-N}	ν_{CN}	ν_{GaC}
$Ga(CN)_3$ (molecular) (Timoshkin and Schaefer, 2000)	SCF/LANL2DZP	1.922	1.142	2533	451
	B3LYP/LANL2DZP	1.922	1.169	2282	431
$Ga(CN)_3$ (framework) (Brousseau et al., 1997)	Exp. – XRD, IR	2.072	1.148	2215	440
$Ga(CN)_3 \cdot 2\ NC_5H_5$ (Chizmeshya et al., 2007)	Exp. – XRD, IR	2.027	1.065	2180	436
	LDA	1.946	1.161	–	–

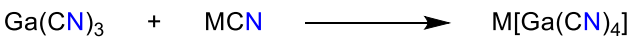

Scheme 39: Synthesis of salts containing the tetracyanido gallide anion (Brousseau et al., 1997).

r_{C-N} = 1.19 Å (BP86/6-311G*(LANL2DZ)) in regard to the isocyanide (Lanzisera and Andrews, 1997b).

Indium tricyanide $In(CN)_3$

In attempts to prepare indium oxycyanide by the action of cyanogen on indium oxyiodide a small amount of material of the analytical composition $In(CN)_3$ was obtained. This compound was extremely deliquescent, unstable in water and causes considerable doubt about the validity of the earlier reports (Goggin et al., 1966a). In contrast to earlier reports, P. L. Goggin et al. could not report a reaction in aqueous solution due to solvolysis. Furthermore, they reported that indium metal reacts with mercury cyanide in liquid ammonia solution, but not in ethanol or liquid hydrogen cyanide solutions. After evaporating the solvent and heating *in vacuo* at 373 K, the product found was $In(CN)_3 \cdot n\,NH_3$. However, pure $In(CN)_3$ could be obtained as sublimate by heating the ammoniate at 573 K in a nitrogen stream. The reaction of HCN gas with indium metal or with indium hydroxide at 623 K also leads to the isolation of small amounts of $In(CN)_3$ (Goggin et al., 1966b).

The initial synthesis of indium tricyanide $In(CN)_3$, as reported by P. L. Goggin et al., was an inefficient procedure that has not been adopted in additional studies (Goggin et al., 1966b). In 1998, D. Williams et al. reported that $In(CN)_3$ can be prepared by treating freshly sublimed $InCl_3$ with an excess of TMS–CN in dry ether/hexane solutions. After extraction with warm hexane, which led to nanoporous cubic $In(CN)_3$ (Scheme 40) (Williams et al., 1998). The crystal structure is similar to those of $Al(CN)_3$ and $Ga(CN)_3$ which have been described earlier. It was also shown that $In(CN)_3$ can be combined with $Ga(CN)_3$ to form solid solutions in which the lattice parameter varies smoothly with concentration across the entire compositional range.

The structural characteristics of $In(CN)_3$ are determined as r_{In-C} = 2.251(1) Å and r_{C-N} = 1.125(1) Å. The cyanide stretching mode was observed at ν_{CN} = 2200 cm^{-1} and the band at ν = 415 cm^{-1} was assigned to the In–CN stretching mode. These structures have zeolitic properties which have been described earlier for Prussian blue-like structures. In this context the authors noted the incorporation of solvent molecules or krypton atoms in the zeolitic structure of $In(CN)_3$ which was verified by powder XRD (Williams et al., 1998). For example, the compound reversibly incorporates krypton atoms into the empty cavities to form $In(CN)_3 \cdot Kr$.

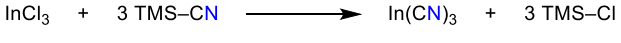

Scheme 40: Synthesis of pure $In(CN)_3$ (Williams et al., 1998).

The molecular structure of gas phase $In(CN)_3$ was computed by A. Y. Timoshkin and H. F. Schaefer (Timoshkin and Schaefer, 2000). The results differ from the solid state structure of $In(CN)_3$ which forms a coordination polymer (framework). The In–C bond length was calculated as r_{In-C} = 2.080 Å while the bond length of the cyanide group is reported as r_{C-N} = 1.169 Å (B3LYP/LANL2DZP). The result of the cyanide absorption band of ν_{CN} = 2274 cm^{-1} is consistent to other $E(CN)_3$ molecules (Timoshkin and Schaefer, 2000).

Thallium

The significant differences in the chemical properties of thallium and indium additionally influence the reaction behavior and substance properties of their compounds. In the last 90 years, various investigations have been carried out and frequently reported on thallium(I) cyanide, especially in aqueous mixtures. As far as the 3rd main group is concerned, thallium is the only element that forms the distinct $E^{I}CN$ compound (E = B, Al, Ga, In, and Tl) (Bassett and Corbet, 1924; Lanzisera and Andrews, 1997b; Penneman and Staritzky, 1958). Many studies of thallium(III) species focused on complexes formed in aqueous solutions and their characteristics (Bányai et al., 2001; Batta et al., 1993; Blixt et al., 1989).

Thallium monocyanide TlCN

In contrast to the compounds of other elements of the 3rd main group, thallium monocyanide, TlCN, has been studied intensively. As a result of the inert pair effect, the oxidation state + I is more stable compared to the lighter group 13 elements. It should be noted that the chemical behavior of thallium(I) is similar to that of an alkali metal. Consequently, TlCN is known for more than 90 years, when H. Bassett and A. S. Corbet studied different aqueous mixtures of TlCN and KCN in 1924 (Bassett and Corbet, 1924). Even though, later findings questioned the existence of $K[Tl(CN)_2]$ announced in their work, it underlines that TlCN was discussed even before the 1930s. In addition to the synthesis of TlCN by reaction of thallium nitrate and potassium cyanide, R. A. Penneman and E. Staritzky described the formation of TlCN by cation exchange using an aqueous solution of potassium cyanide (Penneman and Staritzky, 1958). The IR absorption band of the cyanide stretching mode at ν_{CN} = 2048 cm^{-1} reported in this paper was confirmed by other reports, which included results for the application of thallium cyanide in organic synthesis (Penneman and Staritzky, 1958; Taylor et al., 1978).

E. C. Taylor et al. described a convenient and quantitative preparation of anhydrous thallium(I) cyanide under non-aqueous conditions by the reaction of dry hydrogen cyanide with thallium(I) phenoxide, together with some results on the use of TlCN for the preparation of ketonitriles, cyanoformates and trimethylcyanosilane (Taylor et al., 1978).

Thallium dicyanide $Tl(CN)_2$

A framework compound with the empirical formula $Tl(CN)_2$ was synthesized by D. Williams et al. However, this formal $Tl(CN)_2$ is composed of a thallium mono-cation Tl^+ and a thallium tri-cation Tl^{3+} resulting in a formula of $Tl^{I}Tl^{III}(CN)_4 = TlCN{\cdot}Tl(CN)_3$ (Scheme 41) (Williams et al., 2001).

The structure was described as closely related to disordered $Cd(CN)_2$ with $Pn\bar{3}m$ symmetry. The IR spectrum exhibits two absorption bands for the cyanide stretching mode at $\nu_{CN} = 2209\ cm^{-1}$ and $\nu_{CN} = 2198\ cm^{-1}$, respectively. The higher wave number is assigned to the cyanide groups attached to the Tl^{3+} cation and the smaller wave number is therefore assigned to the stretching mode of the cyanide units of Tl^+. Furthermore, $Tl(CN)_2$ decomposes in presence of air and moisture (Williams et al., 2001).

Thallium tricyanide $Tl(CN)_3$

Due to the redox potentials of Tl^+ and Tl^{3+} the formation of thallium tricyanide $Tl(CN)_3$ was disregarded for a long time, but in the late 1980s, J. Glaser and several co-workers started systematic studies on thallium cyanide complexes in aqueous solution using manifold NMR techniques and could confirm the formation of $Tl(CN)_3$ in solution. The suggestion of E. Penna-Franca and R. W. Dodson that $Tl(CN)_3$ could be existing was verified (Batta et al., 1993; Blixt et al., 1989; Penna-Franca and Dodson, 1955). Furthermore, J. Glaser, M. Sandström and co-workers published structural data of thallium cyanide complexes of the structure $[Tl(CN)_n]^{(3-n)+}$ for n = 2, 3, 4 using X-ray and vibrational spectroscopy techniques in 1995 (Blixt et al., 1995). In the following years equilibrium dynamics including different ligand exchange processes were investigated (Bányai et al., 1997, 2001). A synthesis of $Tl(CN)_3$ using thallium trichloride and trimethylsilyl cyanide by D. Williams et al. was not successful due to the formation of a material $Tl_2(CN)_4$ containing Tl^+ and Tl^{3+}, but four years later results of single crystal XRD experiments on the unstable adduct $Tl(CN)_3{\cdot}OH_2$ (Nagy et al., 2005; Williams et al., 2001).

M. Maliarik, I. Tóth and co-workers dissolved Tl_2O_3 in water in the presence of strongly complexing cyanide ions. By this procedure they were able to identify the formation of $Tl(CN)_{3(aq)}$ by means of ^{205}Tl NMR studies (Nagy et al., 2005). The dominant cyano complex of thallium(III) obtained in this way is $Tl(CN)_{3(aq)}$, which is in equilibrium with bicyano and tetracyano species (Scheme 42). When aqueous solutions of the MCN (M = Na^+, K^+) salts are used to dissolve thallium(III) oxide, the equilibrium in the liquid phase shifts completely to the $[Tl(CN)_4]^-$ complex, which dominates at higher pH values and CN/Tl_2O_3 ratios (Nagy et al., 2005). The $Tl(CN)_3$ can be selectively extracted from aqueous solution containing $Tl(CN)_{3(aq)}$ with diethyl ether. Depending on the water content in the ether phase, $Tl(CN)_3{\cdot}H_2O$ or $Tl^{I}[Tl^{III}(CN)_4]$ crystals can be produced by slow evaporation of the solvent. In the crystal structure of $Tl(CN)_3{\cdot}H_2O$, the thallium(III)-ion has a trigonal-bipyramidal coordination with three cyanide ions in the equatorial plane, while an oxygen atom of the water molecule and a nitrogen atom from a cyanide ligand bonded to an adjacent thallium complex form a linear O–Tl–N fragment. Cyanide ligands act as bridging ligands connecting the thallium units in an infinite zigzag chain structure. Besides the formation of the Tl^{III}–CN complexes, notable redox reactions take place in the $Tl_2O_3/HCN/H_2O$ system. The redox reaction is complete when all thallium is in the form of Tl^{I} (reduction product) and the most stable cyano-complex of thallium(III), $[Tl^{III}(CN)_4]^-$, which yields $Tl^{I}[Tl^{III}(CN)_4]$ upon crystallization (see above) (Nagy et al., 2005).

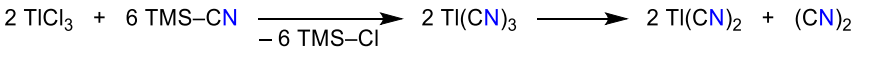

Scheme 41: Synthesis of $Tl(CN)_2$ by D. Williams et al. (Williams et al., 2001).

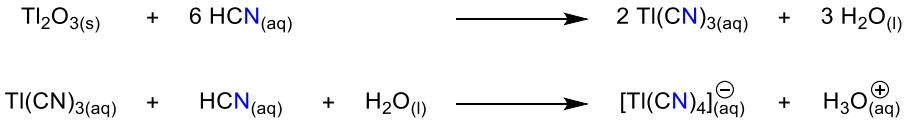

Scheme 42: Synthesis of $Tl(CN)_{3(aq)}$ and $[Tl(CN)_4]_{(aq)}^-$ from Tl_2O_3 in aqueous HCN (Nagy et al., 2005).

Tetracyanidothalliate anion $[Tl(CN)_4]^-$

The tetracyanidothalliate anion $[Tl(CN)_4]^-$ has been prepared in aqueous solutions for the purpose of studying the different resulting species like $Tl(CN)_{3(aq.)}$, $[Tl(CN)_2]^+_{(aq.)}$ or $[TlCN]^{2+}_{(aq.)}$. The determination of different characteristics like complex stability and electrochemical properties was achieved in these studies (Batta et al., 1993; Bányai et al., 1997, 2001; Blixt et al., 1989, 1995; Nagy et al., 2005). In this context, salts like $K[Tl(CN)_4]$ have been synthesized and crystallized by J. Glaser et al. in 1995 (and M. Maliarik, I. Tóth and co-workers – see above) by converting $Tl(ClO_4)_3$ into $K[Tl(CN)_4]$ according to Scheme 43 (Blixt et al., 1989).

The salts $K[Tl(CN)_4]$ and $Tl^I[Tl^{III}(CN)_4]$ are isostructural and derivatives of the Scheelite-type structure. The thallium–carbon distance was determined as $r_{Tl-C} = 2.175(10)$ Å which agrees with the overall tendency of decreasing bond lengths with an increasing number of cyanides. The C–N bond length of the cyanide group was determined as $r_{C-N} = 1.153(14)$ Å (Nagy et al., 2005). A strong absorption band of the cyanide stretching mode was observed at $\nu_{CN} = 2180\ cm^{-1}$ and the Tl–C band at $\nu_{TlC} = 358\ cm^{-1}$ (Blixt et al., 1995). It should be noted that the crystal data of D. Williams et al. (Williams et al., 2001) of $K[Tl(CN)_4]$ and $Tl^I[Tl^{III}(CN)_4]$ differ markedly from the data for the compound of the same composition, reported by M. Maliarik, I. Tóth and co-workers (Nagy et al., 2005).

4th Main group

While the cyanide compounds of the heavier 4th main group elements are not well investigated, the carbon cyanides have been studied by several approaches and the compounds have been analyzed for their characteristics. The inert pair effect also plays a major role in this group. For example, dicyanocarbene, $C(CN)_2$, is a highly reactive covalent molecular substance, while lead(II) dicyanide, $Pb(CN)_2$, is a classic, poorly soluble pseudohalogen salt. The $C(CN)_4$, in turn, can be generated, while the $Pb(CN)_4$ is unknown.

Of practical relevance are the cyanogen $(CN)_2$ and the tricyanomethanide anion $[C(CN)_3]^-$. While the acute toxicity of $(CN)_2$ constitutes a difficult aspect for research facilities, the reactivity and reaction behavior enable unique applications in synthetic chemistry. The $[C(CN)_3]^-$ anion possesses weakly coordinating characteristics due to delocalization effects within the anion and forms ILs with appropriate cations which can be applied in different fields. There are no significant applications known for Si, Ge, Sn or Pb cyanides and the interests in these compounds are so far based on fundamental research.

Carbon

The carbon cyanide compounds are by far the best investigated element cyanide species of all 4th main group compounds. The first reports about cyanogen $(CN)_2$ have been published in 1815 (Figure 28) (Gay-Lussac, 1815).

Cyanogen thus represents one of the earliest known cyanide compounds of all substances studied besides HCN and cyanido ferrate salts (see introduction). Similar to the tetracyanidoborate anion, tricyanomethanide $[C(CN)_3]^-$ has proven to be a WCA for ILs and has been intensively investigated with regard to its properties and possible applications (Brand et al., 2006). While carbon monocyanide CCN has mainly been studied due to spectroscopic interests motivated by observations of interstellar media, dicyanocarbene $C(CN)_2$ has been investigated regarding the appearance as highly reactive intermediate in several reactions (Kakimoto and Kasuya, 1982; Swenson and Renaud, 1965). Tetracyanomethane $C(CN)_4$ was successfully synthesized and characterized in 1969 (Mayer, 1969b).

Carbon monocyanide CCN

Speculations about the existence of the carbon monocyanide cation $[CCN]^+$ in interstellar media constituted the motive for the initial investigations. The first reports were published in the early 1980s. The studies covered experimental reactions of the cation with different small

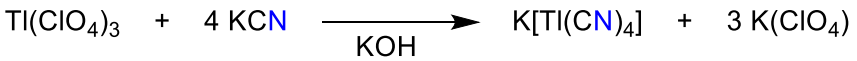

Scheme 43: Synthesis of the potassium salt of $[Tl(CN)_4]^-$ (Blixt et al., 1989).

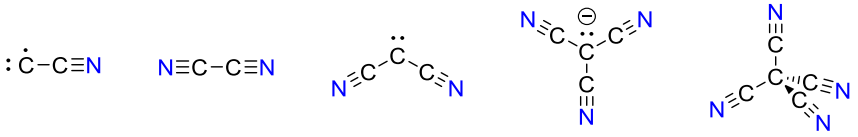

Figure 28: Structures of the mainly spectroscopically studied carbon monocyanide CCN, $(CN)_2$ known since 1815, the highly reactive dicyanocarbene $C(CN)_2$, the $[C(CN)_3]^-$ and tetracyanomethane $C(CN)_4$.

molecules like H_2O, H_2S, HCN, hydrocarbons and other as well as computations of the molecule discussing geometrical characteristics and mechanistic considerations (Knight et al., 1988; Kraemer et al., 1984; Largo-Cabrerizo and Barrientos, 1988; McEwan et al., 1983; Raksit and Bohme, 1985; Tao et al., 2002a, 2002b; Wu et al., 2000). The ion can be generated by laser ablation of graphite and an ensuing reaction with gaseous hydrogen cyanide, similar to the procedure for 3rd main group monocyanides (Parent, 1990). The computational studies found a C–C bond length of r_{C-C} = 1.383 Å and a C–N bond length of r_{C-N} = 1.149 Å (HF/6-31G* and HF/6-31G(d)). The characteristic cyanide stretching mode was calculated to appear between ν_{CN} = 2536 cm^{-1} and ν_{CN} = 2257 cm^{-1} depending on basis set (Knight et al., 1988; Largo-Cabrerizo and Barrientos, 1988). Another study confirmed the band at ν_{CN} = 2529 cm^{-1} by SCF calculations but documented additional values at ν_{CN} = 2342 cm^{-1} (CI–SD) and ν_{CN} = 2249 cm^{-1} (CI-SDQ) (Kraemer et al., 1984). A conclusion derived from the theoretical approaches is that the cyanide isomer is unstable compared to the $[CNC]^+$ cation. Based on these findings, C. G. Freeman, M. J. McEwan and co-workers speculate that the $[CCN]^+$ cation is unlikely to be present in interstellar media (Knight et al., 1988).

The linear CCN molecule and its isomer CNC has initially been studied by A. J. Merer and D. N. Travis in 1965 and 1966, respectively (Merer and Travis, 1965, 1966). Since these first studies, different investigations have been conducted concerning the IR and MW characteristics while both, experimental and computational results were published (Belbruno et al., 2001; Brazier et al., 1987; Georgieva and Velcheva, 2006; Grant Hill et al., 2011; Hakuta and Uehara, 1983; Kakimoto and Kasuya, 1982; Kawaguchi et al., 1984; Ohshima and Endo, 1995). The total number of publications specifically on the rotational spectra and the associated rotational constants is high despite the synthetic irrelevance of this molecule (Brazier et al., 1987; Kohguchi et al., 1997; Oliphant et al., 1990). The studies closer to a synthetic application investigated the kinetic constants of CCN radical reactions (Wang et al., 2006; Zhu et al., 2003). The computational results of bond distances compared in Table 35 vary insignificantly for the C–C bond length and C–N distance, independent on the level of theory and basis sets.

The carbon monocyanide CCN molecule can be generated by a reaction of acetonitrile and microwave-discharge products of sulfur hexafluoride, flash photolysis of diazoacetonitrile or photolysis of cyanotrichloromethane (Hakuta and Uehara, 1983; Merer and Travis, 1965; Zhu et al., 2003).

The anionic $[CCN]^-$ molecule was investigated by several groups mainly for spectroscopic characteristics as well. Among the theoretical approaches, aspects concerning the geometry of cluster molecules $[C_nN]^-$ with $n > 2$ were debated and whether the energetically favored structure would be linear or bent, especially calculations on higher levels of theory indicate a linear structure (Pascoli and Lavendy, 1999; Zhan and Iwata, 1996). The structural data are shown in Table 36.

Calculations of spectroscopic data fit well with the observations of ν_{CN} = 1779 cm^{-1} applying DFT methods and additional scaling results in a further decreased value of ν_{CN} = 1785 cm^{-1} as reported by I. Couturier-Tamburelli et al. (Guennoun et al., 2003). The synthesis of this anion was achieved by different techniques. It was usually prepared

Table 35: Experimental and computational data of CCN (bond lengths in Å; wave numbers in cm^{-1}).

Publication	Exp./calc.	r_{C-C}	r_{C-N}	ν_{CN}
Hakuta and Uehara (1983)	Exp. – LIF	–	–	1916.2
Oliphant et al. (1990)	Exp. – EES	–	–	1930.7
Martin et al. (1994)	CASSCF/pVDZ	1.4152	1.1993	1975.2
	CSSD(T)/TZ2P	1.3908	1.1811	1995.8
Belbruno et al. (2001)[a]	B3LYP/6-311G*	1.372	1.198	–
	B3LYP/cc-pVTZ	1.3680	1.1795	–
	B3LYP/cc-pVQZ	1.3669	1.1780	–
Georgieva and Velcheva (2006)	B3LYP/6–31 + G(d,p)	1.372	1.189	2033
Hill et al. (2011)	CSSD(T)/VDZ-F12	1.3825	1.1857	1923.4
	CSSD(T)/VTZ-F12	1.3808	1.1849	1930.3
	CSSD(T)/VDZ-F12	1.3805	1.1846	1932.3

[a]Calculations of CCN cluster.

Table 36: Experimental and computational data of $[CCN]^-$ (bond lengths in Å; wave numbers in cm^{-1}).

Publication	Exp./calc.	r_{C-C}	r_{C-N}	ν_{CN}
Wang et al. (1995)	RHF/3-21G	1.3443	1.1945	–
Zhan, Iwata (1996)	MP2(full)/6-31G(d)	1.357	1.224	1940.4
	MP2(full)/6-311G(d)	1.360	1.217	1920.4
	MP2(full)/6-311G(df)	1.354	1.213	1940.4
Pascoli, Lavendy (1999)	B3LYP/aug-cc-pVTZ	1.344	1.207	1758
	B3LYP/6-311G*	1.350	1.210	–
Couturier-Tamburelli et al. (2003), Guennoun et al. (2003)	B3LYP/6-31G**	–	–	1860
	Exp. – IR	–	–	1779

with other molecules of the $[C_nN]^-$ constitution and is accessible by laser ablation of different inorganic substances like $K_3[Fe(CN)_6]$, graphite/KCN or graphite/N_2 as well as by UV photoisomerization of cyanoacetylene or dicyanoacetylene and by electron impact on gaseous acetonitrile (Garand et al., 2009; Guennoun et al., 2003; Wang et al., 1995).

The according $[CCN]^{3-}$ anion has so far been calculated twice by P. Pyykkö and Y. Zhao and by M. K. Georgieva et al. and was reported with a characteristic cyanide absorption band at ν_{CN} = 1756 cm^{-1} (HF/6-31G*) or ν_{CN} = 1728 cm^{-1} (B3LYP/6–31 + G(d,p)), respectively (Georgieva and Velcheva, 2006). The C–C and C–N distances were also documented by P. Pyykkö and Y. Zhao (r_{C-C} = 1.315 Å, r_{C-N} = 1.310 Å, HF/6-31G*) (Pyykko and Zhao, 1990). In 1989, G. Boche et al. also reported the synthesis of a lithium dianion containing $[TMS–CCN]^{2-}$, which could be crystallized, and features several independent molecules with different structural parameters in the unit cell. The synthesis begins with a deprotonation of trimethylsilylacetonitrile with either two *n*-butyllithium or lithium diisopropylamide in ether/hexane that leads to the "dianion" Li_2(TMS–CCN), which crystallizes from this solution as $[(Li_2(TMS–CCN))_{12}(Et_2O)_6(C_6H_{14})]$. Twelve "dianions" form an aggregate with a crystallographic inversion center. There are three different "dianion" moieties, which differ in the number of their N–Li and C–Li contacts. The formal dianion, $[TMS–CCN]^{2-}$, can also be considered as an $[CCN]^{3-}$ trianion (with $TMS^+ + 2Li^+$ as counter ions) with bond lengths of r_{C-C} = 1.319 Å, r_{C-N} = 1.235 Å in average (Zarges et al., 1989).

Cyanogen $(CN)_2$

Already in 1959, T. K. Brotherton and J. W. Lynn published a detailed review about cyanogen, $(CN)_2$, a compound that was first successfully synthesized by L. J. Gay-Lussac in 1815, when he thermally decomposed silver cyanide (Brotherton and Lynn, 1959). While it is not settled with certainty that the substance had been prepared earlier than 1815, it is well known that the first preparation of oxalic acid was accomplished by F. Wöhler in 1825 by hydrolysis of cyanogen (Wöhler, 1825a). In the following, we will only briefly describe the chemistry of $(CN)_2$, otherwise we refer to the primary literature as well as the review articles.

Cyanogen is a highly flammable gas at ambient temperature and normal pressure and exothermically combusts in presence of oxygen, whereas a mixture of cyanogen and 14 vol% oxygen is explosive. Its toxicity results from the disproportion with water into hydrogen cyanide and isocyanic acid HNCO (Haas, 1978). Some additional characteristics are given in Table 37 (see also 1.5 HCN sources, toxicology, treatment, and mode of action (Newhouse and Chiu, 2010)).

Cyanogen can be synthesized by several different approaches. In laboratory scales, the decomposition of metal cyanides in an atmosphere of inert gas commonly provides cyanogen in sufficient amounts (Scheme 44). The presence of oxidizing agents can decrease the reaction temperature and increase the yield.

It is better to thermolyze silver cyanide to generate $(CN)_2$ than to use mercury dicyanide, which is easy to sublimate without releasing cyanogen (Haas, 1978). But in general, the decomposition of metal cyanides to obtain cyanogen is used less often in the meantime due to its inefficiency, hazardous nature and the danger of explosions caused by impurities like silver fulminate or mercury fulminate (Brotherton and Lynn, 1959).

The reaction of copper sulfate pentahydrate and potassium cyanide also leads to the formation of cyanogen in laboratory scales and the copper cyanide can be

Table 37: Some experimental data of cyanogen (bond lengths in Å; wave number in cm^{-1}; temperatures in K).

Publication	r_{C-C}[a]	r_{C-N}[a]	$\nu^{as}_{CN,\ exp.}$[b]	T_M	T_B	T_C
Perry and Bardwell (1925)	–	–	–	245.25	251.98	–
Cook and Robinson (1935)	–	–	–	245.3	251.98	–
Pauling et al. (1939)	1.37(2)	1.16(2)	–	–	–	–
Haas (1978)	–	–	2156	245.3	252.0	299.8

[a]Bond lengths determined by electron diffraction. [b]Wave numbers determined by IR spectroscopy.

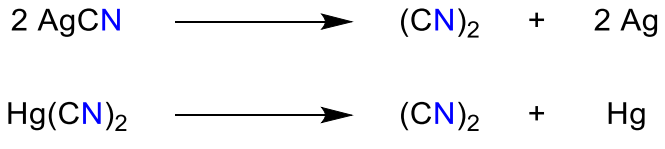

Scheme 44: Cyanogen received by decomposition of metal cyanides (Haas, 1978).

regenerated by addition of iron trichloride causing additional release of cyanogen (Scheme 45) (Haas, 1978).

Another synthetic route is the pyrolysis of diacetylglyoxime, which also avoids the formation of additional toxic by-products and the reaction scale can be adjusted easily (Scheme 46) (Park et al., 1990).

Industrial processes are based on the oxidation of hydrogen cyanide with oxygen. Cyanoformamide and oxamide are accessible on this way as well (Scheme 47). The kind of product, which is preferentially formed, depends on the reaction conditions due to the co-catalytic effect of copper nitrate and the solvent. The use of acetonitrile leads to the formation of cyanogen, aqueous acetic acid increases the formation of cyanoformamide at 303–323 K, while the increase of temperature to 333–353 K favors oxamide (Riemenschneider, 1978).

As a highly reactive compound, cyanogen is an appropriate building block in organic chemistry. The reactions with amines, hydrazine, semicarbazide, aminoguanidine, hydroxylamine, ethene, dienes or magnesium organic compounds are reviewed in detail by T. K. Brotherton and J. W. Lynn (1959).

Cyanogen also polymerizes to black paracyanogen under the influence of heat or light, which has been known since the beginning of the nineteenth century (Delbrück, 1847). The amorphous structure of this polymer consists mostly of carbon atoms being sp^2-hybridized and bridging nitrogen (Figure 29). Heating the polymer to 873–1073 K leads to the release of cyanogen. This structure motiv is supported by a strong IR absorption band at 1500 cm^{-1} and a significantly weaker one at 2200 cm^{-1}. These absorption bands represent the C–N double bond vibration and the terminal C–N triple bond vibration, respectively. Moreover, ^{13}C solid state NMR and conductivity experiments also support the structure of paracyanogen as illustrated in Figure 29 (Maya, 1993).

Dicyanocarbene $C(CN)_2$

The first description of dicyanocarbene $C(CN)_2$, which is also called dicyanomethylene, was published in 1965. The initial report by J. S. Swenson and D. J. Renaud regarded the formation of $C(CN)_2$ as an intermediate. The authors reported that the formation of 1,1-dicyanotetramethylcyclopropane due to *in situ* generated $C(CN)_2$ in presence of tetramethylethylene (TME) proves the existence of the carbene in the reaction mixture as a highly reactive intermediate (Scheme 48) (Swenson and Renaud, 1965).

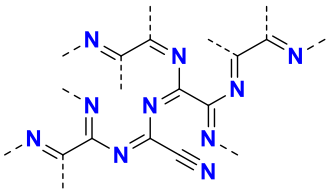

Figure 29: Possible representation of the structure of paracyanogen (representation taken from L. Maya (Maya, 1993) and based on a proposed structure by Brotherton and Lynn (1959).

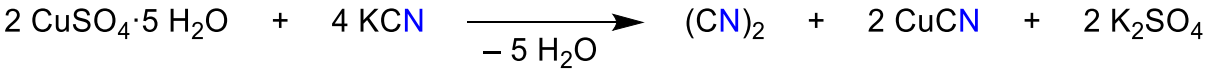

Scheme 45: Alternative formation of cyanogen in laboratory scales (Haas, 1978).

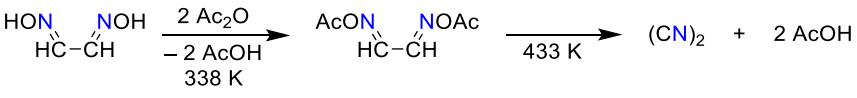

Scheme 46: Cyanogen received by pyrolysis of diacetylglyoxime (Park et al., 1990).

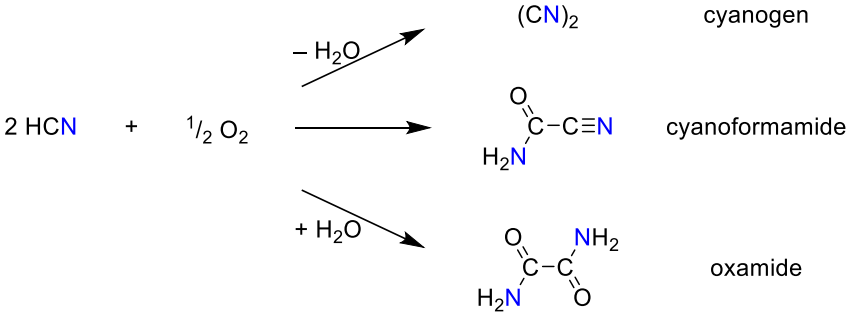

Scheme 47: Formation of cyanogen, cyanoformamide and oxamide by oxidation of hydrogen cyanide (Riemenschneider, 1978).

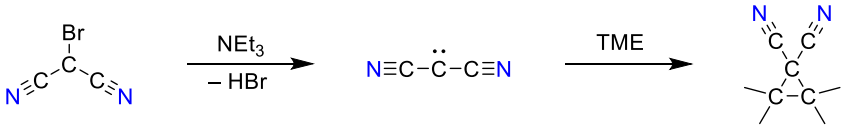

Scheme 48: Formation of 1,1-dicyanotetramethylcyclopropane due to the reaction of *in situ* generated $C(CN)_2$ with tetramethylethylene (TME) (Swenson and Renaud, 1965).

Ensuing this observation, E. Wasserman et al. published results including electron paramagnetic resonance (EPR) measurements of dicyanocarbene resulting from a photolysis of diazomalononitrile (Scheme 49).

Based on their results, E. Wasserman and co-workers interpreted the structure of dicyanocarbene as linear in a fluorolobe matrix but slightly bent at the carbon center in a hexafluorobenzene matrix (Wasserman et al., 1965). This second observation was supported a few years later by R. R. Lucchese and H. F. Schaefer and their calculations using SCF methods (Lucchese and Schaefer, 1977). More recent calculations predict a linear structure of the ground state molecule in contrast to the first theoretical report, but bent structures of excited states have also been calculated (Blanksby et al., 2000; Chaudhuri and Krishnamachari, 2007; Hajgató et al., 2002; Maier et al., 2003). R. Hoffmann and co-workers concluded based on their theoretical approaches that there should be no doubt that the ground state of these molecules, including dicyanocarbene, would be a linear triplet (Hoffmann et al., 1968). Further reports dealt with the experimental and theoretical values for the IR active stretching mode of the cyanide groups and the C–C bond length (Table 38).

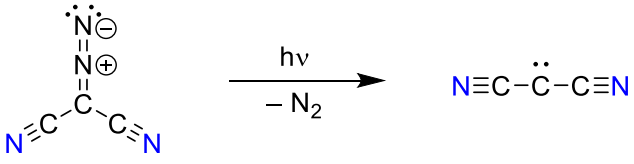

Scheme 49: $C(CN)_2$ formed by photolysis of diazomalononitrile (Wasserman et al., 1965).

Furthermore, the report of R. R. Lucchese and H. F. Schaefer from 1977 noted an interesting inconsistency between the experiment and expectations regarding the bond lengths in the molecule. The C–C distance was calculated as r_{C-C} = 1.41 Å, which is slightly closer to a double than a single bond (r_{cov}(C–C) = 1.50 Å, r_{cov}(C=C) = 1.34 Å) (Lucchese and Schaefer, 1977). This issue can be explained by the resonance structures shown in Figure 30.

Hence, the C–N distance would be expected to have a significantly stronger double bond character. Instead, the calculated value of r_{C-N} = 1.15 Å agrees with the expectations of a C–N triple bond (r_{cov}(C≡N) = 1.14 Å) (Lucchese and Schaefer, 1977; Pyykkö and Atsumi, 2009). Additional studies led to similar results with slightly longer C–N distances of r_{C-N} = 1.183 Å or r_{C-N} = 1.1941 Å, but significantly shorter C–C bond lengths of r_{C-C} = 1.3176 Å or r_{C-C} = 1.310 Å indicating a triple bond character (Blanksby et al., 2000; Hajgató et al., 2002). Some studies also investigated the MS spectra of different dicyanocarbene precursors and detected the $[C(CN)_2]^+$ cation in addition (Blanksby et al., 2000; Hajgató et al., 2002; Smith-Gicklhorn et al., 2002).

Tricyanomethanide $[C(CN)_3]^-$

Due to the high reactivity and strong acidity the synthesis and following isolation of tricyanomethane $HC(CN)_3$, which is also known as cyanoform in regard to the

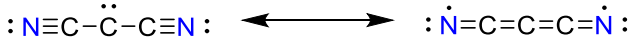

Figure 30: Resonance structures of dicyanocarbene.

Table 38: Some computational data of $C(CN)_2$ (bond lengths in Å; angles in °; wave number in cm^{-1}).

Publication	Method + basis set	state	r_{C-C}	r_{C-N}	< (C–C–C)	ν_{CN}
Lucchese and Schaefer (1977)	SCF/D95V	$^3B_1$	1.407	1.154	132.5	–
		$^1A_1$	1.421	1.160	114.9	–
Blanksby et al. (2000)	B3LYP/6-31 + G(d)	$^3\Sigma_g$	1.3176	1.1941	180.0	–
		$^1A_1$	1.3694	1.1811	123.6	–
Hajgató et al. (2002)	B3LYP/67–311 + G(3df)	$^3B_1$	1.310	1.183	180.0	–
		$^1A_1$	1.359	1.170	125.2	–
Maier et al. (2003)	B3LYP/6-311 + G*	$^3\Sigma_g$	1.312	1.186	180.0	2023.4
Chaudhuri and Krishnamachari (2007)	CASSCF/ANO	$^3\Sigma_g$	1.301	1.197	180.0	1892.4
		$^1A_1$	1.400	1.153	113.2	2348.9

haloform compounds HCX_3 with X = Cl^-, Br^- and I^-, was difficult. However, in 1977 B. Bak and H. Svanholt could identify cyanoform by MW spectroscopy (Bak and Svanholt, 1977). An excellent review on different reported approaches to generate pure cyanoform was given by L. B. McCusker, J. D. Dunitz and co-workers in 2010 (Šišak et al., 2010). Seven years later K. Banert et al. published another report dealing with the formation of $HC(CN)_3$. Their isolation is based on a reaction of the potassium tricyanomethanide and a strong acid, sulfuric acid for example, and following sublimation (Scheme 50) (Banert et al., 2017).

With an approximate pK_a of –5, cyanoform is classified as a super acid. Studies on the crystal structure also led to the discovery of the dicyanoketenimine as a tautomeric species (Šišak et al., 2010).

In 1896 Schmidtmann reported the synthesis of cyanoform, but actually he isolated and identified salts containing the tricyanomethanide anion. His early work included the simple silver and sodium tricyanomethanide salts and he already noticed analogies between the silver tricyanomethanide and silver halides (Brand et al., 2008). His findings were confirmed and pursued three years later by A. Hantzsch and G. Osswald who especially mentioned the similar characteristics of tricyanomethane and trinitromethane and their anions, respectively (Hantzsch and Osswald, 1899). Four years after the initial report of the series of pseudohalogens, L. Birckenbach and K. Huttner devoted a chapter of their essay entitled "Über Pseudohalogene" (About pseudohalogens) to the tricyanomethanide (see 1.2 Cyanide, a classic pseudohalide) (Birckenbach and Kellermann, 1925a, 1930; Birckenbach and Kolb, 1933; Birckenbach and Linhard, 1929; Brand et al., 2007; Jäger et al., 1992). The authors concluded that the reaction behavior and the general characteristics of the tricyanomethanide prove that the concept of pseudohalogens is not limited to inorganic chemistry but can also be applied to organic molecules and that the halogen-like chemical behavior results from the electronic configuration of the valence sphere (Birckenbach et al., 1929b; Brand et al., 2008). In 1922, W. Madelung and E. Kern already described the analogies of tricyanomethanide, dicyanamide and thiocyanate concerning characteristics and reaction behavior (Madelung and Kern, 1922a).

There are various successful synthetic routes to tricyanomethanide salts. The most common methods utilize malononitrile as starting material. The two main procedures are illustrated in a generalized modality in Scheme 51 (Schmidtmann, 1896; Trofimenko et al., 1962).

Aside of the interests in the fundamental characteristics of cyanoform and its anion, tricyanomethanides were investigated for possible applications as ILs and building blocks in coordinative polymers (Batten and Murray, 2003; Bernsdorf et al., 2009a; Brand et al., 2006; Cioslowski et al., 1991; Hipps and Aplin, 1985; Weidinger et al., 2012; Zhang et al., 2003). Starting in the second half of the nineteenth century, various tricyanomethanide salts were synthesized and characterized by different groups and a detailed review on metal containing tricyanomethanide salts (especially Cu(II), Ni(II) and Co(II)) was given by J. Kohout et al. (2000). Several studies on ILs containing $[C(CN)_3]^-$ as WCA have been published in the early years of this century and different synthetic routes towards various carbon based ILs were reported by A. Schulz and co-workers in 2006. The resulting room temperature ionic liquids (RTILs) are distinguished by low melting points and relatively high decomposition points ([EMIM][$C(CN)_3$]: T_M = 262 K, $T_{Dec.}$ = 513 K; [BMIM][$C(CN)_3$]: T_M = 225 K, $T_{Dec.}$ = 543 K) (Brand et al., 2006). Three years later, A. Schulz and co-workers expanded the methodology and synthesized advanced WCAs. The concept included the formation of Lewis acid-base adducts between nitrogen and bulky substituted boron atoms leading to a different group of carbon based ILs (Bernsdorf et al., 2009a). A rather unusual but nevertheless interesting application was investigated in 2009 when Z. Shou and J. M. Shreeve and co-workers described hypergolic ILs based on different WCAs

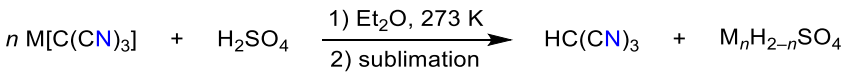

Scheme 50: Synthesis of tricyanomethane by K. Banert, H. Beckers et al. (n = 1, 2) (Banert et al., 2017).

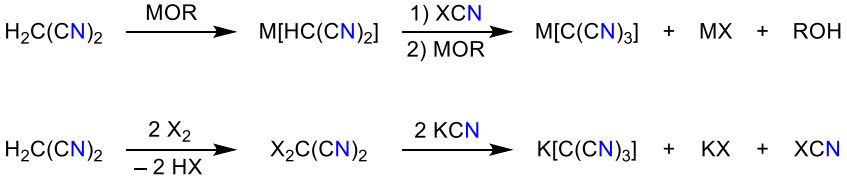

Scheme 51: Generalized synthetic routes to obtain tricyanomethanide salts (Schmidtmann, 1896; Trofimenko et al., 1962).

including tricyanomethanide (Gao et al., 2009). Another possible application are alkylmethylimidazolium cation/tricyanomethanide anion based membranes that exhibit CO_2 selectivity and permeability (Tzialla et al., 2013).

The molecular characteristics of the tricyanomethanide anion were elaborated by different groups and different approaches. The C–C and C–N bond lengths were determined by various computational levels of theory and by XRD (Andersen and Klewe, 1963; Brand et al., 2006; Dixon et al., 1986). Similar to the dicyanocarbene, the C–C distance is shorter than the expected value of a C–C single bond and thereby indicates a significant double bond character which can be explained by the resonance structure shown in Figure 31. Due to the strong delocalization (122.8 kcal mol^{-1} resonance energy) (Brand et al., 2008) within the $[C(CN)_3]^-$ ion, it is planar in contrast to $[H_2CCN]^-$. Note $[HC(CN)_2]^-$ is also planar. A CN group attached to a methanide C atom forms always a linear or nearly linear [< (C–C–N) = 175°] CCN moiety. Upon further CN substitution the C–CN bond lengths increases (CM: 1.380, DCM: 1.391, TCM: 1.406 Å) while the CN bond lengths decreases (CM 1.179, DCM: 1.169, TCM: 1.162 Å). Due to the very good delocalization of the π-electrons, the planar $[C(CN)_3]^-$ anion is only very weakly basic, which conversely means that $HC(CN)_3$ is a very strong acid. There are two almost energy-equal tautomers of the acid, namely non-planar cyanoform $HC(CN)_3$ and a planar ketenimine tautomer $HNC(CN)_2$ (Figure 31) (Banert et al., 2017).

Based on computational results of geometrical properties, frequency analyses have been carried out to predict vibration spectra and to compare them with experimental results (Beaumont et al., 1984; Long et al., 1962). Early calculations of the asymmetric C–N stretching mode from 1986 using a 3-21G basis set predicted the appearance around ν_{CN} = 2471 cm^{-1} (Dixon et al., 1986). These results disagree with experimental values by $\Delta\nu$ = 300 cm^{-1}. With the advancements in computational chemistry and higher levels of theory, this variance was reduced to $\Delta\nu$ = 60 cm^{-1} in 2012 (Weidinger et al., 2012). Some results from different references are compiled in Table 39.

Regarding the computational approaches, the tricyanomethanide anion is computed with D_{3h} symmetry. This assumption was generally confirmed by XRD of different salts. However, observations indicating a C_{2v} distortion depending on the specific salt need to be mentioned (Dixon et al., 1986).

Tetracyanomethane $C(CN)_4$

The synthesis of tetracyanomethane $C(CN)_4$ was achieved by E. Mayer in 1969 by metathesis of cyanogen chloride and silver tricyanomethanide (Scheme 52).

Mayer also recorded IR spectra of the product to determine whether he obtained tetracyanomethane or tricyano-isocyano-methane. According to his interpretation, the spectra confirmed a molecule exhibiting T_d symmetry and consequently the formation of $C(CN)_4$ instead of its isomer and the T_d symmetry was confirmed by ensuing studies (Hester et al., 1970; Mayer, 1969b; Oberhammer, 1971). Furthermore, Mayer documented the high reactivity of $C(CN)_4$ by conducting several experiments. He proved that the highly reactive compound readily undergoes hydrolysis in acidic and basic aqueous solutions (Scheme 53).

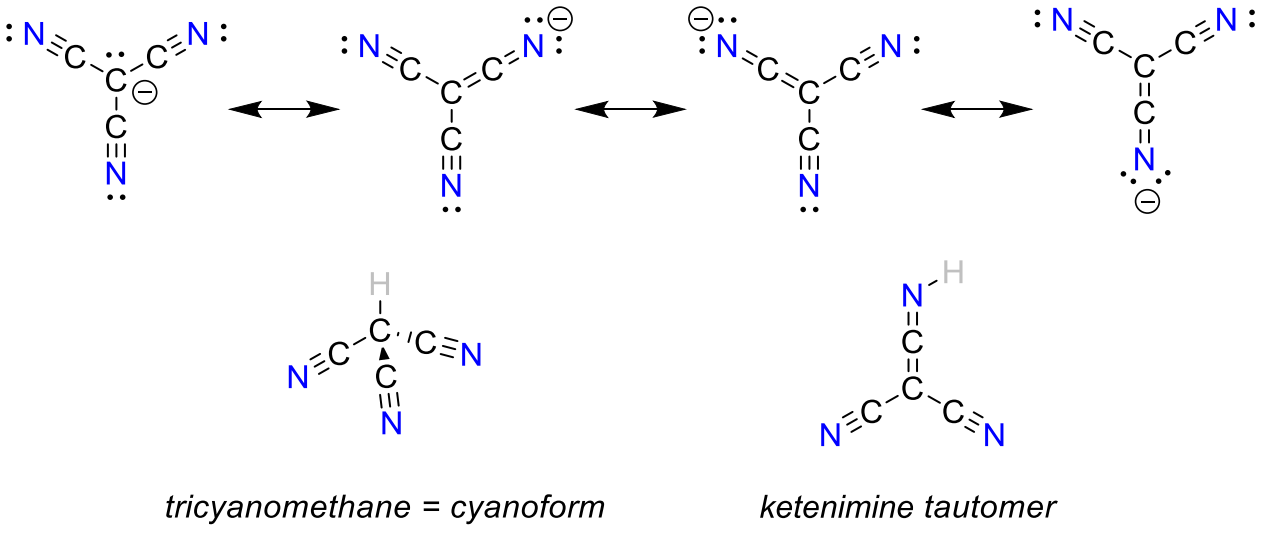

Figure 31: Top: Possible resonance structures of the tricyanomethanide anion and bottom: Tautomers of $HC(CN)_3$.

Table 39: Experimental and computational data of the $[C(CN)_3]^-$ anion (bond lengths in Å; wave numbers in cm^{-1}).

Publication	Exp./calc.	Cation	r_{C-C}	r_{C-N}	$\nu^{as.}_{CN}$
Long et al. (1962)	Exp. – IR	K^+	–	–	2175
Andersen and Klewe (1963)	Exp. – XRD	K^+	1.40	1.15	–
Desiderato and Sass (1965)	Exp. – XRD	$[H_4N]^+$	1.40(1)	1.15(1)	–
Konnert and Britton (1966)	Exp. – XRD	Ag^+	1.54(9)	1.10(9)	–
Köhler and Seifert (1968)	Exp. – IR	$[SnMe_2]^{2+}$	–	–	2185
		$[SnPh_2]^{2+}$	–	–	2175–90
Beaumont et al. (1984)	Exp. – IR	K^+	–	–	2170
Dixon et al. (1986)	Exp. – XRD, IR	$[Fe(Cp)_2]^+$	1.402	1.159	2162
		$[Bu_4N]^+$	–	–	2158
	HF/3-21G	–	1.399	1.149	2471
Cioslowski et al. (1991)	HF/6-31G*	–	1.412	1.145	–
Dua et al. (2000)	B3LYP/6-31 + G*	–	1.4126	1.1732	–
Brand et al. (2006)	Exp. – Raman	$[EMIm]^+$	–	–	2178
	Exp. – Raman	$[BMIm]^+$	–	–	2166
	B3LYP/aug-cc-pVTZ	–	1.406	1.162	2292
Bernsdorf et al. (2009a)	Exp. – IR	K^+	–	–	2171
	exp. – IR	Ag^+	–	–	2174
Weidinger et al. (2012)	Exp. – IR	K^+	–	–	2170
	MP2/aug-cc-pVDZ	–	–	–	2146.7
	B3LYP/aug-cc-pVDZ	–	–	–	2230.9
	B3LYP/aug-cc-pVTZ	–	–	–	2238.1

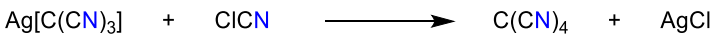

Scheme 52: Synthesis of $C(CN)_4$ by E. Mayer (1969b).

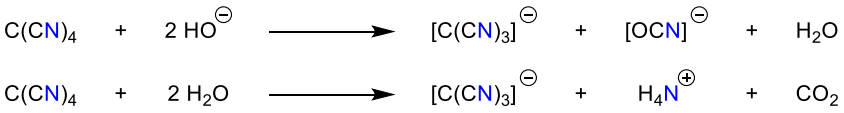

Scheme 53: Hydrolysis of $C(CN)_4$ in acidic and basic aqueous solution (Mayer, 1969b).

Also, the reverse reaction to form tricyanomethanide salts starting with the $C(CN)_4$ occurs with different salts. The conversion with lithium chloride gave lithium tricyanomethanide and cyanogen chloride in quantitative yields (Scheme 54). Additionally, the author mentioned that the formation of the $[C(CN)_3]^-$ anion was partially observed in the KBr pellet which was prepared for IR spectroscopic measurements (Mayer, 1969b).

Other reports investigated structural aspects by electron diffraction in gas phase, single crystal XRD and computations (Britton, 1974; Oberhammer, 1971; Salzner and von Raguè Schleyer, 1992; Wiberg and Rablen, 1993). IR measurements generally confirmed the data obtained by E. Mayer in 1969 (Hester et al., 1970). Due to E. Mayer's findings, a number of studies dealing with $C(CN)_4$ were conducted, but since the report on the crystal structure has been published by D. Britton in 1974, no ensuing experimental studies have been published (Britton, 1974). A compilation of published results is given in Table 40.

Two studies in the early 1990s supplementary discussed the varying properties of carbon tetrahalides. Both studies referred to the destabilizing character of the cyanide being part of the pseudohalogens in contrast to the stabilizing effect of fluorine substituents in compounds of a central carbon (Salzner and von Raguè Schleyer, 1992). According to K. B. Wiberg and P. R. Rablen, the

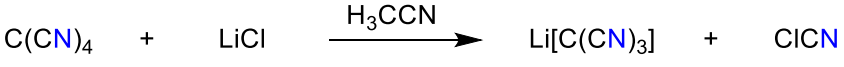

Scheme 54: Reverse reaction of $C(CN)_4$ to form salts containing $[C(CN)_3]^-$ (Mayer, 1969b).

Table 40: Experimental and computational data of $C(CN)_4$ (bond lengths in Å; wave numbers in cm^{-1}).

Publication	Exp./calc.	r_{C-C}	r_{C-N}	ν_{CC}	ν_{CN}
Mayer (1969b)	Exp. – IR	–	–	1058	2273
Hester et al. (1970)	Exp. – IR – solid	–	–	1056	2276
	Exp. – IR – vapor	–	–	1061	2270
Oberhammer et al. (1971)	Exp. – GED	1.484(5)	1.161(3)	–	–
Britton (1974)	Exp. – XRD	1.488	1.168	–	–
Salzner and von Rahué Schleyer (1992)	HF/6-31G**	1.484	1.131	–	–
Wiberg and Rablen (1993)	RHF/6-31G*	1.484	1.131	–	–
	MP2/6-31G*	1.479	1.181	–	–

destabilization is based on the strong π-acceptor properties of the cyanide group and the resulting accumulation of positive charge at the carbon center, which leads to an increasing coulomb repulsion (Wiberg and Rablen, 1993).

Graphitic carbon nitride (g-C_3N_4)

Graphitic carbon nitride (g-C_3N_4) is a class of binary CN layer compounds (often with non-zero hydrogen contents) based on heptazine and poly(triazine imide) units that exhibit different degrees of condensation, properties and reactivities depending on the reaction conditions (*T*, *p*, solvent, starting materials, etc., Scheme 55). Graphitic carbon nitride can be produced by polymerization of cyanamide, dicyandiamide or melamine. There are also methods of synthesizing graphitic carbon nitrides by heating a mixture of melamine and uric acid in the presence of alumina or by condensation of melamine and cyanuric chloride with triethylamine as solvent under supercritical conditions. Pyrolysis of melamine (in the presence of hydrazine) also yields g-C_3N_4. Graphitic carbon nitride (g-C_3N_4) has attracted much attention because of its high activity and efficient absorption of visible light. It is a binary CN layer compound with high chemical and thermal stability due to the strong covalent bond between the carbon and nitrogen atoms in the conjugated layer structure. Graphitic carbon nitride has a moderate band gap energy of 2.7 eV (460 nm), which can harvest visible light, and a suitable CB and VB edge position for both water reduction and oxidation. For this reason, g-C_3N_4 has quickly become a modern area of research as a potential "green" photocatalyst and has already expanded the field of photocatalysis. There is an abundance of review articles (Chen and Bai, 2020; Darkwah and Ao, 2018; Liu et al., 2020; Ong et al., 2016; Rhimi et al., 2020; Wen et al., 2017; Zhang et al., 2019) as well as articles dealing with its synthesis, characterization and application, which we do not wish to repeat here and therefore refer to these publications.

Silicon

Silicon cyanide compounds (cyanosilanes) have not been studied as intensively as carbon cyanides. The silicon monocyanide SiCN (Apponi et al., 2000; Flores, 2005; Guélin et al., 1986; Jin-chai et al., 2001; Largo-Cabrerizo, 1988; Maier et al., 1998; McCarthy et al., 2001; Ng et al., 2006; Pham et al., 2006; Richardson et al., 2003; Yamamoto and Okabe, 2011) has primarily been studied while the number of reports on $Si(CN)_2$ (Maier and Reisenauer, 2005; Sakai and Inagaki, 1990) and $Si(CN)_4$ is comparatively small. Salts bearing the octahedral hexacyanidosilicate, $[Si(CN)_6]^{2-}$, have been reported recently (Harloff et al., 2020a, 2019b; Smallwood et al., 2019). About neutral binary Si–CN

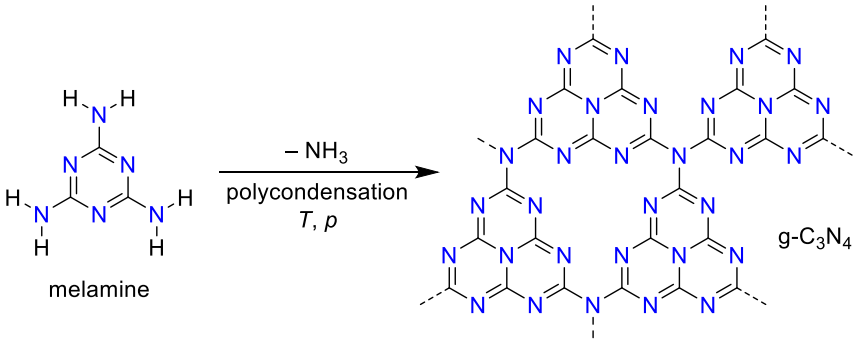

Scheme 55: Synthesis of g-C_3N_4 (Chen and Bai, 2020; Darkwah and Ao, 2018; Liu et al., 2020; Ong et al., 2016; Rhimi et al., 2020; Wen et al., 2017; Zhang et al., 2019).

compounds (e.g. SiCN and $Si(CN)_2$) (Fukushima and Ishiwata, 2013; Guélin et al., 1986; Maier and Reisenauer, 2005; Maier et al., 1998; Mandal and Roesky, 2010; McCarthy et al., 2001; Richardson et al., 2003), which have been studied in an argon matrix or observed in the envelope of a star (Guélin et al., 1986, 2004; Mandal and Roesky, 2010), little is known, although cyanide-containing silanes, such as cyanotrimethylsilane (TMS–CN), are well known in organic chemistry for their versatile use as cyanosilylation reagents in combination with Lewis acids or bases (Bither et al., 1958; Booth and Frankiss, 1968; Groutas, 2001; Kalikhman et al., 2007; North et al., 2012). The more highly substituted dicyanodimethylsilane can be used as a protecting group (Mai and Patil, 1986; Ryu, 2001; Ryu et al., 1978), while the tricyanomethylsilane has not yet been isolated but is believed to be formed *in situ* in a reaction of $MeSiCl_3$ with KCN (Duboudin et al., 1983).

Silicon monocyanide SiCN and its substituted cation

The term "SiCN" is also commonly used in material sciences for amorphous solids and nanoparticles containing mainly silicon, carbon and nitrogen and should not be confused with the silicon monocyanide molecule which has so far not been synthesized in significant amounts (Jinchai et al., 2001; Ng et al., 2006; Pham et al., 2006).

The motivation behind the investigation of the silicon monocyanide radical $[SiCN]^{\cdot}$ corresponds with those of many other lighter element monocyanide compounds. An initial report about a new molecule observed in the envelope of the star IRC + 10216 in 1986 was followed by theoretical studies regarding the characteristics of this compound (Guélin et al., 1986). According to these calculations, the cyanide and its isomer $[SiNC]^{\cdot}$ both presumably appear linear in the $^2\Pi$ ground state with the cyanide being the more stable isomer at several MP levels, but not at UHF level being the isocyanide the favored isomer (Largo-Cabrerizo, 1988). A more extensive study was conducted by G. Maier et al. in 1998 including additional computations and IR measurements of prepared $[SiCN]^{\cdot}$ molecules trapped in an argon matrix (Maier et al., 1998).

Both studies reported findings on the isomerization barrier, which is reported to be ΔE = 75 kJ mol^{-1} and isomerization occurring at a wave length of 366 nm. This aspect was additionally highlighted in a detailed report by N. A. Richardson et al. including calculations using numerous levels of theory. The results matched the predictions by A. Largo-Cabrerizo from 1988 well, even though the levels of theory explicitly differ (Largo-Cabrerizo, 1988; Richardson et al., 2003). Although some levels of theory indicate that the isocyanide is the stable isomer, both authors concluded that the cyanide species is predicted to be more stable by about $\Delta E \approx 9$ kJ mol^{-1} and that the barrier of isomerization accounts for about $\Delta E(\mathrm{TS}) \approx 95$ kJ mol^{-1} (Table 41). The detailed report by N. A. Richardson et al. illustrates the significance of the employed computational method (Richardson et al., 2003). Due to the interest of astronomers and astrophysicists, P. Thaddeus and coworkers recorded and analyzed radio and rotational spectra of the molecule (Apponi et al., 2000; McCarthy et al., 2001).

By treatment of TMS–CN with [TMS–H–TMS]WCA ($[WCA]^- = [B(C_6F_5)_4]^-$), it was possible to prepare the first example of a bissilylated $[TMS–CN–TMS]^+$ ion, a so-called pseudohalonium cation, in high yields. It is thermally stable up to 461 K and the Si–CN–Si moiety is almost linear

Table 41: Some computational data of $[SiCN]^{\cdot}$ (bond lengths in Å; wave numbers in cm^{-1}; energies in kJ mol^{-1}).

Publication	Method + basis set	r_{Si-C}	r_{Si-N}	ν_{CN}	ΔE(iso.)	ΔE(TS)
Largo-Cabrerizo (1988)	UHF/6-31G(d)	1.866	1.746	2135	−10.0	–
	MP2/6-31G(d)	–	–	–	9.6	85.8
	MP3/6-31G(d)	–	–	–	3.8	–
Maier et al. (1998)	B3LYP/6-311G**	1.857	1.752	2046.1	10.5	–
Richardson et al. (2003)	SCF/TZ2P	1.8812	1.7471	2458	−16.66	101.07/91.27
	SCF/cc-pVTZ	1.8826	1.7461	2459	−20.72	101.57/89.51
	CCSD/TZ2P	1.8717	1.7577	2185	9.29	95.33/99.65
	CCSD/cc-pVTZ	1.8663	1.7502	2194	6.32	94.50/95.75
	CCSD(T)/TZ2P	1.8697	1.7594	2102	12.02	91.82/99.56
	CCSD(T)/cc-pVTZ	1.8635	1.7514	2109	9.46	90.85/95.63
Flores (2005)	B3LYP/6-311G*	1.851	1.743	–	8.0	87.50
	QCISD/6-311G*	1.863	1.751	–	–	–
	MRCISD/cc-pVDZ	1.879	1.785	–	–	–
Yamamoto and Okabe (2011)	B3LYP/6–311 ++ G(3df,3pd)	1.846	1.733	–	1.993	–

(<(C^1–N–Si^1) = 176.8(2)° and < (N–C^1–Si^2) = 178.5(2)°) with rather long Si–C (1.890(2) Å) and Si–N (1.888(2) Å) bond lengths (Schulz and Villinger, 2010).

Dicyanosilylene $Si(CN)_2$

Studies on dicyanosilylene are rare but the accessible reports consist of detailed theoretical calculations and even experimental results from gas phase reactions of silicon with cyanogen. The initial report was published by S. Sakai and S. Inagaki in 1990 and additional information were contributed by G. Maier and H. P. Reisenauer in 2005, especially, the formation of three different open-chain silylenes, dicyanosilylene, cyano(isocyano)silylene and di(isocyano)-silylene, originating from a cyclic intermediate (Maier and Reisenauer, 2005; Sakai and Inagaki, 1990). In the following year, M. Z. Kassaee et al. also examined different silylenes including dicyanosilylene in a theoretical approach (Kassaee et al., 2006). Regarding the energetic difference between dicyanosilylene and di(isocyano) silylene, the calculations by G. Maier and H. P. Reisenauer indicate a lower energy of $Si(NC)_2$. Due to the singlet ground state, an angled geometry results from the quantum mechanical calculations with < (C–Si–C) = 94.3° and a nearly linear Si–C–N angle of about < (Si–C–N) ≈ 170.4° (B3LYP/6-311 + G(3df,3pd)) (Maier and Reisenauer, 2005). The characteristics of $Si(CN)_2$ are given in Table 42.

Silicon tetracyanide $Si(CN)_4$

Silicon tetracyanide has been studied once by C. Glidewell in 1981 who determined the Si–C bond length of the tetrahedral molecule as r_{Si-C} = 1.756 Å and the bond length of the cyanide group as r_{C-N} = 1.163 Å in a theoretical study (MNDO) (Glidewell, 1981). A. Schulz and co-workers describe the formation of $Si(CN)_4$ in the thermal decomposition of $[^nPr_3NH]_2[Si(CN)_6]$ (Harloff et al., 2019b).

Hexacyanidosilicates $[Si(CN)_6]^{2-}$

Starting from fluoridosilicate precursors in pure cyanotrimethylsilane, TMS–CN, a series of different ammonium salts $[R_3NMe]^+$ (R = Et, ^{n}Pr, ^{n}Bu) were synthesized with $[SiF(CN)_5]^{2-}$ and $[Si(CN)_6]^{2-}$ dianions in simple, temperature-controlled $F^-/[CN]^-$-exchange reactions (Figure 32, Schemes 56 and 57). With decomposable, non-innocent cations like $[R_3NH]^+$, metal salts of the type $M_2[Si(CN)_6]$ (M = Li^+, K^+) could be prepared by neutralization reactions with corresponding metal hydroxides. The ionic liquid $[BMIm]_2[Si(CN)_6]$ (T_M = 345 K, $[BMIm]^+$ = 1-butyl-3-methyl-imidazolium) was obtained by a salt metathesis reaction (Harloff et al., 2019b).

Starting from chloride-containing precursors to synthesize salts with the $[Si(CN)_6]^{2-}$ dianion does not work well (e.g. $SiCl_4$ with two equivalents of [WCC]CN and four equivalents of AgCN; Scheme 56) (Campbell et al., 2015). All attempts at a full hexa-substitution failed, even when using a large excess of both cyanide sources.

P. Portius and co-workers also reported this problem and attempted to further convert the respective isolated compounds $(PPN)_2[Si(CN)_xCl_y]$ ($x + y = 6$) to the corresponding hexacyanidosilicate by multiple isolation/reaction with PPN[CN] ($[WCC]^+$ = $[PPN]^+$ = $[(Ph_3P)_2N]^+$) (Smallwood et al., 2019). However, it can be assumed that a

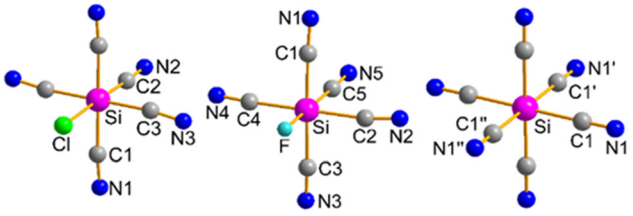

Figure 32: Ball-and-stick representation of the molecular anion structure in the crystal: Left: $[Ph_4P]_2[SiCl_{0.78}(CN)_{5.22}] \cdot 4\ CH_3CN$. Middle: $[^nPr_3NH]_2[SiF(CN)_5]$. Right: $[^nPr_3NH]_2[Si(CN)_6]$. Cations and solvent molecules are omitted for clarity (Harloff et al., 2019b).

Table 42: Computational data of $Si(CN)_2$ and its isomers (bond lengths in Å; angles in °; wave numbers in cm^{-1}; energies in kJ mol^{-1}).

Publication	Method + basis set	Compound	r_{Si-X}	r_{C-N}	< (A–Si–A)	< (Si–A–B)	$\nu^{as}_{CN,\ calc.}$	$\Delta E_{rel.}$
Maier and Reisenauer (2005)	B3LYP/6-311 + G(3df,3pd)	$Si(CN)_2$	1.872	1.157	94.3	170.4	2252	0.0
		NCSiNC	1.886/1.751	1.156/1.180	95.8	166.5/169.8	2261/2095	−0.8
		$Si(NC)_2$	1.758	1.179	97.0	165.0	2089	−8.0
Kassaee et al. (2006)	B3LYP/6–311++G**	$Si(CN)_2$	1.88	1.16	94.2	170.0	–	–
	MP2/6-311G**	$Si(CN)_2$	1.87	1.18	93.8	172.1	–	–

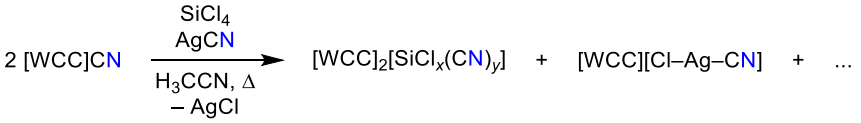

Scheme 56: Synthesis of salts bearing the $[Si(CN)_xCl_y]^{2-}$ ($x + y = 6$) ion (Campbell et al., 2015).

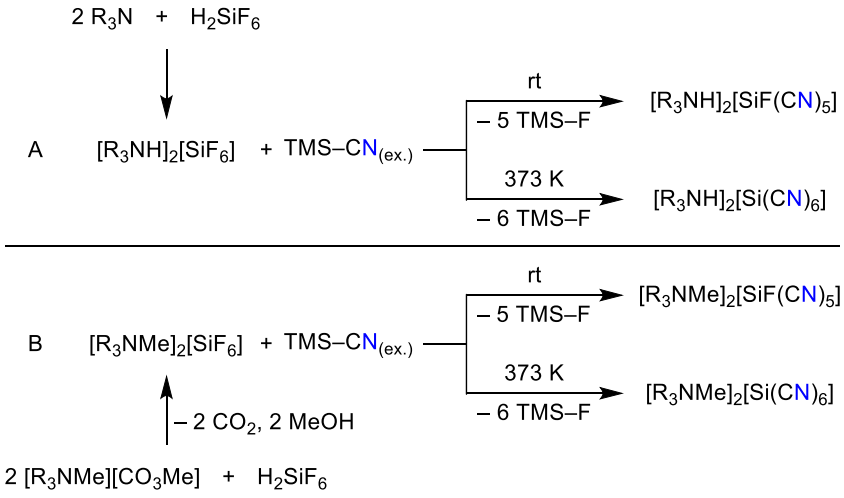

Scheme 57: Synthesis of salts bearing the $[Si(CN)_6]^{2-}$ ion (Finger and Sundermeyer, 2016; Glasnov et al., 2012; Holbrey et al., 2010; Jost et al., 2016; Thielemann and Spange, 2017; Zheng et al., 2007).

small chloride content always remains, as A. Schulz and co-workers were able to show (Harloff et al., 2019b). Therefore, the two synthesis routes A and B in Scheme 57 are more suitable for synthesizing highly pure, chloride-free $[Si(CN)_6]^{2-}$ salts. As shown in Scheme 57, amines NR_3 (R = Et, ^{n}Pr) can be reacted directly with aqueous hexafluorosilicic acid, H_2SiF_6, leading to the formation of the corresponding $[R_3NH]_2[SiF_6]$ salts in good yields. Secondly, ammonium methyl carbonates, ionic liquids with a decomposable anion (Finger and Sundermeyer, 2016; Glasnov et al., 2012; Holbrey et al., 2010; Jost et al., 2016; Thielemann and Spange, 2017; Zheng et al., 2007), were treated with aqueous H_2SiF_6, resulting in the preparation of tetraalkylated ammonium salts $[R_3NMe]_2[SiF_6]$ (R = Et, ^{n}Pr and ^{n}Bu) in very good yields. With the hexafluoridosilicates in hand, reaction with a large excess of TMS–CN, as a cyanidation reagent, led to the formation of salts containing the $[SiF(CN)_5]^{2-}$ ion (after 2 h at 298 K). However, when the temperature was raised to 373 K, the reaction led exclusively to the formation of $[Si(CN)_6]^{2-}$ salts (reaction time of 2 h). With small amounts of $GaCl_3$ as Lewis acid catalyst added to the reaction mixture, the reaction time could be shortened (Bläsing et al., 2016a, 2016b).

The great advantage of $[R_3NH]_2[Si(CN)_6]$ salts over $[R_3NMe]_2[Si(CN)_6]$ salts is that the former have a decomposable, non-innocent cation (Bläsing et al., 2016a; Bresien et al., 2015a). Therefore, these salts are particularly suitable for the synthesis of metal salts, as they can be reacted with corresponding metal bases (Scheme 58, eq. 1). The potassium salt can be converted into the BMIm salt in a mixture of H_2O/CH_2Cl_2 at 298 K. Thermal treatment of $[R_3NH]_2[Si(CN)_6]$ results in the liberation of HCN, free amine and $Si(CN)_4$ (Scheme 58, eq. 3) (Harloff et al., 2019b).

Functionalized imidazolium cations were combined with the hexacyanidosilicate anion by salt metathesis reactions with $K_2[Si(CN)_6]$, whereby ionic compounds of the general formula $[R\text{-}Ph(^n Bu)Im]_2[Si(CN)_6]$ (R = 2-Me, 4-Me, 2,4,6-Me = Mes, 2-MeO, 2,4-F, 4-Br; $[Im]^+$ = imidazolium). All synthesized imidazolium hexacyanidosilicates decompose when thermally treated above 368 K (369–437 K). Furthermore, the hexa-borane adduct $[Mes(^n Bu)Im]_2\{Si[CN\cdot B(C_6F_5)_3]_6\}\cdot 6\,CH_2Cl_2$ (Figure 33), which is thermally stable up

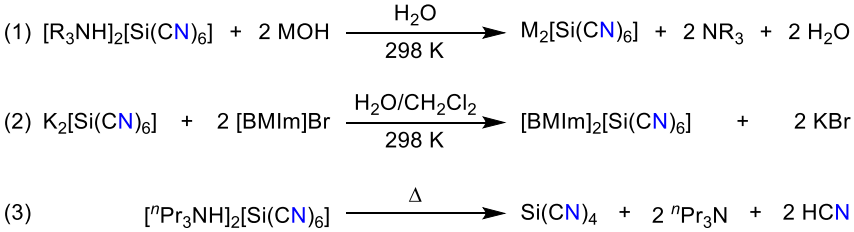

Scheme 58: Synthesis of salts bearing the $[Si(CN)_6]^{2-}$ ion (Harloff et al., 2019b).

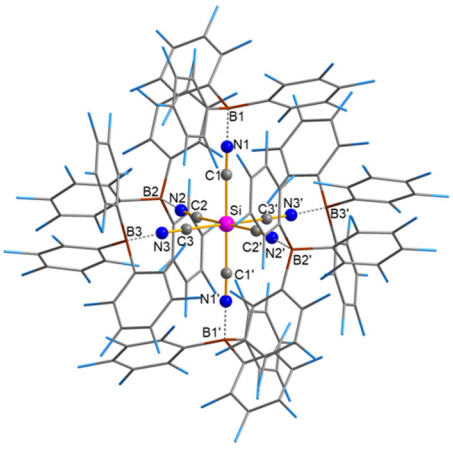

Figure 33: Molecular structure of the $\{Si[CN{\cdot}B(C_6F_5)_3]_6\}^{2-}$ anion (Harloff et al., 2020a).

to 488 K, is obtained from the reaction of $[Mes(^nBu)Im]_2[Si(CN)_6]$ with Lewis acid $B(C_6F_5)_3$ (Harloff et al., 2020a).

Germanium

While germanium monocyanide and its ions have exclusively been studied theoretically (Petrie, 1999b; Wang et al., 2005), germanium(II) and germanium(IV) cyanide have been prepared successfully (Bither et al., 1958; Bundhun et al., 2012; Menzer, 1958; Onyszchuk et al., 1986). Recently, salts containing the $[Ge(CN)_6]^{2-}$ anion were prepared (Smallwood et al., 2019).

Germanium monocyanide GeCN

S. Petrie examined trends of the main group elements of the third row and noted that GeCN is linear and the stable isomer in contrast to the lighter third row element monocyanides. Additionally, the barrier of isomerization appears to be lower compared to the corresponding potassium, calcium and gallium compounds.

Furthermore, they calculated the germanium cyanide cation and documented that its characteristics are comparable to those of isoelectronic GaCN in terms of the molecular geometry and the more stable isocyanide isomer (Petrie, 1999b). These results were confirmed by Q. Wang et al. in a detailed study concerning exclusively GeCN and its ions in 2005. According to their results, the cyanide species is the favored isomer of the anionic compound. A triplet state is documented for the anion while the singlet state of the isocyanide species is energetically favored by the cation (Wang et al., 2005). Selected calculated values are given in Table 43.

Table 43: Computational data of GeCN, its isomer and the cationic and anionic species (bond lengths in Å; wave numbers in cm^{-1}; energies in kJ mol^{-1}).

Publication	Method + basis set	Compound	r_{Ge-X}	r_{C-N}	ν_{CN}	$\Delta E_{rel.}$
Petrie (1999b)	MP2(full)/6-31G*	GeCN	1.996	1.148	–	–
		GeNC	1.774	1.189	–	–
		$[GeCN]^+$	1.909	1.199	–	–
		$[GeNC]^+$	1.798	1.219	–	–
Wang et al. (2005)	B3LYP/6-311G(d)	GeCN	1.9593	1.1648	2178	0.00
		GeNC	1.8773	1.1857	2039	21.48
		$^1[GeCN]^+$	1.9211	1.1658	2227	800.9
		$^3[GeCN]^+$	1.9590	1.1682	2123	1115.28
		$^1[GeNC]^+$	1.7949	1.2060	1975	780.21
		$^3[GeNC]^+$	2.0411	1.1630	2091	1050.09
		$^1[GeCN]^-$	1.9843	1.1733	2089	–100.06
		$^3[GeCN]^-$	2.0063	1.1703	2113	–182.50
		$^1[GeNC]^-$	1.9629	1.1808	2037	–49.95
		$^3[GeNC]^-$	1.9925	1.1771	2077	–137.75
	QCISD/6-311G(d)	GeCN	1.9738	1.1732	2140	–
		GeNC	1.8846	1.1907	2045	–
		$^1[GeCN]^+$	1.9203	1.1734	2194	–
		$^3[GeCN]^+$	2.0147	1.1778	2072	–
		$^1[GeNC]^+$	1.7882	1.2102	1978	–
		$^3[GeNC]^+$	2.3799	1.2534	1745	–
		$^1[GeCN]^-$	2.0185	1.1771	2111	–
		$^3[GeCN]^-$	2.0362	1.1771	2094	–
		$^1[GeNC]^-$	2.0016	1.1839	2072	–
		$^3[GeNC]^-$	2.0218	1.1829	2075	–

Germanium dicyanide $Ge(CN)_2$

J. Satge and co-workers reported the successful synthesis of germanium dicyanide $Ge(CN)_2$ among other germanium(II) pseudohalogens in 1986 by different synthetic routes following Scheme 59 (Onyszchuk et al., 1986).

In contrast to the exchange reaction using trimethylsilyl cyanide TMS–CN, the reaction of germanium diiodide and silver cyanide leads to the highest yields (80%), but also the use of mercury(II) dicyanide is possible. After removal of the solvent the product is obtained as a viscous liquid being very sensitive to moisture and showing a dominant absorption band at ν_{CN} = 2090 cm^{-1} assigned to the cyanide stretching mode. The authors also reported further experiments carried out on $Ge(CN)_2$ including cycloadditions, insertion reactions or formation of Lewis acid-base complexes being so far the only experimental study on the preparation and chemical behavior of $Ge(CN)_2$ (Onyszchuk et al., 1986). A theoretical study by H. F. Schaefer and co-workers highlighted germanium dicyanide and investigated isomers and electronic states which led to the perception that the dicyanide isomer in the singlet ground state is energetically favored. The Ge–C bond length was calculated as $r_{Ge–C}$ = 1.970–2.005 Å (MP2, BLYP) and the bond length of the cyanide group as $r_{C–N}$ = 1.156–1.196 Å (BHLYP, MP2). Additionally, the cation (doublet ground state, $r_{Ge–C}$ = 1.890 Å, $r_{C–N}$ = 1.176 Å, B3LYP) and anion (doublet ground state, $r_{Ge–C}$ = 2.022 Å, $r_{C–N}$ = 1.178 Å, B3LYP) of $Ge(CN)_2$ were calculated (Bundhun et al., 2012).

Germanium tetracyanide $Ge(CN)_4$

In 1958, two independent reports were published describing the preparation of germanium tetracyanide $Ge(CN)_4$. W. Menzer converted the germanium tetraiodide with silver cyanide while T. A. Bither et al. utilized germanium chloride and trimethylsilyl (iso)cyanide (Scheme 60) (Bither et al., 1958; Menzer, 1958).

The products were described as hygroscopic and insoluble in several solvents. The decomposition occurred by heating as well as immediately at air forming hydrogen cyanide (Bither et al., 1958; Menzer, 1958). With the exception of an elemental analysis reported by T. A. Bither and co-workers, no analytical identification of the molecule has been performed and no further studies have been published since these early reports.

Hexacyanidogermanate $[Ge(CN)_6]^{2-}$

The $[PPN]^+$ salt with $[Ge(CN)_6]^{2-}$ counterion has been synthesized, isolated, and fully characterized in the reaction of (PPN)CN and $GeCl_4$ (Smallwood et al., 2019). However, more forcing conditions are required for the final reaction step $[Ge(CN)_5Cl]^{2-} + CN^- \rightarrow [Ge(CN)_6]^{2-} + Cl^-$. In order to complete the $Cl^-/[CN]^-$-exchange, the chloride-containing product was further treated with NaCN in MeCN to give $[PPN]_2[Ge(CN)_6]$ after re-crystallization. $[PPN]_2[Ge(CN)_6]$ is moderately air sensitive and dissolves readily in polar aprotic solvents without noticeable dissociation.

Tin

Although tin halides are well known and organotin compounds are applied in organic syntheses, the cyanide compounds have been object of only a few studies. Whereas tin dicyanide $Sn(CN)_2$ was prepared and analyzed by Mössbauer spectroscopy, tin tetracyanide $Sn(CN)_4$ was applied as a starting material but not characterized (Harrison, 1972; Harrison and Stobart, 1973; Jung et al., 2010; Renz et al., 2009a). Recently, salts containing the $[Sn(CN)_6]^{2-}$ anion were prepared (Smallwood et al., 2019).

Tin dicyanide $Sn(CN)_2$

Whereas tin(II) halides are well known, tin(II) cyanide, $Sn(CN)_2$, has not been studied intensively. So far, only two

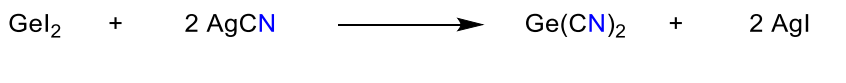

Scheme 59: $Ge(CN)_2$ received by silver cyanide or exchange reaction using trimethylsilyl cyanide (Onyszchuk et al., 1986).

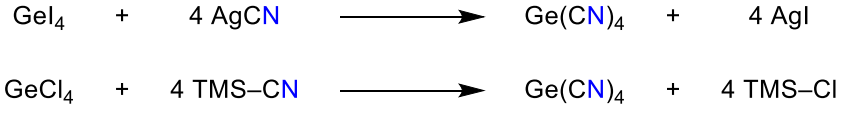

Scheme 60: Synthesis of $Ge(CN)_4$using germanium tetrahalides (Bither et al., 1958; Menzer, 1958).

reports by P. G. Harrison from 1972 to 1973 are available (Harrison, 1972; Harrison and Stobart, 1973). The synthesis was achieved by protolysis of dicyclopentadienyl tin(II) with hydrogen cyanide to give a colorless, air sensitive solid with absorption bands at ν_{CN} = 2168 cm^{-1} and ν_{CN} = 2179 cm^{-1} in the IR spectrum (Scheme 61) (Harrison, 1972; Harrison and Stobart, 1973). It should be noted that the carbodiimide $Sn(CN_2)$ has been isolated from the solid-state metathesis reaction between equimolar amounts of $Li_2(CN_2)$ and $SnCl_2$ (Löber et al., 2019).

Tin tetracyanide $Sn(CN)_4$

Similar to the tin(II) compound, tin(IV) cyanide $Sn(CN)_4$ has not been studied intensively as well. F. Renz et al. published two reports on the investigation of pentanuclear clusters with tin tetracyanide as bridging unit between iron complexes. The $Sn(CN)_4$ was reported to be accessible by conversion of tin(IV) chloride and potassium cyanide (Scheme 62) (Jung et al., 2010; Renz et al., 2009a).

An adduct of $Sn(CN)_4$ was obtained in the reaction of SnF_4 with an excess of TMS–CN resulting in the formation of $Sn(CN)_4$·2 MeCN (Smallwood et al., 2019).

Hexacyanidostannate(IV) $[Sn(CN)_6]^{2-}$

As early as 1987, K. B. Dillon et al. studied the reaction of SnX_4 (X = Cl^-, Br^-) with $[^nBu_4N]CN$ but failed to isolate $[^nBu_4N][Sn(CN)_6]$ as they found always cyanohalogenostannates(IV) of the type $[^nBu_4N]_2[SnX_m(CN)_n]$ ($m + n = 6$). However, on the basis of ^{119}Sn NMR studies a resonance at ca. –917 ppm was assigned to the $[Sn(CN)_6]^{2-}$ ion in solution (Dillon and Marshall, 1987). In 2019, P. Portius and coworkers described the synthesis of $[PPN]_2[Sn(CN)_6]$ from $Sn(CN)_4$·2 MeCN (see above) and an excess of [PPN]CN (Scheme 63). The ν_{CN} stretching modes of the slightly distorted octahedral anion (r_{Sn-C} = 2.06(1) – 2.10(1) Å) were found at 2157, 2153, 2146 cm^{-1} in the solid and at 2157.3 cm^{-1} in solution (Smallwood et al., 2019).

$$Sn(Cp)_2 + 2\,HCN \longrightarrow Sn(CN)_2 + 2\,HCp$$

Scheme 61: Synthesis of $Sn(CN)_2$ by protolysis (Harrison, 1972; Harrison and Stobart, 1973).

$$SnCl_4 + 4\,KCN \longrightarrow Sn(CN)_4 + 4\,KCl$$

Scheme 62: Synthesis of $Sn(CN)_4$ by F. Renz et al. (Jung et al., 2010; Renz et al., 2009a).

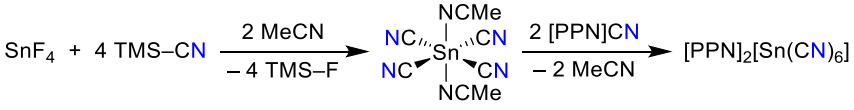

Scheme 63: Synthesis of $[PPN]_2[Sn(CN)_6]$ (Smallwood et al., 2019).

Lead

Except for the observations by R. M. Kroeker and J. Pacansky of $Pb(CN)_2$ formed by treating a magnesium layer, which has a monolayer of cyanoacetic acid and is coated with lead, with an electron beam, there is just one article reporting the quantitative formation of lead dicyanide by treatment of lead dihydroxide with an excess of potassium cyanide (Herz and Neukirch, 1923; Kroeker and Pacansky, 1982). But a retry of this reaction in an aqueous system led to a mixture of $Pb(CN)_2$ having two distinct signals in a Raman spectrum (ν = 2057 cm^{-1} and ν = 2085 cm^{-1}) and a lead compound containing nitrate and hydrogenoxide, where the isolation of lead dicyanide in quantitative amounts was not possible (Schulz et al., 2021). In a US patent from 1954 the synthesis of $Pb(CN)_2$ is described: $Pb(CN)_2$ is prepared by heating a dialkyllead dicyanide, such as diethyllead dicyanide, at 393–533 K. After sublimation a solid material, $Pb(CN)_2$, was isolated (Shapiro et al., 1954).

Astonishingly, also in the CCSD data base there is no entry of $Pb(CN)_2$. The only known and structurally characterized ternary Pb–C–N compounds are lead tricyanomethanides $Pb[C(CN)_3]_2$ (Deflon et al., 2006), lead dicyanamide $Pb[N(CN)_2]_2$ (Jürgens et al., 2002), and lead cyanamide Pb[NCN] (Zhao et al., 2018), which were synthesized from salt metathesis reactions of $PbCl_2$ with $Ag[C(CN)_3]$, $Na[N(CN)_2]$ or $Ag_2[NCN]$.

5th Main group

The 5th main group is dominated by trisubstituted homoleptic cyanides due to the characteristic oxidation states (III) and (V) of the later elements.

The most important pnictogen monocyanides are nitrogen and phosphorus monocyanide, which are triplet biradicals. Die P–C bond is elongated and smaller in energy compared to the N–C bond, which leads to no formation of the nitrene configuration and the cyanide group is characterized by a triple bond. This is confirmed by shortened bond lengths and increased wave numbers of the stretching mode.

The pnictogen dicyanides are also dominated by nitrogen and phosphorus dicyanide. The differences of these two compounds mainly base on the various electronegativities. Hence, the central nitrogen atom of the dicyanamide anion has a significant negative charge, while the phosphorus atom has a positive charge. On the other hand, the dicyanamide anion is characterized by an angle of 120° indicating sp^2-hybridization while the phosphorus species shows an angle of about 90° pointing to a square planar structure.

In regard to the pnictogen tricyanide compounds, the increase of the period of the central atom leads to a decrease of hybridization, to an increasing wave number of the stretching mode of the cyanide groups and to a decreasing angle between the cyanide groups. The diminishment of the angle is analogous to the less coordinated pnictogen cyanide compounds, while the increase of the wave number is contrary to the trends of the pnictogen mono- and dicyanides.

R. Dronskowski et al. investigated in detail the interactions in $[E(CN)_3]_n$ (E = N–Sb, n = 1–3 and ∞) by means of computations. They found a significant preference for chain-like structures over molecular units (such as monomers, dimers or trimers) the heavier the pnictogen E. In addition, evidence of cooperativity in chains of pnictogen-linked $E(CN)_3$ species is discussed. It is assumed that the pnictogen bonds are strengthened by such a cooperative effect (George et al., 2014).

Nitrogen

Cyanonitrene NCN and its ions

Many publications of cyanonitrene were published in the middle of the twentieth century (Milligan et al., 1965). The synthesis can be carried out as a photolysis of cyanogen azide using UV light at wavelengths of 280–300 nm or as a thermal decomposition (Scheme 64) (Dammeier and Friedrichs, 2010).

Scheme 64: Synthesis of cyanonitrene by photolysis or thermal decomposition (Dammeier and Friedrichs, 2010).

On that way H. Okabe and A. Mele could determine, that the bond dissociation energy of the $N–CN_3$ bond is $\Delta(NCN_3)$ = (414.5 ± 20.9) kJ mol^{-1} and the standard formation enthalpy is $\Delta_f H°(NCN)$ = (481.5 ± 20.9) kJ mol^{-1} (Okabe and Mele, 1969). In 1997, G. B. Ellison and co-workers published another synthetic route of cyanonitrene in terms of a radiation of cyanamine using oxide ion chemistry. The formed cyanonitrene anion is separated and photodetached by light of a CW Ar III ion laser with a wavelength of λ = 351.1 nm. The removed photoelectrons are focused and detected by passing them through an energy analyzer. The electron affinity of the radical is calculated from its photoelectron spectra and the determined thermochemistry compared to computational results (Clifford et al., 1997).

The supposed occurrence in interstellar matter and the radical structure of the cyanonitrene led to many theoretical studies of the molecular structure (Armstrong et al., 2000; Blanksby et al., 2000; Jiang et al., 2003; Schiavon et al., 2012; Yang et al., 2011). A. G. Anastassiou and H. E. Simmons reported a triplet ground state of cyanonitrene, which is lower in energy in contrast to three possible singlet states due to repulsion considerations and described by three mesomeric structures (Figure 34). Furthermore, they argued, the two unpaired electrons should be distributed among two degenerated, orthogonal molecular orbitals (Anastassiou and Simmons, 1967). In addition, experimental and computational values of the cyanonitrene and its isomers are compared in Table 44.

Dicyanamide $[N(CN)_2]^-$

In 1922 W. Madelung and E. Kern published their studies on the synthesis and properties of dicyanamides (Madelung and Kern, 1922a; Madelung and Kern, 1922b). The consideration of properties was based on the diagonal relationship of the periodic table of elements and could be confirmed by them. Sodium dicyanamide can be technically prepared by introducing gaseous cyanogen chloride into a mixture of sodium hydrogencyanamide and sodium hydroxide solution, according to a patent by F. Thalhammer and H. Trautz in 2000 (Scheme 65) (Thalhammer and Trautz, 2000).

As early as 1922, W. Madelung and E. Kern recognized that sodium dicyanamide at “dark red heat” trimerizes to trisodium tricyanmelaminate (Scheme 66). In 1997, the

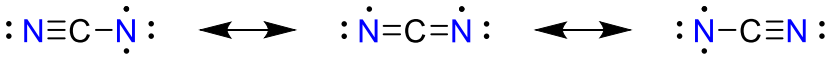

Figure 34: Lewis representation of the triplet ground state of cyanonitrene (Anastassiou and Simmons, 1967).

Table 44: Experimental and computational values of cyanonitrene (bond lengths in Å; wave numbers in cm^{-1}; electron affinity (E_A) in eV).

Compound	Exp./calc.	r_{C-N}	ν_{CN}	E_A
$[NCN]^-$	B3LYP/6-31 + G(d)	1.2404 (Blanksby et al., 2000)	–	–
NCN	Exp. – LES, IR, NIPS	1.230944(14) (Beaton et al., 1996)	1197 (Milligan and Jacox, 1966)	2.484 (Clifford et al., 1997)
	B3LYP/6-31 + G(d)	1.2341 (Blanksby et al., 2000)	–	2.50 (Blanksby et al., 2000)
$[NCN]^+$	B3LYP/6-31 + G(d)	1.2377 (Blanksby et al., 2000)	–	–

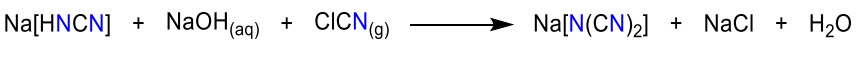

Scheme 65: Synthesis of $Na[N(CN)_2]$ (Thalhammer and Trautz, 2000).

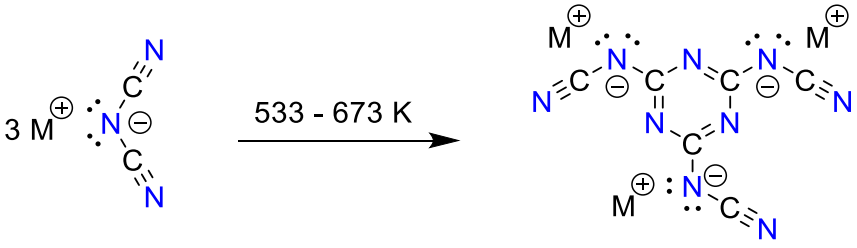

Scheme 66: Trimerization of $M[N(CN)_2]$ (Purdy et al., 1997).

group of A. P. Purdy studied the preparation and properties of lithium dicyanamide. In the cause of this study they discovered a trimerization reaction, which was investigated thermoanalytically for the first time (Purdy et al., 1997). A. P. Purdy and co-workers were able to show, among other things, with DSC measurements that the sodium dicyanamide trimerizes in the temperature range of 553–673 K and the lithium dicyanamide trimerizes in the temperature range of 533–653 K. In a series of papers, W. Schnick and co-workers confirmed the assumptions of W. Madelung and E. Kern and the data of A. P. Purdy et al. on the trimerization of sodium dicyanamide (Irran et al., 2001, 2002; Jürgens et al., 1998, 2000, 2001, 2002, 2005; Lotsch et al., 2004).

Furthermore, this work of W. Schnick and co-workers provided many interesting results on sodium dicyanamide (including IR data, DSC measurements on a reversible phase transition and powder diffractograms of the both phases), on its trimerization (including DSC measurements on the irreversibility of this solid reaction) and on the trisodium tricyanmelaminate (including a powder diffractogram of the anhydrous compound, a powder diffractogram, and a single crystal X-ray structural analysis of the trihydrate). Another 2001 publication of the group of W. Schnick on the preparation and properties of potassium dicyanamide and rubidium dicyanamide was concerned with the trimerization to tripotassium tricyanmelaminate and to trirubidium tricyanmelaminate, respectively (Scheme 66) (Irran et al., 2001). W. Schnick and co-workers described, among other things, that the potassium dicyanamide melts at 505 K, in the temperature range of 583–703 K its anions trimerize, and the melt solidifies during the formation of the tripotassium tricyanamide. For rubidium dicyanamide W. Schnick and co-workers found a melting point of 463 K and a temperature range of 533–643 K for the trimerization of its anions, although here, too, the melt solidifies. The cesium dicyanamide was already characterized by P. Starynowicz in 1991 by a single crystal X-ray structure analysis (Starynowicz, 1991). With the strong Lewis acid $B(C_6F_5)_3$, both dicyanamide, $[N(CN)_2]^-$, and its trimer tricyanomelaminate, $[C_3N_3(NCN)_3]^{3-}$ form stable adduct-anions, $\{N[CN{\cdot}B(C_6F_5)_3]_2\}^-$ and $\{C_3N_3[NCN{\cdot}B(C_6F_5)_3]_3\}^{3-}$ (Bernsdorf et al., 2009b; Voss et al., 2011).

Lab synthesis of dicyanamides usually begins with commerically available disodium cyanamide, $Na_2[NCN]$, which is treated with cyanogen bromide in an aqueous solution and the solvent is then removed by distillation (Scheme 67). It should be noted that the reaction of cyanogen bromide and cyanamide (H_2NCN, monomer of melamine)

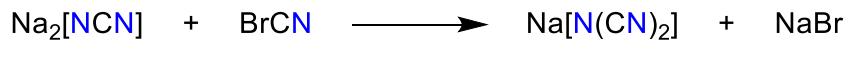

Scheme 67: Synthesis of the sodium salt of dicyanamide (Madelung and Kern, 1922a).

does not lead to the expected product. The cyanamide is stable in aqueous solution, tends to oligomerize and acts as acid (Madelung and Kern, 1922a).

In 1964, H. Köhler analyzed IR spectra of the sodium dicyanamide and different dicyanamide complexes and found for $Na[N(CN)_2]$ a stretching mode for $\nu_{CN} = 2179\ cm^{-1}$ (Köhler, 1964). Further studies on the dicyanamide anion in different salts, its symmetry and behavior in IR light were published by M. Kuhn and R. Mecke (Table 45) (Kuhn and Mecke, 1961a). On the basis of the IR active modes they could confirm a bent structure of C_{2v} symmetry with a partial double bond character within the N–CN unit indicating the importance of mesomeric structures in the Lewis picture (Figure 35).

H. Köhler et al. studied potassium dicyanamide and determined its structure experimentally (Table 46) (Köhler et al., 1977).

Computed data (B3LYP/6–311++G**) (Schalley et al., 1998) of the dicyanamide anion, $[N(CN)_2]^-$, the neutral radical, $[N(CN)_2]^{\cdot}$, and the cation, $[N(CN)_2]^{+\cdot}$ are summarized in Table 47 indicating that the loss of electrons increases the enthalpy of formation while the zero-point vibrational energy (ZPVE) decreases.

The experimental and computational vibrational spectra of sodium dicyanamide were analyzed by M K.

Table 45: IR data of different metal dicyanamide salts (wave numbers in cm^{-1}) (Kuhn and Mecke, 1961a).

Compound	Na^+	Ag^+	Cu^+	Cu^{2+}	Hg^{2+}	Pb^{2+}
$\nu^{sym.}{}_{CN}$	2179	2183	2247	2203	2165	2125/60
$\nu^{as.}{}_{CN}$	2232	2227	2283	2273	2251	2217

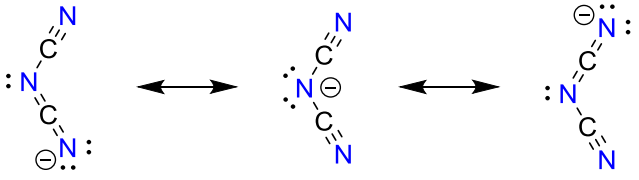

Figure 35: Mesomeric structures of the dicyanamide anion.

Table 47: Total energy E_{tot}, ZPVE (in Hartree) and formation enthalpy ($\Delta_f H$ in kJ mol^{-1}) of the dicyanamide anion, radical and cation (E_{tot} calculated using B3LYP/6–311 + G**) (Schalley et al., 1998).

Compound	$E_{tot.}$	*ZPE*	$\Delta_f H$
$[N(CN)_2]^-$	−240.4649	0.0211	23.0
$[N(CN)_2]^{\cdot}$	−240.3366	0.0192	360.1
$[N(CN)_2]^+$	−239.9035	0.0189	1498.0

Georgieva in 2005 showing good agreement to calculated data (Table 48). As illustrated by a population analysis, the negative net charges are found at all nitrogen atoms with a slightly more negative charge on the central N atom (−0.72e), while a positive charge of + 0.94e sits on both carbon atoms (Figure 36) (Brand et al., 2009).

In 2009, N. Carrasco et al. repeated the formation of Titan's (moon of the Saturn) tholins (see 2.7 $[HCNH]^+$ cation and the $[H(HCN)_n]^+$ cluster ion series), which is a polymeric mixture of high-nitrogen carbon compounds discovered on Titan for the first time (Sagan and Khare, 1979), when they could detect dicyanamide. In that experiment plasma radio frequency discharges are initialized in an atmosphere of nitrogen and methane. The formed products were investigated spectroscopically using IR spectroscopy, mass spectrometry and scanning electron microscopy. Characteristic mass-charge ratios are $m/z = 66.01$ of the dicyanamide ion as well as $m/z = 40.01$ and $m/z = 26.00$ of the fragments $[NCN]^-$ and $[CN]^-$, respectively (Carrasco et al., 2009).

In addition, D. Ergöçmen and J. M. Goicoechea prepared the heavier homologue of the dicyanamide, the cyaphocyanamide anion $[N(CN)(CP)]^-$. Sodium phosphanide was added to the N-precursor dimethyl-N-cyanocarbonimidate

Table 48: Experimental and computational IR data of $Na[N(CN)_2]$ (wave numbers in cm^{-1}).

Publication	Exp./calc.	$\nu^{sym.}{}_{CN}$	$\nu^{as.}{}_{CN}$
Georgieva and Binev (2005)	Exp. – IR	2179	2232
	MP2/6-31G*	2183	2199
	B3LYP/6-31G*	2209	2186

Table 46: Experimental and computational bond length (in Å) and bond angles (in°) of the dicyanoamide radical, anion and cation.

Compound	Exp./calc.	r_{C-N}	r_{N-CN}	< (C–N–C)	< (N–C–N)
$[N(CN)_2]^-$	Exp. – XRD[a] (Köhler et al., 1977)	1.155/1.145	1.304/1.317	120.8	172.6/172.9
$[N(CN)_2]^-$	B3LYP/6–311++G** (Schalley et al., 1998)	1.180	1.315	122.6	173.4
$[N(CN)_2]^{\cdot}$	B3LYP/6–311++G** (Schalley et al., 1998)	1.182	1.302	124.1	173.1
$[N(CN)_2]^+$	B3LYP/6–311++G** (Schalley et al., 1998)	1.198	1.280	130.9	171.8

[a]As potassium salt.

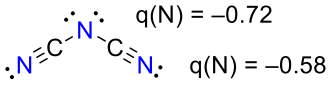

Figure 36: Negative partial charge distributation of the dicyanamide ion (Brand et al., 2009).

leading to the sodium salt Na[N(CN)(CP)] and two equivalents of methanol (Scheme 68) (Ergöçmen and Goicoechea, 2021).

Nitrogen tricyanide $N(CN)_3$

Although $N(CN)_3$ is a very simple molecule, it is unknown. On the one hand, this is due to the lack of suitable precursors, and on the other hand to the well-known isomeric equilibrium with the dicyano-carbodiimide (Scheme 69), which is very unstable with regard to oligomerization or polymerization. While tricyanamine has so far been elusive and has only been investigated theoretically (Riggs and Radom, 1985; Williams and Damrauer, 1971), there are experimental, i.e. spectroscopic, indications of the existence of dicyano-carbodiimide at very low temperatures (Ar matrix). However, it must be pointed out that the existence could not be confirmed in subsequent experiments (Sato et al., 2003, 2004). Although tricyanamine was mentioned by E. C. Franklin in his book "The Nitrogen System of Compounds" (Franklin, 1935), tricyanamine or its structural isomer dicyano-carbodiimide have only be observed as short-lived intermediates and all published procedures so far are of little preparative use.

In 2007, P. Politzer and co-workers published calculations dealing with directed, covalent bonds of molecules RX_3 including nucleophiles and central atoms of the 5th main group, which led to the σ-hole concept. The geometry and electrostatic potential of $N(CN)_3$ was optimized using DFT calculations. The ability for induction and resonance leads to a strong electron-withdrawing character of the cyanide group resulting in a planar structure of $N(CN)_3$. The length of the carbon-nitrogen bond was found of 1.365 Å (B3PW91/6-31G**) indicating a distinct double bond character, which was confirmed by NBO analysis. The hybridization of the central nitrogen atom is sp^2 and it possesses a *2p* orbital, which is orthogonally orientated to the molecular plane (Figure 37) (Murray et al., 2007a).

Polymerization of $N(CN)_3$ formally leads to $(C_3N_4)_x$. As previously explained for graphitic g-(C_3N_4) (see 6.1.6 Graphitic carbon nitride (g-C_3N_4)), the single-source concept is probably the most promising for attempts to produce a metastable carbonitride. This means that a reactive molecular precursor would be used, which can be condensed into a three-dimensional composite via the polymer intermediate stage. The simplest molecule with the right composition is the hypothetical tricyanamine $N(CN)_3$, which is in equilibrium with dicyano-carbodiimide NC–N=C=N–CN via the well-known amine-imide structural isomerism (Scheme 69).

Phosphorus

Based on typical oxidation states of phosphorus, especially compounds with three and five substituents, such as PCl_3 and PCl_5, are known. Accordingly, the phosphorus tricyanide is known, which is also probably the best-known

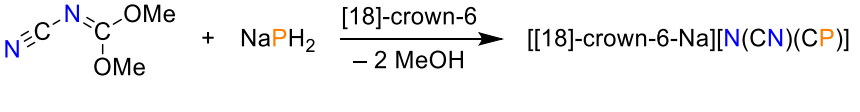

Scheme 68: Synthesis of the cyaphocyanamide anion $[N(CN)(CP)]^-$ (Ergöçmen and Goicoechea, 2021).

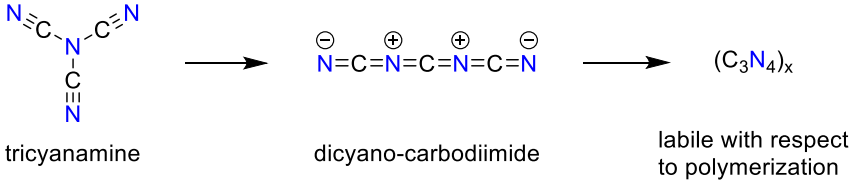

Scheme 69: Isomerism between tricyanamine and dicyano-carbodiimide.

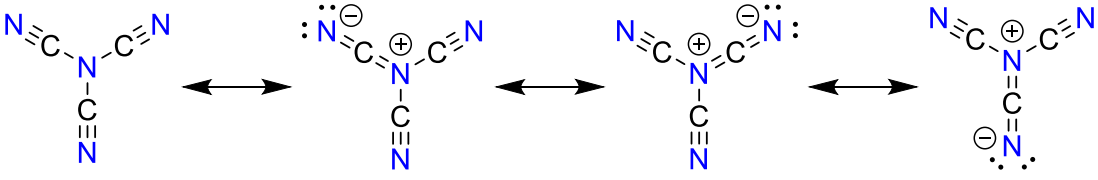

Figure 37: Lewis representations of the nitrogen tricyanide (Murray et al., 2007a).

phosphorus cyanide compound, while the phosphorus pentacyanide $P(CN)_5$ has not yet been studied in as much detail as $P(CN)_3$. The reason for this is the redox instability of $P(CN)_5$ with regard to the release of cyanogen, $(CN)_2$. It is known that CN ligands have a comparatively low oxidation potential, which is reflected in the low thermal stability of $P(CN)_5$, which easily releases cyanogen at room temperature to form $P(CN)_3$. Also, the related $[P(CN)_6]^-$ ion, on the other hand, is presumably stabilized by hyperconjugation. However, the synthesis of the $[P(CN)_6]^-$ ion using conventional methods from (fluoro)phosphorus precursors is complicated by an affinity of $P(CN)_5$ for F^- (590 kJ mol^{-1}), which is far greater than that for $[CN]^-$ (198 kJ mol^{-1}) and could not be realized so far (Bläsing et al., 2016b; Bresien et al., 2015b; Smallwood et al., 2019).

Cyanophosphide PCN

The synthetic route often bases on an *ac* discharge in a mixture of gaseous starting materials, for example a dilute mixture of red phosphorus vapor and cyanogen (p = 1.33 Pa) in presence of argon gas (p = 4.67 Pa). But the use of phosphorus trichloride or phosphine in flash photolysis as phosphorus precursors in an atmosphere of nitrogen is also possible (Scheme 70) (Basco and Yee, 1968a; Halfen et al., 2012).

The existence of small phosphoric molecules in interstellar matter inspired A. Largo et al. to carry out theoretical studies on PCN and its isomer PNC and also their ions. The ground state of both linear isomers is $^3\Sigma^-$, the C–N bond length is not affected and very similar to the cyanide radical and also the P–N bond has a typical length of a single bond. In contrast to the isovalent CN_2, the bond lengths of PCN are less affected by mesomeric effects. The

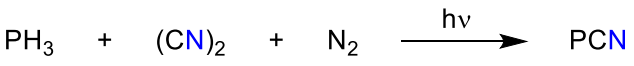

Scheme 70: Flash photolysis of PCN using phosphine, cyanogen and nitrogen gas (Basco and Yee, 1968a).

two unpaired electrons are also mainly located at the phosphorus atom. Furthermore, a nitrene isomer with a P–C triple and a C–N single bond is not located as a minimum structure, which is a consequence of the high bond energy of the C–N triple bond ($\Delta_B H$ = 888 kJ mol^{-1}) in contrast to a C–P triple bond ($\Delta_B H$ = 515 kJ mol^{-1}). The proton affinity of the phosphorus atom is 541.8 kJ mol^{-1}, the proton affinity of the nitrogen atom of PCN is 752.8 kJ mol^{-1} (Largo and Barrientos, 1991; Pham-Tran et al., 2006) (Table 49).

Dicyanophosphide $[P(CN)_2]^-$

Dicyanophosphide, $[P(CN)_2]^-$, is well described (Harloff et al., 2020b; Schmidpeter and Zwaschka, 1977a, 1977b; Schmidpeter et al., 1985a; Sheldrick et al., 1979). A. Schmidpeter and F. Zwaschka first reported on the synthesis and properties of the ion in 1977 (Schmidpeter and Zwaschka, 1977a). $[P(CN)_2]^-$ is stable in the form of the crown ether sodium salt both as a solid and in solution. The preparation is carried out by reacting $P(CN)_3$ with diethyl phosphites, $Na[PO(OEt)_2]$, and [18]-crown-6 in THF under cooling to 253 K. In this case the product crystallizes with crown ether and THF in ratio of 1:1:1 (Scheme 71). It is also possible to use other alkali metal salts, for example KF, to transform the $P(CN)_3$ into its phosphide anion in presence of crown ether. In all cases the crown ether is important to stabilize the salt as solid or in solution (Schmidpeter and Zwaschka, 1977a, 1977b; Schmidpeter et al., 1985a; Sheldrick et al., 1979).

Another synthetic route is based on the degradation of white phosphorus, P_4, by the cyanide ion (as MCN salt). The $[CN]^-$ ion as a strong anionic nucleophile is able to generate different PCN-ions in the presence of acetonitrile and stoichiometric amounts of [18]-crown-6, but mainly the $[P(CN)_2]^-$ can be isolated (Scheme 72). The observed dicyanophosphide salt [18]-crown-6-K][$P(CN)_2$] has an orthorhombic crystal lattice with the space group $Pna2_1$ (Schmidpeter et al., 1985a).

The crown ether is essential to increase the solubility of the cyanide salt. The increasing dark-red color of the

Table 49: Experimental data of PCN and computational data of PCN and its cation (bond lengths in Å; dipole moments μ in D; wave numbers in cm^{-1}).

Compound	Exp./calc.	r_{P-C}	r_{C-N}	μ	$\nu^{sym.}{}_{CN}$
PCN[a]	Exp. – MW (Halfen et al., 2012)	1.732(2)	1.167(2)	–	–
	B3LYP/cc-pVTZ (El-Yazal et al., 1997)	1.7237	1.1697	2.68	2037
	UHF/6-31G* (Largo and Barrientos, 1991)	1.724	1.174	2.42	1771
$[PCN]^+$	B3LYP/cc-pVTZ (El-Yazal et al., 1997)	1.6901	1.1783	3.67	2045
	UHF/6-31G* (Largo and Barrientos, 1991)	1.675	1.193	3.85	2030

[a]Ground state $^3\Sigma^-$ of PCN.

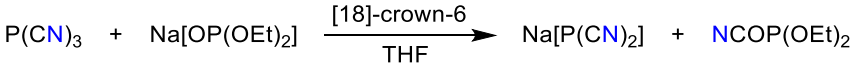

Scheme 71: Synthesis of dicyanophosphide using an alkaline diethylphosphite salt in presence of crown ether (Schmidpeter and Zwaschka, 1977a, 1977b; Schmidpeter et al., 1985a; Sheldrick et al., 1979).

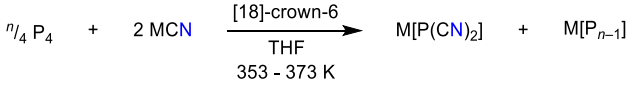

Scheme 72: Synthesis of the dicyanophosphide anion (M = [18]-crown-6-Na, [18]-crown-6-K, NEt_4, NBu_4, $N(PPh_3)_2$) (Schmidpeter et al., 1985a).

reaction mixture indicates the reaction process due to the formation of polymeric phosphides. Though the ratio $n/2$ of phosphorus and cyanide determines the formation of the polymeric phosphide, but the largest observed phosphide has the index n = 16 which corresponds with the best stoichiometry (Scheme 73). A higher ratio leads to free cyanide anions and a smaller ratio means unreacted phosphorus. Furthermore, the formation of different phosphides ($n \leq 16$) hinders the isolation of the pure salt $M[P(CN)_2]$ (Schmidpeter et al., 1985a). It is also possible to influence the equilibrium between phosphorus and dicyanophosphide on one side and phosphorus tricyanide/polyphosphides on the other side to increase the amount of the dicyanophosphide anion (Scheme 73). In this context, A. Schmidpeter et al. reported a strong influence of different nucleophiles on the equilibrium. For example, X = $[CN]^-$ led to a shift to the left side, but in case of X = H^- a shift to the right side was observed (Schmidpeter et al., 1985a).

In 2018, L. B. Macdonald and co-workers published a new approach to the dicyanopnictides $[E(CN)_2]^-$ (E = P, As). Similar to an approach reported by A. Schmidpeter the phosphino ligand bis(diphenylphosphino)ethane (dppe) in $[dppeE][BPh_4]$ (E = P, As) was displaced by cyanide ligands using tetraphenylphosphonium cyanide $[PPh_4]CN$ as cyanide source (Binder et al., 2018).

In the crystal the nitrogen atoms of the cyanides are aligned towards the cation, but the phosphorus atom is not, which leads to bent cyanide groups as shown in Table 50. Dicyanophosphide is angled, in crystalline $[[18]\text{-crown-6-K}][P(CN)_2]$, the nitrogen of the CN group coordinates to the K^+ ion so that zigzag P–C–N···K···N–C–P chains are present in the crystal (Schmidpeter et al., 1985a). The calculated negative net charge (C: −0.16; N: −0.36) is delocalized on the cyanide group corresponding to the shortened P–C bond and widened C–P–C angle in contrast to the $P(CN)_3$, whereas the phosphorus has a slightly positive net charge of +0.05 (Figure 38). Due to the high negative charge on the nitrogen atom, the anion coordinates to cations via nitrogen (Sheldrick et al., 1979).

In ^{31}P NMR spectra the shift of the phosphorus in dicyanophosphides (δ = −193 ppm) is nearly independent of the solvent and the cation (Schmidpeter and Zwaschka, 1977b). With regard to ^{13}C NMR spectra the chemical shift of the carbon is at about δ = 132.1 ppm with a coupling constant of $^1J(^{31}P–^{13}C)$ = 106.2 Hz, which is similar to organic nitriles (Schmidpeter et al., 1985a).

Only recently it was found that salts containing the phosphaethynolate anion, $[OCP]^-$, react with HCN, leading to the formation of the dicyanophosphide anion in a previously unknown decomposition process. In the case of [PPN][OCP], for example, the reaction with pure HCN as reaction medium and solvent led to the decomposition of the phosphaethynolate anion and finally to the formation of $[PPN][P(CN{\cdot}HCN)_2]$ (Figure 39). This is an exergonic

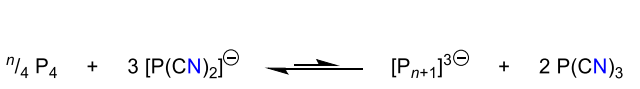

Scheme 73: Equilibrium of dicyanophosphide $[P(CN)_2]^-$ (Schmidpeter et al., 1985a).

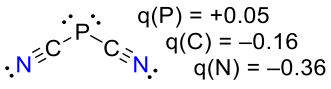

Figure 38: Calculated net charges of dicyanophosphide (Sheldrick et al., 1979).

Table 50: Experimental and computational data of $[[18]\text{-crown-6-Na}][P(CN)_2]$ (bond lengths in Å; angles in °; wave numbers in cm^{-1}).

Exp./calc.	r_{P-C} (Sheldrick et al., 1979)	r_{C-N} (Sheldrick et al., 1979)	< (C–P–C) (Sheldrick et al., 1979)	< (P–C–N) (Sheldrick et al., 1979)	$\nu^{sym.}_{CN}$ (Schmidpeter et al., 1985a)	$\nu^{as.}_{CN}$ (Schmidpeter et al., 1985a)
Exp. – XRD, IR	1.76(2)/1.72(2)	1.155	95.0(10)	169(2)/175(2)	2120	2097
STO-3G	1.77	1.16	94.7	175.3	–	–

process according to calculations ($\Delta_r G° = -35.8$ kcal mol^{-1}). It was assumed that formaldehyde is formed as a by-product according to the following reaction equation: $[PCO]^- + 4\ HCN \rightarrow [P(CN{\cdot}HCN)_2]^- + H_2CO$. Its $[PPN]^+$-salt crystallized in the form of an HCN solvate with the formation of a bent $[P(CN{\cdot}HCN)_2]^-$ anion (Figure 39) (Bläsing et al., 2020).

Dicyanophosphide can be regarded as a pseudohalide; accordingly, $P(CN)_3$ could be described as an inter-pseudohalogen compound. This is consistent with the electrophilic transfer of the cyano radical to the dialkyl phosphite in the course of the above-mentioned synthesis.

Phosphorus tricyanide $P(CN)_3$

The phosphorus tricyanide, $P(CN)_3$, which was first mentioned by M. Cenedella in 1835 (Cenedella, 1835), is widely characterized. However, the start of the chemistry of phosphorus tricyanides dates back to 1863, when H. Hübner and G. Wehrhane described the isolation of "long, snow-white needles or hexagonal plates of cyanophosphorus" (German: Cyanphosphor), $P(CN)_3$, in the reaction of PCl_3 with three equivalents of AgCN at 393–413 K (Scheme 74) (Hübner and Wehrhane, 1863; Wehrhane and Hübner, 1864). In 1958, T. A. Bither et al. described the isolation of the entire series of $E(CN)_3$ (E = P, As, Sb and Bi) obtained by treating pnictogen(III) chlorides ECl_3 with three equivalents of TMS–CN in xylene under reflux conditions. All these species were characterized from elemental analyses only (Bither et al., 1958). In 1964, K. Emerson et al. carried out crystallographic studies on monocrystals (Emerson and Britton, 1964), which were synthesized by addition of phosphorus trichloride in excess to silver cyanide in carbon tetrachloride under reflux (Scheme 74) (Davies et al., 1976; Kirk and Smith, 1968).

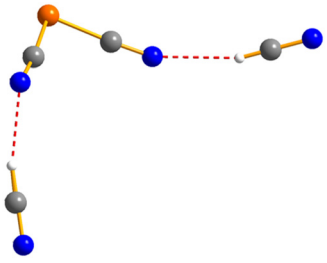

Figure 39: Structure of the $[P(CN{\cdot}HCN)_2]^-$ ion in $[PPN][P(CN{\cdot}HCN)_2]$ (color code: P = orange, N = blue, C = grey, H = white) (Bläsing et al., 2020).

This synthesis was significantly improved in 1971 by C. E. Jones and K. J. Coskran (Jones and Coskran, 1971). When reacting PCl_3 with AgCN in acetonitrile (MeCN) under a nitrogen atmosphere, the reaction already proceeds at room temperature within 2 h with good yield. Alternatively, PBr_3 can also be reacted with AgCN in MeCN (Maier, 1963) or diethyl ether (Et_2O) (Dillon and Platt, 1982). Another route is the reaction of phosphorus trichloride and methoxydimethylsilyl cyanide (Krolevets et al., 1991) achieving a 96.7% yield of $P(CN)_3$ in 10–25 min at 303–323 K.

The phosphorus tricyanide sublimes at 323–333 K at normal pressure (Coskran and Jones, 1971). $P(CN)_3$ is moisture-sensitive and hydrolyzes to H_3PO_3 and HCN (Gall and Schüppen, 1930). Work must therefore be carried out under protective gas and in dry solvents. Suitable solvents for $P(CN)_3$ include MeCN, nitromethane ($MeNO_2$) and 2-nitropropane (Wilkie and Parry, 1980) as well as dioxane and benzene (Kirk and Smith, 1968). In solution, $P(CN)_3$ exists as a dimer or tetramer (Kirk and Smith, 1968). C. A. Wilkie and R. W. Parry found that the phosphorus atom in $P(CN)_3$ can act as a Lewis acidic center (Wilkie and Parry, 1980). Due to the Lewis acidic character of the P atom, there are a number of adducts of the form $[P(CN)_3X]^-$ (X = Cl^-, Br^-, I^-) (Dillon et al., 1982; Sheldrick et al., 1981).

The crystals of $P(CN)_3$ have the shape of flat colorless needles. The unit cell of the crystals is tetragonal (space group $I\bar{4}2d$) with the parameters $a = b = 14.00$ Å and $c = 10.81$ Å (Emerson and Britton, 1964). The $P(CN)_3$ molecules are trigonal-pyramidal with approximate C_{3v} symmetry in tetragonal crystals. The P–C–N angles are slightly bent and therefore smaller than 180°. O. Sala and co-workers assumed packing effects for this rather surprising bent PCN units (Miller et al., 1965). Having a closer look on the environment of the phosphorus atom, there are three

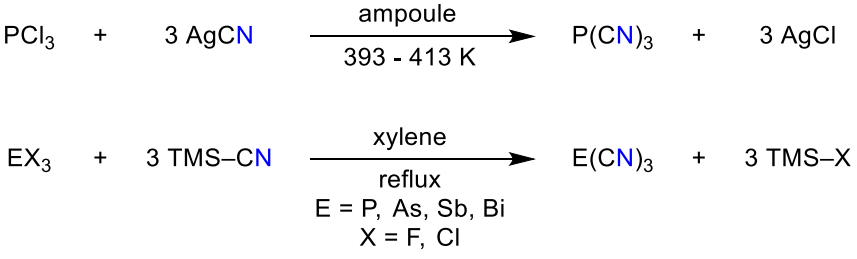

Scheme 74: Synthesis of $P(CN)_3$ (Davies et al., 1976; Emerson and Britton, 1964; Kirk and Smith, 1968).

nitrogen atoms additionally to three cyanide groups, which are closer to the phosphorus atom than the normal van der Waals distance, leading to intermolecular interactions and a roughly octahedral environment around each phosphorus atom. This means, the coordination around the P atom might be described as [3 + 3], that means there are three covalently bonded cyanide groups and three very loosely bonded cyanide groups of adjacent $P(CN)_3$ molecules (Emerson and Britton, 1964). Furthermore, the small bond angles at the phosphorus might be affected by a strong *s* character of the lone pair (Coskran and Jones, 1971). Experimental and theoretical structural data are listed in Table 51.

The standard formation enthalpy of gaseous $P(CN)_3$ was reported to be $\Delta_f H° = (494.6 \pm 25.1)$ kJ mol^{-1} (Davies et al., 1976). The chemical shifts of $P(CN)_3$ are summarized in Table 52 and the vibrational data in Table 53.

Tetracyanidophosphate(III) anion $[P(CN)_4]^-$ and tetracyanido phosphonium cation $[P(CN)_4]^+$

R. W. Parry et al. described the formation of the $[P(CN)_4]^-$ ion in the reaction of potassium cyanide with phosphorus tricyanide in acetonitrile (Scheme 75). Only NMR data as well as vibrational data were given (Wilkie and Parry, 1980). C. A. Wilkie and R. W. Parry could not observe a signal in the ^{13}C NMR spectrum, which clearly relates to the carbon atom of the cyanide groups. But they assumed, that the signal lies under the signal of the acetonitrile due to an expected downfield shift, which would mean a chemical shift of about δ (*C*N) ≈ 118 ppm. The added cyanide also causes a shift of the signal in the ^{31}P NMR spectrum of about 53.6 ppm to more negative values (δ (^{31}P) = –192.7 ppm). Compared to PCl_3 and four times coordinated equivalent $[PCl_4]^+$ the direction of the chemical shift is opposite. C. A. Wilkie and R. W. Parry discussed the different charges of the ions and the different changes of symmetry as possible reasons, because PCl_3 changes from C_{3v} to T_d by addition of a formal Cl^+, but $P(CN)_3$ changes from C_{3v} to C_s by addition of the cyanide. The infrared spectrum of $K[P(CN)_4]$ displayed bands at 2195, 2160, 2097, and 2070 cm^{-1}, suggesting a distorted trigonal-bipyramidal structure in the solid state (Table 54) (Wilkie and Parry, 1980).

Investigations by A. Schmidpeter et al. have shown, however, that the $[P(CN)_4]^-$ ion is indeed formed in solution by the addition of $[CN]^-$ to $P(CN)_3$, but then rapidly decays in the sense of an intermolecular redox reaction. This produces dicyanophosphide, $[P(CN)_2]^-$, as well as the "unusual" anion $[C_{10}N_{10}P_2]^{2-}$, whose structure was published in the same paper (Schmidpeter et al., 1985b).

Table 52: NMR data of phosphorus tricyanide (in acetonitrile, chemical shifts in ppm).

Compound	Exp./calc.	δ (^{31}P)	δ (^{13}C)
$P(CN)_3$	Exp.	–138.3 (Coskran and Jones, 1971) –137.83 (Tattershall, 1990)	110.54 (Tattershall, 1990)

Table 53: Selected vibrational data (wave numbers in cm^{-1}) of $E(CN)_3$ and $E(CN)_3$·2 THF (Arlt et al., 2016a).

Compound	IR[a]	Raman[b]
$P(CN)_3$[c]	2205(m)	2207(10)
$As(CN)_3$[c]	2209(m), 2199(s)	2208(7), 2198(8)
$Sb(CN)_3$	2293(w), 2251(m), 2188(m, br)	2248(0.5), 2187(8)
$Bi(CN)_3$	2291(m), 2254(s), 2174(m, br)	2256(1), 2171(7)
$Sb(CN)_3$·2 THF	2170(m)	2185(7,br)
$Bi(CN)_3$·2 THF	2154(m)	2158(10,br)

[a]Nicolet 380 FT-IR spectrometer with a Smart Orbit ATR at 298 K. [b]LabRAM HR 800 Horiba Jobin YVON Raman spectrometer (red laser 633 nm, 17 mW) at 298 K. [c]$E(CN)_3$ (E = P, As) was prepared for comparison only.

Table 51: Experimental average and computational data using different methods of phosphorus tricyanide (bond lengths in Å; angles in °; wave numbers in cm^{-1}).

Publication	Exp./calc.	r_{P-C}	r_{C-N}	< (C–P–C)	< (P–C–N)	$\nu^{sym.}_{CN}$
Miller et al. (1965)	Exp. – Raman	–	–	–	–	2206
Emerson and D. Britton (1964)	Exp. – XRD	1.803(29)/ 1.786(27)/ 1.774(27)	1.124(47)/ 1.158(44)/ 1.165(44)	93.7(2)/ 93.2(2)/ 93.6(2)	170.7(3)/ 172.2(3)/ 171.9(3)	–
J. O. Jensen (2004a)	HF/6-311G**	1.791	1.130	98.3	174.1	2567
	B3LYP/6-311G**	1.790	1.155	98.6	172.4	2308
	MP2/6-311G**	1.786	1.179	97.6	173.1	2110

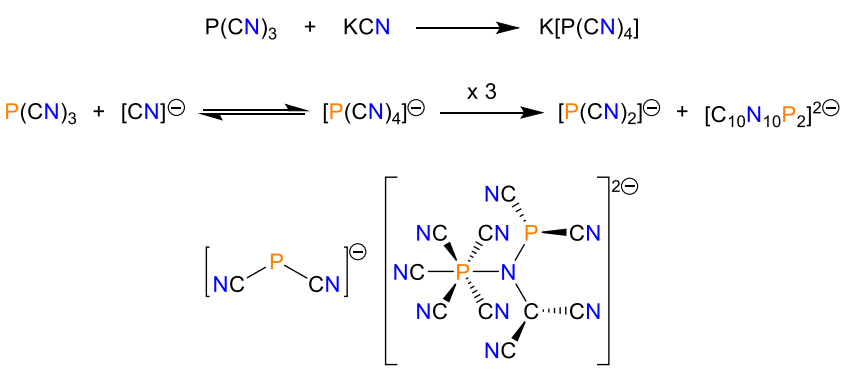

Scheme 75: Top: Synthesis of the phosphorus tetracyanide anion by R. W. Parry et al. (Wilkie and Parry, 1980). Bottom: Decomposition of $[P(CN)_4]^-$ (Schmidpeter et al., 1985b).

Table 54: IR data of $[P(CN)_4]^-$ and related assignments (wave numbers in cm^{-1}) (Wilkie and Parry, 1980).

ν_{CN}	Symmetry
2070	B_1, sym., eq.
2097	B_2, sym., ax.
2160	A_1, sym., eq.
2195	A_1, sym., ax.

Furthermore, if one reacts $[P(CN)_2]^-$ with X_2 (X = Br, I), one obtains the $[P(CN)_2X_2]^-$ anion in the course of an oxidative addition. Similarly, X–CN adds to the $[P(CN)_3X]^-$ ion. With Cl_2, on the other hand, only $P(CN)_2Cl$ is formed (Schmidpeter and Zwaschka, 1979).

Tetracyanido phosphonium cation $[P(CN)_4]^+$: In addition to the anion $[P(CN)_3X]^-$ mentioned above, the cation $[P(CN)_4]^+$ was also found, but only in solution together with other tetra(pseudo)halogen phosphonium cations (Dillon and Platt, 1983). Different $[PBr_{4-n}(CN)_n]^+$ (n = 0–4) species were generated in the reaction of PBr_5 with $Zn(CN)_2$ in liquid bromine, which led to four new resonances in the ^{31}P NMR spectrum. ^{31}P NMR data of $[PBr_{4-n}(CN)_n]^+$ (n = 0–4; δ (^{31}P) = –76.5, –49.3, –40.3, –33.3 and –41.9 ppm) were reported by K. B. Dillon et al. The $[P(CN)_4]^+$ assignment at –41.9 ppm was confirmed by measurements on a $P(CN)_3/(CN)_2$ system, where in addition to these resonances the signals of $P(CN)_3$ (–130.6 ppm) and $P(CN)_5$ (–98.4 ppm) are assigned (Dillon and Platt, 1983). Isolation of solid $[P(CN)_4]^+$ salts was not achieved.

Phosphorus pentacyanide $P(CN)_5$

H. Gall and J. Schüppen carried out experiments dealing with penta-coordinated phosphates in 1930 (Gall and Schüppen, 1930). They tried to completely substitute the chloride atoms of phosphorus pentachloride PCl_5 by cyanide and thiocyanate groups. When they heated a mixture of PCl_5 and an excess of silver cyanide to a temperature of 403 K, they noticed the formation of large quantities of cyanogen (Scheme 76). But in this setup only phosphorus tricyanide was formed due to the high reaction temperature.

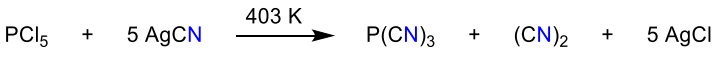

Scheme 76: Release of cyanogen during the reaction of PCl_5 and silver cyanide (Gall and Schüppen, 1930).

Based on this observation, they also heated a mixture of phosphorus tricyanide and cyanogen in a closed tube and realized a degradiation of the $P(CN)_3$ crystals concluding that phosphorus pentacyanide was formed reversibly, which was confirmed by vapor pressure measurements (Scheme 77) (Gall and Schüppen, 1930). Due to the absence of analytical data of the product, the isolation must be questioned critically. Hence, so far, the *in situ* generation of $P(CN)_5$ was only proposed and it should be noted that $P(CN)_5$ should decompose rapidly at standard conditions.

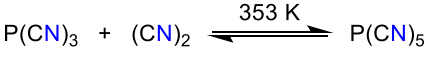

Scheme 77: Phosphorus pentacyanide formed in an equilibrium reaction (Gall and Schüppen, 1930).

Hexacyanidophosphate(V) anion $[P(CN)_6]^-$

Despite many attempts, the hexacyanidophosphate(V) anion $[P(CN)_6]^-$ has not been synthesized until now and has just been a hypothetical counterion in computational study e.g. by J. E. Bara and co-workers in 2012 or A. Schulz and co-workers in 2016 (Bläsing et al., 2016b; Shannon et al., 2012). However, as early as 1967, H. W. Roesky reported the synthesis of $[^nBu_4N][PCl_4(CN)_2]$ starting from PCl_5 and an excess of KCN (Scheme 78) (Roesky, 1967). Furthermore, H. W. Roesky was able to show that under the same reaction

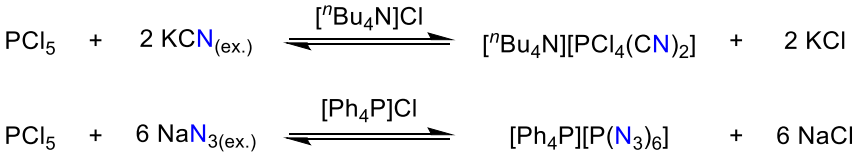

Scheme 78: Attempted synthesis of $[P(CN)_6]^-$ starting from PCl_5 (Roesky, 1967).

conditions he could isolate $[Ph_4P][P(N_3)_6]$, but not a salt containing the $[P(CN)_6]^-$ ion.

In 1982, K. B. Dillon and A. W. G. Platt reported the formation of $[Et_4N][PCl_{6-n}(CN)_n]$ (n = 1–3) when they treated $[PCl_6]^-$ salts with AgCN (Scheme 79). However, none of these salts were isolated and fully characterized (Dillon and Platt, 1982). P. J. Chevrier et al. published ^{19}F NMR data of the $[PF_5(CN)]^-$-ion (Chevrier and Brownstein, 1980), and somewhat later K. B. Dillon et al. ^{31}P NMR data of reaction mixtures containing $[PF_{6-n}(CN)_n]^-$- ($1 \le n \le 4$) and $[PF_3Cl_{3-n}(CN)_n]^-$-ions ($1 \le n \le 3$) (Dillon and Platt, 1982). These reaction mixtures were obtained when PF_5 was treated with $[Et_4N]CN$ or $[PCl_4(CN)_2]^-$ salts with AgF.

The first cyanido(fluorido)phosphate, $[BMIm][PF_3(CN)_3]$ ($[BMIm]^+$ = 1-butyl-3-methylimidazolium), was isolated in the reaction of $[BMIm][PCl_3(CN)_3]$ and $Ag[BF_4]$ after four days of reaction (Tatsumi et al., 2012). Furthermore, $[^nBu_4N][PF_2(CN)_4]$ was isolated in the reaction of $[^nBu_4N][PF_6]$ with an excess of TMS–CN under autogenous pressure in a steel autoclave at high temperatures (453–483 K, Scheme 79) (Bresien et al., 2015a, 2015b; Ellinger, Franke, et al., 2014; Ellinger, Harloff, et al., 2014; Sievert et al., 2015). By salt metathesis starting from $[^nBu_4N][PF_2(CN)_4]$, a series of different $M[PF_2(CN)_4]$ (M = Ag^+, K^+, Li^+, $[H_5O_2]^+$, $[EMIm]^+$; $[EMIm]^+$ = 1-ethyl-3-methylimidazolium) was successfully isolated and fully characterized.

The reaction of $[PF_6]^-$-salts with TMS–CN under Lewis acid catalyzed conditions was studied in detail by A. Schulz and co-workers (Bläsing et al., 2016b; Bresien et al., 2015b). This group was able to show that the best results, i.e. certain cyanido(fluorido)phosphate anions of the general formula $[PF_{6-n}(CN)_n]^-$ (n = 1–4) can be generated by a very mild Lewis acid catalyzed synthesis protocol. Salts containing the $[PF_{6-n}(CN)_n]^-$ ion (n = 1–4) can thus be isolated on a preparative scale (Scheme 80). It was also possible to detect the anion $[PF(CN)_5]^-$ but not the anion $[P(CN)_6]^-$. The formation of the $[P(CN)_6]^-$-anion is thermodynamically not allowed as DFT calculations showed. All steps up to $[PF(CN)_5]^-$ ion are exergonic only the 6th substitution step $[PF(CN)_5]^- + CN^- \rightarrow [P(CN)_6]^-$ is endergonic (Table 55) in accord with the experimental observations

Table 55: Calculated gas phase Gibbs energies for the consecutive substitution reactions (ΔG_{298} in kcal mol^{-1}, M06-2X/aug-cc-pVDZ level of theory) (Bläsing et al., 2016b; Bresien et al., 2015b).

Reaction step			ΔG_{298}
$[PF_6]^-$ + TMS–CN	→	$[PF_5CN]^-$ + TMS–F	−9.12
$[PF_5CN]^-$ + TMS–CN	→	[*cis*-$PF_4(CN)_2]^-$ + TMS–F	−5.59
$[PF_5CN]^-$ + TMS–CN	→	[*trans*-$PF_4(CN)_2]^-$ + TMS–F	−6.83
[*trans*-$PF_4(CN)_2]^-$ + TMS–CN	→	[*fac*-$PF_3(CN)_3]^-$ + TMS–F	−2.48
[*trans*-$PF_4(CN)_2]^-$ + TMS–CN	→	[*mer*-$PF_3(CN)_3]^-$ + TMS–F	−3.07
[*cis*-$PF_4(CN)_2]^-$ + TMS–CN	→	[*fac*-$PF_3(CN)_3]^-$ + TMS–F	−3.72
[*cis*-$PF_4(CN)_2]^-$ + TMS–CN	→	[*mer*-$PF_3(CN)_3]^-$ + TMS–F	−4.31
[*mer*-$PF_3(CN)_3]^-$ + TMS–CN	→	[*trans*-$PF_2(CN)_4]^-$ + TMS–F	+ 0.24
[*fac*-$PF_3(CN)_3]^-$ + TMS–CN	→	[*trans*-$PF_2(CN)_4]^-$ + TMS–F	−0.35
[*mer*-$PF_3(CN)_3]^-$ + TMS–CN	→	[*cis*-$PF_2(CN)_4]^-$ + TMS–F	−2.47
[*fac*-$PF_3(CN)_3]^-$ + TMS–CN	→	[*cis*-$PF_2(CN)_4]^-$ + TMS–F	−3.06
[*cis*-$PF_2(CN)_4]^-$ + TMS–CN	→	$[PF(CN)_5]^-$ + TMS–F	−0.09
[*trans*-$PF_2(CN)_4]^-$ + TMS–CN	→	$[PF(CN)_5]^-$ + TMS–F	−2.80
$[PF(CN)_5]^-$ + TMS–CN	→	$[P(CN)_6]^-$ + TMS–F	+ 2.48
$[PF_6]^-$ + 6 TMS–CN	→	$[P(CN)_6]^-$ + 6 TMS–F	−19.10

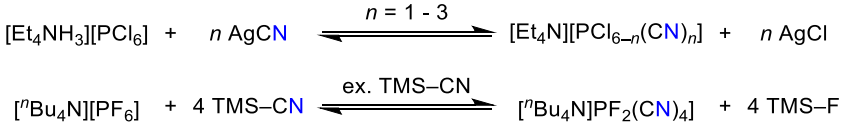

Scheme 79: Synthesis of cyanido-chlorido and cyanido-fluorido phosphates (El-Yazal et al., 1997; Jensen, 2004b; Jung et al., 2010; Küppers et al., 2007; Leibovici, 1973; Sheldrick et al., 1981).

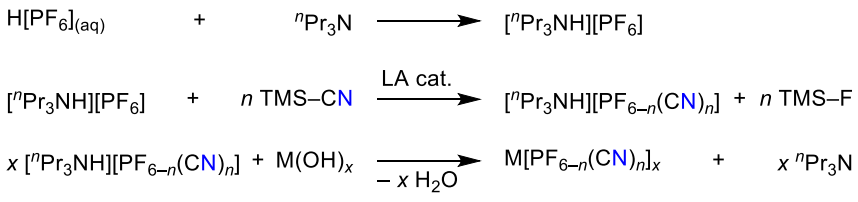

Scheme 80: Lewis acid catalyzed $F^-/[CN]^-$-exchange reactions leading to the formation of salts bearing the $[PF_{6-n}(CN)_n]^-$ (n = 1– 4) ion (Bläsing et al., 2016b).

Table 56: ^{13}C, ^{19}F and ^{31}P NMR shifts (298 K in D_2O) of all $[PF_{6-n}(CN)_n]^-$ ions along with coupling constants (*J*) and multiplicity (*M*) (Bläsing et al., 2016b).

Reaction step	$\delta^{31}P$	M	$\delta^{19}F$	M	$\delta^{13}C$	M	$^1J_{PF}$	$^2J_{FF}$	$^1J_{PC}$	$^2J_{FC}$
$[PF_6]^-$	−144.6	sept	−73.0	d	–	–	707	–	–	–
$[PF_5CN]^-$	−158.4	dquin	−47.1	dd	126.0	dquin	740	56	331	77
			−75.1	dquin			762	56		
[*trans*-$PF_4(CN)_2]^-$	−170	quin	−31.5	d	124.3	dquin	739	–	320	71
[*cis*-$PF_4(CN)_2]^-$	−183.1	tt	−41.3	dt	127.7[a]	dddt	710	43	247	37/41/53
			−54.3	dt			764	43		
[mer-$PF_3(CN)_3]^-$	−211.3	dt	−8.7	dt	124.6	ddt	780	35	262	80/54/35/19
			−39.9	dd	127.7	ddt	681	35	183	
[*fac*-$PF_3(CN)_3]^-$	−219.3	q	−40.5	d	[b]	dq	742	–	[b]	42[c]
[*trans*-$PF_2(CN)_4]^-$	[b]	t	−48.8	d	[b]	dt	632	–	[b]	[b]
[*cis*-$PF_2(CN)_4]^-$	−269.1	t	−6.1	d	125.7	dt	730	–	218	65
					128.1	dt			143	38
$[PF(CN)_5]^-$	−316.5	d	20.1	d	[b]	dd	708	–	[b]	[b]
$[P(CN)_6]^-$	[b]	s	–	–	[b]	d	[b]	–	[b]	[b]

[a]^{13}C NMR data of the Li salt in d_6-DMSO. [b]Not observed. [c]$^2J_{FC}$ taken from ^{19}F NMR spectrum.

(Bläsing et al., 2016b; Bresien et al., 2015b). NMR data of all fluorido-cyanido phosphates are listed in Table 56.

Arsenic

Although $As(CN)_3$ was first described in 1892 (Guenez, 1892), there are very few publications on the chemistry of arsenic cyanides. All of them essentially concern $As(CN)_3$, i.e. with arsenic in the oxidation state + III. The experimental and theoretical IR and Raman data of $As(CN)_3$ were also studied in detail (Cyvin et al., 1973; Edwards and Fawcett, 1987; Jensen, 2004b; Largo and Barrientos, 1991; Leibovici, 1973; Magnusson, 1986; Nagarajan, 1966).

Arsenic cyanide AsCN

The arsenic cyanide radical is rarely analyzed, but in 1968 it was part of a study by N. Basco and K. K. Yee, which deals with the absorption spectrum of flash photolysis of cyanogen and arsenic trichloride or arsane in an inert nitrogen atmosphere (Scheme 81).

AsCN was detectable during a period of τ = 150 ms, reaches its maximum of absorption intensity after τ = 3 ms and showed the largest triplet splitting of about 550 cm^{-1} of the 5th main group monocyanides (NCN: 40 cm^{-1}, PCN: 104 cm^{-1}) due to enhanced spin–orbit interaction (Basco and Yee, 1968b).

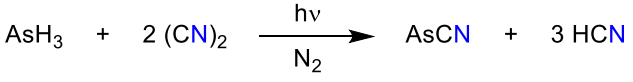

Scheme 81: Formation of arsenic cyanide by flash photolysis of cyanogen and arsane (Basco and Yee, 1968b).

Ab initio calculations, using the G2 and G2(QCI) procedures, have been performed by S. Petrie on the various isomers of AsCN, which are summerized in Table 57 (Petrie, 1999).

In relation to both isomers, the triplet state is more stable than the singlet state associated with a triplet-singlet gap of about $\Delta H_{0K}° = 90$ kJ mol^{-1}. Additionally, the cyanide isomer is 58.3 kJ mol^{-1} on G2 level and about 57 kJ mol^{-1} on G2(QCI) lower in energy than the isocyanide isomer, which implies the arsenic cyanide in triplet state is the most stable species (Table 58) (Petrie, 1999).

Dicyanoarsenide $[As(CN)_2]^-$

Similar to the synthesis of the analog $[P(CN)_2]^-$ L. B. Macdonald and co-workers published a new approach to the $[As(CN)_2]^-$. The starting material [dppeAs][BPh_4] (dppe = bis(diphenylphosphino)ethane) was obtained by a one-pot reaction of dppe, Na[BPh_4] and arsenic trichloride $AsCl_3$ as a pale-yellow solid based on M. Driess' approach. Then the phosphino ligand dppe in [dppeAs][BPh_4] was

Table 57: Computational structural data of AsCN and AsNC (bond lengths in Å; angles in °) (Petrie, 1999).

Compound	Method + basis set	r_{As-E}	r_{C-N}	< (As–A–B)
AsCN	MP2(full)/6-31G*	1.853	1.191	85.58
AsNC	QCISD(fc)/6-31G*	1.816	1.200	81.01

Table 58: Computational data of the arsenic cyanide and isocyanide on different levels of theory (ZPE, $\Delta_f H_{0K}°$ and bond strength D_{As-E} in kJ mol^{-1}; E_0 in E_h including ZPE; AsNC in $^1\Sigma$ at QCISD/6-31G*) (Petrie, 1999).

Compound	State	HF/6-31G*	G2		G2(QCI)		
		ZPE	E_0	$\Delta_f H_{0\,K}°$	E_0	$\Delta_f H_{0\,K}°$	$D_{As-E,\,0\,K}$
AsCN	$^1\Sigma$	19.6	−2326.939	470.0	−2326.940	473.0	276.5
	$^3\Sigma$	16.6	−2326.973	380.2	−2326.974	383.2	366.2
AsNC	$^1\Sigma$[a]	18.4	−2326.917	528.3	−2326.918	530.3	219.1
	$^3\Sigma$	13.8	−2326.951	438.5	−2326.953	439.8	309.6

[a]AsNC in $^1\Sigma$ calculated at QCISD/6-31G*.

displaced by cyanide ligands using tetraphenylphosphonium cyanide $[PPh_4]CN$ as cyanide source similar to an approach reported by A. Schmidpeter (Binder et al., 2018).

Arsenic tricyanide $As(CN)_3$

Arsenic tricyanide was synthesized for the first time in 1892 by M. E. Guenez by mixing cyanogen iodide and arsenic in carbon disulfide (Scheme 82) (Guenez, 1892). In 1958, T. A. Bither et al. described the isolation of $As(CN)_3$, which were obtained by treating pnictogen chlorides ECl_3 with three equivalents of TMS–CN in xylene under reflux conditions (Bither et al., 1958). $As(CN)_3$ was only characterized on the basis of elemental analysis (Bither et al., 1958; Jones and Coskran, 1971).

The crystal structure was solved by K. Emerson and D. Britton in 1963. Their synthesis was an anhydrous reaction of silver cyanide and arsenic trichloride in acetonitrile by heating to reflux or using a glass tube under vacuum at 373 K (Scheme 83) (Emerson and Britton, 1963). The group of O. Sala reported a formation of arsenic trioxide in spite of careful exclusion of moisture during heating to reflux. Although, the use of the glass tube leads to smaller amounts of the oxide, the group carried out a sublimation to remove the oxide, but the product is still contaminated with arsenic trioxide (Miller et al., 1965). $As(CN)_3$ can also be synthesized directly from $AsCl_3$ with TMS–CN without the need for another solvent. This reaction already proceeds at room temperature and after the removal of all volatile products, a white substance is obtained which can be washed with *n*-hexane (decomposition point at 492 K) (Arlt et al., 2017). P. Deokar et al. carried out the reaction utilizing arsenic trifluorides and

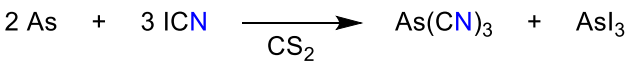

Scheme 82: Synthesis of arsenic tricyanide using arsenic and cyanogen iodide (Guenez, 1892).

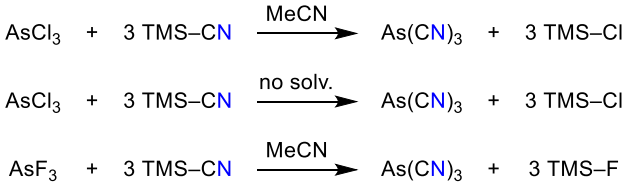

Scheme 83: Synthesis of arsenic tricyanide by K. Emerson and D. Britton (1963) S. Arlt et al. (Arlt et al., 2017) and P. Deokar et al. (Deokar et al., 2016).

an excess trimethylsilyl cyanide in acetonitrile (Deokar et al., 2016).

$As(CN)_3$ is highly moisture-sensitive and it should be noted that purification by vacuum sublimation increases decomposition (Edwards et al., 1976). IR and Raman data of all $E(CN)_3$ (E = P, As, Sb, Bi) spezies are summarized in Table 53.

Arsenic tricyanide forms monoclinic crystals, space group C_2 with four molecules in a unit cell. The molecules approximately exhibit C_{3v} symmetry including one bent cyanide group showing external interaction to one arsenic of the neighboring layer. The molecules are orientated roughly vertical to the *c*-axis and to the chains in neighboring layers (Emerson and Britton, 1963). R. Haiges and co-workers have redetermined the $As(CN)_3$ structure. The newly determined structure also shows an $As(CN)_3$ molecule with the approximate C_{3v} symmetry expected for an isolated trivalent As atom, containing three ligands and a sterically active free valence electron pair. The As–C bond distances are 1.956(3), 1.964(3) and 1.964(2) Å and the C–N distances of 1.133(3) and 1.134(3) Å, respectively, are very similar (Table 59). The arsenic atom is additionally coordinated by three N atoms from neighbouring cyano groups, resulting in a coordination number of six for the arsenic atom [3 + 3] (3 covalent + 3 van der Waals bonds). It can be seen that the As–C–N groups deviate significantly from linearity with an average angle of 174.8(4)°. The same is true for the non-linear geometry of $P(CN)_3$. The three As···N bridge bond distances of 2.704(3), 2.823(2), and 2.837(3) Å are much shorter than the van der Waals value of 3.40 Å,

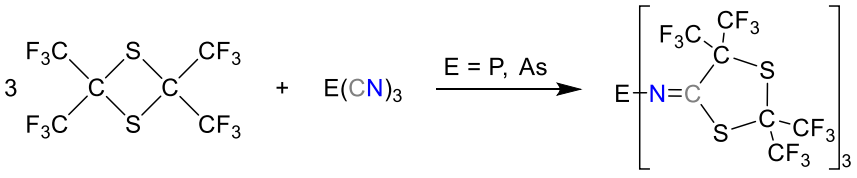

Scheme 84: Reaction of $E(CN)_3$ species with hexafluorothioacetone (Roesky and Dhathathreyan, 1984; Roesky et al., 1985).

indicating a strong association in the solid state (Deokar et al., 2016).

Furthermore, H. W. Roesky described the insertion of $P(CN)_3$ and $As(CN)_3$ into the dimer of hexafluorothioacetone (Scheme 84) (Roesky and Dhathathreyan, 1984; Roesky et al., 1985). R. Haiges and co-workers reported also on the adduct formation of $As(CN)_3$ with 2,2′-bipyridine (2,2′-bipy) leading to the formation of $As(CN)_3$·(2,2′-bipy) (Deokar et al., 2016).

Cyanidoarsenates and the unusual $[AsC_4N_4]^-$ ion

In principle, there are two ways to generate cyanidoarsenates (Scheme 85) in analogy to the cyanido phosphates or heavy pnictogens Sb and Bi. A. Schulz and co-workers reported two routes: (i) the reaction of $E(CN)_3$ with weakly coordinating cyanide salts of the type [Cat]CN ($[Cat]^+$ = e.g. $[PPh_4]^+$, $[PPN]^+ = [Ph_3P{-}N{-}PPh_3]^+$ and (ii) the treatment of EX_3 with [Cat]CN in the presence of molar amounts of TMS–CN (X = halogen) (Schmidpeter et al., 1985b; Arlt et al., 2016b). Interestingly, the formation of $[P(CN)_4]^-$ was described as a very labile intermediate in the reaction of $P(CN)_3$ with CN^- sources, which rapidly decomposes to $[NC{-}P{-}CN]^-$ and the unusual $[C_{10}N_{10}P_2]^{2-}$ (Schmidpeter et al., 1985b), while the formation and isolation of the heavy cyanidopnictogen anions of the type $[E(CN)_{3+n}]^{n-}$ (E = Sb, Bi) was only achieved when EX_3 was treated with cyanide salts and TMS–CN (Arlt et al., 2016b), since $E(CN)_3$ (E = Sb, Bi) are high polymer species that are almost insoluble in common organic solvents, so that no reaction was observed even after several days of reaction time and under reflux. It was shown that $As(CN)_3$ does not form stable $[E(CN)_{3+n}]^{n-}$ salts like phosphorus and unlike the heavier antimony and bismuth, which do form stable salts with $[E(CN)_{3+n}]^{n-}$ ions.

The chemistry of arsenic cyanides was found to be completely different from the chemistry of the heavier analogues antimony and bismuth as well as the lighter congener phosphorus. The reaction of $As(CN)_3$ with cyanide salts led to the formation of an unknown cyanido arsazolide heterocycle, which is a structural isomer of the desired $[As(CN)_4]^-$ (Arlt et al., 2017). The formation of this

Table 59: Experimental and computational data of $As(CN)_3$ (bond lengths in Å; angles in °; wave numbers in cm^{-1}).

Publication	Exp./calc.	r_{As-C}	r_{C-N}	< (C–As–C)	< (As–C–N)	$\nu^{sym.}_{CN}$
Emerson and Britton (1963)	Exp. – XRD	1.82(5)/ 1.85(5)/ 1.96(5)	1.13(7)/ 1.19(7)/ 1.14(7)	87.6(3.5)/ 91.5(3.5)/ 91.5(3.5)	175(8)/ 171(8)/ 168(8)	–
Edwards et al. (1976)	Exp. – Raman	–	–	–	–	2205
Deokar et al. (2016)	Exp. – XRD, IR	1.964(3)/ 1.964(2)/ 1.956(3)	1.134(3)/ 1.133(3)/ 1.138(3)	89.94(10)/ 90.56(10)/ 90.47(10)	174.5(3)/ 175.7(2)/ 174.5(2)	2209
	B3LYP/aug-cc-pVDZ//-PP	1.93518	1.16280	95.49	170.86	2289

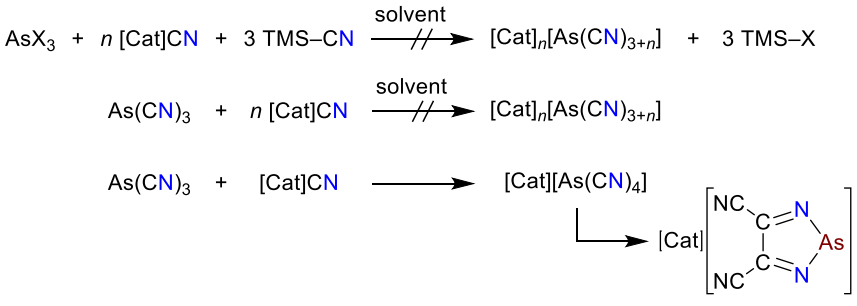

Scheme 85: Synthesis of salts containing $[As(CN)_{3+n}]^{n-}$ ions (X = F^-, Cl^-; n = 1–3; $[Cat]^+$ = $[PPh_4]^+$, $[PPN]^+ = [Ph_3P{-}N{-}PPh_3]^+$; solvent = excess TMS–CN, CH_3CN, ionic liquids) (Arlt et al., 2017).

unusual heterocycle is discussed on the basis of computation featuring an arsenic-mediated C–C coupling of cyanides. $[As(CN)_4]^-$ salts with various counterions such as $[PPh_4]^+$, $[PPN]^+$, Ag^+ and $[BMIm]^+$ are reported, where $[BMIm][AsC_4N_4]$ is a low temperature ionic liquid (T_M = 211 K).

First the authors treated $AsCl_3$ with MCN in TMS–CN which always led to the formation of $[PPh_4]_2[As(CN)_3Cl_2]$ as shown in Figure 40. To avoid the $Cl^-/[CN]^-$-substitution problem, $As(CN)_3$ was used in a second series of experiments (Scheme 85). Regardless of the stoichiometry, cyanide source and solvent (e.g. CH_3CN, TMS–CN) or even ionic liquids such as [BMIm][OTf], $[OTf]^- = [F_3CSO_2O]^-$, always the structural isomer of $[As(CN)_4]^-$, the 4,5-dicyano-1,3,2-diazarsolide, $[AsC_4N_4]^-$ (Figure 40, Scheme 85), was isolated in quite good yields (up to 70%). As calculations show, heterocyclic $[AsC_4N_4]^-$ is formed in an unusual isomerization process starting from its structural isomer $[As(CN)_4]^-$, which is first formed as a transient species when $As(CN)_3$ is treated with $[CN]^-$. Then two arsenic-mediated C–C coupling steps occur, which finally lead to the formation of the aromatic ring system $[AsC_4N_4]^-$, which can be regarded as a resonance-stabilized pseudohalide (Arlt et al., 2017).

$[As^{III}(CN)_6]^{3-}$: There is only one report on this ion by L. Kahlenberg and J. V. Steinle (1923). They studied the redox potential of many salts and amongst these they also treated a solution of silver cyanide in aqueous potassium cyanide with arsenic. They write: "The reaction probably takes place as indicated by this equation: $3K[Ag(CN)_2] + As = K_3[As(CN)_6] + 3Ag$." No analytical data are presented. Furthermore, **$[As^V(CN)_6]^-$** was mentioned in a Japanese patent on tetracyanidoborates, in which the authors calculated the highest occupied molecular orbital energy level of a great number of cyanide containing anions. Though the $[As(CN)_6]^-$ has the smallest energy of –6.744 eV, which is also smaller than –6.561 eV of $[P(CN)_6]^-$, –5.961 eV of $[Si(CN)_5]^-$ or –5.809 eV of $[B(CN)_4]^-$ (Hagiwara et al., 2011).

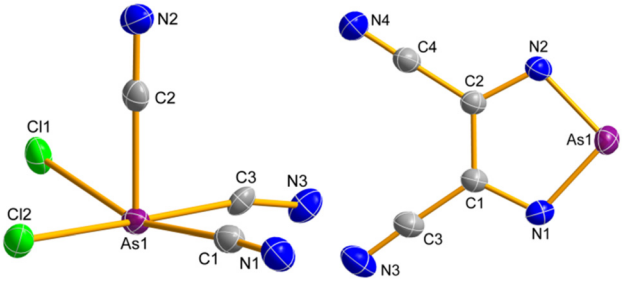

Figure 40: Left: ORTEP representation of $[As(CN)_3Cl_2]^{2-}$ and Right: Heterocyclic $[AsC_4N_4]^-$ in the crystal (Arlt et al., 2017).

Antimony

There are only very few publications on antimony cyanides, most of them are dedicated to the oxidation state(-III). It was only in 2016 that the chemistry of $Sb(CN)_3$ was taken up again by two research groups (Arlt et al., 2016a, 2016b; Deokar et al., 2016).

Antimony tricyanide $Sb(CN)_3$

$Sb(CN)_3$ was synthesized for the first time in 1958 by heating a mixture of trimethylsilyl cyanide TMS–CN dissolved in xylene and freshly sublimated antimony trichloride to reflux (Scheme 86). The white powder antimony tricyanide, which decomposes at temperatures higher than 473 K, was identified by elementary analysis (Bither et al., 1958; Jones and Coskran, 1971).

Another synthetic route is the electrochemical preparation of $Sb(CN)_3$, which was published by H. Schmidt and H. Meinert in 1958. The dissolved product is obtained at the antimony anode due to electrolysis of silver cyanide, which is also dissolved in pyridine, and can be isolated as colorless, hygroscopic crystals by evaporation of the solution (Schmidt and Meinert, 1958). The reaction of the antimony trifluorides with TMS–CN in acetonitrile in the presence of stoichiometric amounts of 2,2′-bipyridine (2,2′-bipy) led to the formation of the corresponding 2,2′-bipyridine adduct, $Sb(CN)_3{\cdot}$(2,2′-bipy) (Deokar et al., 2016).

A. Schulz and co-workers reacted pnictogen trifluoride EF_3 with three equivalents of TMS–CN in various organic solvents such as acetonitrile or THF (Arlt et al., 2016a, 2016b). They also carried out the reaction in a large excess of TMS–CN. All these experiments resulted in the quantitative conversion of EF_3 to $E(CN)_3$ (E = Sb, Bi), which were

$$SbCl_3 + 3\ TMS{-}CN \xrightarrow[xylene]{\Delta} Sb(CN)_3 + 3\ TMS{-}Cl$$

Scheme 86: Synthesis of antimony tricyanide using antimony trichloride and TMS–CN (Bither et al., 1958).

$$EF_3 + 3\ TMS{-}CN \xrightarrow[\Delta]{solvent} E(CN)_3 + 3\ TMS{-}F$$

Scheme 87: Synthesis of polymeric $E(CN)_3$ species (E = Sb, Bi; solvent = MeCN, TMS–CN, THF) (Roesky, 1967).

obtained as highly amorphous white powders (Scheme 87). Both species are almost insoluble in standard organic solvents. Hence, it was not possible to produce single crystals of both $E(CN)_3$ species by this method. Therefore, both species could only be characterized by elemental analysis and vibrational spectroscopy (Table 53). Mass spectrometric investigations showed no specific molecular peak. Moreover, both $Sb(CN)_3$ and $Bi(CN)_3$ hydrolyse slowly to E_2O_3, as shown by powder X-ray diffraction studies, and decompose without melting above 472 K ($Sb(CN)_3$) and 439 K ($Bi(CN)_3$), respectively. All these results indicate the presence of high polymer structured $E(CN)_3$ species that exhibit strong intermolecular interactions, as predicted by the group of R. Dronskowski (George et al., 2014).

However, it was shown that molecular $Sb(CN)_3$ and $Bi(CN)_3$ species, once formed in the synthesis process, can be stabilized in ionic liquids. To avoid oligomerization of the molecular $E(CN)_3$ species, different ionic liquids were used as reaction media instead of (polar) organic solvents (Ahmed and Ruck, 2011; Freudenmann et al., 2011). By this approach it was possible to prevent the *in situ* formed $E(CN)_3$ molecules from oligomerization by anion formation with the counterion of the ionic liquid (Scheme 3, Scheme 88). For example, in the reaction of SbF_3 with TMS–CN in presence of [BMIm][OTf] ($[BMIm]^+$ = 1-butyl-3-methylimidazolium, $[OTf]^-$ = triflate = $[CF_3SO_3]^-$), it was possible to isolate and fully characterize [BMIm] $[Sb(CN)_3(OTf)]$ in the first reaction step of the reaction sequence depicted in Scheme 88.

The structure of the $Sb(CN)_3$ adducts is characterized by a trigonal-pyramidal arrangement of the three cyanide groups as illustrated in Figure 41. In addition, there are three further van der Waals interactions with two solvent molecules and an adjacent CN group, so that here, too, one can speak of a formal [3 + 3] coordination or a distorted octahedral coordination sphere, quite in analogy to the lighter species $E(CN)_3$ (E = P, As).

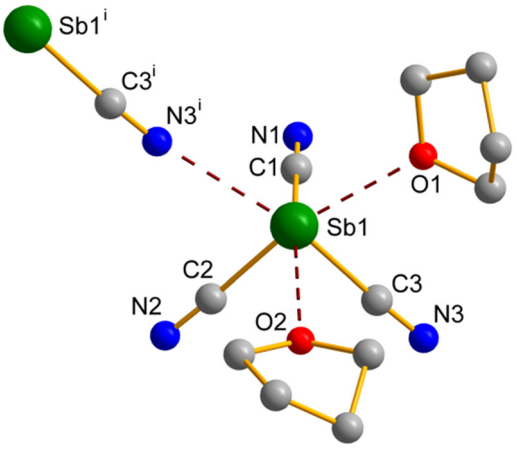

Figure 41: Molecular structure of $Sb(CN)_3 \cdot 2$ THF in the crystal.

Cyanidoantimonates $[Sb^{III}(CN)_{3+n}]^{n-}$ and $[Sb^{V}(CN)_6]^-$

The quest for cyanidoantimonates began with U. Müller who observed the formation of the $[SbCl_5(CN)]^-$ anion upon addition of MCN (M = Na^+, K^+) to a solution of $SbCl_5$ in SO_2 (Müller, 1973). M. K. Rastogi studied the reaction of $SbCl_3$ with KCN which afforded the formation of $K_2[SbCl_3(CN)_2]$ (Rastogi, 1987). In 2009 F. Renz and co-worker reported the isolation of an iron salt containing the $[Sb(CN)_6]^-$ ion from the reaction of $[SbCl_6]^-$ with KCN in acetone under reflux for six days (Renz et al., 2009b). In the light of the rather poor analytical data (ESI-MS and IR data, Mössbauer spectra) the formation of $[Sb(CN)_6]^-$ ion seems to be rather doubtful. Actually, neither the mentioned ESI-MS and IR data, nor any elemental analysis data at all could be found. A retry clearly showed that it is impossible to get a complete $Cl^-/[CN]^-$-exchange by this procedure starting from $[SbCl_6]^-$.

When SbF_3 is reacted with TMS–CN, only the insoluble polymer $Sb(CN)_3$ is obtained, regardless of the solvent used. No molecular $Sb(CN)_3$ solvent adducts could be isolated (Arlt et al., 2016b). However, when SbF_3 is treated with three equivalents of TMS–CN in the presence of n equivalents of [WCC]CN (n = 1–3) in acetonitrile, $[WCC]_2[E(CN)_5]$ salts are obtained (Scheme 89). In addition to $[WCC]_2[Sb(CN)_5]$ (Arlt et al., 2016b), quantities of $Sb(CN)_3$ were always detected, depending on the stoichiometry of [WCC]CN used, which is why the yields were rather low (between 20 and 30%). Thus, when only one equivalent of [WCC]CN was used, mixtures of $Sb(CN)_3$ and $[Sb(CN)_5]^{2-}$ were always observed. It was impossible to isolate or even

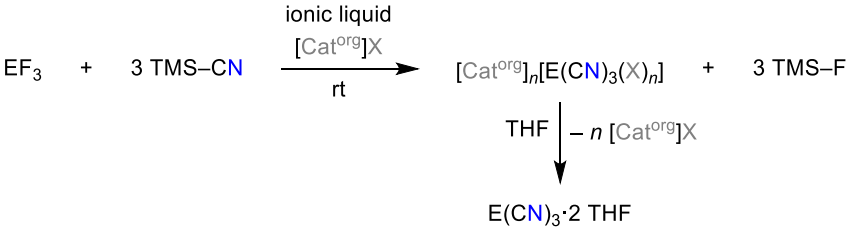

Scheme 88: Synthesis of $E(CN)_3 \cdot 2$ THF in ionic liquids ($[BMIm]^+$ = 1-butyl-3-methylimidazolium, $[EMIm]^+$ = 1-ethyl-3-methylimidazolium; $[OTf]^- = [CF_3SO_3]^-$) (Roesky, 1967).

$$SbF_3 + 3\ TMS{-}CN + n\ [WCC]CN \xrightarrow{MeCN} [WCC]_n[Sb(CN)_{3+n}] + 3\ TMS{-}F$$

Scheme 89: Synthesis of cyanido antimonates (Arlt et al., 2016b).

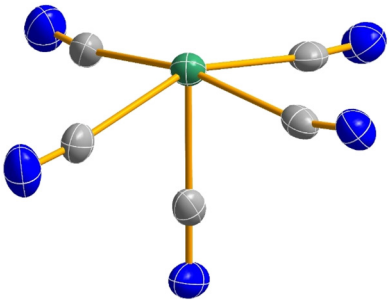

Figure 42: Molecular structure of $[Sb(CN)_5]^{2-}$ in the crystal (color code: blue = nitrogen, grey = carbon, green = antimony) (Arlt et al., 2016b).

observe the [WCC][Sb(CN)$_4$] salts. When three equivalents of [WCC]CN were added, only [WCC]$_2$[Sb(CN)$_5$] salts could be isolated in addition to an excess of [WCC]CN. No formation of [WCC]$_3$[Sb(CN)$_6$] was observed (Arlt et al., 2016b). The structures of [PPN]$_2$[Sb(CN)$_5$] and [Ph$_4$P]$_2$[Sb(CN)$_5$] have been determined (Figure 42). Both structures consist of well-separated cations and $[Sb(CN)_5]^{2-}$ anions without significant cation···anion contacts. $[Sb(CN)_5]^{2-}$ adopts a highly distorted square pyramidal geometry. There are no significant inter-anion interactions. The basal Sb–C distances range between 2.305(4) and 2.479(5) Å, while the apical Sb–C distances are much shorter at 2.142(4) Å (Arlt et al., 2016b).

Bismuth

Bi(CN)$_3$ is very similar to Sb(CN)$_3$ in terms of synthesis and structure, as it also occurs as a polymer. The cyanido bismuthates, on the other hand, show a much greater variety.

Bismuth dicyanide Ph$_3$Bi(CN)$_2$

Until now, no homoleptic bismuth dicyanide has been published in literature, but several multivalent bismuth derivatives consisting of two cyanide groups and some organic substituents, for example phenyl groups. The first synthesis of triphenylbismuth dicyanide using triphenylbismuth dichloride and potassium cyanide was published by R. G. Goel and H. S. Prasad (Scheme 90).

$$Ph_3BiCl_2 + 2\ KCN \longrightarrow Ph_3Bi(CN)_2 + 2\ KCl$$

Scheme 90: Synthesis of triphenylbismuth dicyanide by R. G. Goel and H. S. Prasad (1973).

Table 60: Experimental spectroscopic data of the CN group of Ph$_3$Bi(CN)$_2$ (wave numbers in cm^{-1}) (Goel and Prasad, 1973).

spectrum	ν_{CN}
IR	2128, 2135, 2140
Raman	2136

Furthermore, IR and Raman spectra of triphenylbismuth dicyanide, which can be obtained as colorless crystals, were published (Table 60) (Goel and Prasad, 1973). However, cyanide is also a common ligand of many different bismuth complexes, e.g. tetraethylamine-dicyano-diphenyl bismuthate. However, these organo-bismuth complexes are not part of this article and the reader is referred to the relevant literature (Allman et al., 1979).

Bismuth tricyanide Bi(CN)$_3$

One of the first synthesis of bismuth tricyanide was published by H. Schmidt and H. Meinert in 1958. The synthetic route is similar to the electrochemical preparation of antimony tricyanide as the bismuth compound is obtained at the bismuth anode due to electrolysis of silver cyanide dissolved in pyridine (Scheme 91). As described for E(CN)$_3$ (E = P, As, Sb, see above) also Bi(CN)$_3$ can be prepared by treating BiCl$_3$ with three equivalents of TMS–CN in xylene under reflux conditions (Bither et al., 1958; Jones and Coskran, 1971). The reaction of BiCl$_3$ with TMS–CN was reported to be incomplete leading only to mixed chloride/cyanide bismuth species. However, Bi(CN)$_3$ can be prepared utilizing the same procedure as discussed for Sb(CN)$_3$ (see 7.4.1 Antimony tricyanide Sb(CN)$_3$, Scheme 87, Scheme 88) (Arlt et al., 2016a). IR and Raman data of all E(CN)$_3$ (E = P, As, Sb, Bi) spezies are summarized in Table 53. The bismuth tricyanide is also a colorless solid (Schmidt and Meinert, 1958).

Crystals of Bi(CN)$_3$·2 THF were studied exhibiting also a [3 + 3] coordination around the bismuth atom as found for the analogous antimony compound. Both THF adducts E(CN)$_3$·2 THF (E = Sb, Bi) are highly moisture-sensitive and decompose above 485 and 409 K, respectively, under release of THF as shown by DSC/TGA experiments.

$$Bi + 3\ AgCN \longrightarrow Bi(CN)_3 + 3\ Ag$$

Scheme 91: Electrochemical preparation of bismuth tricyanide by H. Schmidt and H. Meinert (Schmidt and Meinert, 1958).

Cyanidobismuthates $[Bi^{III}(CN)_{3+n}]^{n-}$ and $[Bi^{V}(CN)_6]^-$

The reaction of *in situ* generated $Bi(CN)_3$ with different amounts of $[Ph_4P]CN$ and [PPN]CN yielded salts with the ternary ions $[Bi(CN)_5]^{2-}$, $[Bi_2(CN)_{11}]^{5-}$ and $[Bi(CN)_6]^{3-}$ (synthesis analogous to the reaction with $Sb(CN)_3$; Scheme 86 - 88, Figure 43) (Arlt et al., 2016b). It was shown that the bismuth reaction mixture is highly dynamic with respect to the CN ligand sphere around the formal Bi^{3+} cation and that, depending on solubility, concentration and temperature, different products can be isolated as illustrated in Figure 43. All structures display an active valence electron pair at the central atom of the bismuth^{III} ions and Bi–C bonds that can be either asymmetrically (three shorter bonds + *x* longer bonds) or symmetrically (with rather long averaged bonds). In the presence of weakly coordinating cations (e.g. $[Ph_4P]^+$ and $[PPN]^+$), the solid state structures of salts containing $[Bi(CN)_5]^{2-}$ anions contain well-separated cations and monomeric anions that have a sterically active lone pair and a monomeric square-based pyramidal (pseudo-octahedral) structure. The $[Bi(CN)_5 \cdot MeCN]^{2-}$ acetonitrile adduct ion shows a strongly distorted octahedral structure that is better understood as a [5 + 1] coordination. The $[Ph_4P]_6[Bi_2(CN)_{11}]CN$ salt consists of separate cations and anions, as well as well-separated $[Bi_2(CN)_{11}]^{5-}$ and $[CN]^-$ ions. The structure of $[Bi_2(CN)_{11}]^{5-}$ ion can be described as two square-based pyramidal $[Bi(CN)_5]^{2-}$ fragments connected by a disordered bridging $[CN]^-$ ion, resulting in a distorted octahedral environment around the two Bi centers. Here, the steric effect of the lone pair is much less pronounced, but still present.

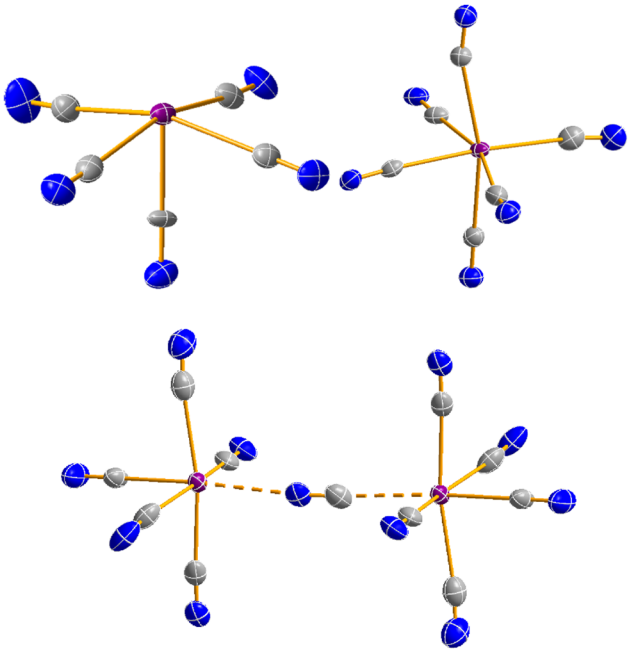

Figure 43: Molecular structures of different cyanido bismuthates (Arlt et al., 2016b).

6th Main group

When an oxygen atom is formally linked to a $[CN]^-$ ion with its electron sextet, the cyanate ion, $[OCN]^-$, is formed, which is a pseudohalogen just like the cyanide ion itself. The cyanate ion is by far the most important chalcogen-cyanide compound, followed by the thiocyanate, $[SCN]^-$. The heavy chalcogen congeners are also pseudohalide ions (see 1.2 Cyanide, a classic pseudohalide). The cyanate is the eponym of all monocyanides of this main group. As typical pseudohalides they easily generate salts in presence of different metal cations. Cyanates are of great industrial (e.g. synthesis of polymers) as well as biological importance (Arnold et al., 1957; Barton et al., 1991, 1999; Bauer and Gnauck, 1987; Bauer et al., 1986, 1998; Bernsdorf and Köckerling, 2012; Britton and Dunitz, 1965a; Decius et al., 1965; Eyster and Gillette, 1940; Fang and Shimp, 1995; Grenier-Loustalot et al., 1996; Hamerton and Hay, 1998; Hendricks and Pauling, 1925; Kalmutzki et al., 2013; Kertes, 1979; Kotch et al., 1995; Maki and Decius, 1958, 1959; Marcos-Fernández et al., 1999; Moreno et al., 2013; Okubo and Ise, 1972; Osei Owusu et al., 1996; Rabalais et al., 1969a, 1969b; Reghunadhan Nair et al., 2001; Schalke, 2006; Shorter, 1978). Especially the latter also applies to the thiocyanates (Aguirre et al., 2010; Akcil, 2003; Anderson, 1980; Anderson et al., 1990; Azizitorghabeh et al., 2021; Bahta et al., 1997; Banerjee, 1996; Betts et al., 1979; Bezsudnova et al., 2007; Bhunia et al., 2000; Castanheiro et al., 2016; Dash et al., 2009; Du Plessis et al., 2001; Ebbs, 2004; Happold et al., 1958; Jensen and Tuan, 1993; Kelly and Baker, 1990; Kim and Katayama, 2000; Kwon et al., 2002; McDonald et al., 1969; Mudder et al., 1991; Palatinszky et al., 2015; Ryu et al., 2015; Stafford and Callely, 1969; Staib and Lant, 2007; Stott et al., 2001; Stratford et al., 1994; Sorokin et al., 2001; Wald et al., 1939; Watts and Moreau, 2016; Wilson and Harris, 1961; Wijeyasinghe and Anthopoulos, 2015; Willemin and Lumen, 2017; Wilson et al., 1960; Youatt, 1954). However, these aspects are not examined in this review, nor are the many inorganic salts of cyanates and thiocyanates (Bahta et al., 1997; Bernsdorf and Köckerling, 2012; Britton and Dunitz, 1965a; Schalke, 2006; McDonald et al., 1969; Norbury et al., 1973; Schultz, 1996; Wilson and Harris, 1961; Wijeyasinghe and Anthopoulos, 2015).

Formally, all chalcogenates, $[ECN]^-$ (E = O, S, Se, Te, and Po), can also be considered as chalcogen monocyanides, where the interaction between the chalcogen and the cyanide group decreases along the group.

Accordingly, the charge between the oxygen and nitrogen atoms of the cyanate anion is approximately equally distributed, but the negative charge on the nitrogen atom increases the heavier the chalcogen is due to a decrease in electronegativity towards the tellurocyanate. Another aspect is the reduced influence of resonance structures, which reduce the π-interaction of the heavier elements.

The formal dicyanides of the type $E(CN)_2$ are also known. The neutral chalcogen tetracyanide, $E(CN)_4$, compounds are only known from selenium and tellurium, which are not stable in the long term. Their structure can be discussed as a pseudo-trigonal-bipyramidal arrangement and the unpaired electrons are in axial position.

Oxygen

Cyanate radical $[OCN]^{\cdot}$ and cyanate anion $[OCN]^{-}$

Modern cyanate chemistry began with a dispute between Friedrich Wöhler and Justus v. Liebig (Liebig and Gay-Lussac, 1824a, 1824b; Liebig and Wöhler, 1830; Wöhler, 1824, 1825b). The latter was of the opinion that the elemental analysis of silver cyanate (AgNCO) published by F. Wöhler must be wrong, as it was the same as the one he had found for silver fulminate (AgCNO). The dispute was settled when the isomerism of these compounds was discovered (Berzelius, 1832). Incidentally, it is remarkable that the two congenial minds had been working with isomeric acids since their early youth: F. Wöhler with (iso) cyanic acid and J. v. Liebig with fulminic acid and their salts; already at the age of 15 J. v. Liebig had copied the preparation of silver fulminate from a market trader. Last but not least, F. Wöhler's urea synthesis from ammonium cyanate was a milestone in the history of chemistry ($[NH_4]OCN \rightarrow H_2NC(O)NH_2$) (Wöhler, 1828).

Cyanate radical $[OCN]^{\cdot}$

Large sources of natural free cyanate radicals are not known, but smaller amounts of cyanates are reported to be part of carbon-star atmospheres in regard to CNO processing and intermediates of the cyanate radical are still existing in exhaust gases of modern combustion engines during reduction processes of nitric oxides (Du and Zhang, 2013; Morris and Wyller, 1967).

The cyanate radical has a linear structure and exhibits $C_{\infty v}$ symmetry. Cyanate radicals can be generated by photolysis of isocyanic acid using UV light in a noble gas matrix at low pressure and low temperature. According to H. Okabe, HNCO is prepared by heating powdery cyanuric acid in an evacuated vessel, whereas D. E. Milligan and M. E. Jacox heated up the cyclic trimer. But also the reaction of carbon atoms of cyanogen azide with NO or the reaction of oxygen atoms with CN can result in the formation of $[OCN]^{\cdot}$. Using UV light the isocyanic acid can directly dissociate in hydrogen and the cyanate radical, but photolytic isomerization to HNCO and its photodissociation forming the cyanate radical is also possible (Scheme 92) (Milligan and Jacox, 1967a, 1967b; Okabe, 1970).

In 1985, D. D. Bell and R. D. Coombe published a study on the photolysis of chlorine isocyanate to form cyanate radicals and discussing several standard enthalpies of formation (Scheme 93) (Bell and Coombe, 1985). As early as 1974, C. Thomson and B. J. Wishart could confirm the linear structure of the cyanate radical by computations (Table 61). Based on population analysis data, the dipole moment of the radical was estimated to be 0.504 D (LCAO-MO-SCF/BA + P, Table 62) (Thomson and Wishart, 1974).

Cyanate anion $[OCN]^{-}$

The cyanate anion $[OCN]^{-}$ is much more stable than the radical and can be isolated as anion in salts with metal or WCCs as counter cation (Bernsdorf and Köckerling, 2012; Britton and Dunitz, 1965a; Decius et al., 1965; Galliart and Brown, 1972; Hendricks and Pauling, 1925; Hennings et al., 2011; Kertes, 1979; Maki and Decius, 1958; Schalke, 2006). Furthermore, it is an ambidentate nucleophile and able to bind protons or metal centers at both ends. If the proton is bound at the nitrogen atom, the product is called cyanic acid, if it is bound to the oxygen atom, the isomer is called isocyanic acid. At room temperature, isocyanic acid clearly predominates. However, esters of both isomers exist, e.g. ethyl cyanate, Et–OCN, and ethyl isocyanate, Et–NCO. The cyanate ion should be represented by at least three mesomeric structures (Scheme 94). The constitutional isomer of the

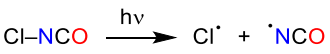

Scheme 93: Photolysis of chlorine isocyanates to form the cyanate radical (Bell and Coombe, 1985).

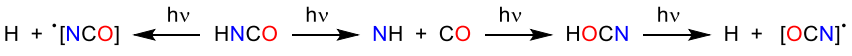

Scheme 92: Formation of the cyanate radical by vacuum-ultraviolet photolysis (Milligan and Jacox, 1967a, 1967b; Okabe, 1970).

Table 61: Structural data of the cyanate radical (bond lengths in Å; angles in °; wave numbers in cm^{-1}).

Publication	Exp./calc.	r_{C-N}	r_{C-O}	< (O–C–N)	ν_{CO}	ν_{CN}
Chase et al. (1974)	Exp.	1.23	1.18	180	1275	1922
Thomson and Wishart (1974)	LCAO-MO-SCF/DZ + P	1.259	1.191	180	–	–
	LCAO-MO-SCF/BA + P	1.226	1.134	180	–	–
Yu et al. (1992)	HF/6-31G*	1.231	1.160	180	1407	1959
	MP2/6-31G*	1.253	1.166	180	–	–
Léonard et al. (2007)	MRCI/cc-pVQZ	1.230	1.178	180	1270.8	1987.6

Table 62: Population analysis of the valence orbitals within the cyanate radical as reported by B. Thomson and B. J. Wishart (1974).

MO	N	C	O
4*s*	0.0228	0.5369	1.4403
5*s*	1.2054	0.7653	0.0294
6*s*	0.0537	0.2106	1.7357
7*s*	1.7375	0.2118	0.0507
1*p*	0.1064	1.2493	2.6434
2*p*	1.9431	0.7588	0.2982
Total	7.0679	5.7339	8.1983

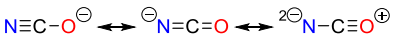

Scheme 94: Lewis representation of the $[OCN]^-$ ion.

cyanate is called fulminate $[CNO]^-$ and its corresponding acid is called fulminic acid. In comparison to the cyanates, the fulminates are more unstable, which also corresponds to the name fulminic acid derived from fulmination, which is a synonym of detonation or bang. But on the other hand, fulminate salts are stable enough to carry out X-ray structure analyses (Britton and Dunitz, 1965b).

Both KOCN and NaOCN are commercially available. Alkali metal cyanate is obtained by melting urea and alkali metal carbonate (Scheme 95) (Müller et al., 2014). Metal hydroxide is only useful for laboratory synthesis (Schalke, 2006). Urea is the preferred source for the cyanate part of the molecule, with ammonium carbonate being formed as a by-product in reversal of F. Wöhler's urea synthesis. The endothermic reaction requires strong heating above 473 K for a prolonged period of time to achieve a reasonable conversion. This process does not achieve a complete conversion, but only a product with a purity of approx. 89–92%. The reaction takes place in a urea melt with a high content of dispersed solids. The main impurity is metal carbonate with small amounts of metal allophanate ($H_2NC(O)NHCO_2M$), cyanuric acid, biuret and urea. Higher purities > 95% are achieved by directly using technical-grade MOCN and urea to decrease the amount of by-products in the technical-grade MOCN. In this case, temperatures up to 873 K are required. Metathesis reactions can produce cyanate salts other than NaOCN and KOCN. The synthesis of $[NH_4]OCN$ can be generated by reversing F. Wöhler's urea synthesis ($H_2NC(O)NH_2 \rightarrow [NH_4]OCN$) (Boatright, 1954). The synthesis of $[NH_4]OCN$ can also be achieved by a catalytic reaction (with the catalysts Pt, Cu/Ni, Ru or Os). In this process, NO is reduced with CO and H_2 to $[NH_4]OCN$ (Cant et al., 2003, 2004, 2005a, 2005b; Chambers et al., 2001; Dalla Betta and Shelef, 1976; Unland, 1973; Voorhoeve and Thimble, 1978). It was the C. C. Cummins group that studied nitrogen fixation with transition metal complex to form the N_2-derived terminal nitrido ligand in $NMo–(N[^tBu]Ar)_3$ (Ar = 3,5-$Me_2C_6H_3$). The latter complex was shown to form $OCN–Mo–(N[^tBu]Ar)_3$ in the reaction with CO (Cozzolino et al., 2014). An elegent way to synthesize [WCC]OCN salts represents the nucleophilic desilylation of trimethylsilyl cyanate by methylcarbonate-containing ILs (Harloff et al., 2019a).

The cyanate ion has a linear structure, exhibits $C_{\infty v}$ symmetry (Cozzolino et al., 2014; Galliart and Brown, 1972;

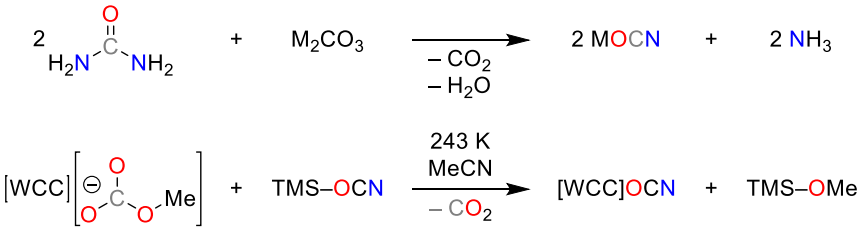

Scheme 95: Synthesis of alkali metal and WCC cyanates (Müller et al., 2014).

Hennings et al., 2011; MacLean et al., 2003; Schalke, 2006). Its silver salt forms monoclinic crystals, space group $P2_1/m$ (Britton and Dunitz, 1965a). One could expect a coordination of the cation to both ends of the cyanate, so coordination to the nitrogen and oxygen, but in fact long chains are reported because of two silver cations linearly coordinating to one nitrogen atom. Though, the silver nitrogen distance of r_{Ag-N} = 2.115(8) Å is in the range of a typical silver cyanide bond. In contrast, the distance between the silver cation and the harder oxygen of r_{Ag-O} = 2.996(8) Å is much longer causing a weaker interaction (Britton and Dunitz, 1965a). Using neutron powder diffraction (MacLean et al., 2003), it was shown that in the structure of ammonium cyanate, the NH_4^+ cation forms N–H–N hydrogen bonds to four cyanate N atoms at alternate corners of a distorted cube (Figure 44), rather than the alternative arrangement with N–H···O hydrogen bonds to cyanate O atoms at the other four corners. With two formula units of $[NH_4]NCO$ in the tetragonal unit cell in the space group $P4/nmm$ the linear cyanate anions lie along the fourfold axes, and the N atom of the ammonium cation is on a site with $\bar{4}$ symmetry. Recently, salts bearing the cyanate ion in a hydrogen-bonded HCN matrix $[OCN(HCN)_3]^-$, were reported (Bläsing et al., 2020). Due to a detailed review dealing with three-atomic cyanate and thiocyanate and especially their alkaline, ammonium and thallium(I) salts, the growth of crystals, properties and phase transitions were reported by A. Fuith, this class of CN containing substances is just discussed briefly (Fuith, 1997).

Computational studies confirm the linear structure of the anion in the gas phase and an NBO analysis show a well-balanced charge distribution on nitrogen and oxygen (Table 63). In comparison to carbon both terminal elements are more electronegative having an electron-withdrawing effect on carbon and causing a positive partial charge

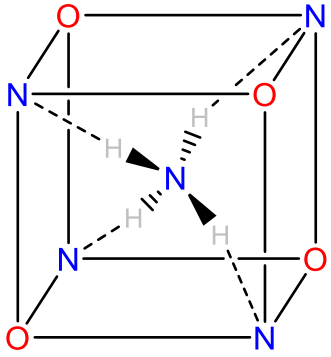

Figure 44: Schematic illustration of the N–H···N hydrogen bonding in $[NX_4]OCN$ (X = H, D).

Table 63: Natural Bond Orbital (NBO) atomic charges (in a.u.) of the cyanate ion at BP86/cc-pVQZ (Lu et al., 2014).

NBO	O	C	N
q_E	−0.72	0.50	−0.78

(Lu et al., 2014). Selected experimental and computational data are listed in Table 64.

In 2018, T. M. Klapötke and co-workers reported the synthesis of isocyanic acid using potassium cyanate and stearic acid, which is similar to the synthesis of hydrogen cyanide by A. Schulz and co-workers in 2016 (Labbow et al., 2016). Based on the X-ray diffraction experiment similarities of carbon dioxide and the isocyanic acid, which can also be called the imide of CO_2, are discussed. In the crystal the acid also forms zigzag chains with N···HN hydrogen bonds of 2.14 Å (Evers et al., 2018).

The trimerization and polymerization of cyanic acid are well known (Scheme 96). Trimerization reactions of isocyanates (R–NCO) have been investigated in many ways, e.g. for the preparation of cyclic cyanurate esters, which show great performance as adhesives, composites, resins etc. (Arnold et al., 1957; Barton et al., 1991, 1999; Bauer and Gnauck, 1987; Bauer et al., 1986, 1998; Fang and Shimp, 1995; Grenier-Loustalot et al., 1996; Hamerton and Hay, 1998; Kotch et al., 1995; Marcos-Fernández et al., 1999; Osei Owusu et al., 1996; Reghunadhan Nair et al., 2001; Seifer, 2002; Williams, 1948).

Although a large number of derivatives of cyanuric acid are known in organic chemistry, there are only a few structurally characterized metal cyanurates. Salts of cyanuric acid have been mentioned since the mid-eighteenth century (Kalmutzki et al., 2013; Seifer, 2002; Williams, 1948). The first reported compounds containing anions of cyanuric acid were transition metal cyanurate complexes, mainly of nickel, copper and cobalt. Structures with trivalent cyanurate anions were isolated and fully characterized by H. J. Meyer and co-workers (Scheme 97) (Kalmutzki et al., 2013). The preparations of cyanurate compounds $LiSr(O_3C_3N_3)$ and $Li_3Sr_2F(O_3C_3N_3)_2$ were possible due to using the concept of solid-state metathesis reactions.

Dicyanoether $O(CN)_2$

Experimentally, dicyanoether $O(CN)_2$ has been investigated by C. W. Hand and R. M. Hexter in 1970 (Hand and Hexter, 1970). Flash photolysis of a mixture of cyanogen and ozone and followed by a rapid scanning using an IR

Table 64: Experimental and computational data of the cyanate anion and different cyanate salts (bond lengths in Å; angles in °; wave numbers in cm^{-1}).

Compound	Exp./calc.	r_{C-N}	r_{C-O}	< (O–C–N)	$\nu^{as.}$	$\nu^{sym.}$
$[OCN]^-$	Exp. – UV (Jacox, 1990)	–	–	–	2338	1289
	B3LYP/aug-cc-pVTZ (Moreno et al., 2013)	1.184	1.221	180	–	–
	CCSD(T)/cc-pVQZ (Lu et al., 2014)	1.192	1.230	180	2188	1232
	CCSD(T)/aug-cc-pV5Z (Léonard et al., 2010)	1.193		180	2166.1	1228.0
AgNCO	Exp. – XRD (Britton and Dunitz, 1965a)	1.195(11)	1.180(11)	–	–	–
NaOCN	Exp. – XRD (170 K)/Raman (Reckeweg et al., 2010)	1.227(16)	1.192(17)	180	2178	1215
KOCN	Exp. – XRD (Nambu, 2003)/Raman (Brooker and Wen, 1993)	–	1.1988(4)	180	2181	1207
$[ND_4]OCN$	Exp. – XRD (MacLean et al., 2003) (14 K)	1.191(5)	1.215(5)	180	–	–
	Exp. – XRD (MacLean et al., 2003) (288 K)	1.192(7)	1.174(8)	180	–	–

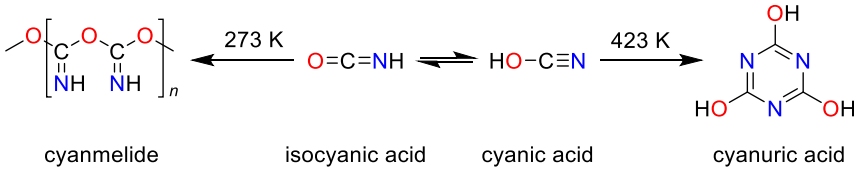

Scheme 96: Oligomers and polymers of (iso) cyanic acid (Huthmacher and Most, 2000).

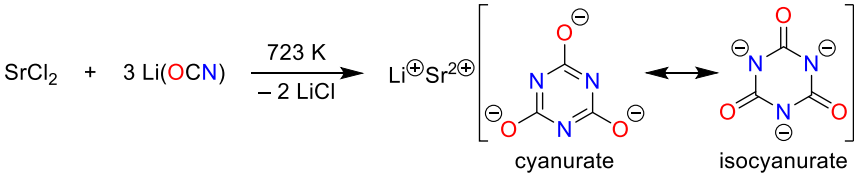

Scheme 97: Synthesis of salts bearing the trimeric cyanate ion (Kalmutzki et al., 2013).

spectrometer led to the detection of the $O(CN)_2$ molecule. Besides $O(CN)_2$, a further product was observed. The asymmetrical product evolved from the terminal addition of oxygen in its ground state to the cyanogen. On the other hand, the symmetrical product $O(CN)_2$ is the result of an insertion of singlet oxygen into the C–C bond of the cyanogen (Scheme 98).

One of the new absorption band at (2205 ± 10) cm^{-1}, which appeared within 20 µs was assigned to the formation of $O(CN)_2$. After 70 µs the band reaches the maximum of intensity and fell off gradually during several minutes (Hand and Hexter, 1970). In 1977, D. Poppinger and L. Radom published the first computations on the geometrical and energetical properties of R–OCN fragments (Poppinger and Radom, 1978). Due to limited computing capacity, the cyanate group was supposed to be linear, so the geometry optimization was restricted to the bond length and bond angle of the substituent R of R–OCN

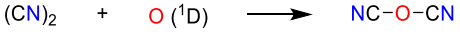

Scheme 98: Flash photolysis of cyanogen and ozone to form dicyanoether (Hand and Hexter, 1970).

Table 65: Computational data of cyanogen isocyanate, cyanogen cyanate and cyanoformonitrile oxide using HF/STO-3G (bond lengths in Å; angles in °; $E_{rel.}$ in kJ mol^{-1}) (Poppinger and Radom, 1978).

Compound	Symmetry	r_{NC-X}	< (C–X–Y)	$E_{rel.}$
(NC)NCO	C_s	1.381	123.5	0.0
(NC)O(CN)	C_{2v}	1.369	111.4	157.0
(NC)CNO	$C_{\infty v}$	1.392	180.0	261.3

(Table 65). With the presumption of linear cyanate groups, the dicyanoether was found to exhibit C_{2v} symmetry. Interestingly, dicyanoether does not represent the lowest lying isomer as it is 157.0 kJ mol^{-1} above the cyanoisocyanate, (NC)NCO.

Furthermore, the product of terminal addition of oxygen in its ground state is the most unstable compound. After all, these compounds with R = CN show the same order of stability as R = CH_3 and the authors noted that the isocyanate structure is the most stable one, because the lone pair of nitrogen is a better *p* donor than the lone pair of oxygen. The change to a bigger basis set 4-31G including polarization functions leads to the bending of the angle

< (O–C–N) = 175.6° and an decrease of symmetry from C_{2v} to C_s (Poppinger and Radom, 1978). J. B. Moffat could confirm the bond lengths and bond angles reported by D. Poppinger and L. Radom. In regard to the compounds of Table 65 the C–N distances of the cyanide groups (r_{N-CX} = 1.160/1.159/1.163 Å) are in the typical range of a triple bond and the C–O bonds of dicyanoether are slightly shortened due to a back-bonding of unpaired electrons of oxygen into antibonding orbitals of the cyanide groups (Moffat, 1979; Poppinger and Radom, 1978).

Oxocyanogen $(OCN)_2$ – the cyanate dimer

In 1977, the formation of an $(OCN)_2^-$ species, which was part of an equilibrium of the cyanate anion $[OCN]^-$ and a complex HNCOOH formed by irradiation of OH radical/$[OCN]^-$ mixture, was reported by J. G. Leopold and M. Faraggi (Scheme 99). By means of pulse radiolysis of cyanate anion solutions, kinetic studies led to the assumption of the *in situ* formation of an $[(OCN)_2]^-$ species (Leopold and Faraggi, 1977).

Experimental evidence of the existence of an $(CNO)_2$ species, isomer of $(OCN)_2$, was published in 1984. Time-resolved mass spectrometry of the decomposition products after thermal explosion (at 430 K) of mercury fulminate showed mass peak at m/z = 84 that could allocated to the $(CNO)_2$ dimer (Scheme 100) which further breaks down into more stable species such as ONC–CN, O, N_2O and $(CN)_2$ (Tang et al., 1984).

In 1981, M. S. Delgado and V. Fernandez published the reaction of silver cyanate and bromine and a stabilization of $(OCN)_2$ using titanium tetrachloride to isolate the dimer, but polymerization was assumed, which hindered the unambiguous identification of the dimer (Delgado and Fernandez, 1981). In 1996, A. Schulz and T. M. Klapötke reported the formation of dioxocyan as a reactive intermediate in the reaction of silver cyanate and bromine, which dissociated under release of nitrogen (Scheme 101).

Due to fast decomposition of the dioxocyan, its isolation and spectroscopic analyses were not possible. Computational studies at MP2(full)/6-31G(d,p) were also carried out to distinguish between isomers of O–O and N–N linked dimers showing that the diisooxocyan is the thermodynamically more stable isomer lying 343.7 kJ mol^{-1} lower in energy than the oxygen linked isomer. In addition, the N–N bond is significantly shortened and the bond length of r_{N-N} = 1.385 Å is in between a typical single and double bond. In contrast to this shortened bond, the O–O bond of the dioxocyan is much weaker (r_{O-O} = 1.622 Å, Table 66) (Schulz and Klapötke, 1996). In the same year, G. Maier et al. generated and identified $(OCN)_2$ by matrix IR spectroscopy (Maier et al., 1996a). It was generated by UV irradiation of oxalic acid diazide and azidoformyl isocyanate in argon at 10 K and by high vacuum flash pyrolysis of the same precursors at 1173 K. Although $(OCN)_2$ proved stable at 80 K, it polymerized and was not in pure form at room temperature. In 2008, T. Pasinszki also published detailed studies on cyanate dimers of different configurations and could also confirm, that the diisooxocyan is the thermodynamically most stable isomer (Table 67) (Pasinszki, 2008).

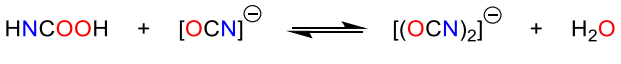

Scheme 99: Pulse radiolysis to form the $[(OCN)_2]^-$ dimer (Leopold and Faraggi, 1977).

Sulfur

As for oxygen, the monocyanide $[SCN]^{\cdot}$ radical, the thiocyanide anion, $[SCN]^-$, and the dicyanide, $S(CN)_2$ are also known for sulfur. However, while the number of CN groups attached to the oxygen atom is (so far) limited to two, three and four CN groups have also been found for sulfur. Since thiocyanate plays a major role in both inorganic and bioorganic chemistry (see introduction), only the essentials such as synthesis and structure are discussed here, otherwise reference is made to the many review articles (Anderson, 1980; Azizitorghabeh et al., 2021; Bahta et al., 1997; Bezsudnova et al., 2007; Castanheiro et al., 2016; Dash et al., 2009; Ebbs, 2004; Happold et al., 1958; Jensen and Tuan, 1993; McDonald et al., 1969; Sorokin et al., 2001;

Scheme 100: Thermal explosion of mercury fulminate forming $(OCN)_2$ as an intermediate of decomposition (Tang et al., 1984).

Scheme 101: The reaction of silver cyanate and bromine leads to dioxocyan as an intermediate (Schulz and Klapötke, 1996).

Table 66: Computational data of $(OCN)_2$ dimers (bond lengths in Å; angles in °).

Compound ABC–DEF	Method + basis set	r_{A-B}	r_{B-C}	r_{C-D}	r_{D-E}	r_{E-F}	< (A–B–C)	< (B–C–D)	< (C–D–E)	< (D–E–F)
OCN–NCO (Schulz and Klapötke, 1996)	MP2(FU)/6-31G(d,p)	1.181	1.238	1.385	1.238	1.181	168.5	123.3	123.3	168.5
NCO–OCN (Schulz and Klapötke, 1996)	MP2(FU)/6-31G(d,p)	1.190	1.296	1.622	1.296	1.190	176.5	104.6	104.6	176.5
ONC–CNO (Pasinszki, 2008)	B3LYP/6-311 + G(2d)	1.201	1.165	1.340	1.165	1.201	180.0	180.0	180.0	180.0
OCN–CNO (Pasinszki, 2008)	B3LYP/6-311 + G(2d)	1.212	1.162	1.319	1.210	1.162	173.5	159.0	141.7	172.5
NCO–CNO (Pasinszki, 2008)	B3LYP/6-311 + G(2d)	1.196	1.180	1.351	1.307	1.151	168.5	135.9	117.0	175.1
CNO–CNO (Pasinszki, 2008)	B3LYP/6-311 + G(2d)	1.173	1.341	1.349	1.179	1.198	166.8	112.9	135.6	169.6
OCN–NCO (Pasinszki, 2008)	B3LYP/6-311 + G(2d)	1.163	1.221	1.376	1.221	1.163	170.5	125.0	125.0	170.5
NCO–NCO (Pasinszki, 2008)	B3LYP/6-311 + G(2d)	1.154	1.297	1.458	1.239	1.156	175.1	110.1	112.9	171.1
CNO–NCO (Pasinszki, 2008)	B3LYP/6-311 + G(2d)	1.173	1.321	1.465	1.241	1.155	171.6	108.2	111.9	171.5

Table 67: Computational data of $(OCN)_2$ dimers (total energy in a.u.; relative energy and dissociation energy at 298 K in kJ mol^{-1}; wave numbers in cm^{-1}).

Compound ABC–DEF	Method + basis set	$E_{tot.}$	$E_{rel.}$	$D_{ABC-DEF}$	ν_{CD}	ν_{DEF}
OCN–NCO (Schulz and Klapötke, 1996)	MP2(full)/6-31G(d,p)	−335.23422	0.0	–	–	–
NCO–OCN (Schulz and Klapötke, 1996)	MP2(full)/6-31G(d,p)	−335.103437	82.9	–	–	–
ONC–CNO (Pasinszki, 2008)	B3LYP/6-311 + G(2d)	−336.076636	347	332	634	1588
OCN–CNO (Pasinszki, 2008)	B3LYP/6-311 + G(2d)	−336.152341	148	288	737	1596/1296[a]
NCO–CNO (Pasinszki, 2008)	B3LYP/6-311 + G(2d)	−336.072284	356	117	–	1429
CNO–CNO (Pasinszki, 2008)	B3LYP/6-311 + G(2d)	−335.980380	592	144	–	1410
OCN–NCO (Pasinszki, 2008)	B3LYP/6-311 + G(2d)	−336.209270	0	188	837	1514
NCO–NCO (Pasinszki, 2008)	B3LYP/6-311 + G(2d)	−336.134348	193	21	805	1324
CNO–NCO (Pasinszki, 2008)	B3LYP/6-311 + G(2d)	−336.046988	418	56	797	1301

[a]CNO and NCO stretching vibration.

Stott et al., 2001; Wald et al., 1939; Watts and Moreau, 2016; Willemin and Lumen, 2017; Wilson et al., 1960).

Thiocyanate radical $[SCN]^{\bullet}$ and $[SCN]^{-}$ ion

Thiocyanate radical $[SCN]^{\bullet}$

The thiocyanate radical, $[SCN]^{\cdot}$, can be generated by photolytic dissociation of methyl isothiocyanate, using KrF or ArF excimer laser. Prior to the dissociation, methyl isothiocyanate was very diluted by helium. $[SCN]^{\cdot}$ has also been detected after radio frequency discharge of methyl thiocyanate and the reaction between CN and OCS (Scheme 102). To avoid higher thermal excitation, conditions of supersonic free jet expansion are used to obtain fluorescence excitation spectra (Northrup and Sears, 1989).

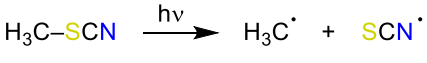

Scheme 102: Photolytic dissociation of methyl isothiocyanate to obtain the thiocyanate radical (Northrup and Sears, 1989).

Additional experimental studies focusing on the Renner-Teller effect of the linear thiocyanate radical, which exhibits $C_{\infty v}$ symmetry, confirmed the $^2\Pi$ state to be the electronic ground state (Northrup and Sears, 1990). Its fluorescent lifetime is reported to be t_0 = 165 ns (Ohtoshi et al., 1984). Furthermore, the bond lengths were calculated based on observed rotational constants (Table 68) (Maeda et al., 2007).

DFT calculations could confirm experimental values and the electron affinity of E_A = 3.51 eV (339 kJ mol^{-1}),

Table 68: Experimental and calculated structural data of the thiocyanate radical (bond lengths in Å).

Publication	Exp./calc.	r_{C-N}	r_{S-N}
Maeda et al. (2007)	Exp. – SWS	1.1831(18)	1.6301(14)
Li et al. (2012)	MP2/aug-cc-pVDZ	1.1563	1.6879
Chen et al. (2008)	MP2/6–311 + G(3df,2p)	1.15	1.66
	B3LYP/6–311 + G(3df,2p)	1.17	1.63

which was calculated by J. G. Dillard and J. L. Franklin, was re-adjusted to be E_A = 3.52 eV by H.-L. Chen et al. using CCSD(T)/aug-cc-PVQZ//B3LYP/6–311 + G(3df,2p) (Chen et al., 2008; Dillard and Franklin, 1968). Photoionization mass spectrometry led to an adiabatic ionization potential of IP = 10.689(5) eV and the standard formation enthalpy was reported to be $\Delta_f H°$ = (304.4 ± 3.3) kJ mol^{-1} (Ruscic and Berkowitz, 1994).

Thiocyanate anion [SCN]$^-$

Thiocyanates are the salts of thiocyanic acid, HSCN (initially known as *Schwefelblausäure* = German for sulfur blue acid). Thiocyanic acid was observed as early as 1790 by Winterl, 1799 by C. Buchholz (Buchholz, 1799), 1804 by Rink and produced in 1808 by R. Porret (Köhler, 1914). Its composition was determined by J. J. Berzelius in 1820 and he also introduced the old name rhodanic acid (from Greek for red), since ferric thiocyanate is a deep red complex. Thiocyanate salts can be prepared from cyanides and sulfur in the melt (Scheme 103) (Köhler, 1914). In addition to thiocyanic acid (HSCN), an isomer is also known, namely isothiocyanic acid (HNCS also thiocarbimide). Both types of acid are labile with respect to decomposition. The thiocyanate ion, like the azide, cyanide or cyanate, is called a linear pseudohalide, which easily forms salts with alkali metals such as potassium thiocyanate (KSCN, also potassium rhodanide) (Birckenbach and Kellermann, 1925a; Brand et al., 2006, 2007; Kauffman et al., 1968; Stopenko et al., 1986). But also non-metal main group thionates are known (Bahta et al., 1997; McDonald et al., 1969; Wijeyasinghe and Anthopoulos, 2015). As early as 1873, L. Lössner et al. converted phosphorus trichloride with KSCN into $P(SCN)_3$ in an alcoholic solution (Lössner et al., 1873). Shortly thereafter, the reaction of PCl_3, $AsCl_3$ and $SbCl_3$ with metal thiocyanates (MSCN, M = alkali metal) was studied by different groups (Dixon, 1901). The formation of the thiocyanates $P(SCN)_3$, $As(SCN)_3$ and $Sb(SCN)_3$ was assumed since upon contact of these $E(SCN)_3$ (E = P, As, and Sb) species with water, thiocyanic acid was observed. In 1902, A. E. Dixon studied the reaction of PCl_3 with KSCN in detail in order to investigate the behavior of $P(SCN)_3$ towards alcohol (Dixon, 1902). It was E. Söderbäck who advanced the thiocyanate-chemistry and dealt in particular with the synthesis of free HSCN and its salts. In the course of these investigations, he examined the effect of HSCN-ether solutions on pure arsenic and antimony, whereby he could isolate a yellow hygroscopic oily solid (Söderbäck, 1919). To date, various synthetic routes to $P(SCN)_3$ have been published, most of them starting from PCl_3 and metal thiocyanates such as AgSCN, $Hg(SCN)_2$, or $[NH_4]SCN$ (Fluck et al., 1965; Gall and Schüppen, 1930). Also, pure heavy $E(NCS)_3$ (E = Sb, Bi) species were obtained from the reaction of EF_3 and an excess of TMS–SCN (Arlt et al., 2019). Furthermore, the cluster ion $[SCN(HCN)_3]^-$ was isolated when WCC[SCN] is recrystallized from liquid HCN (Bläsing et al., 2020)

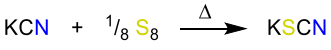

Scheme 103: Synthesis of potassium thiocyanate (Köhler, 1914).

Thiocyanates fulfill several functions in organisms, for example degradation product of the cyanide detoxication or oxidation of thiocyanate by enzymes like eosinophil peroxidase to form hypothiocyanous acid HOSCN, which is present in the oral cavity, airway or alimentary tract and has got antimicrobial properties (Chandler and Day, 2015). Also the thiocyanate anion itself is analyzed due to biological activities, for example the affinity to bind to hemoglobin (Kumar Sau et al., 2003). Furthermore, the formation of bonds to organic substituents leading to isothiocyanates is possible, which is interesting in respect to bonding of nitric monoxide radicals or the prevention of inhibition of the immune system by reduced macrophage migration (Noshita et al., 2009; Spencer et al., 2015).

Structurally, many thiocyanate salts have already been characterized. For example, in 1971 Z. Igbal published structural data of sodium thiocyanate, which were rectified by P. H. van Rooyen and J. C. A. Boeyens in 1975 using single crystal XRD and observed characteristic vibrational bands (Table 69). The sodium thiocyanate forms orthorhombic crystals, space group *Pnma*, the sodium is octahedral coordinated by three sulfur and three nitrogen atoms in *fac* arrangement and the thiocyanate anion can be regarded to be linear (Iqbal, 1971; van Rooyen and Boeyens, 1975). The crystal structures of thiocyanate salts (M = alkali, $[NH_4]^+$, Tl^+), their crystal growth, properties and phase transitions in comparison to cyanates, azides and bifluorides ($[HF_2]^-$) have been reviewed in detail by A. Fuith (1997).

The calculations on KSCN by K. Urabe and co-workers were carried out in the framework of the rigid ion model. To

Table 69: Experimental and computational data of sodium and potassium thiocyanate (bond lengths in Å; angles in °; wave numbers in cm^{-1}).

Compound	Exp./calc.	r_{C-N}	r_{S-C}	< (S–C–N)	ν_{CN}	ν_{SC}
NaSCN	Exp. – XRD, IR (Iqbal, 1971; van Rooyen and Boeyens, 1975)	1.168(18)	1.663(9)	179.0(8)	2070/2090	750/760
KSCN	Exp. – XRD, Raman (Akers et al., 1968; Dao and Wilkinson, 1973)	1.149(14)	1.689(13)	178.3(1)	2050(2)	749(2)
KSCN	Rigid ion model (Kanamori et al., 1981)	1.15	1.79	180	2050	749

analyze the mesomeric stability of this compound they also calculated the distribution of negative charge (q(K) = 0.747, q(S) = −0.194, q(C) = −0.161, q(N) = −0.392) identifying a main focus of negative charge on the nitrogen (Kanamori et al., 1981). In contrast to sodium thiocyanate the space group of potassium thiocyanate is *Pbcm* and it exhibits longer S–C bonds and shorter C–N bonds. Although, the sulfur-carbon bond is 0.12 Å shorter than a typical single bond, the Lewis picture should include at least mesomeric structures as depicted in Figure 45 (Akers et al., 1968). The chemical shift of ^{15}N and ^{13}C were measured using Li[SCN] dissolved in DMF ($\delta[^{15}N]$ = –160 ppm, $\delta[^{13}C]$ = 150–152 ppm) (Vaes et al., 1978).

Dirhodan, NCS–SCN (Allenstein and Lattewitz, 1964; Fieser et al., 2006; Nolan et al., 1975; Kuhn and Mecke, 1960, 1961b; Kuhnhen, 1977; Schoneshofer et al., 1970; Seel and Wesemann, 1953; Wizemann et al., 1969). As classical pseudohalide thiosulfate can be oxidized to form dirhodan, the dimer of the $[SCN]^{\cdot}$ radical. As early as 1919, E. Söderbäck tried to oxidize the $[SCN]^-$ ion to dirhodan using nitrous acid (Scheme 104) (Söderbäck, 1919). However, when an aqueous solution of potassium rhodanide and potassium nitrite was acidified, the result was not dirhodan but the intensely red nitrosyl rhodanide, which had already been observed in 1852 by J. Besnou and later also by E. W. Davy (Scheme 104) (Seel and Wesemann, 1953).

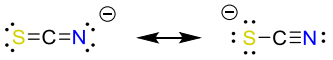

Figure 45: Mesomeric structures of the thiocyanate anion.

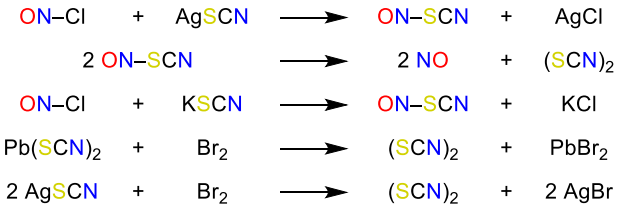

Scheme 104: Different routes for the synthesis of $(SCN)_2$ (Emerson, 1966; Fitzgerald and Bowie, 2004; Rogers and Gross, 1952; van Rooyen and Boeyens, 1975).

All the authors mentioned report that nitrosyl rhodanide can easily be decomposed with the release of nitrogen oxide. Since dirhodan is hydrolysed by water (Schoneshofer et al., 1970), nitrosyl rhodanide must be prepared in a non-aqueous solvent (Seel and Wesemann, 1953). The preparation of a solution of nitrosyl rhodanide in liquid sulfur dioxide, which is obtained by reacting nitrosyl chloride with a solution of potassium rhodanide, proved to be particularly advantageous. In this quantitative reaction, potassium chloride precipitates. After careful evaporation of the intensely red solution *in vacuo* and at low temperatures, the solid nitrosyl rhodanide is obtained, which rapidly changes into completely colorless dirhodan with the elimination of nitrogen oxide. The decomposition of the dirhodan (T_M = 288–289 K) leads to an orange-red solid substance. Another method for the synthesis of dirhodan is based on $Pb(SCN)_2$ and bromine in ether at temperatures between 273 and 283 K (Scheme 104) (Kuhn and Mecke, 1960).

$K(SCN)_3$. If three equivalent KSCN are treated with two equivalent [NO]SCN, the interesting yellow potassium trirhodanide, $K(SCN)_3$, which is analogous to the better-known potassium triiodide, KI_3, is obtained after NO cleavage.

Thiocyanate cation $[SCN]^+$

Equally to the $[SCN]^{\cdot}$ radical only a few experimental studies of the thiocyanate cation $[SCN]^+$ are published in literature. The first evidence of the cation was published by B. Ruscic and J. Berkowitz in 1994 as a result of hydrogen abstraction of HNCS by atomic fluorine, but the spectra showed several autoionizing features. A second route was the formation of the dirhodane (dithiocyane, see above) using silver thiocyanate and chlorine and in the second step it was photolytically ionized in a mass spectrometer (Scheme 105). The correlated standard formation enthalpy was reported to be $\Delta_f H°$ = (1336.4 ± 3.8) kJ mol^{-1} (Ruscic and Berkowitz, 1994).

In 2004, mass spectrometric studies on methylene-isothiocyanate, which was formed by dissociative electron ionization of 2-mercaptoimidazole, were reported and confirmed by tandem mass spectrometry. The neutralization-reionization spectrum showed a peak at m/z = 58, which was

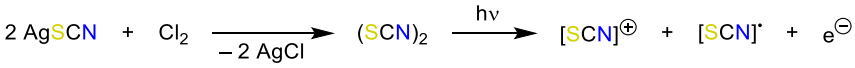

Scheme 105: Formation of the thiocyanate cation (Ruscic and Berkowitz, 1994).

allocated to the thiocyanate cation due to removal of the methylene group from $[H_2C–NCS]^+$ (Reddy et al., 2004). M. Fitzgerald and J. H. Bowie could also generate the thiocyanate cation by charge reversal of the thiocyanate anion directly in the collision cell of a mass spectrometer by single collisions with oxygen. In their computational studies they could additionally show that the isomerization from thiocyanate cations in the triplet state to thiofulminate cations is endothermic by 86.2 kJ mol^{-1} and correlated to an activation barrier of 188.8 kJ mol^{-1}, whereas the change of the isomers in the singlet state is less endothermic by 76.2 kJ mol^{-1}. The calculated parameters of the triplet ground state and the singlet state are shown in Table 70 and all isomers exhibit $C_{\infty v}$ symmetry (Fitzgerald and Bowie, 2004).

Evidence for the formation of $[SCN]^+$ ion was also found in the fragmentation reaction of methylenethiocyanate investigated by E. Cortés et al. in 2009. Based on photoelectron photoion coincidence (PEPICO) and photoelectron photoion photoion coincidence (PEPIPICO) spectra it was shown that the fragmentation processes leading to formation of $[CH_3]^+$ and $[SCN]^+$ ions dominate the dissociation of CH_3SCN excited at the S 2*p* levels (Cortés et al., 2009).

Sulfur dicyanide $S(CN)_2$

In 1919, E. Söderbäck published a detailed article dealing with the free thiocyanate radical, starting with J. v. Liebig's experiments ($Ag[SCN] + Cl_2$) to obtain the radical, presenting several attempts to synthesize the free radical and collecting characteristic chemical properties (Söderbäck, 1919). In this context, he also described F. Linnemann's synthesis (Linnemann, 1861) of sulfur dicyanide $S(CN)_2$ due to a reaction of cyanogen iodide and silver thiocyanate and R. Schneider's attempt (Schneider, 1885) to synthesize dirhodane, $(SCN)_2$, but due to several analyses R. Schneider assumed a rapid decomposition of the dimer to form the dicyansulfide and dicyantrisulfide $S_3(CN)_2$ (Scheme 106) (Söderbäck, 1919).

At that time the homologous series of cyanosulfanes was extended quickly and also contained the dithiocyanate $(SCN)_2$, sulfur dithiocyanate $S(SCN)_2$ and disulfur dithiocyanate $S_2(SCN)_2$ based on the same synthetic route of mercury thiocyanate and sulfur–halogen compounds (Scheme 107).

Isolated colorless crystals of $S(CN)_2$ sublime easily at normal pressure, melt at 335 K and in addition to its low sublimation temperature the compound tends to polymerize easily (Feher and Weber, 1958). The dipole moment of SCN was determined to be μ = 2.28 D using electron diffraction experiments and under assumption of an carbon-sulfur-carbon angle of < (C–S–C) = 105° identical to dimethyl sulfide (Rogers and Gross, 1952). Furthermore, several results of structure determination, for example using single crystal XRD experiments, were published during the 1960s and during the last 15 years (Table 72). K. Emerson as well as K.-H. Linke and F. Lemmer reported different parameters for each CN group, which led to an asymmetric molecule, but this fact could not be confirmed by later studies (Emerson, 1966; Linke and Lemmer, 1966a). The small distances of neighboring molecules in the crystal, which are smaller than the van der Waals radii, are striking and could be interpreted using the σ-hole concept established some years ago (Donald and Tawfik,

Table 70: Computational data of $[SCN]^+$ in different electronic states ($E_{tot.}$ in Hartree; bond lengths in Å; dipole moment μ in D) (Fitzgerald and Bowie, 2004).

Compound	State	$E_{tot.}$ [a]	$r_{A–B}$ [b]	$r_{B–C}$ [b]	μ
$[SCN]^+$	$^1\Pi$	–489.83203	1.593	1.211	1.98
$[SNC]^+$	$^1\Pi$	–489.80298	1.547	1.245	1.63
$[SCN]^+$	$^3\Sigma$	–489.87300	1.594	1.213	2.25
$[SNC]^+$	$^3\Sigma$	–489.84011	1.561	1.232	2.07

[a]$E_{tot.}$ calculated at CCSD(T)/aug-cc-pVDZ and zpe included. [b]Bond length calculated at B3LYP/6-31G + (d).

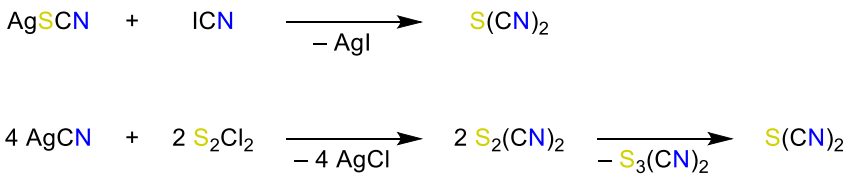

Scheme 106: Reactions of F. Linnemann and R. Schneider obtaining dicyansulfide (Söderbäck, 1919).

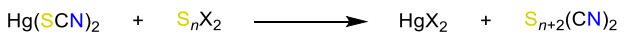

Scheme 107: Synthetic route of homologous cyanosulfanes (Feher and Weber, 1958).

2013; Murray et al., 2007b; Politzer et al., 2007), which implies, that the half-filled *p* bonding orbital of group V to VII atoms showing electron deficiency interacts with a nucleophile, whereas the intensity depends on its electronegativity, polarizability and the electron-withdrawing character of the group to which it is bonded. So, the outer surface of the chalcogen atoms has regions of positive electrostatic potential, which noncovalently interact with the lone pairs of the nitrogen atom of a neighboring cyanide group causing a denser package in the crystal (Murray et al., 2007b; Politzer et al., 2007).

Several spectroscopic studies specified the structure determination (Table 71), for example, D. A. Long and D. Steele could confirm C_{2v} symmetry and discussed various C–S–C angles due to different assumed bond dipole moments using IR and Raman spectra (Long and Steele, 1963).

Experimental and computational data of chemical shifts fit well, especially regarding the ^{13}C species the difference between theory and experiment is about $\Delta\delta \approx 5$ ppm (δ (^{13}C, exp., CD_2Cl_2) = 100.1 ppm, δ (^{13}C, calc.) = 105.0 ppm), regarding ^{14}N the difference is large (δ (^{14}N, exp., CD_2Cl_2) = 293.4 ppm, δ (^{14}N, calc.) = 338.4 ppm). All calculations were carried out at B3LYP/6-311 + G* (Burchell et al., 2006).

Table 71: IR and Raman data of $S(CN)_2$ in different matrices (wave numbers in cm^{-1}).

Publication	Method	Matrix	$\nu^{sym.}_{SC}$	$\nu^{sym.}_{CN}$
Long and Steele (1963)	Exp. – IR	Solid	752	2190
	Exp. – Raman	Solid	–	2191
Fehér and Weber (1958)	Exp. – Raman	In bromoethane	680	2186
Burchell et al. (2006)	Exp. – IR	In KBr	697	–
	Exp. – Raman	Solid	693	2196

Furthermore, dicyansulfide is an alkaline compound due to its lone pairs at the sulfur atom and both nitrogen atoms, which can also interact with electrophiles. In accordance to the HSAB principle of Pearson, pairs of acids and bases of the same strength are most stable, which implies, that the nitrogen atoms can interact with two Lewis acids, for example antimony or arsenic pentafluoride, forming strong diadducts (Minkwitz et al., 1991; Pearson, 1968).

Thiocyanogen $(SCN)_2$

The syntheses of thiocyanogen published by F. Linnemann and R. Schneider based on the reaction of silver cyanide and disulfur dicyanide and subsequently formation of sulfur dicyanide $S(CN)_2$ and sulfur dithiocyanate $S(SCN)_2$ (Scheme 106) (Söderbäck, 1919) as well as the reaction of mercury thiocyanate and sulfur–halogen compounds (Scheme 107) (Feher and Weber, 1958) reported by F. Fehér and H. Weber have already been named. In the 2000s, J. D. Woollins and co-workers also dealed with sulfur-cyanogen compounds and reported a synthesis of thiocyanogen based on the reaction of silver thiocyanate and molecular bromine at –20 °C. They reported carbon and nitrogen NMR data and also noticed the polymerization of thiocyanogen forming polycyanogen at ambient temperature (Burchell et al., 2004, 2006).

Tricyanosulfonium cation $[S(CN)_3]^+$

There is only one article in literature published by R. Minkwitz and V. Gerhard dealing with the $[S(CN)_3]^+$ cation. The synthesis is a halogen-pseudohalogen exchange at tribromosulfonium hexafluoroarsenate in liquid sulfur dioxide at lower temperatures (Scheme 108). The reaction takes 24 h under exclusion of light, when silver bromide

Table 72: Experimental and computational data of $S(CN)_2$ reported in different studies (bond lengths in Å; angles in °).

Publication	Exp./calc.	r_{S-C}	r_{C-N}	< (S–C–N)	< (C–S–C)	Space group
Emerson (1966)	Exp. – XRD	1.736(15)/ 1.718(18)	1.118(21)/ 1.134(23)	177.49(1.34)/ 176.43(1.70)	95.60(78)	*Pbca*
Linke and Lemmer (1966a)	Exp. – XRD	1.87/2.07	1.02/1.20	177/144	96	*Pbca*
Burchell et al. (2006)	Exp. – XRD	1.74(2)/1.72(2)	1.12(2)/1.13(2)	177(1)/176(2)	95.6(8)	–
	B3LYP/6-311 + G*	1.71	1.16	175	99.6	–
Kisiel et al. (2013)	FIR spectra, CCSD(T)/ aug-cc-pVTZ	1.6972(4)	1.1602(4)	175.14(5)	98.36(3)	–
	CCSD(T)/aug-cc-pVTZ	1.7059	1.1617	175.37	97.77	–

$$[SBr_3][AsF_6] + 3\,AgCN \xrightarrow[233\ K]{SO_2} [S(CN)_3][AsF_6] + 3\,AgBr$$

Scheme 108: Synthesis of the $[S(CN)_3]^+$ cation (Minkwitz and Gerhard, 1991).

and an excess of silver cyanide are removed from the dissolved product by filtration.

The product is a colorless solid, is sensitive to hydrolysis and decomposes at 364 K. The results of their spectroscopic measurements are listed in Table 73. The ^{13}C NMR spectrum shows one signal at $\delta = 85.4$ ppm, which implies a significant high field shift in comparison to $S(CN)_2$ (δ = 100–102 ppm) (Minkwitz and Gerhard, 1991).

Tetracyanosulfonium cation $[S(CN)_4]^{2+}$

The tetracyanosulfonium dication $[S(CN)_4]^{2+}$ was described theoretically by I. A. Koppel et al. (B3LYP/6-311 + G**) (Koppel et al., 2002). This publication deals with the generalized principle of superstrong Brønsted acids, in which sulfur tetracyanide is a fragment of a major compound and substitutes the oxygen atom of nitrous acid, acetalaldehyde or nitroxyl (Figure 46). The calculated distances of the four sulfur–cyanide bonds are not equal and listed in Table 74 as well as the calculated deprotonation enthalpy $\Delta H°_{acid}$ and acidity $\Delta G°_{acid}$ to estimate the Brønsted acid behavior.

Table 73: Experimental data of IR and Raman spectra of $[S(CN)_3]^+$ (wave numbers in cm^{-1}) (Minkwitz and Gerhard, 1991).

Method	Matrix	$\nu^{sym.}_{SC}$	$\nu^{as.}_{SC}$	$\nu^{sym.}_{CN}$
IR	Solid	–	564	2230
Raman	Solid	638	568	2242

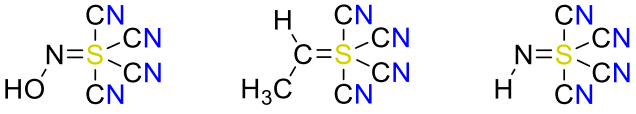

Figure 46: The oxygen atom of nitrous acid, acetalaldehyde and nitroxyl is substituted by R = $S(CN)_4$ (Koppel et al., 2002).

Table 74: Computational data of R = $S(CN)_4$ containing compounds (bond lengths in Å; gas phase acidity and proton affinity in kJ mol^{-1}) (Koppel et al., 2002).

Compound	r_{S-C}	$\Delta H°_{acid}$	$\Delta G°_{acid}$
$HON{=}S(CN)_4$[a]	1.78/1.91/1.84/1.83	–	–
$CH_3CHC{=}S(CN)_4$	1.92/1.92/2.22/2.22	1022.0	983.5
$[CH_2HC{=}S(CN)_4]^-$	1.92/1.92/2.23/2.23	–	–
$HN{=}S(CN)_4$	1.79/1.79/1.90/1.83	1277.0	1240.1

[a]This structure forms fragments during structure optimization.

Selenium

Selenium cyanide hydrogen compounds are unstable acids, but some of their salts are storable for longer periods of time. For example, they can be found in wastewater of oil and gas industries, especially coal-fired power plants using flue gas desulfurization, and are toxic (Petrov et al., 2012; Vadhanavikit and Ganther, 1988). In regard to chemical properties and resulting biological activity selenium and sulfur are very similar to each other. For example, in some cases the sulfur atom of the amino acid cysteine is replaced by selenium forming selenocysteine. Accordingly, selenium cyanide compounds possess several biological activities similar to the sulfur cyanide compounds discussed before (Badiello, 1992; Huber and Criddle, 1967; Shrift and Virupaksha, 1963). In some studies the application of organo selenium compounds as cancerostatic drugs are tested, which are synthesized using selenocyanates (Bouchet et al., 2011; El-Bayoumy and Sinha, 2004).

Selenocyanate $[SeCN]^-$ and the triselenocyanate $[(SeCN)_3]^-$ ion

Selenocyanate, $[SeCN]^-$, is known for a long time and its stability enables commercial trade. The contact to air leads to decomposition of these hydroscopic compounds forming potassium cyanide and red selenium, which necessitates its handling under inert gas atmosphere. The synthesis runs in reverse direction in terms of an insertion of elementary, powdered selenium into potassium cyanide (Scheme 109) (Kaufmann and Kögler, 1926).

The first crystal structure determination of the selenocyanate anion (with K^+ as counter ion) was published by D. D. Swank and R. D. Willett in 1965 reporting a nearly linear structure, which is slightly perturbed due to packing effects (Swank and Willett, 1965). The space group of

$$KCN + Se \xrightarrow{\Delta} KSeCN$$

Scheme 109: Insertion of red selenium into potassium cyanide to form potassium selenocyanate (Kaufmann and Kögler, 1926).

potassium selenocyanate crystals is $P2_1/c$. Within the standard deviation, the CN bond length is in the range of a triple bond, but the Se–C bond length of $r_{Se–C}$(exp.) = 1.829 Å is significantly shorter than the expected single bond length of $r_{Se–C}$(calc.) = 1.94 Å, which indicates a partial double bond character, but does not affect the CN bond due to the higher difference in electronegativities (Table 75) (Swank and Willett, 1965).

Detailed information about all alkali metal selenocyanates MSeCN with M = Li to Cs are summarized by F. Tambornino and co-workers including syntheses, spectroscopic data as well as crystal structures and computations (Shlyaykher et al., 2021).

Silver selenocyanate complexes dissolved in acetonitrile were studied by means of IR spectroscopy (ν_{SeC} = 530–560 cm^{-1}, ν_{CN} = 2070–2110 cm^{-1}, ν_{bent} = 380–410 cm^{-1}) (Singh, 1980).

Selenocyanogen $(SeCN)_2$ and selenium dicyanide $Se(CN)_2$

Selenium dicyanide $Se(CN)_2$ is significantly more stable than the oxygen species $O(CN)_2$ and can be obtained as a pure substance. The crucial step of its synthesis is the disproportionation of selenocyanogen in selenium dicyanide and selenium diselenocyanate, which can be separated by sublimation at 323 K. The selenocyanogen can be synthesized on two different routes. The first one is a reaction of potassium selenocyanate and iodine pentafluoride and the second one is a salt metathesis of potassium selenocyanate in presence of silver nitrate and following oxidation by iodine (Scheme 110) (Aynsley et al., 1964; Burchell et al., 2004, 2006; Linke and Lemmer, 1966b).

The first structure determination by single crystal XRD was published by A. C. Hazell in 1963. He assumed that selenium dicyanide would form orthorhombic crystals, space group *Cmca* (Hazell, 1963). Detailed structural data are shown in Table 76. In 1966, K.-H. Linke and F. Lemmer also published a study on the structure of selenium dicyanide correcting the space group to *Pbca* and lowering the symmetry to C_s because of two non-equivalent cyanide groups, which differ due to the carbon–nitrogen bond and the bond angle < (Se–C–N). After all, they suggest to call it selenocyanocyanide instead of selenium dicyanide (Linke and Lemmer, 1966b). Publications of T. M. Klapötke et al. and J. D. Woollins and co-workers confirmed the results of K.-H. Linke and F. Lemmer in principle, but they all differ due to the C–Se–C angle. On the other hand, they all report very small intermolecular distances of nitrogen and selenium atoms in the crystal of 2.74–2.82 Å, which is significantly smaller than the sum of the van der Waals radii (3.45 Å) and is explained by the σ-hole concept mentioned in chapter 8.2.2 (Burchell et al., 2006; Klapötke et al., 2008). The first IR and Raman spectroscopic measurements were carried out in 1964 and were confirmed experimentally and computationally (Table 77). NMR spectroscopic data of $Se(CN)_2$ in deuterated dichloromethane were reported by J. D. Woollins and co-workers in 2006 (Table 78) (Burchell et al., 2006).

The mesomerism of π-bond electrons and lone pairs causes an interaction of the selenium and carbon atom, which is stronger than a typical single bond and correlates with calculated bond orders of 1.27 regarding Se–C and 2.92 with regard to C–N (Burchell et al., 2006). In 1981, G. Jonkers et al. also analyzed the ionization energy using ultraviolet photoelectron spectroscopy and asserted that the ionization energy E_I = 10.96 eV of $Se(CN)_2$ is in the range of elementary carbon (Table 79) (Jonkers et al., 1981).

Table 75: Experimental and computational structural data of the selenocyanate anion (bond lengths in Å; angle in °).

Publication	Exp./calc.	$r_{Se–C}$	$r_{C–N}$	< (Se–C–N)
Swank and Willett (1965)	Exp. – XRD	1.829(25)	1.117(26)	178.8(2.5)
Petrie (1999a)	MP2(full)/6-31G*	1.832	1.147	–

Selenium diselenocyanate $Se(SeCN)_2$, triselenocyanate $[(SeCN)_3]^-$, and selenium triselenocyanate $[Se(SeCN)_3]^-$

Selenium diselenocyanate, $Se(SeCN)_2$, synthesized from KSeCN in an oxidation process, was first described by A. Verneuil (Verneuil, 1886). $Se(SeCN)_2$ is formed along with $Se(CN)_2$, as rearrangement product of selenocyanogen, $(SeCN)_2$ (Scheme 111). The same products are obtained when Se_2Br_2 is treated with AgCN or $Pb[(SeCN)_2] + Br_2$. W. Muthmann and E. Schröder observed the formation of

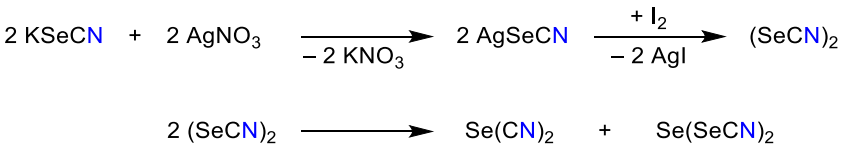

Scheme 110: Synthesis of selenocyanogen and its disproportionation to selenium dicyanide (Linke and Lemmer, 1966b).

Table 76: Experimental and computational data of $Se(CN)_2$ (bond lengths in Å; angles in °).

Publication	Exp./calc.	r_{Se-C}	r_{C-N}	< (C–Se–C)	< (Se–C–N)
Hazell (1963)	Exp. – XRD	1.86(10)	1.42(15)	119(6)	177(6)
Linke and Lemmer (1966b)	Exp. – XRD	2.08/2.01	1.07/1.27	99	168/155
Klapötke et al. (2008)	Exp. – XRD	1.862(7)/1.870(7)	1.138(8)/1.131(8)	91.3(3)	179.2(7)/176.3(6)
Burchell et al. (2006)	B3LYP/6-311 + G*	1.86	1.16	97	175

Table 77: Some spectroscopic data of $Se(CN)_2$ (wave numbers in cm^{-1}).

Publication	Exp./calc.	$\nu^{sym.}_{SeC}$	$\nu^{as.}_{SeC}$	$\nu^{sym.}_{CN}$	$\nu^{as.}_{CN}$
Aynsley et al. (1964)	IR (KBr)	516	(608)	2183	2175
	Raman (in CH_3CN)	514	598	–	2178
Burchell et al. (2006)	IR (KBr)	–	509	–	2179
	Raman (solid)	512	–	2188	–
	B3LYP/6-311 + G*	540	524	2282	2269

Table 78: Experimental and computational NMR data of $Se(CN)_2$ in CD_2Cl_2 (chemical shifts in ppm) (Burchell et al., 2006).

Compound	δ ($^{13}C\{^1H\}$, 67.9 MHz)	δ (^{14}N, 21.7 MHz)	δ (^{77}Se, 67.9 MHz)
$Se(CN)_2$ in CD_2Cl_2	91.5	299.8	0.29
$Se(CN)_2$ at B3LYP/6-311 + G*	106.9	355.2	574.87

Table 79: Experimental and computational (Hartree-Fock-Slater/double zeta) ionization energies (in eV) (Jonkers et al., 1981).

Method	1st E_I	2nd E_I
Exp. – UVPE	10.96(5)	13.82(5)
HFS/DZ	10.9	12.2

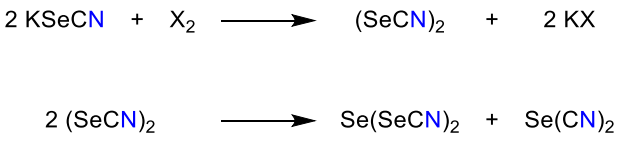

Scheme 111: Synthesis of $Se(SeCN)_2$ (X = Br^-, I^-) (Verneuil, 1886).

$Se(SeCN)_2$ in the reaction of KSeCN with nitrogen dioxide (Aksnes et al., 1954; Challenger et al., 1926; Kaufmann and Kögler, 1926; Muthmann and Schröder, 1900; Rogers and Gross, 1952). The molecule is C_2 symmetric with Se–C–N angles of 164° and Se–Se bond lengths of 2.33 Å and Se–C bond lengths of 1.83 Å (Figure 47).

Triselenocyanate ion $[(SeCN)_3]^-$. Probably the first triselenocyanate salt with potassium as counterion was produced by A. Verneuil in 1886 (Verneuil, 1886). The cesium salt bearing the triselenocyanate ion was first isolated by L. Birckenbach and K. Kellermann in 1925 (Scheme 112) (Birckenbach and Kellermann, 1925b). Half a century later in a series of papers S. Hauge et al. isolated and fully characterized the alkali salts $M[(SeCN)_3]$ (M = K^+, Rb^+, Cs^+). The potassium and rubidium salts were isolated as hemihydrates (Hauge et al., 1971a, 1971b, 1975). The alkali metal salts are prepared by oxidation of the corresponding selenocyanates dissolved in water with bromine dissolved in benzene (Scheme 112). Furthermore, it was found that at ambient temperature a mixture of $[(SeCN)_3]^-$ and $[Se(SeCN)_3]^-$ crystallizes indicating an equilibrium (Scheme 112). An alternative is the reaction of $Se(SeCN)_2$ with $[CN]^-$ (Hauge et al., 1971a). $Cs[(SeCN)_3]$ crystallized in monoclinic space group *C*2/*c* (Hauge et al., 1975). The three selenium chains are almost linear (178.3(1)°) with Se–Se bond lengths of 2.650(3) Å, which is significantly longer than the Se–Se single bond (cf. Σr_{cov}(Se) = 2.32 Å, Figure 47) (Pyykkö and Atsumi, 2009).

Selenium triselenocyanate, $[Se(SeCN)_3]^-$, was synthesized by the reaction of $Se(SeCN)_2$ and MCN in water (M = K^+, Rb^+, Cs^+) in a rather complex reaction (Hauge et al., 1971a).

Selenium tetracyanide $Se(CN)_4$

The selenium tetracyanide $Se(CN)_4$ could not be synthesized until now. A reaction of selenium tetrafluoride and trimethylsilyl cyanide TMS–CN at 223 K, which was carried out by T. M. Klapötke et al. in 2008, did not lead to $Se(CN)_4$, but its decomposition products $Se(CN)_2$ and $(CN)_2$ could be detected (Scheme 113) which indicates the *in situ* generation.

Due to computational studies the selenium dicyanide is significantly more stable than its oxidized species and in

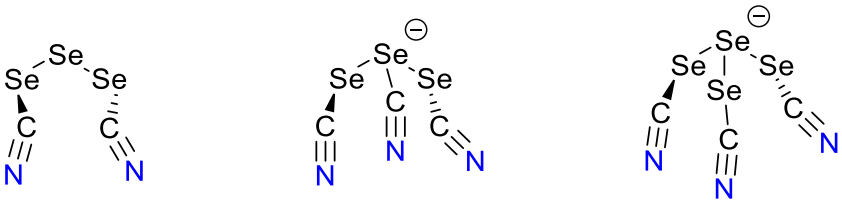

Figure 47: Schematic representation of the molecular structure of $Se(SeCN)_2$, $[(SeCN)_3]^-$ and $[Se(SeCN)_3]^-$.

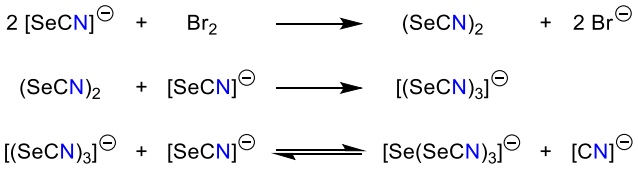

Scheme 112: Synthesis of $[(SeCN)_3]^-$ (Birckenbach and Kellermann, 1925b).

detail the reductive decomposition represented in Scheme 113 implies a gain of energy of ΔE = –300.4 kJ mol^{-1} calculated at MP2/cc-pVTZ (Klapötke et al., 2008). Additional computational data of $Se(CN)_2$ and $Se(CN)_4$ are represented in Table 80.

The calculated $Se(CN)_4$ exhibits pseudo trigonal-bipyramidal structure and the free valance electron pair is located at an equatorial position. The calculated bond lengths also indicate a significant elongation of the Se–C bond in axial positions and a slightly elongated bond of the axial cyanide groups (Klapötke et al., 2008).

Table 80: Calculated data of $Se(CN)_2$ and $Se(CN)_4$ (E in a.u.; *zpe* in kJ mol^{-1}; bond lengths in Å; angles in °) (Klapötke et al., 2008).

	$Se(CN)_2$	$Se(CN)_4$
Point group	C_{2v}	C_{2v}
State	$^1A_1$	$^1A'$
$-E$	194.610124	379.814761
zpe	40.82	78.92
r_{Se-C}	1.842	1.854 (eq.)
		2.066 (ax.)
r_{C-N}	1.176	1.178 (eq.)
		1.180 (ax.)
< (C–Se–C)	94.9	102.5 (eq.–eq.)
		167.1 (ax.–ax.)
		86.0 (ax.–eq.)

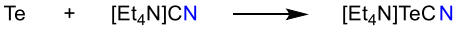

Scheme 114: Synthesis of the tellurium monocyanide anion (Downs, 1968).

Tellurium

Tellurocyanate $[TeCN]^-$

Salts of tellurocyanate, $[TeCN]^-$, with alkali metal cations like sodium or potassium could not be isolated, so weakly coordinating cations (WCC) are necessary to stabilize the anion. The first synthesis was published by A. W. Downs in 1968 based on a new signal in the Raman spectrum at 2080 cm^{-1}. After a reaction of tellurium and tetraethylammonium cyanide in DMF slightly yellow crystals were obtained, which included a stoichiometric amount of DMF (Scheme 114) (Downs, 1968).

To obtain crystals, which include no solvent molecules, are more stable and less sensitive to hydrolysis, the reaction was carried out in acetonitrile using tetramethylammonium cyanide or tetraphenylarsonium cyanide (Austad et al., 1971). Due to the increased stability, XRD experiments of the solvent free tetraphenylarsonium tellurocyanate were possible and the stretching mode of the cyanide group was observed at 2081 cm^{-1} in the IR spectrum.

Nine years later in 1977, M. P. Cava and co-workers published the first synthesis of an alkali metal tellurocyanate salt obtained in a reaction of tellurium and alkaline cyanide dissolved in dry dimethyl sulfoxide at 373 K under inert atmosphere leading to a pale-yellow solution (Scheme 115). But the salt could not be isolated and tellurium was formed after addition of water, acetone or diethylether (Spencer et al., 1977).

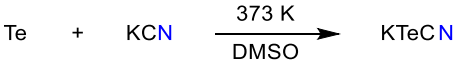

Scheme 115: First synthesis of potassium tellurocyanate (Spencer et al., 1977).

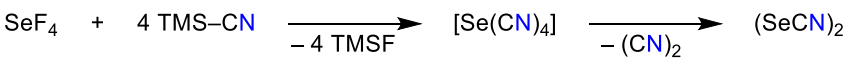

Scheme 113: Reaction to synthesize $Se(CN)_4$, which could not be isolated but its decomposition products (Klapötke et al., 2008).

Only a few spectroscopic studies of the tellurocyanate were reported due to its sensitivity and instability. Some of these spectroscopic data are shown in Table 81. The calculated data were obtained by extrapolation of force constants k and interaction force constants k_{EC} of experimental values of the preceding cyanates $[OCN]^-$, $[SCN]^-$ and $[SeCN]^-$ (Greenwood et al., 1964).

Tellurium dicyanide $Te(CN)_2$

The first synthesis and elementary analysis of tellurium dicyanide $Te(CN)_2$ was published by H. E. Cocksedge in 1908. The synthesis was based on a reaction of tellurium tetrabromide and silver cyanide (Scheme 116). The product was sublimed to obtain crystals of 70.9% tellurium (calc. 71.0%) and 28.8% CN (calc. 29.0%), which are sensitive to hydrolysis and decomposed into tellurium and cyanogen at 373 K (Cocksedge, 1908).

More than 50 years later H. P. Fritz and H. Keller repeated the synthesis published by H. E. Cocksedge, the product was purified by high vacuum sublimation and an IR measurement was carried out using the received pale-pink crystals. The bands at ν_{CN} = 2181 cm^{-1} and ν_{CN} = 2179 cm^{-1} were assigned to the C–N stretching mode and the asymmetrical tellurium–carbon stretching mode was observed at ν_{TeC} = 403 cm^{-1}. Due to two bands of the cyanide group and in comparison to other chalcogene halide compounds they assumed a bent structure of the $Te(CN)_2$, although only one fundamental of the Te–C bond was found. They also reported the thermal decomposition of $Te(CN)_2$ at 353 K (Fritz and Keller, 1961).

A complete structure characterization including XRD measurements were reported by T. M. Klapötke et al. in 2008. In addition to the synthetic route of H. E. Cocksedge using tellurium tetrabromide, T. M. Klapötke et al. could report a synthesis starting with tellurium tetraiodide. In regard to the IR and Raman spectrum they also observed two bands of the cyanide group at ν_{CN} = 2176 cm^{-1} and ν_{CN} = 2168 cm^{-1}, but additionally they could identify two fundamentals at ν_{TeC} = 410 cm^{-1} and ν_{TeC} = 398 cm^{-1} originating from the Te–C bond and finally confirming the bent structure. The two signals in the mass spectrum (EI) were related to the parent ion $[Te(CN)_2]^+$ (m/z = 182) and to the fragment $[TeCN]^+$ (m/z = 156). To obtain NMR spectra, the product was dissolved in deuterated THF. The chemical shift of the C atom is at δ (^{13}C) = 86.2 ppm, the chemical shift of the N atom at δ (^{14}N) = –70 ppm and the chemical shift of Te at δ (^{125}Te) = 567 ppm. The coupling constant of C and Te is reported to be $^1J(^{125}Te\text{-}^{13}C)$ = 330.2 Hz. In the ^{14}N NMR spectrum extra signals of dinitrogen (δ (^{14}N) = –71.5 ppm) and cyanogen (δ (^{14}N) = –123 ppm) were found. A solution of $Te(CN)_2$ in diethyl ether was layered by n-heptane and cooled to 248 K receiving colorless needles suitable for X-ray structure elucidation. Decomposition being faster than crystallization was problematic. The space group is $R\bar{3}c$, the bent structure is confirmed (<(C–Te–C) = 85.4(2)°) and two pairs of bond lengths are reported (r_{Te-C} = 2.090(5) Å respectively r_{Te-C} = 2.091(6) Å and r_{C-N} = 1.131(7) Å respectively r_{C-N} = 1.149(7) Å) (Klapötke et al., 2008).

The tellurium dicyanide exhibits C_{2v} symmetry in gas phase, but in regard to the experimental crystal structure the symmetry is decreased due to electrostatic interaction of lone pairs of neighboring cyanide groups, which is explained by the σ-hole concept mentioned in chapter 8.2.2. This causes a nearly square-planar coordination of $Te(CN)_2$ due to solvent molecules, which are included in the crystal. Both effects cause a significant variation of experimental and computational data (George et al., 2015).

Table 81: Selected experimental spectroscopic data of K[TeCN] and computational data of the tellurocyanate anion (bond lengths in Å; wave numbers in cm^{-1}).

Method	r_{Te-C}	r_{C-N}	ν_{TeC}	ν_{CN}
Exp. (Loewenschuss and Marcus, 1996)	1.904	1.153	459	2086
Extrapolation (Greenwood et al., 1964)	–	–	455–457	2083–2086

Tellurium tricyanide $Te(CN)_3$

Homoleptic threefold cyanide substituted tellurides $Te(CN)_3$ are not stable and require one more halogen to gain a certain level of stability (Fritz et al., 2008).

Tellurium tetracyanide $Te(CN)_4$

Tellurium tetracyanide $Te(CN)_4$ is less investigated due to its high sensitivity and its tendency to explosively decompose at air or temperatures higher than 253 K. In 2004, T. M. Klapötke et al. published a synthesis of $Te(CN)_4$ based on a reaction of tellurium tetrafluoride and four

Scheme 116: First synthesis of tellurium dicyanide (Cocksedge, 1908).

equivalents of trimethylsilyl cyanide, TMS–CN, dissolved in dichloromethane, which is similar to the reaction of $Se(CN)_4$ (Scheme 117) (Table 82).

The product was isolated in form of a colorless powder and was analyzed by Raman spectroscopy due to its low solubility in common solvents (Table 83). The identification of four different carbon–nitrogen stretching modes implies the presence of two axial and two equatorial cyanide groups. Furthermore, computational studies of $Te(CN)_4$ were carried out using different methods and basis sets (Table 84).

The computational results imply two pairs of cyanide groups and C_{2v} symmetry leading to a trigonal-bipyramidal structure. The reductive decomposition of tellurium tetracyanide forming tellurium dicyanide and cyanogen is exothermic (ΔE = –357.8 kJ mol^{-1}, MP2(fc)/cc-pVTZ) illustrating the high instability of $Te(CN)_4$ (Scheme 118) (Klapötke et al., 2004, 2008).

Tellurium hexacyanide $Te(CN)_6$

Tellurium hexacyanide $Te(CN)_6$ could not be synthesized until now and computational studies of this compound are rare. T. M. Klapötke et al. published results of calculations at B3LYP/cc-pVTZ and MP2(fc)/cc-pVTZ in 2004 (Table 85).

The centered tellurium atom is octahedral coordinated by cyanide groups (point group O_h). The reductive decomposition of tellurium hexacyanide forming tellurium tetracyanide and cyanogen is exothermic (ΔE = –343.32 kJ mol^{-1}, MP2(fc)/cc-pVTZ) illustrating the high instability of $Te(CN)_6$ (Scheme 119). However, the received tellurium tetracyanide itself also decomposes yielding tellurium dicyanide and cyanogen (Klapötke et al., 2004).

$$TeF_4 + 4\ TMS{-}CN \xrightarrow[253\ K]{CH_2Cl_2} Te(CN)_4 + 4\ TMS{-}F$$

Scheme 117: Synthesis of $Te(CN)_4$ accordingly the synthesis of $Se(CN)_4$ (Klapötke et al., 2004; Klapötke et al., 2008).

Table 82: Selected computational data of $Te(CN)_2$ (zpe in kJ mol^{-1}; bond lengths in Å; angles in °; wave numbers in cm^{-1}) (Klapötke et al., 2008).

Method + basis set	*zpe*	r_{Te-C}	r_{C-N}	< (C–Te–C)	ν_{CN}
B3LYP/cc-pVQZ	40.57	2.054	1.153	94.46	2274/2266
MP2(fc)/cc-pVQZ	39.05	2.021	1.177	93.19	2101/2100

Table 83: C–N stretching modes of $Te(CN)_4$ in the Raman spectrum (wave numbers in cm^{-1}) (Klapötke et al., 2004, 2008).

Compound	$\nu_{CN,1}$	$\nu_{CN,2}$	$\nu_{CN,3}$	$\nu_{CN,4}$
$Te(CN)_4$	2204	2191	2149	2129

$$Te(CN)_4 \longrightarrow Te(CN)_2 + (CN)_2$$

Scheme 118: Decomposition of tellurium tetracyanide (Klapötke et al., 2004, 2008).

Polonium

Since polonium is extremely rare on earth, e.g. traces in uranium pitchblende (uraninite), and is also highly radioactive, it is not surprising that nothing is known about polonium cyanide.

7th Main group

Formally, all halogen cyanides (also cyanogen halides), X–CN (X = F^-–I^-) can be regarded as halogen-pseudohalogen

Table 85: Selected computational data of $Te(CN)_6$ (zpe in kJ mol^{-1}; bond lengths in Å; angles in °; wave numbers in cm^{-1}) (Klapötke et al., 2004).

Method + basis set	*zpe*	r_{Te-C}	r_{C-N}	< (C–Te–C)	ν_{CN}
B3LYP/cc-pVTZ	125.49	2.118	1.153	90	2292–2297
MP2(fc)/cc-pVTZ	118.69	2.078	1.179	90	2062–2070

$$Te(CN)_6 \longrightarrow Te(CN)_4 + (CN)_2$$

Scheme 119: Reductive decomposition of tellurium hexacyanide (Klapötke et al., 2004).

Table 84: Selected computational data of $Te(CN)_4$ (total energies in a.u.; zpe in kJ mol^{-1}; bond lengths in Å; angles in °; wave numbers in cm^{-1}) (Klapötke et al., 2004, 2008).

Method + basis set	$E_{tot.}$	*zpe*	r_{Te-C}	r_{C-N}	< (C–Te–C)	ν_{CN}
B3LYP/cc-pVTZ	–639.4585	88.91	2.074/2.227	1.152/1.155	84.35/104.06	2300/2295/2265/2263
MP2(FC)/cc-pVTZ	–637.7936	77.00	2.042/2.180	1.176/1.180	83.53/105.60	2089/2086/2057/2053

compounds. Their aggregate state ranges from gaseous to solid at ambient temperatures and normal pressure and the melting and boiling points increase in accordance to the atomic number. Their reaction behavior is manifold and they tend to oligomerize forming the corresponding cyanuric halides, e.g. $(XCN)_3$. The solid structure of cyanogen fluoride is not experimentally confirmed, but there are many indications, that all cyanogen halides are crystallizing in the cyanogen bromide or iodide type. But in general, it can be assumed that all XCN molecules show a chain-like orientation of the molecules in the crystal.

The application of cyanogen halides of the smaller homologues fluorine, chlorine and bromine has not been intensively studied and is limited due to the instability of these compounds, quite in contrast to ICN, which has a quite diverse chemistry.

Fluorine

Cyanogen fluoride FCN, isocyanic fluoride FNC and their ions

Cyanogen fluoride FCN and isocyanic fluoride FNC

The first description of cyanogen fluoride FCN was published by V. E. Cosslett in 1931 being the latest cyanogen halide that was found. The colorless solid sublimes at 201 K and forms a colorless, sharp smelling gas. Synthesis was achieved in the reaction of silver fluoride and cyanogen iodide or bromide carried out in an evacuated glass ampulla at 493 K (Scheme 120) (Cosslett, 1931). It should be noted that this synthesis could not be repeated by E. E. Aynsley et al. in 1959 (Aynsley et al., 1959).

Moreover, it was reported that the pyrolysis of cyanuric fluoride in a stream of nitrogen at 1573 K and 67 mbar led to the formation of cyanogen fluoride (Scheme 121).

In this context, F. S. Fawcett and R. D. Lipscomb reported a boiling point of T_B = 229 K, a melting point at T_M = 191 K and characteristic bands at ν_{CN} = 2290 cm^{-1} and ν_{CF} = 1078 cm^{-1} were allocated to the cyanogen fluoride in good accordance to earlier assignments (Fawcett and Lipscomb, 1960; Panas, 1994). But they also studied alternative routes of pyrolysis to obtain FCN and at the end of several tests of different precursors they patent their formation of FCN by pyrolysis (Fawcett and Lipscomb, 1964; Lipscomb and Smith, 1961).

A synthetic route to obtain FCN, but requiring smaller instrumental effort was published by E. Mayer in 1969 and is based on the reaction of cesium fluoride and tetracyanomethane, although this method was already used to obtain the heavier compounds cyanogen chloride and bromide (Scheme 122) (Mayer, 1969c).

And in the early 1970s, Du Pont submitted another patent on the formation of FCN which describes fluorination of a solution of sodium cyanide using elemental fluorine (Scheme 123) and analyzing the escaping gas stream after 10 mins of reaction (Grakauskas, 1970).

The MW spectra of cyanogen fluoride suggest a C–F bond length of about 1.262 Å and a carbon–nitrogen bond length of about 1.159 Å, which is in good accordance to computations (r_{C-F} = 1.26–1.29 Å, r_{C-N} = 1.15–1.18 Å) (Bhattacharyya et al., 2007a; Degli Esposti et al., 1982; Lee and Racine, 1995; Lee et al., 1995; Ruoff, 1970; Schmiedekamp et al., 1980; Tyler and Sheridan, 1963). Based on MW spectra the dipole moment was determined being μ = 2.17 D, which is also in good accordance to computational studies (μ = 2.13–2.31 D) (Bhattacharyya et al., 2007a; Lee and Racine, 1995; Tyler and Sheridan, 1963; Sheridan et al., 1960; Zúñiga et al., 2012).

The crystal structures of the homologous cyanogen halides are known for several years, but until now the structure determination of cyanogen fluoride by single crystal XRD has not been possible. Based on computational studies two possible crystal structures were proposed, which are analogous to the non-polar, crystalline cyanogen chloride or polar hydrogen cyanide depending on the chosen structure modell. For each basic type two unit cells, an orthorhombic and a tetragonal one, can be derived (Table 88) (Panas, 1994).

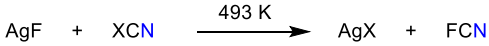

Scheme 120: Synthesis of cyanogen fluoride published by Cosslett (X = Br^-, I^-) (Cosslett, 1931).

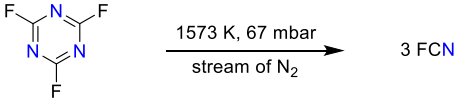

Scheme 121: Synthesis of cyanogen fluoride by thermolysis of cyanuric fluoride (Fawcett and Lipscomb, 1960; Panas, 1994).

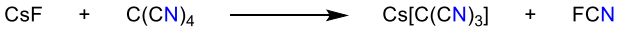

Scheme 122: Synthesis of FCN reported by E. Mayer (Mayer, 1969c).

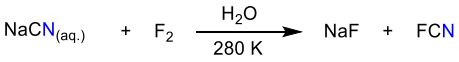

Scheme 123: Fluorination of sodium cyanide in solution patented by Du Pont (Grakauskas, 1970).

The extremely unstable isocyanic fluoride was synthesized by D. E. Milligan and M. E. Jacox by ultraviolet photolysis of cyanogen fluoride and characterized using IR spectroscopy (Milligan and Jacox, 1967a, 1967b). The patent of Du Pont also reports the formation of isocyanic fluoride using potassium isocyanide instead of sodium cyanide (Scheme 123) (Grakauskas, 1970). Additionally, some theoretical studies are dealing with the constitution isomers of cyanogen fluoride (Tables 86 and 87). In regard to computations the N–F bond length is in the range of 1.31–1.33 Å and the C–N bond length in the range of 1.15–1.20 Å (Lee et al., 1995; Schmiedekamp et al., 1980). Furthermore, bands of streching modes of ν_{CN} = 2214 cm^{-1} and ν_{NF} = 964 cm^{-1} are supposed and the mechanism of photochemical isomerization of cyanogen fluoride in contrast to dissociation is discussed (Zhang et al., 2007).

Table 88: Possible crystal structures of cyanogen fluoride (dimensions of unit cell in Å; volumes in $Å^3$) (Panas, 1994).

Parameter	ClCN type tetragonal	ClCN type orthorhombic	HCN type tetragonal	HCN type orthorhombic
Space group	*P4/nmm*	*Pmmn*	*I4mm*	*Imm*
a	4.76	4.50	4.29	–
b	4.76	4.87	4.29	–
c	5.40	5.50	5.45	–
V	122.35	120.53	100.30	–
Z	2	2	2	2

Cyanuric fluoride, $(FCN)_3$ (also known as trifluorotriazine, cyanuric trifluoride, trifluoro-s-triazine, 2,4,6-Trifluorotriazine, 2,4,6-trifluro-s-triazin, trifluoro-1,3,5-triazine), which is the trimer of FCN, is commercially

Table 86: Some experimental and computational data of cyanogen fluoride (bond lengths in Å; wave numbers in cm^{-1}).

Publication	Exp./calc.	r_{F-C}	r_{C-N}	ν_{FC}	ν_{CN}
Aynsley et al. (1959)	Exp. – IR	1.26	1.16	1077	2290
Fawcett and Lipscomb (1960)	Exp. – IR	–	–	1078	2290
Tyler and Sheridan (1963)	Exp. – MW	1.262	1.159	–	–
Esposti et al. (1982)	Exp. – MW	1.26240	1.15928	–	–
Lee et al. (1995)	CCSD(T)/cc-pVDZ	1.2826	1.1779	–	–
	CCSD(T)/cc-pVTZ	1.2701	1.1632	1077	2312
	CCSD(T)/cc-pVQZ	1.2670	1.1596	–	–
Lee and Racine (1995)	CCSD/TZ2P	1.270	1.153	1087	2404
	CCSD(T)/TZ2P	1.275	1.162	1060	2331
Wang et al. (1998)	CASSCF(6,6)/6-31G*	1.2630	1.1698	1132.3	2409.8
	MP2/6-31G*	1.2828	1.1825	1060.6	2267.4
	MP2/6-311G(2df)	1.2640	1.1689	1082.2	2291.5
	CCSD(T)/6-311G*	1.2717	1.1665	1068.2	2350.6
	CCSD(T)/6-311G(2d)	1.2733	1.1625	1055.8	2322.2
Bhattacharyya	MP2/cc-pVTZ	1.27	1.17	1074.16	2277.52
et al. (2007a)	CCSD/cc-pVTZ	1.27	1.15	1104.23	2422.87
	CCSD(T)/cc-pVTZ	1.27	1.16	1078.47	2350.36
Zhang et al. (2007)	B3LYP/6-311G**	–	–	1088.0	2419.6

Table 87: Selected experimental and computational data of isocyanic fluoride (bond lengths in Å; wave numbers in cm^{-1}).

Publication	Exp./calc.	r_{F-N}	r_{C-N}	ν_{FN}	ν_{CN}
Milligan and Jacox (1967a), (1967b)	Exp. – IR	–	–	928	2123
Lee et al. (1995)	CCSD(T)/cc-pVDZ	1.3199	1.2011	–	–
	CCSD(T)/cc-pVTZ	1.3097	1.1842	935	2109
Lee and Racine (1995)	CCSD/TZ2P	1.310	1.173	967	2220
	CCSD(T)/TZ2P	1.321	1.184	912	2126
Bhattacharyya	MP2/cc-pVTZ	1.30	1.19	987.20	2127.65
et al. (2007a)	CCSD/cc-pVTZ	1.30	1.17	997.44	2248.01
	CCSD(T)/cc-pVTZ	1.31	1.18	948.01	2157.39
Zhang et al. (2007)	B3LYP/6-311G**	–	–	963.5	2214.0

available as it is widely used as a fluorinating agent in the conversion of carboxylic acids into acyl fluorides. It is used as a precursor for fibre-reactive dyes and a specific reagent for tyrosine residues in enzymes (Anderson and Frick, 1972; Chambers and Tamura, 1985; Fawcett and Lipscomb, 1964; Grisley et al., 1958; Groβ et al., 2000; Kober and Grundmann, 1959; Kober et al., 1962; Maxwell et al., 1958; Nenajdenko, 2014; Rusinov et al., 2014; Sheridan et al., 1960; Shmel'kova et al., 1989; Zúñiga et al., 2012). Most synthesis processes for the preparation of cyanuric fluorides are based on cyanuric chloride, which can be converted to cyanuric fluoride by Cl^-/F^--exchange using various fluoride sources (Scheme 124). When using alkali fluorides, it is necessary to use COF_2 as a catalyst to allow lower temperatures (Anderson and Frick, 1972).

Cyanogen fluoride anion $[FCN]^-$ and isocyanic fluoride anion $[FNC]^-$

Neither the cyanogen fluoride anion, which is an odd electron species, nor the isocyanic fluoride anion could be synthesized or isolated until now. The isomeric structures and other properties were analyzed in several computational studies. Some of these data, bond angles, bond lengths and spectroscopic data for example, reported by different working groups are represented in Tables 89 and 90.

The calculated bond lengths significantly vary depending on the chosen method and basis set. The F–C bond length of the cyanogen fluoride anion is in the range of 1.53–1.72 Å, whereas the F–N bond length of the isocyanic fluoride anion is in the range of 1.86–2.10 Å. The variation of the C–N bond length is smaller, but also depends on method, basis set and isomer ($[FCN]^-$: 1.18–1.21 Å; $[FNC]^-$: 1.17–1.19 Å).

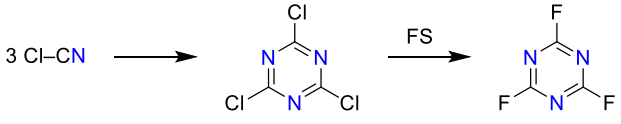

Scheme 124: Synthesis of cyanuric fluoride starting from cyanuric chloride (FS = fluoride source, MF, SbF_3; M = alkali metal with COF_2 as catalyst) (Anderson and Frick, 1972).

Cyanogen fluoride cation $[FCN]^+$

Similar to the cyanogen fluoride anion the cation species could also not be synthesized until now. But several computational studies have been published during the last decades, for example by A. K. Das and co-workers (Bhattacharyya et al., 2007a) and D.-C. Wang et al. (1998). Selected structural and spectroscopic data are listed in Table 91.

Difluorocyan cation $[F_2(CN)]^+$

Calculations of the difluorocyan cation $[F_2(CN)]^+$ and its structure were published by P. Pyykkö and N. Runeberg in 1991 and T. M. Klapötke and co-workers considered the linear cation to be an adduct of a fluorine atom and the cyanogen fluoride cation (Pyykkö and Runeberg, 1991). Their synthesis is a two-step-reaction. After the reaction of

Table 89: Selected computational data of the cyanogen fluoride anion (bond lengths in Å; angles in °; wave numbers in cm^{-1}).

Publication	Exp./calc.	r_{F-C}	r_{C-N}	< (F–C–N)	ν_{FC}	ν_{CN}
Gauld et al. (1997)	MP2/6-31G(d)	1.607	1.201	130.6	–	–
	QCISD/6-31G(d)	1.616	1.205	129.1	–	–
	QCISD/6-311 + G(2d,f,p)	1.531	1.197	128.1	–	–
	PW-P86/IGLO-III	1.718	1.192	131.3	–	–
Guerra (1999)	UQCISD/6-311G(d,p)	1.638	1.195	128.9	–	–
	UQCISD/6-311 + G(d,p)	1.603	1.199	128.1	–	–
Sommerfeld (2001)	MP2/TZV(d) + p	1.6538	1.1887	130.4	–	–
	SDCI/TZV(d) + p	1.6007	1.1799	128.5	–	–
	CCD/TZV(d) + p	1.6423	1.1826	128.7	–	–
	CCSD/TZV(d) + p	1.7056	1.1848	131.1	534.8	2013.1
	CCSD/TZV(2df) + sp	1.5314	1.1928	128.6	–	–
	CCSD(T)/TZV(d) + p	1.7215	1.1920	131.6	–	–
	CCSD(T)/TZV(2df) + sp	1.5661	1.1989	128.8	–	–
Bhattacharyya et al. (2007b)	B3LYP/cc-pVTZ	1.67	1.18	129.9	534.86	1972.17
	MP2/cc-pVTZ	1.58	1.19	131.0	816.17	2056.13
	CCSD/cc-pVTZ	1.57	1.19	127.7	605.22	1887.52
	CCSD(T)/cc-pVTZ	1.59	1.20	129.0	612.11	1891.68

Table 90: Selected computational data of the isocyanic fluoride anion (bond lengths in Å; angles in °; wave numbers in cm^{-1}).

Publication	exp./calc.	r_{F-N}	r_{C-N}	< (F–N–C)	ν_{FN}	ν_{CN}
Sommerfeld (2001)	MP2/TZV(d) + p	1.8592	1.1937	141.6	–	–
	SDCI/TZV(d) + p	2.1002	1.1682	180.0	–	–
	CCD/TZV(d) + p	2.0173	1.1769	150.3	–	–
	CCSD/TZV(d) + p	2.0128	1.1803	180.0	324.0	2117.1
	CCSD/TZV(2df) + sp	1.9874	1.1747	180.0	–	–
	CCSD(T)/TZV(d) + p	2.0000	1.1880	165.3	–	–
	CCSD(T)/TZV(2df) + sp	1.9625	1.1837	161.9	–	–
	B3LYP/cc-pVTZ	2.06	1.17	150.1	307.39	2105.08
Bhattacharyya	MP2/cc-pVTZ	1.86	1.19	144.1	368.36	1949.63
et al. (2007b)	CCSD/cc-pVTZ	2.00	1.18	180.0	335.20	2114.95
	CCSD(T)/6–311 + G(2d,2p)	1.98	1.18	180.0	372.66	2052.87

Table 91: Some computational data of $[FCN]^+$ (bond lengths in Å; wave numbers in cm^{-1}).

Author	Exp./calc.	r_{F-C}	r_{C-N}	ν_{FC}	ν_{CN}
D.-C. Wang et al. (1998)	CASSCF(5,6)/6-31G*	1.1979	1.2362	1170.1	2219.1
	MP2/6-31G*	1.2139	1.2128	1350.5	3021.0
	MP2/6-311G(2df)	1.1962	1.2106	1339.7	2763.0
	CCSD(T)/6-311G*	1.2050	1.2315	1145.8	2195.1
	CCSD(T)/6-311G(2d)	1.2062	1.2299	1133.9	2159.8
	IFCA	1.205	1.223	1134	2160
	MP2/cc-pVTZ	1.20	1.21	1342.26	2795.49
Bhattacharyya	CCSD/cc-pVTZ	1.20	1.22	1170.21	2218.79
et al. (2007a)	CCSD(T)cc-pVTZ	1.21	1.23	1151.81	2187.14

hydrogen cyanide and arsenic pentafluoride in liquid hydrogen fluoride the received cation $[HCNH]^+$ is fluorinated using an excess of elementary fluorine (Scheme 125).

T. M. Klapötke and co-workers could characterize the cation using IR and Raman spectroscopy, but could not isolate the salt due to decomposition at ambient temperatures. The experimental data reported by T. M. Klapötke and co-workers, their computational results and the data of P. Pyykkö and N. Runeberg are summarized in Table 92 (Pyykkö and Runeberg, 1991; Tornieporth-Oetting et al., 1991).

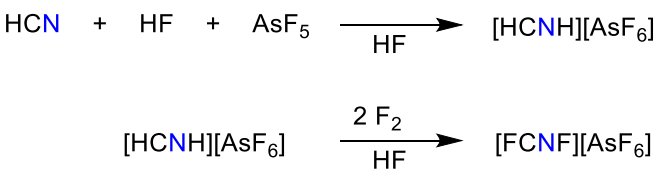

Scheme 125: Two-step-synthesis of the difluorocyan cation by Tornieporth-Oetting et al. (1991).

Table 92: Experimental Raman data and computational data of $[F_2(CN)][AsF_6]$ (bond lengths in Å; wave numbers in cm^{-1}).

Exp./calc.	r_{F-CNF}	r_{FC-NF}	r_{FCN-F}	$\nu(\sigma_g)$	$\nu(\sigma_u)$	$\nu(\sigma_u)$	$\nu(\pi_g)$	$\nu(\pi_g)$
Exp. – Raman (Tornieporth-Oetting et al., 1991)	–	–	–	2587	1378*	729	456	243
HF/6-31G[a] (Tornieporth-Oetting et al., 1991)	–	–	–	2565	1312	774	457	230
HF/6-31G[a] (Pyykkö and Runeberg, 1991)	1.215	1.108	1.261	3017	1544	911	537	270
MP2/6-31G[a] (Pyykkö and Runeberg, 1991)	1.241	1.147	1.282	–	–	–	–	–

[a]IR data.

Chlorine

Cyanogen chloride ClCN, isocyanic chloride ClNC and their ions

Cyanogen chloride (also known as chlorine cyanide, chlorocyanogen, chlorcyan) is both an industrial chemical needed to build a variety of organic/inorganic products (e.g. cyan amide, $H_2N–CN$, in the reaction with ammonia), but it is also a chemical warfare agent (1.5 HCN sources, toxicology, treatment, and mode of action (Newhouse and Chiu, 2010)) (Romano et al., 2007). It hydrolyzes in water to form HCl and HOCN.

Cyanogen chloride ClCN and isocyanic chloride ClNC

The first synthesis of cyanogen chloride ClCN was carried out by C.-L. Berthollet in 1787 and several studies were published since that time (Jennings and Scott, 1919). During the World War I it was used as a warfare agent due to its toxicity. Many different synthetic routes have been reported in the earlier years, especially wet chemical methods based on the reaction of cyanides and elementary chlorine in aqueous solution. One example is the reaction of potassium cyanide and chlorine water carried out by A. Hantzsch and L. Mai (Scheme 126). To avoid side reaction, an excess of chlorine water is necessary (Hantzsch and Mai, 1895).

Therefore, several working groups tried to find synthetic routes with less experimental effort resulting in the use of *in situ* formed potassium tetracyanozincate instead of potassium cyanide (Scheme 127) (Klemenc and Wagner, 1938; Schröder, 1958).

An anhydrous synthesis of cyanogen chloride is the reaction of chlorine and a mixture of potassium cyanide and sand to distribute heat (Jennings and Scott, 1919). R. Varma and A. J. Signorelli reported a similar route using dichlorine monoxide and silver cyanide (Scheme 128) (Varma and Signorelli, 1969).

W. Sundermeyer also discussed molten salts and their use as reaction media. As an example of halogen-pseudohalogen exchange, he studied the reaction of

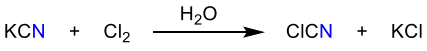

Scheme 126: Synthesis of cyanogen chloride by A. Hantzsch and L. Mai (Hantzsch and Mai, 1895).

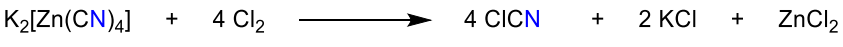

Scheme 127: Synthesis of cyanogen chloride using potassium tetracyanozincate (Schröder, 1958).

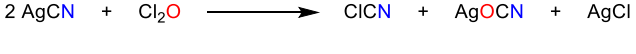

Scheme 128: Anhydrous synthesis of cyanogen chloride by R. Varma and and A. J. Signorelli (Varma and Signorelli, 1969).

potassium cyanide and chlorine to form cyanogen and potassium chloride. Discussing the cyanogen chloride as a possible intermediate, he reported that the reaction of potassium cyanide and chlorine may lead to cyanogen chloride in nearly quantitative yields in the first step (Sundermeyer, 1965). Additionally, several industrial synthetic routes were developed. For example, a patent of Degussa includes the reaction of chlorine and hydrogen cyanide, which is formed *in situ* using hydrogen peroxide and hydrogen chloride (Scheme 129).

Catalysts are Lewis acids, copper dichloride or aluminum trichloride for example (Heilos et al., 1971; Heimberger and Schreyer, 1975). The immediate reaction of chlorine and hydrogen cyanide in liquid phase at low temperatures and in presence of a catalyst is protected by a patent owned by the Bayer AG (Scheme 130). Catalysts are Lewis acids like phosphorus trichloride and side products of this reaction are cyanuric chloride and hydrogen chloride (Enders, 1972). In 2007, Evonik published a patent for a continuous process for ClCN that is particularly suitable for industrial scale. The process is based on sodium cyanide, which is reacted with chlorine in aqueous solution to form cyanogen chloride (Tautz and Blumberg, 2007).

Under standard conditions cyanogen chloride is a colorless gas, which liquefies under normal pressure at 286 K and changes to solid state at 266 K (Chadwick and Edwards 1973). Especially MW spectroscopy was used to extensively investigate cyanogen chloride in gaseous state. The carbon–nitrogen bond length is reported to be in the

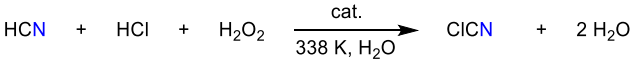

Scheme 129: Industrial formation of cyanogen chloride protected by patent of Degussa (Heilos et al., 1971; Heimberger and Schreyer, 1975).

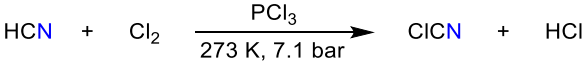

Scheme 130: Industrial formation of cyanogen chloride protected by patent of Bayer AG (Enders, 1972).

range of 1.14–1.17 Å and the chlorine–carbon bond length in the range of 1.62–1.64 Å (Townes et al., 1947, 1948; Tyler and Sheridan, 1963; Smith et al., 1948). In regard to MW spectroscopy the experimental dipole moment of cyanogen chloride is μ = 2.80 D, which is in accordance to the calculated value of μ = 2.869 D (Kellö and Sadlej, 1992; Tyler and Sheridan, 1963). Based on IR spectra the band at 2219 cm^{-1} was allocated to the C–N stretching mode and the band at 714 cm^{-1} was assigned to the C–Cl stretching mode by W. O. Freitag and E. R. Nixon, which is in good accordance to the Raman spectra of M. Pézolet and R. Savoie (Freitag and Nixon, 1956; Pézolet and Savoie, 1971).

In 1956 the first structure determination using single crystal XRD of solid cyanogen chloride was published by R. B. Heiart and G. B. Carpenter. It forms orthorhombic crystals, space group *Pmmn*, and each unit cell contains two molecules. Similar to the later homologs the molecules exhibit a substructure of chains along the *c*-axis. They argued that the bond lengths are decreased to r_{Cl-C} = 1.57(1) Å and r_{C-N} = 1.16(2) Å and due to these intermolecular interactions along the chains, respectively (Heiart and Carpenter, 1956).

Next to experimental results, several computational studies have been published in literature (Bhattacharyya et al., 2007a; Destro et al., 1988; Lee and Racine, 1995; Lee et al., 1995; Schmiedekamp et al., 1980; Støgard, 1976; Zhang et al., 2007). A summary of these data in comparison to the experimental values are represented in Tables 93 and 94. Computational data of the isocyanic chloride are also included, although the isomerization product could not be

Table 93: Some experimental and computational data of cyanogen chloride (bond lengths in Å; wave numbers in cm^{-1}).

Publication	Exp./calc.	r_{Cl-C}	r_{C-N}	ν_{ClC}	ν_{CN}
Townes et al. (1947)	Exp. – MW	1.64	1.15	–	–
Smith et al. (1948)	Exp. – MW	1.630	1.163	–	–
Townes et al. (1948)	Exp. – MW	1.629	1.163	–	–
Freitag and Nixon (1956)	Exp. – IR	–	–	714	2219
Heiart and Carpenter (1956)	Exp. – XRD	1.57(1)	1.16(2)	–	–
Tyler and Sheridan (1963)	Exp. – MW	1.631	1.159	–	–
Pézolet and Savoie (1971)	Exp. – Raman	–	–	728	2205
Støgård (1976)	HF (no 3d of Cl)	1.684	1.150	–	–
	HF (with 3d of Cl)	1.657	1.151	–	–
Lee and Racine (1995)	CCSD/TZ2P	1.652	1.155	729	2313
	CCSD(T)/TZ2P	1.655	1.164	716	2236
Lee et al. (1995)	CCSD(T)/cc-pVDZ	1.6604	1.1800	–	–
	CCSD(T)/cc-pVTZ	1.6437	1.1656	707	2209
	CCSD(T)/cc-pVQZ	1.6384	1.1619	–	–
Bhattacharyya	MP2/cc-pVTZ	1.63	1.17	754.55	2139.38
et al. (2007a)	CCSD/cc-pVTZ	1.64	1.16	749.54	2318.78
	CCSD(T)/cc-pVTZ	1.64	1.17	737.80	2241.87
Zhang et al. (2007)	B3LYP/6-311G**	–	–	737.4	2316.4

Table 94: Some experimental and computational data of isocyanic chloride (bond lengths in Å; wave numbers in cm^{-1}).

Publication	Exp./calc.	r_{Cl-N}	r_{C-N}	ν_{ClN}	ν_{CN}
Milligan and Jacox (1967a, 1967b)	Exp. – IR	–	–	615	2074
Destro et al. (1988)	SCF/STO-3G	1.693	1.179	–	–
	SCF/3-21G	1.690	1.165	–	–
	SCF/6-31G*	1.619	1.157	–	–
Lee et al. (1995)	CCSD(T)/cc-pVDZ	1.6612	1.2009	–	–
	CCSD(T)/cc-pVTZ	1.6371	1.1845	702	2069
Bhattacharyya	MP2/cc-pVTZ	1.62	1.19	734.87	2074.88
et al. (2007a)	CCSD/cc-pVTZ	1.63	1.18	733.94	2185.78
	CCSD(T)/cc-pVTZ	1.64	1.18	706.99	2105.81
Zhang et al. (2007)	B3LYP/6-311G**	–	–	685.2	2149.8

isolated, but D. E. Milligan and M. E. Jacox reported that photolysis experiments similar to the formation of isocyanic fluoride and spectroscopic analysis may indicate the formation of ClNC (Milligan and Jacox, 1967a, 1967b).

Cyanuric chloride $(ClCN)_3$, the trimer of cyanogen chloride, is commonly produced on a large scale worldwide by trimerization of cyanogen chloride (Burger and Hornbaker, 1953; Grundmann and Kober, 1956; Grundmann and Kreutzberger, 1954, 1955; Goubeau et al., 1954; Huthmacher and Most, 2000; Ruoff, 1970; Kreutzberger, 2006; Romano et al., 2007; Tautz and Blumberg, 2007). The synthesis of $(ClCN)_3$ usually proceeds in two steps. The hydrocyanic acid is converted into cyanogen chloride, which is directly trimerized to cyanuric chloride. The dry cyanogen chloride is trimerized at 573 K on activated carbon. The ClCN yield in this process exceeds 95%; the $(ClCN)_3$ yield exceeds 90% (Scheme 131) (Huthmacher and Most, 2000).

Catalysts for the cyanogen chloride trimerization as activated carbon are, among others, molten cyanuric acid chloride, molten aluminum chloride, eutectic mixtures of tetrachloroaluminates, aluminum silicates, and Zeolites doped with metal oxides or sulphides. In some of these processes, ''tetrameric cyanogen chloride'' (2,4-dichloro-6-isocyanodichloro-5-triazine) is a by-product; its conversion to cyanuric chloride is catalyzed by iron oxide. In the laboratory, ClCN trimerizes in benzene or chloroform solution in the presence of hydrogen chloride (Diels, 1899). For further details on the chemistry of cyanuric chloride, we refer to the review article by K. Huthmacher (Huthmacher and Most, 2000).

Cyanogen chloride anion $[ClCN]^-$ and isocyanic chloride anion $[ClNC]^-$

Similar to the fluorine species, the cyanogen chloride anion $[ClCN]^-$ and the isocyanic chloride anion $[ClNC]^-$could not be isolated until now. The data of a theoretical study are represented in Table 95 (Bhattacharyya et al., 2007b).

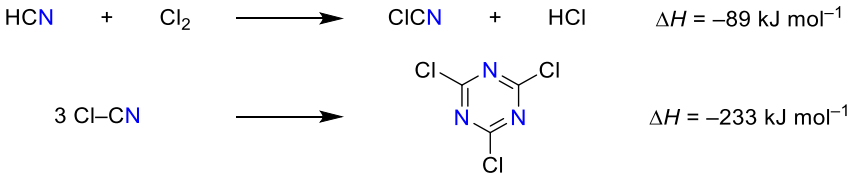

Scheme 131: Two-step synthesis of cyanuric chloride (Huthmacher and Most, 2000).

Table 95: Computational data of the isomers $[ClCN]^-$ and $[ClNC]^-$ reported by I. Bhattacharyya et al. (bond lengths in Å; angles in °; wave numbers in cm^{-1}) (Bhattacharyya et al., 2007b).

Compound	Method + basis set	r_{Cl-E}	r_{C-N}	< (F–A–B)	ν_{ClE}	ν_{CN}
$[ClCN]^-$	B3LYP/cc-pVTZ	2.44	1.16	167.9	251.74	2169.11
	MP2/cc-pVTZ	2.22	1.18	131.2	1072.59	2086.36
	CCSD/cc-pVTZ	2.37	1.17	179.7	293.05	2181.28
	CCSD(T)/cc-pVTZ	2.33	1.18	158.0	338.83	2123.1
$[ClNC]^-$	B3LYP/cc-pVTZ	2.46	1.17	178.6	204.58	2126.79
	MP2/cc-pVTZ	2.27	1.19	144.0	352.30	2053.93
	CCSD/cc-pVTZ	2.34	1.18	180.0	274.90	2126.68
	CCSD(T)/6–311 + G(2d,2p)	2.37	1.18	179.9	269.61	2067.89

Table 96: Some experimental and computational data of the cyanogen chloride cation (bond lengths in Å; wave numbers in cm^{-1}).

Publication	Exp./calc.	r_{Cl-C}	r_{C-N}	ν_{ClC}	ν_{CN}
Fulara et al. (1985)	Exp – PES	–	–	827	1914
Jacox and Thompson (2007)	Exp. – IR	–	–	832.0	1919.4
Wang et al. (1998)	CASSCF(5,6)/6-31G*	1.5717	1.2326	819.8	2005.4
	MP2/6-31G*	1.5592	1.1921	928.6	2975.7
	MP2/6-311G(2df)	1.5526	1.1885	913.2	2878.4
	CCSD(T)/6-311G*	1.5732	1.2152	826.5	1981.2
	CCSD(T)/6-311G(2d)	1.5800	1.2127	800.2	1959.8
	IFCA	1.556	1.214	800	1960
Bhattacharyya et al. (2007a)	MP2/cc-pVTZ	1.56	1.19	912.29	2897.20
	CCSD/cc-pVTZ	1.57	1.21	837.73	2040.04
	CCSD(T)/cc-pVTZ	1.57	1.21	833.96	2062.42

Cyanogen chloride cation $[ClCN]^+$ and isocyanic chloride cation $[ClNC]^+$

Besides some computational studies of the cyanogen chloride cation $[ClCN]^+$ and its isomer there are only two experimental investigations (Fulara et al., 1985; Jacox and Thompson, 2007). M. E. Jacox and W. E. Thompson reported vibrational data of the cations. After formation of the cations using cyanogen chloride, which was exposed to a beam of neon atoms excited in a microwave discharge, the reactive species were included in a neon matrix and analyzed IR spectroscopically (Jacox and Thompson, 2007). J. P. Maier and co-workers used a combination of present emission spectra and photoelectron spectroscopy (PES) to identify the cation and to determine its structural parameters (Table 96) (Fulara et al., 1985).

On excitation of ClCN at energies between 16.6 and 16.85 eV, followed by rapid quenching of the products in solid neon at 4.3 K (see above), prominent infrared absorptions result from both photoisomerization and photoionization of the ClCN. In regard to the isocyanic chloride cation, a band at 1952.8 cm^{-1} was allocated to the C–N stretching mode and the band at 734.8 cm^{-1} was assigned to the Cl–N stretching mode by M. E. Jacox and W. E. Thompson (2007).

Bromine

Cyanogen bromide BrCN, isocyanic bromide BrNC and their ions

Just like ClCN, BrCN is a commercially available substance that is frequently used in both inorganic and organic chemistry because, unlike ClCN, it is a solid (Bhattacharyya et al., 2010; Chau et al., 1993; Geller and Schawlow, 1955; Hartman and Dreger, 1931; Holland et al., 2004; Hollas and Sutherley, 1971; Jacox and Thompson, 2007; Kellö and Sadlej, 1992; Lee, 1995; Lord and Woolf, 1954; Mishra et al., 2006; Nolan et al., 1975; Oberhauser, 1927; Pasternack and Dagdigian, 1976; Pézolet and Savoie, 1971; Rösslein et al., 1989; Ruoff, 1970; Salud et al., 1993; Smith et al., 1948; Slotta, 1934; Tyler and Sheridan, 1963; Zhang et al., 2007).

Cyanogen bromide BrCN and isocyanic bromide BrNC

At standard conditions cyanogen bromide BrCN is a colorless, transparent solid. In spite of its toxicity, cyanogen bromide is a frequently used reagent in biochemical and biological studies. To synthesize this compound in laboratory scale, a reaction of dissolved sodium or potassium cyanide and elementary bromine at low temperature is used (Scheme 132). Purification of the product by distillation is difficult due to the boiling point of T_B = 335 K which is quite close to its melting point of T_M = 325 K (Baum, 1908; Scholl, 1896; Slotta, 1934; Steinkopf, 1925).

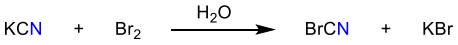

Scheme 132: Synthesis of cyanogen bromide published by R. Scholl (1896).

Another synthetic route of cyanogen bromide is the reaction of bromine and potassium thiocyanate leading to cyanogen bromide and some side products, potassium bromide and hydrogen bromide for example (Scheme 133) (König, 1911).

Cyanogen bromide can also be isolated after a reaction of bromine monochloride and sodium cyanide. To avoid the use of bromine monochloride, this method has been modified to form this compound *in situ* by addition of chlorine to a solution of sodium cyanide and sodium bromide (Scheme 134) (Dodonow, 1926).

Additionally, several industrial synthetic routes were developed. The synthetic route of cyanogen chloride, which is protected by a patent of Degussa (Scheme 129), was modified and can also be used to isolate the bromine species (Scheme 135). Similar to the formation of cyanogen chloride catalysts are Lewis acids, copper dichloride or aluminum trichloride for example (Heimberger and Schreyer, 1975).

The anhydrous formation of cyanogen bromide based on a reaction of trimethylsilyl cyanide TMS–CN and homo- or heteronuclear halogens, bromine monochloride for example, is another industrial process and protected by a patent of Bayer AG (Scheme 136).

The synthesis of cyanogen bromide using sodium cyanide and sodium hypobromite, which is formed *in situ*, was protected by a patent of Syngenta Limited in 2001 (Scheme 137). A small temperature range is preferred to avoid hydrolysis of the product and buffer, especially borates, maintain the preferred pH range (Jackson et al., 2001).

The cyanogen bromide has been structurally investigated several times. Studies of the gas phase using MW spectroscopy led to bond lengths of r_{Br-C} = 1.79 Å and r_{C-N} = 1.16 Å, respectively (Le Guennec et al., 1992; Smith et al., 1948; Tyler and Sheridan, 1963; Townes et al., 1947, 1948). J. K. Tyler and J. Sheridan also reported an experimental dipole moment μ = 2.94 D, while the calculated dipole moment is μ = 3.187 D (Kellö and Sadlej, 1992; Tyler and Sheridan, 1963). Several working groups also analyzed IR and Raman spectra in respect of the BrC and CN stretching mode. Depending on the publication, bands at about ν_{BrC} = 575 cm^{-1} were assigned to the BrC and bands at

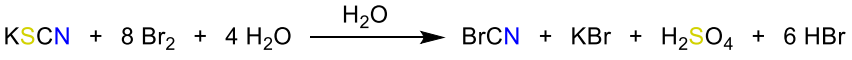

Scheme 133: Synthesis of cyanogen bromide published by W. König (1911).

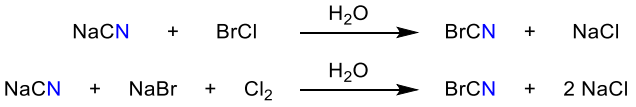

Scheme 134: Synthesis of BrCN using bromine monochloride (Dodonow, 1926).

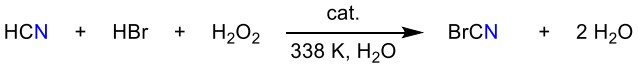

Scheme 135: Industrial formation of cyanogen bromide protected by patent of Degussa (Heimberger and Schreyer, 1975).

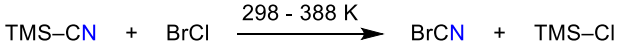

Scheme 136: Industrial generation of cyanogen bromide (patent of Bayer AG) (Faß et al., 1984).

ν_{CN} = 2187–2200 cm^{-1} to the CN stretching mode (Bandy et al., 1970; Freitag and Nixon, 1956; Klapötke and Schulz, 1996; Pézolet and Savoie, 1971; Thomas and Orville-Thomas, 1969).

The first study of cyanogen bromide determining bond lengths and molecular constitution using electron diffraction experiments was published by J. Y. Beach and A. Turkevich in 1939 (Beach and Turkevich, 1939). Cyanogen bromide forms orthorhombic crystals, space group *Pnmm*, and each unit cell contains two molecules. The reported bond lengths are r_{Br-C} = 1.79(2) Å and r_{C-N} = 1.13(4) Å being nearly identical to the bond lengths in gas phase (vide supra). Similar to the cyanogen chloride discussed above the molecules exhibit a substructure of chains along the *a*-axis corresponding to intermolecular interactions along these chains and shortening intermolecular distances (Geller and Schawlow, 1955). Additionally, several computational studies have been published in literature and selected data are listed in Table 97 along with reported experimental data (Bhattacharyya et al., 2010; Holland et al., 2004; Klapötke and Schulz, 1996; Lee, 1995; Mishra et al., 2006; Zhang et al., 2007).

Similar to the lighter homologs, isocyanic bromide has also been investigated computationally, whereas its isolation has failed until now and only one experimental evidence of its formation was published in literature (Table 98) (Bhattacharyya et al., 2010; Lee, 1995; Milligan and Jacox, 1967a, 1967b; Zhang et al., 2007).

Cyanuric bromide (BrCN)$_3$, can be obtained by the polymerization of BrCN similar to the methods described for the trimerization of cyanuric chloride, (ClCN)$_3$ (see Scheme 131) (Smolin and Rapoport, 1959). For example, by allowing a BrCN solution in ether to stand, to add HBr at ambient temperatures or to add $AlBr_3$ in nitromethane. Also the reaction of $K_3[Fe(CN)_6]$ with bromine yields $(BrCN)_3$ at 473 K in good yields. $(BrCN)_3$ also features the same s-triazine ring structure as discussed for $(XCN)_3$ (X = F$^-$, Cl$^-$; vide supra).

Cyanogen bromide cation [BrCN]$^+$

The cyanogen bromide cation [BrCN]$^+$ was formed by exposure of cyanogen bromide to a beam of excited helium atoms and studied by laser excitation spectroscopy (LES). Based on the analysis of recorded spectra M. A. Hanratty and co-workers could report Br–C and C–N bond lengths of the cation as listed in Table 99 (Rösslein et al., 1989). IR spectroscopy was used by M. E. Jacox and W. E. Thompson to identify the cation in a similar way to the formation of the cyanogen chloride cation described before (Jacox and Thompson, 2007). The bond lengths, which were determined using photoelectron spectroscopy (PES), are similar to those of LES and in the range of the calculated values (Chau et al., 1993).

Bromine bromocyanate [Br(BrCN)]$^-$ and bromine tribromocyanate [Br(BrCN)$_3$]$^-$

The polyhalogen pseudohalide [Br(BrCN)]$^-$ was synthesized by adding one equivalent of BrCN to [PNP]Br ([PNP] = $[Ph_3PNPPh_3]$) in acetonitrile (Schmidt et al., 2019). The compound crystallizes in the triclinic space group $P\bar{1}$ (Scheme 138). The polyhalogenpseudohalide

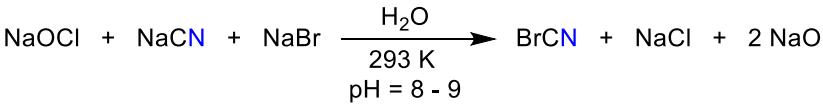

Scheme 137: Industrial formation of cyanogen bromide protected by patent of Syngenta Limited (Jackson et al., 2001).

Table 97: Some experimental and computational data of the cyanogen bromide (bond lengths in Å; wave numbers in cm^{-1}).

Publication	Exp./calc.	r_{Br-C}	r_{C-N}	ν_{BrC}	ν_{CN}
Beach and Turkevich (1939)	Exp. – ED	1.79(2)	1.13(4)	–	–
Townes et al. (1947)	Exp. – MW	1.79	1.15	–	–
Smith et al. (1948)	Exp. – MW	1.789	1.160	–	–
Townes et al. (1948)	Exp. – MW	1.790	1.158	–	–
Geller and Schawlow (1955)	Exp. – XRD	1.79	1.15	–	–
Freitag and Nixon (1956)	Exp. – IR	–	–	575	2200
Tyler and Sheridan (1963)	Exp. – MW	1.789	1.158	–	–
Thomas and Orville-Thomas (1969)	Exp. – IR	–	–	577	2188
Bandy et al. (1970)	Exp. – IR	–	–	573	2193
Pézolet and Savoie (1971)	Exp. – Raman	–	–	577	2187
Le Guennec et al. (1992)	Exp. – MW	1.7891	1.1586	–	–
Klapötke and Schulz (1996)	Exp. – IR	–	–	574	2200
	MP2/6-31G*	1.791	1.185	–	–
Lee (1995)	CCSD(T)/TZ2P	1.810	1.165	577	2218
Holland et al. (2004)	MP2/6-311G**	1.790	1.178	–	–
Mishra et al. (2006)	B3LYP/aug-cc-pVTZ(RECP)	1.7899	1.1531	585	2289
	CCSD(T)/aug-cc-pVTZ(RECP)	1.7966	1.1662	–	–
Zhang et al. (2007)	B3LYP/6-311G**	–	–	581.1	2294.0
Bhattacharyya et al. (2010)	MP2/(SDB-aug-)cc-pVTZ	1.78	1.18	601.81	2111.70
	CCSD/(SDB-aug-) cc-pVTZ	1.79	1.16	600.44	2281.64
	CCSD(T)/(SDB-aug-) cc-pVTZ	1.80	1.17	594.00	2197.07

Table 98: Some experimental and computational data of the isocyanic bromide (bond lengths in Å; wave numbers in cm^{-1}).

Publication	Exp./calc.	r_{Br-N}	r_{C-N}	ν_{BrN}	ν_{CN}
Milligan and Jacox (1967a, 1967b)	Exp. – IR	–	–	–	2067
Lee (1995)	CCSD(T)/TZ2P	1.800	1.183	561	2089
Zhang et al. (2007)	B3LYP/6-311G**	–	–	543.8	2134.4
Bhattacharyya et al. (2010)	MP2/(SDB-aug-)cc-pVTZ	1.77	1.19	593.36	2061.01
	CCSD/(SDB-aug-)cc-pVTZ	1.78	1.18	587.90	2142.73
	CCSD(T)/(SDB-aug-)cc-pVTZ	1.79	1.19	568.88	2090.18

Table 99: Some experimental and computational data of the cyanogen bromide cation (bond lengths in Å; wave numbers in cm^{-1}).

Publication	Exp./calc.	r_{Br-C}	r_{C-N}	ν_{BrC}	ν_{CN}
Rösslein et al. (1989)	Exp – LES	1.745(14)	1.195(16)	–	–
Salud et al. (1993)	Exp – IR	–	–	–	1905.93
Chau et al. (1993)	Exp. – PES	1.745(14)	1.195(16)	–	–
Jacox and Thompson (2007)	Exp. – IR	–	–	–	1907.7
Mishra et al. (2006)	B3LYP/aug-cc-pVTZ(RECP)	1.7304	1.1868	640	1989
	CCSD(T)/aug-cc-pVTZ(RECP)	1.7218	1.2039	640	1925

consists of a bromide ion coordinated by a BrCN molecule in an almost linear structure with a rather long Br–Br bond (< (Br–Br–C1) = 176.3(1)°, r_{Br-Br} = 3.011(1) Å; cf. Σr_{cov}(Br) = 2.28 Å; Scheme 138) (Pyykkö and Atsumi, 2009).

The polypseudohalogen anion is comparable to the known trihalides such as $[Br_3]^-$ or $[Cl_3]^-$. Quantum chemical calculations show that the energy required for the cleavage of $[Br]^-$ in $[Br_3]^-$ is 37 kJ mol^{-1} higher than that for $[Br(BrCN)]^-$.

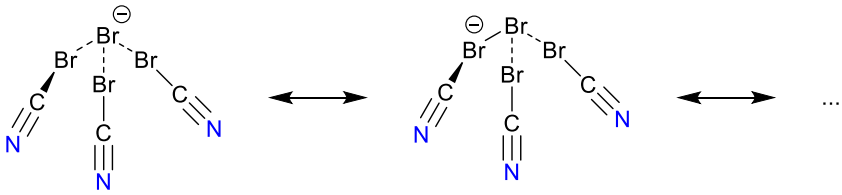

Scheme 138: Important Lewis representations of $[Br(BrCN)]^-$ and $[Br(BrCN)_3]^-$.

From a mixture of three equivalents of BrCN and [PNP]Br in acetonitrile, the pseudohalogen salt [PNP][$Br(BrCN)_3$] (monoclinic space group $P2_1/n$; Scheme 138) crystallizes. In the anion the central bromide ion is coordinated by three BrCN molecules in a distorted pyramidal structure. The Br···BrCN bond lengths are significantly elongated (3.089(1) Å) compared to a Br–Br single bond (cf. $\Sigma r_{cov}(Br) = 2.28$ Å). All Br–Br–C angles are nearly linear (169°–176°). Both ions, $[Br(BrCN)]^-$ and $[Br(BrCN)_3]^-$, can be referred to as BrCN adducts of a bromide anion of the type $[Br]^- \cdot n$ (BrCN) with $n = 1$ and 3.

Iodine

In contrast to the cyanide compounds of chlorine and bromine, the cyanogen iodide compounds show a quite manifold chemistry. Some polyiodine-pseudohalide anions are synthesized and purified in form of their alkali metal salts enabling structural characterizations. Their structural properties are quite similar to the well-known poly-iodide anions.

Cyanogen iodide ICN and derived ions

Cyanogen iodide ICN

Studies on cyanogen iodide ICN go back to the nineteenth century when F. Wöhler and other chemists investigated these compounds systematically. The cyanogen iodide is a very poisonous, colorless solid forming crystalline needles, melts at about 420 K and decomposes at higher temperatures leading to cyanogen and iodine (Chadwick and Edwards 1973). One of the first synthetic routes was published by H. Davy and F. Wöhler. They observed that the reaction of iodine and mercury cyanide or silver cyanide led to the formation of cyanogen iodide (Scheme 139). F. Wöhler preferred silver cyanide as starting material due to an easier purification by sublimation of the cyanogen iodide (Wöhler, 1821).

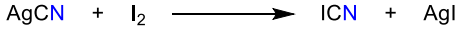

Scheme 139: Synthesis of cyanogen iodide published by F. Wöhler (1821).

During his studies on nitrogen triiodide in the 1880s, F. Raschig observed that the reaction of this compound and an aqueous solution of potassium cyanide or potassium thiocyanate led to the formation of cyanogen iodide, which was easily isolated by extraction (Scheme 140) (Raschig, 1885).

Cyanogen iodide can also be obtained by partial transformation of hydrogen cyanide with iodine into ICN and HI which is described as an equilibrium reaction (Scheme 141) (von Meyer, 1887).

In regard to the smaller homologs chlorine and bromine, the formation of cyanogen halides using the elemental halogen has already been discussed. In this context the formation of cyanogen iodide using iodine and a metal cyanide as cyanide source is also possible (Scheme 142) (Bak and Hillebert, 1952). Additionally, the reaction of potassium cyanide and heteronuclear instead of homonuclear halogens, for example I–Cl, also yields cyanogen iodide (Scheme 142) (Birckenbach and Huttner, 1929; Cornog et al., 1938).

Studies of the gas phase of cyanogen iodide using MW spectroscopy led to the determination of the bond lengths ($r_{I-C} = 2.00$ Å and $r_{C-N} = 1.16$ Å) (Smith et al., 1948; Townes et al., 1948; Tyler and Sheridan, 1963). J. K. Tyler and J. Sheridan also reported an experimental dipole moment $\mu = 3.71$ D, while the calculated dipole moment is $\mu = 3.628$ D (Kellö and Sadlej, 1992; Tyler and Sheridan, 1963). The vibrational modes of cyanogen iodide were analyzed using IR, Raman and photoelectron spectroscopy. In general the IC stretching band is in the range of 452–487 cm^{-1} and the CN stretching band at about 2171–2188 cm^{-1} (Freitag and Nixon, 1956; Hemple and Nixon, 1967; Hollas and Sutherley, 1971).

Based on a crystal structure determination of cyanogen iodide, published by J. A. A. Ketelaar and J. W. Zwartsenberg in the 1930s, this compound forms rhombohedral crystals with the space group $R\bar{3}m$, and each unit cell contains one molecule. The reported bond lengths are $r_{I-C} = 2.03$ Å and $r_{C-N} = 1.18$ Å being nearly identical to the bond lengths in the gas phase (Ketelaar and Zwartsenberg, 1939).

The metastabile isocyanic iodide, INC, was formed from its constitution isomer ICN by photoisomerization and was analyzed using spectroscopic measurements combined with

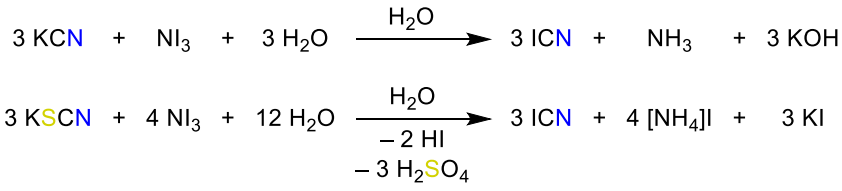

Scheme 140: Reaction of nitrogen triiodide and potassium cyanide or potassium thiocyanate to form ICN (Raschig, 1885).

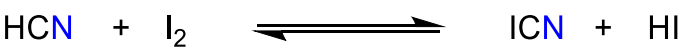

Scheme 141: Equilibrium of hydrogen cyanide and iodine with ICN and hydrogen iodide (von Meyer, 1887).

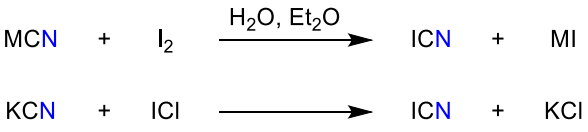

Scheme 142: Cyanogen iodide formed by alkaline cyanide and homonuclear, elemental halogen (M = Na^+, K^+; top) or potassium cyanide and I–Cl (bottom) (Bak and Hillebert, 1952; Birckenbach and Huttner, 1929; Cornog et al., 1938).

computations (Larsen et al., 2002; Samuni et al., 1994). Computational data compared to experimental data are listed in Tables 100 and 101.

Cyanur iodide $(ICN)_3$, was first prepared by P. Klason. It can either be obtained by a Cl^-/I^--exchange starting from cyanuric chloride or by trimerization of ICN (Scheme 143) (Klason, 1886; Smolin and Rapoport, 1959).

ICN adducts. Normally, in the ICN molecule, the nitrogen atom is a strong Lewis basic center, while the iodine can already act as a weak Lewis acid. To give one example: The reaction behavior of trimethylsilylphosphanimine, TMS–N–PPh_3, towards the pseudohalogen species X–CN (X = Cl^-, Br^- and I^-), in particular the intermediate formation of [TMS–N(PPh_3)–XCN] adduct complexes, was investigated in solution (Kempe et al., 2001). It was shown that only the ICN adduct is metastable in solution with respect to further reaction to Ph_3PNCN and TMS–X and can be trapped. Raman and X-ray data of the ICN adduct showed a very labile donor-acceptor complex in which the iodine atom of the ICN moiety is loosely bound to the nitrogen atom of TMS–$NPPh_3$. There are two different, rather long N···I bonds with bond lengths of 2.634(1) and 2.739(14) Å (Kempe et al., 2001).

Cyanogen iodide anion $[ICN]^-$

In 2012, E. M. Miller et al. described photoelectron spectroscopy experiments on the $[ICN]^-$ anion, which was previously formed in a gas matrix using an electron beam. In order to generate $[ICN]^-$ or $[ICN]^-$ Ar, CO_2 or Ar gas was passed over a solid sample of ICN. The gas was expanded into the source chamber through a heated, pulsed general valve nozzle. The gas pulse interacts with a counter-propagating 1-keV electron beam, producing anions through secondary electron attachment. The reported

Table 100: Some experimental and computational data of the cyanogen iodide (bond lengths in Å; wave numbers in cm^{-1}).

Publication	Exp./calc.	r_{I-C}	r_{C-N}	ν_{IC}	ν_{CN}
Smith et al. (1948)	Exp. – MW	1.995	1.159	–	–
Townes et al. (1948)	Exp. – MW	1.995	1.158	–	–
Freitag and Nixon (1956)	Exp. – IR	–	–	451.5	2176
Tyler and Sheridan (1963)	Exp. – MW	1.994	1.159	–	–
Hemple and Nixon (1967)	Exp. – IR	–	–	485.8	2188
Hollas and Sutherley (1971)	Exp. – PES	1.994	1.159	452	2176
Simpson et al. (1972)	Exp. – MW	1.995(1)	1.158(1)	–	–
Samuni et al. (1994)	Exp. – IR	1.992	1.160	487	2171
	HF/D95v(RECP)	1.998	1.140	530.1	2543.5
	QCISD(T)/D95v(RECP)	2.013	1.185	486.6	2178.6
	HF/(SBK)RECP	2.005	1.153	531.7	2547.5
	QCISD(T)/(SBK)RECP	2.026	1.197	480.3	2159.5
Holland et al. (2004)	MP2/6-311G**	2.003	1.178	–	–
Bhattacharyya et al. (2010)	MP2/(SDB-aug-)cc-pVTZ	1.99	1.18	516.49	2086.44
	CCSD/(SDB-aug-)cc-pVTZ	2.00	1.16	507.99	2278.54
	CCSD(T)/(SDB-aug-) cc-pVTZ	2.01	1.17	499.73	2200.32

Table 101: Some experimental and computational data of the isocyanic iodide (bond lengths in Å; wave numbers in cm^{-1}).

Publication	Exp./calc.	r_{I-N}	r_{C-N}	ν_{IN}	ν_{CN}
Samuni et al. (1994)	Exp. – IR	–	–	494	2057.5
	HF/D95v(RECP)	1.950	1.163	551.0	2364.6
	QCISD(T)/D95v(RECP)	1.991	1.203	479.2	2073.2
	HF/(SBK)RECP	1.966	1.173	550.4	2348.2
	QCISD(T)/(SBK)RECP	2.014	1.214	469.9	2026.5
Larsen et al. (2002)	Exp. – IR	2.004	1.203	459	2073
Bhattacharyya et al. (2010)	MP2/(SDB-aug-)cc-pVTZ	1.97	1.19	516.52	2040.96
	CCSD/(SDB-aug-)cc-pVTZ	1.97	1.18	516.03	2157.65
	CCSD(T)/(SDB-aug-) cc-pVTZ	1.98	1.19	500.71	2052.40

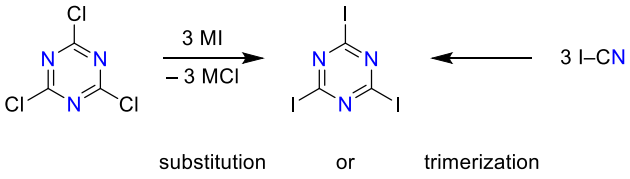

Scheme 143: Synthesis of cyanuric iodide (M = H, alkaline metal) (Klason, 1886; Smolin and Rapoport, 1959).

results are presented in Table 102 in comparison to a computational study of A. B. McCoy (McCoy, 2013; Miller et al., 2012).

Cyanogen iodide cation $[ICN]^+$

This transient cyanogen iodide cation $[ICN]^+$ was formed by collision ionization in a special apparatus and was characterized by photoelectron spectroscopy (Fulara et al., 1985; Hollas and Sutherley, 1971). The structural and spectroscopic data are given in Table 103.

Table 102: Selected experimental and computational data of the cyanogen iodide anion (bond lengths in Å; wave numbers in cm^{-1}).

Publication	Exp./calc.	r_{I-C}	r_{C-N}	ν_{IC}
Miller et al. (2012)	Exp. – PES	2.65	–	235.2
McCoy (2013)	MR-SO-CISD/ aug-cc-pVTZ(-PP)	2.65	1.16	235

Table 103: Some experimental data of $[ICN]^+$ (bond lengths in Å; wave numbers in cm^{-1}).

Publication	Exp./calc.	r_{I-C}	r_{C-N}	ν_{IC}	ν_{CN}
Hollas and Sutherley (1971)	Exp. – PES	1.934	1.180	500	2050
Fulara et al. (1985)	Exp. – PES	–	–	535	2082

Cyanoiodine cation $[ICN]^{2+}$

In 1997, R. Minkwitz and T. Hertel reported the synthesis of the cyanoiodine cation $[ICN]^{2+}$ in form of its nitrate, which is just stable at temperatures below 228 K, carrying out a reaction of cyanogen iodide and excess of chlorine nitrate at 203 K (Scheme 144). The received yellow solid was characterized using IR and Raman spectroscopy. The band at 2200–2212 cm^{-1} was assigned to the CN stretching mode and the band at 469 cm^{-1} in the IR spectrum and 473 cm^{-1} in the Raman spectrum was allocated to the IC stretching mode (Minkwitz and Hertel, 1997). Cyanoiodine(III) dinitrate is a yellow, hydrolysis-sensitive solid that decomposes above 228 K to release ICN and N_2O_5. At 203 K it can be stored undecomposed for several weeks.

Dicyanoiodate anion $[I(CN)_2]^-$

The dicyanoiodate anion $[I(CN)_2]^-$ is formed in an aqueous solution of cyanogen iodide and an excess of cyanide anions (Scheme 145). Furthermore, in 1933, D. M. Yost and W. E. Stone determined the stability of the anions in the chemical equilibrium as illustrated in Scheme 145 and estimated the equilibrium constant (Yost and Stone, 1933).

The first systematic study on salts containing the dicyanoiodate anion was carried out by B. M. Chadwick et al. Counterions of these salts were cesium, tetraphenylphosphonium and tetraphenylarsonium cations.

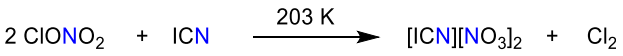

Scheme 144: Synthesis of the cyanoiodine cation by Minkwitz and Hertel (1997).

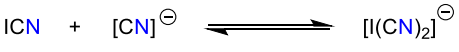

Scheme 145: Cyanogen iodide and cyanide forming the dicyanoiodate anion in equilibrium (Yost and Stone, 1933).

In case of the cesium species, the cesium chloride was added to a mixture of saturated aqueous solution of potassium cyanide and a saturated solution of cyanogen iodide in ethanol. The salts of these two bulky cations ($[Ph_4P]^+$, $[Ph_4As]^+$) were obtained using a similar route after a reaction of potassium cyanide and saturated aqueous solution of cyanogen iodide and following addition of the chloride salt dissolved in water (Scheme 146). All salts were finally characterized by IR and Raman spectroscopy (Chadwick et al., 1980).

In the 1980s, K.-F. Tebbe and co-workers published several syntheses and characterizations of different salts containing the dicyanoiodate anion. The synthesis of the pure potassium salt, based on a reaction of potassium cyanide and elemental iodine, was reported in 1988 (Scheme 147). After the addition of solid iodine to a saturated aqueous solution of potassium cyanide at ambient temperature, a colorless solid is formed and slow cooling of the solution leads to crystals suitable for single crystal XRD.

The use of cyanogen iodide instead of pure iodine also led to the formation of the dicyanoiodate anion (Scheme 148). Therefore, a saturated aqueous solution of potassium cyanide was added to a solution of cyanogen iodide using different solvents. The crystallisation started at 255 K after six weeks (Tebbe and Krauß, 1988).

The addition of rubidium bromide to this reaction mixture in a solvent mixture of water and ethanol also led to a salt of dicyanoiodate. But this salt contained two different types of cations, the potassium and rubidium cation (Scheme 149, $x = 0.6$) (Tebbe and Fröhlich, 1983a).

Due to variation of the reaction conditions they used different solvents and they observed that the use of ethanol caused the formation of an additional product, which coordinated to the expected salt forming adducts (Scheme 150).

They proposed that the formation of the (diamino) oxalic acid diethyl ether was caused by partial solvolysis of cyanogen iodide to iodine and cyanogen, which already reacted with two solvent molecules (Tebbe and Fröhlich, 1983b; Tebbe and Krauß, 1988).

The $[I(CN)_2]^-$ anion is nearly linear in the solid state as predicted by the VSEPR model. This is true for both the C–I–C unit and the two ICN units. The I–C bond can be understood as a 3-center-4-electron bond (Scheme 151). Experimental data of salts containing the $[I(CN)_2]^-$ ion are summarized in Tables 104 and 105 (Chadwick et al., 1980).

$$KCN + ICN + CsCl \xrightarrow[EtOH]{H_2O} Cs[I(CN)_2] + KCl$$

$$KCN + ICN + [Ph_4E]Cl \xrightarrow{H_2O} [Ph_4E][I(CN)_2] + KCl$$

Scheme 146: Synthesis of $[I(CN)_2]^-$ containing salts by B. M. Chadwick et al. (E = P, As) (Chadwick et al., 1980).

$$2\,KCN + I_2 \xrightarrow{H_2O} K[I(CN)_2] + KI$$

Scheme 147: Synthesis of the pure potassium salt published by Tebbe and Krauß (1988).

$$KCN + ICN \xrightarrow{H_2O} K[I(CN)_2]$$

Scheme 148: Synthesis of the potassium salt using cyanogen iodide instead of iodine (Tebbe and Krauß, 1988).

$$KCN + ICN + RbBr \xrightarrow[EtOH]{H_2O} K_xRb_{1-x}[I(CN)_2]\cdot 0.5\,(EtOCNH)_2$$

Scheme 149: Synthesis of a dicyanoiodide salt of two different cations ($(EtOCNH)_2$ = (diimino)oxalic acid diethyl ether; $x = 0.6$) (Tebbe and Fröhlich, 1983a).

(Iodocyano)iodine ions $[I_2(CN)]^-$ and $[I_2(CN)]^+$

(Iodocyano)iodide anion $[I_2(CN)]^-$

Similar to the measurement of the equilibrium constant of the dicyanoiodate anion, D. M. Yost and W. E. Stone also determined the equilibrium constant of the formation of the (iodocyano)iodide anion $[I_2(CN)]^-$ (Scheme 152), which is the only report on this anion (Yost and Stone, 1933). As discussed before for the $[I(CN)_2]^-$ ion, the $[I_2(CN)]^-$ anion should be linear and the bonding within the I–I–C moiety can also be understood as a 3-center-4-electron bond.

(Iodocyano)iodonium cation $[I_2(CN)]^+$

In contrast to BrCN and ClCN, which do not form stable salts of the type $[XCNX]^+[AsF_6]^-$ (X = Cl^- or Br^-) due to the thermodynamically favourable adduct formation $XCN{\cdot}AsF_5$ and elimination of Cl–F and Br–F, ICN does react with $[I]^+$ donors to yield compounds containing the $[ICNI]^+ = [I_2(CN)]^+$ ion as demonstrated by I. Tornieporth-Oetting and T. M. Klapötke. They investigated the reactions of triiodonium hexafluoroarsenate, $[I_3][AsF_6]$, and different cyanide containing compounds. For example, the reaction of $[I_3][AsF_6]$ and cyanogen iodide led to the formation of the (iodocyano) iodonium hexafluoroarsenate, $[I_2(CN)][AsF_6]$, which was characterized by IR and Raman spectroscopy. To obtain

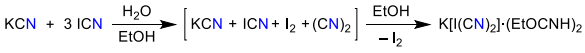

Scheme 150: Formation of (diimino)oxalic acid diethyl ether by solvolysis of cyanogen iodide in presence of ethanol (Tebbe and Fröhlich, 1983b; Tebbe and Krauß, 1988).

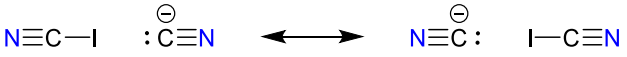

Scheme 151: 3-Center-4-electron bond in $[I(CN)_2]^-$ (Chadwick et al., 1980).

$[I_2(CN)][AsF_6]$, a suspension of $[I_3][AsF_6]$ in trichlorofluoromethane was added to cyanogen iodide dissolved in carbon disulfide at 283 K or it can be directly generated from ICN, I_2 and AsF_5 (Scheme 153).

Due to its high instability, crystals of the $[I_2(CN)][AsF_6]$ could not be obtained (Tornieporth-Oetting and Klapötke, 1990, 1991), but structural data were computed (Klapötke, 1997). The $[ICNI]^+$ cation adopts a linear structure with a I–C–N–I connectivity (Scheme 154). Selected experimental and theoretical data are summarized in Table 106. Strong hyperconjugative effects within the π-electronic system along the I–C–N–I are discussed [p-LP(I) → π*(C–N)].

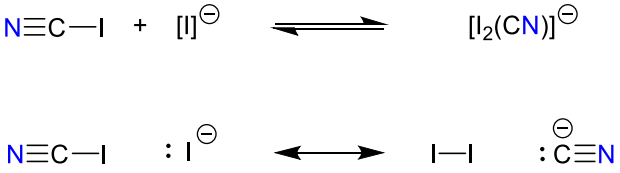

Scheme 152: Equilibrium of cyanogen iodide, iodide and the (iodocyano)iodide anion (Yost and Stone, 1933).

(Diiododicyano)iodide anion $[I_3(CN)_2]^-$

The first synthesis of the dicyanotriiodide or (diiododicyano)iodide anion, $[I(ICN)_2]^- = [I_3(CN)_2]^-$ (Figure 48), was reported by K.-F. Tebbe and co-workers. The potassium, rubidium and cesium salts were obtained by addition of two equivalents of cyanogen iodide to the potassium, rubidium or cesium iodide in aqueous solution (Scheme

Table 104: Experimental data of salts containing $[I(CN)_2]^-$ (bond lengths in Å; wave numbers in cm^{-1}).

Compound	r_{I-C} [a]	r_{C-N} [a]	$\nu^{sym.}_{IC}$ [b]	$\nu^{as.}_{IC}$ [c]	$\nu^{sym.}_{CN}$ [b]	$\nu^{as.}_{CN}$ [c]
$Cs[I(CN)_2]$ (Chadwick et al., 1980)	–	–	434	431	2118	2109
$[Ph_4P][I(CN)_2]$ (Chadwick et al., 1980)	–	–	440	–	2124	2110
$[Ph_4As][I(CN)_2]$ (Chadwick et al., 1980)	–	–	–	–	2121.5	2110
$K[I(CN)_2]$ (Tebbe and Krauß, 1988)	2.298(6)	1.129(7)	–	–	–	2115
$K[I(CN)_2]\cdot(EtOHNC)_2$ (Tebbe and Fröhlich, 1983b)	2.302(3)	1.121(5)	422	425	2126	2108
$K_{0.6}Rb_{0.4}[I(CN)_2]\cdot 0.5\ (EtOCNH)_2$ (Tebbe and Fröhlich, 1983a)	2.265(8)/ 2.351(10)	1.117(12)/ 1.096(12)	–	415– 440	–	2155/2100/ 2060/22016

[a]Bond lengths obtained by XRD. [b]Wave numbers of symmetric vibrations obtained by Raman spectroscopy. [c] Wave numbers of asymmetric vibrations obtained by IR spectroscopy.

Table 105: Crystallographic data of salts synthesized by K.-F. Tebbe et al. (bond lengths in Å; angles in °; volumes in $Å^3$).

parameter	$K[I(CN)_2]$ (Tebbe and Krauß, 1988) monoclinic	$K[I(CN)_2]\cdot(EtOHNC)_2$ (Tebbe and Fröhlich, 1983b) triclinic	$K_{0.6}Rb_{0.4}[I(CN)_2]\cdot 0.5\ (EtOCNH)_2$ (Tebbe and Fröhlich, 1983a) monoclinic
Space group	$C2/m$	$P\bar{1}$	$P2_1/c$
a	7.3637(9)	4.285(1)	4.3634(8)
b	4.5144(4)	9.259(2)	19.335(3)
c	9.0800(8)	10.350(2)	12.405(2)
α	90.00	63.41(1)	90.00
β	92.56(1)	76.33(2)	92.30(2)
γ	90.00	78.58(2)	90.00
V	301.54(5)	354.8	1046
Z	2	1	4

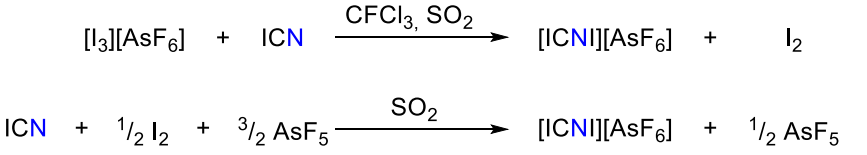

Scheme 153: Synthesis of $[I_2(CN)][AsF_6]$ (Binnewies et al., 2016; Pettersson et al., 1998; Werner et al., 1988).

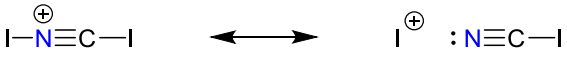

Scheme 154: Important Lewis representations of the $[ICNI]^+$ cation (Klapötke, 1997).

155) (Frölich and Tebbe, 1982; Krauß and Tebbe, 1986; Tebbe et al., 1983c).

Additionally, a salt of the $[I_3(CN)_2]^-$ anion having a potassium-2.2.2-cryptand cation ($[(Crypt)K]^+$) was synthesized adding an excess of cyanogen iodide to the KI crown ether complex dissolved in ethanol (Scheme 156) (Tebbe and Grafe-Kavoosian, 1996).

All mentioned salts were characterized using single crystal XRD and IR spectroscopy (Tables 107 and 108). Similar to the pentaiodide anion, the anions of these salts also show a V-shaped structure in solid state (Figure 48) (Tebbe and Grafe-Kavoosian, 1996). The $[I_3(CN)_2]^-$ ion is best described as $[I(ICN)_2]^-$, that is as an iodide, I^-, briding two ICN molecules.

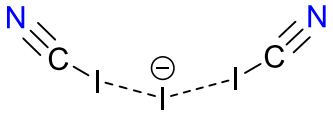

Figure 48: V-shaped structure of $[I_3(CN)_2]^-$ (Tebbe and Grafe-Kavoosian, 1996).

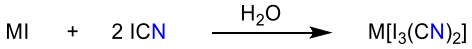

Scheme 155: Synthesis of $[I_3(CN)_2]^-$ salts by K.-F. Tebbe and coworkers (M = K^+, Rb^+, Cs^+) (Frölich and Tebbe, 1982; Krauß and Tebbe, 1986; Tebbe et al., 1983c).

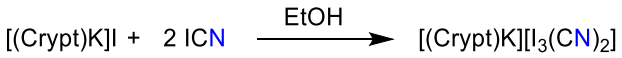

Scheme 156: Synthesis of a complex containing the $[I_3(CN)_2]^-$ anion (Tebbe and Grafe-Kavoosian, 1996).

8th Main group

Noble gas cyanides

The chemistry of the nobel gases mainly focuses on the later homologs krypton and xenon due to the increasing strength of Rg–E bonds the heavier the rare gas (Rg). Especially xenon is able to form manifold compounds with electronegative elements, several xenon fluorides for example (Binnewies et al., 2016).

As a consequence of the group electronegativity of the cyanide group, which is significantly smaller in comparison to the strongly electronegative fluorine, noble gas cyanides could not be received on common synthetic routes and could not be formed in industrial scales. Nevertheless, some working groups reported indications of the existence of short-lived nobel gas cyanide species in excited states. And additionally, several computational studies were published to maintain experimental data or predict compounds, which have not been synthesized until now (Arppe et al., 2012; Fiedler et al., 2002; Han et al., 2008a, 2008b; Jana et al., 2018; Lin and Heaven, 1991; Lin et al., 1994; Pan et al., 2015; Pettersson et al., 1998; Thoma et al., 1994; van de Burgt et al., 1984; Werner et al., 1988; Zhu et al., 2015).

For example, H.-J. Werner et al. studied excited helium cyanide radical complexes. Assuming very weak intermolecular interaction, they carried out several calculations of their structures, although there is no experimental evidence of their existence (Werner et al., 1988).

Table 106: Some experimental and computational data of the (iodocyano)iodonium cation (bond lengths in Å; wave numbers in cm^{-1}).

Publication	Exp./calc.	r_{I-C}	r_{I-N}	r_{C-N}	$\nu_{IC,\ NI}$	$\nu_{IC,\ NI}$	ν_{CN}
Tornieporth-Oetting and Klapötke (1990)	Exp. – IR	–	–	–	470	700	2330
Klapötke (1997)	Exp. – IR, Raman	–	–	–	179	590	2200
	AM1/6-31G(d) (LANL2DZ)	1.939	1.916	1.163	223	760	2494
	PM3/6-31G(d) (LANL2DZ)	1.896	1.892	1.165	287	1032	2438
	RHF/6-31G(d) (LANL2DZ)	2.023	2.030	1.132	181	615	2585
	RMP2/6-31G(d) (LANL2DZ)	1.986	0.020	1.176	179	624	2205
	RMP4(SDQ1)/6-31G(D) (LANL2DZ)	2.001	0.021	1.167	178	615	2285

Table 107: Crystallographic data of $[I_3(CN)_2]^-$ salts synthesized by K.-F. Tebbe and co-workers (lengths in Å; angles in °; volumes in Å^3; [CryptK] = [potassium-2.2.2-cryptand]).

Parameter	$K[I_3(CN)_2]$ (Krauß and Tebbe, 1986) monoclinic	$Rb[I_3(CN)_2]$ (Tebbe et al., 1983c) orthorhombic	$Cs[I_3(CN)_2]$ (Frölich and Tebbe, 1982) orthorhombic	$[CryptK][I_3(CN)_2]$ (Tebbe and Grafe-Kavoosian, 1996) triclinic
Space group	*C*2/*m*	*Pmmn*	*Pmmn*	$P\bar{1}$
a	7.364	16.246(7)	16.494(4)	11.923(2)
b	4.514	6.795(4)	6.726(1)	11.972(2)
c	9.080	4.397(2)	4.592(1)	12.781(3)
α	90.00	90.00	90.00	69.79(2)
β	92.56	90.00	90.00	72.67(2)
γ	90.00	90.00	90.00	75.79(1)
V	301.5	485.4	509.4	1613.5(8)
Z	2	2	2	2

Table 108: Experimental data of salts containing the $[I_3(CN)_2]^-$ anion (bond lengths in Å; angles in °; wave numbers in cm^{-1}).

Compound	r_{I-I}[a]	r_{I-C}[a]	r_{C-N}[a]	< (I–I–I)[a]	< (I–C–N)[a]	ν_{IC}[b]	ν_{CN}[b]
$Rb[I_3(CN)_2]$ (Tebbe et al., 1983c)	3.271(1)	2.11(2)	1.13(3)	128.69(5)	177(1)	415	2154
$Cs[I_3(CN)_2]$ (Tebbe et al., 1983c; Frölich and Tebbe, 1982)	3.306(1)	2.08(2)	1.07(2)	123.12(5)	179(2)	–	2168
$[CryptK][I_3(CN)_2]$[c] (Tebbe and Grafe-Kavoosian, 1996)	3.2025(7)	2.075(7)/2.100(5)	1.108(10)/1.070(7)	88.64(1)	178.(6)/174.5(6)	–	–

[a]Bond lengths and angles obtained by XRD. [b]Wave numbers obtained by IR spectroscopy. [c][CryptK] = [(Cryptand-2.2.2)K].

Studies on the chemistry of (cyanide) radicals in nobel gas matrices by M. Heaven led to the proof of different complexes formed by excited radicals and nobel gas atoms (Heaven, 1992). Using a special experimental setup they could obtain short-lived neon cyanide radical complexes by laser induced photochemical excitation of cyanogen iodide anions in a beam of neon and helium gas (70%: 30%) and verified their existence by LIF spectroscopy (Lin and Heaven, 1991; van de Burgt et al., 1984). They could also form argon cyanide radical cluster and exciplexes of cyanide radicals and argon atoms on a similar way using a beam of argon and helium (14%: 86%) (Lin et al., 1994; Han et al., 2008a, 2008b).

The exciplex of cyanide radicals of krypton and xenon atoms was reported by V. A. Apkarian et al. in 2002. A thin layer of a mixture of the nobel gas and deuterated hydrogen cyanide in the guest-to-host ratio of 1:1000 was deposited on magnesium difluoride at 20–30 K. The exciplex is formed by photolysis of the hydrogen cyanide leading to the cyanide radicals. The existence of this exciplex in noble gas matrix was proven by UV/vis and fluorescence spectroscopy. The visible absorption and the ground state vibrational infrared emission of the CN–Xe complex were studied in an argon matrix by A. Thoma et al. in 1994. In this early study cyanide radicals being precursor of those exciplexes were received from dicyanoacetylene in a self-igniting pulsed discharge source (Fiedler et al., 2002; Thoma et al., 1994).

Another working group carried out computations and predicted the formation of organo xenon and radon compounds (Scheme 157). The formation of xenon or radon CN compounds is an exergonic process of ΔE(Xe) = –68 kJ mol^{-1} and ΔE(Rn) = –71 kJ mol^{-1}, respectively. They also published structural parameters of $Rg(CN)_2$ (bond lengths of r_{Xe-C} = 2.192 Å and r_{Rn-C} = 2.268 Å) (Fitzsimmons and Klobukowski, 2013). Earlier computational studies on xenon complexes by C. C. Lovallo et al., dealing with the same reaction, revealed bond lengths of r_{Rg-C} = 2.202–2.246 Å. The predicted C–N bond lengths are in the range of r_{C-N} = 1.133–1.180 Å depending on the basis set (Lovallo and Klobukowski, 2002).

Besides binary noble gas cyanide species, E–Rg–CN (E = H, Au, halogens etc., Rg = rare gase), were also investigated (Arppe et al., 2012; Pan et al., 2015; Pettersson et al., 1998; Zhu et al., 2015). For example, the synthesis of

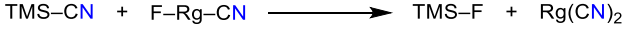

Scheme 157: Simulated reaction to synthesize nobel gas dicyanide compounds (Rg = Xe, Rn) (Fitzsimmons and Klobukowski, 2013).

the new noble gas compounds HXeCN, HXeNC and HKrCN was reported. HKrCN was the first stable compound with a Kr–C bond. These molecules were formed in solid Xe and Kr by first photolysing monomeric HCN with a 193 nm ArF laser at 7.5 K. The photolysis generates isolated hydrogen atoms and CN radicals, as detected by IR spectroscopy and laser-induced fluorescence (Pettersson et al., 1998). Another publication reports on the preparation and characterization of noble gas molecules of the type ClXeCN, ClXeNC and BrXeCN. These molecules were synthesized by 193 nm photolysis and thermal annealing of ClCN and BrCN in a xenon matrix (Arppe et al., 2012). A similar report deals with FRgCN (Rg = Kr, Xe), which were also prepared in low-temperature Kr and Xe matrices. These F–Rg–CN molecules were produced by UV photolysis of FCN in the matrices and subsequent thermal annealing. The FCN precursor is produced by depositing the $(FCN)_3$ containing matrix gas by a microwave discharge (Zhu et al., 2015).

Final remarks

More than 315 years have passed since the beginning of cyanide chemistry with the discovery of Berlin Blue in 1706. Starting from the pseudohalogen concept, according to which the cyanide ion is to be regarded as such, cyanide chemistry of the main group elements developed enormously at the end of the nineteenth and in the twentieth century. Since then, both organic cyanide chemistry, which has not been covered here, and inorganic cyanide chemistry have become important fields with industrial, biological and fundamental significance. Although cyanide compounds are mostly toxic, they have found their way into modern industrial society. Despite all this, we are still far from fully understanding the cyanide ion in its compounds. For example, the oligomerization reactions, cyclisation reactions or redox reactions are often still not fully understood, as are such unusual reactions as the isomerization of $[As(CN)_4]^-$ to an unusual cyclic cyanidoarsenate ion of the type $[AsC_4N_4]^-$.

We are confident that further experimental research also in basic research as well as improved computational methods will further highlight the unique properties of this very versatile two-atomic CN ligand.

Author contributions: All the authors have accepted responsibility for the entire content of this submitted manuscript and approved submission.
Research funding: None declared.
Conflict of interest statement: The authors declare no conflicts of interest regarding this article.

References

Abelson, P. H. Chemical events on the primitive earth. *Proc. Natl. Acad. Sci. U.S.A.* **1966**, *55*, 1365.
Adams, W. S. Some results with the COUDÉ Spectrograph of the mount Wilson Observatory. *Astrophys. J.* **1941**, *93*, 11.
Adrian, F. J.; Cochran, E. L.; Bowers, V. A.; Weatherley, B. C. ESR spectrum and structure of HCN^- in KCl at 4°K. *Phys. Rev.* **1969**, *177* (1), 129–135.
Aguirre, N. V.; Vivas, B. P.; Montes-Morán, M. A.; Ania, C. O. Adsorption of thiocyanate anions from aqueous solution onto adsorbents of various origin. *Adsorpt. Sci. Technol.* **2010**, *28* (8–9), 705–716.
Ahmed, E.; Ruck, M. Homo- and heteroatomic polycations of groups 15 and 16. Recent advances in synthesis and isolation using Room temperature ionic liquids. *Coord. Chem. Rev.* **2011**, *255* (23–24), 2892–2903.
Akcil, A. Destruction of cyanide in gold mill effluents: biological versus chemical treatments. *Biotechnol. Adv.* **2003**, *21* (6), 501–511.
Akers, C.; Peterson, S. W.; Willett, R. D. A refinement of the crystal structure of KSCN. *Acta Crystallogr. Sect. B Struct. Crystallogr. Cryst. Chem.* **1968**, *24* (8), 1125–1126.
Aksnes, O.; Foss, O.; Schultz, G.; Sörensen, N. A. The crystal structure of selenium diselenocyanate. *Acta Chem. Scand.* **1954**, *8*, 1787–1795.
Al-Azmi, A.; Elassar, A. Z. A.; Booth, B. L. The chemistry of diaminomaleonitrile and its utility in heterocyclic synthesis. *Tetrahedron* **2003**, *59* (16), 2749–2763.
Alkorta, I.; Elguero, J. Non-conventional hydrogen bonds. *Chem. Soc. Rev.* **1998**, *27* (2), 163.
Allen, T. L.; Goddard, J. D.; Schaefer, H. F. A possible role for triplet H_2CN^+ Isomers in the formation of HCN and HNC in Interstellar Clouds. *J. Chem. Phys.* **1980**, *73* (7), 3255–3263.
Allenstein, E.; Lattewitz, E. Versuche Zur Darstellung von N-Rhodanaminen. *Z. Anorg. Allg. Chem.* **1964**, *333* (1–3), 1–9.
Allman, T.; Goel, R. G.; Prasad, H. S. Organobismuth compounds. *J. Organomet. Chem.* **1979**, *166* (3), 365–371.
Altman, R. S.; Crofton, M. W.; Oka, T. High resolution infrared spectroscopy of the v_1 (NH stretch) and v_2 (CH stretch) bands of $HCNH^+$. *J. Chem. Phys.* **1984a**, *81* (10), 4255–4258.
Altman, R. S.; Crofton, M. W.; Oka, T. Observation of the infrared v_2 band (CH stretch) of protonated hydrogen cyanide $HCNH^+$. *J. Chem. Phys.* **1984b**, *80* (8), 3911–3912.
Amano, T.; Tanaka, K. Difference frequency laser spectroscopy of $HCNH^+$: observation of the isotopic species and the hot bands. *J. Mol. Spectrosc.* **1986**, *116* (1), 112–119.
Ambient Water Quality Criteria: Report from US Environmental Protection Agency (EPA), the Office of Water Regulations and Standards [Criteria and Standards Division], the Office of Research and Development [Environmental Criteria and Assessment Office], Carcinogen Assessment Group and Environmental Research Laboratories; Washington D.C., **1980**.
Anastassiou, A. G.; Simmons, H. E. Cyanonitrene. Reaction with saturated hydrocarbons. *J. Am. Chem. Soc.* **1967**, *89* (13), 3177–3184.
Andersen, P.; Klewe, B. X-ray investigation of potassium tricyanomethanide $(KC(CN)_3)$. *Nature* **1963**, *200*, 464.
Anderson, P. M. Purification and properties of the inducible enzyme cyanase. *Biochemistry* **1980**, *19* (13), 2882–2888.
Anderson, R. W.; Frick, H. R. *Synthesis of cyanuric fluoride* **1972**, 3641020.
Anderson, P. M.; Sung, Y.; Fuchs, J. A. The cyanase operon and cyanate metabolism. *FEMS Microbiol. Lett.* **1990**, *87* (3–4), 247–252.

Anderson, M. A.; Steimle, T. C.; Ziurys, L. M. The millimeter and submillimeter rotational spectrum of the MgCN radical ($X^2\Sigma^+$). *Astrophys. J.* **1994**, *429*, L41.

Andreas, H. "Cyan-industrie" – Anfänge Einer Chemischen Industrie in Deutschland Im 18. Jahrhundert. *Mitt. - Ges. Dtsch. Chem., Fachgruppe Gesch. Chem.* **2017**, *25*, 47–56.

Andrussow, L. Über die Katalytische Oxidation von Cyanwasserstoffsäure und Ammoniak (Ein Vergleich). *Ber. Dtsch. Chem. Ges.* **1926**, *59* (3), 458–461.

Andrussow, L. Über die Katalytische Oxidation von Ammoniak-Methan-Gemischen Zu Blausäure. *Angew. Chem.* **1935**, *48* (37), 593–595.

Andrussow, L. Blausäuresynthese und die Schnell Verlaufenden Katalytischen Prozesse in Strömenden Gasen. *Chem. Ing. Tech.* **1955**, *27* (8–9), 469–472.

Anex, D. S.; Davidson, E. R.; Douketis, C.; Ewing, G. E. Vibrational spectroscopy of hydrogen cyanide clusters. *J. Phys. Chem.* **1988**, *92* (10), 2913–2925.

Anseeuw, K.; Delvau, N.; Burillo-Putze, G.; De Iaco, F.; Geldner, G.; Holmström, P.; Lambert, Y.; Sabbe, M. Cyanide poisoning by fire smoke inhalation. *Eur. J. Emerg. Med.* **2013**, *20* (1), 2–9.

Apponi, A. J.; McCarthy, M. C.; Gottlieb, C. A.; Thaddeus, P. The radio spectra of SiCCH, SiCN, and SiNC. *Astrophys. J.* **2000**, *536* (1), 55–58.

Arlt, S.; Harloff, J.; Schulz, A.; Stoffers, A.; Villinger, A. Molecular $E(CN)_3$ (E = Sb, Bi) species synthesized from ionic liquids as solvates. *Chem. Eur J.* **2016a**, *22* (45), 16012–16016.

Arlt, S.; Harloff, J.; Schulz, A.; Stoffers, A.; Villinger, A. Cyanido antimonate(III) and bismuthate(III) anions. *Inorg. Chem.* **2016b**, *55* (23), 12321–12328.

Arlt, S.; Harloff, J.; Schulz, A.; Stoffers, A.; Villinger, A. Arsenic-mediated C–C coupling of cyanides leading to cyanido arsazolide $[AsC_4N_4]^-$. *Chem. Eur J.* **2017**, *23* (52), 12735–12738.

Arlt, S.; Harloff, J.; Schulz, A.; Stoffers, A.; Villinger, A. Heavy neutral and anionic pnictogen thiocyanates. *Inorg. Chem.* **2019**, *58* (8), 5305–5313.

Arlt, S.; Bläsing, K.; Harloff, J.; Laatz, K. C.; Michalik, D.; Nier, S.; Schulz, A.; Stoer, P.; Stoffers, A.; Villinger, A. Pseudohalogen chemistry in ionic liquids with non-innocent cations and Anions. *ChemistryOpen* **2021**, *10* (2), 62–71.

Armstrong, J.; Degoricija, L.; Hildebrand, A.; Koehne, J.; Fleming, P. E. The ionization energies of the isomers of CN_2. *Chem. Phys. Lett.* **2000**, *332* (5–6), 591–596.

Arnold, R. G.; Nelson, J. A.; Verbanc, J. J. Recent advances in isocyanate chemistry. *Chem. Rev.* **1957**, *57* (1), 47–76.

Arp, H. P. H.; Decken, A.; Passmore, J.; Wood, D. J. Preparation, characterization, X-ray crystal structure, and energetics of cesium 5-cyano-1,2,3,4-tetrazolate: Cs[NCCNNNN]. *Inorg. Chem.* **2000**, *39* (9), 1840–1848.

Arppe, T.; Khriachtchev, L.; Lignell, A.; Domanskaya, A. V.; Räsänen, M. Halogenated xenon cyanides ClXeCN, ClXeNC, and BrXeCN. *Inorg. Chem.* **2012**, *51* (7), 4398–4402.

Arulsamy, N.; Bohle, D. S.; Doletski, B. G. Synthesis and thermal decomposition studies of new nitroso- and nitrodicyanomethanide salts. *Inorg. Chem.* **1999**, *38* (11), 2709–2715.

Atoji, M. Neutron structure analysis of cubic CaC_2 and KCN. *J. Chem. Phys.* **1971**, *54* (8), 3514–3516.

Austad, T.; Songstad, J.; Åse, K.; Omfeldt, M.; Lagerlund, I.; Ehrenberg, L. Stable salts of the tellurocyanate ion. *Acta Chem. Scand.* **1971**, *25*, 331–333.

Aynsley, E. E.; Dodd, R. E.; Little, R. *Proc. Chem. Soc.*, London **1959**, 241–284.

Aynsley, E. E.; Greenwood, N. N.; Sprague, M. J. The oxidation of potassium selenocyanate by iodine pentafluoride. *J. Chem. Soc.* **1964**, 704–708.

Azizitorghabeh, A.; Wang, J.; Ramsay, J. A.; Ghahreman, A. A review of thiocyanate gold leaching – chemistry, thermodynamics, kinetics and processing. *Miner. Eng.* **2021**, p. 106689.

Badiello, R. Physical-chemical properties of selenium-containing inorganic radicals and their reactivity with amino acids and enzymes. *Phosphorus, Sulfur Silicon Relat. Elem.* **1992**, *67* (1–4), 7–10.

Baglin, F. G.; Coulter, G. L.; Durig, J. R. Low frequency vibrations of molecular crystals, VIII. The far infrared spectrum of polycrystalline hydrogen and deuterium cyanide. *Mol. Cryst. Liq. Cryst.* **1970**, *10* (1–2), 47–60.

Bahta, A.; Parker, G. A.; Tuck, D. G. Critical survey of stability constants of complexes of thiocyanate ion (technical report). *Pure Appl. Chem.* **1997**, *69* (7), 1489–1548.

Bak, B.; Hillebert, A. Cyanogen iodide. *Org. Synth.* **1952**, *32*, 29.

Bak, B.; Svanholt, H. The existence of gaseous cyanoform as observed by microwave spectra. *J. Mol. Struct.* **1977**, *37* (1), 153–156.

Bak, B.; Clementi, E.; Kortzeborn, R. N. Structure, vibrational spectra, dipole moment, and stability of gaseous LiCN and LiNC. *J. Chem. Phys.* **1970**, *52* (2), 764–772.

Bandy, A. R.; Friedrich, H. B.; Person, W. B. Absolute infrared intensities of the fundamental absorption bands in solid cyanogen halides. *J. Chem. Phys.* **1970**, *53* (2), 674–681.

Banerjee, G. Phenol- and thiocyanate-based wastewater treatment in RBC reactor. *J. Environ. Eng.* **1996**, *122* (10), 941–948.

Banert, K.; Chityala, M.; Hagedorn, M.; Beckers, H.; Stüker, T.; Riedel, S.; Rüffer, T.; Lang, H. Tricyanomethane and its ketenimine tautomer: generation from different precursors and analysis in solution, argon matrix, and as a single crystal. *Angew. Chem. Int. Ed.* **2017**, *56* (32), 9582–9586.

Bányai, I.; Glaser, J.; Losonczi, J. Equilibrium dynamics in the thallium(III)-cyanide system in aqueous solution. *Inorg. Chem.* **1997**, *36* (25), 5900–5908.

Bányai, I.; Glaser, J.; Tóth, I. Cyanide exchange on $Tl(CN)_4^-$ in aqueous solution studied by 205Tl and 13C NMR spectroscopy. *Eur. J. Inorg. Chem.* **2001**, *2001* (7), 1709–1717.

Barrientos, C.; Largo, A. Ionization and protonation of (MgCN): an ab initio study of some gas-phase properties of the first magnesium compound in space. *J. Mol. Struct.: Theochem.* **1995**, *336* (1), 29–37.

Barton, J. M.; Greenfield, D. C. L.; Hamerton, I.; Jones, J. R. A study of the cyclotrimerisation and polymerisation of aryl cyanates using 13C and 15N nuclear magnetic resonance spectroscopy, Fourier transform infra-red spectroscopy and differential scanning calorimetry. *Polym. Bull.* **1991**, *25* (4), 475–482.

Barton, J. M.; Chaplin, A.; Hamerton, I.; Howlin, B. J. A new synthetic route for the preparation of alkenyl functionalized aryl cyanate ester monomers. *Polymer.* **1999**, *40* (19), 5421–5427.

Basco, N.; Yee, K. K. Spectra attributed to the PCN and HPCN free radicals. *Chem. Commun. (London)* **1968a**, 152–153.

Basco, N.; Yee, K. K. Spectrum attributed to the AsCN free radical. *Chem. Commun. (London)* **1968b**, 153–154.

Baskin, S. I.; Horowitz, A. M.; Nealley, E. W. The antidotal action of sodium nitrite and sodium thiosulfate against cyanide poisoning. *J. Clin. Pharmacol.* **1992**, *32* (4), 368–375.

Bassett, H.; Corbet, A. S. Ccxvii. A phase rule study of the cupro-, argento-, auro- and thallo-cyanides of potassium. *J. Chem. Soc. Trans.* **1924**, *125* (1660), 1660–1675.

Batta, G.; Banyai, I.; Glaser, J. 2D NMR exchange spectroscopy with spy nuclei for thallium(III) cyano complexes in aqueous solution. *J. Am. Chem. Soc.* **1993**, *115* (15), 6782–6785.

Batten, S. R.; Murray, K. S. Structure and magnetism of coordination polymers containing dicyanamide and tricyanomethanide. *Coord. Chem. Rev.* **2003**, *246* (1–2), 103–130.

Bauer, M.; Gnauck, R. Thermischer und Thermisch-Oxidativer Abbau von Polycyanuraten und deren Kombinationen Mit Polyglycidethern. *Acta Polym.* **1987**, *38* (12), 658–661.

Bauer, M.; Bauer, J.; Kühn, G. Analytik von Prepolymeren und Polymeren Aromatischer Cyansäureester. 1. IR-spektroskopie. *Acta Polym.* **1986**, *37* (4), 218–220.

Bauer, J.; Höper, L.; Bauer, M. Cyclotrimerization reactivities of mono- and difunctional cyanates. *Macromol. Chem. Phys.* **1998**, *199* (11), 2417–2423.

Baum, F. Zur Darstellung von Bromcyan und Cyanamid-Derivaten. *Ber. Dtsch. Chem. Ges.* **1908**, *41* (1), 523–524.

Bauschlicher, C. W.; Partridge, H. Mg^+-ligand binding energies. *Chem. Phys. Lett.* **1991**, *181* (2–3), 129–133.

Bauschlicher, C. W.; Langhoff, S. R.; Partridge, H. Ab initio study of BeCN, MgCN, CaCN and BaCN. *Chem. Phys. Lett.* **1985**, *115* (2), 124–129.

Beach, J. Y.; Turkevich, A. The electron diffraction investigation of the molecular structures of cyanogen chloride and cyanogen bromide. *J. Am. Chem. Soc.* **1939**, *61* (2), 299–303.

Beaton, S. A.; Ito, Y.; Brown, J. M. Laser excitation spectroscopy of the $\tilde{A}^3\Pi_u$–$X^3\Sigma^-_g$ transition of the NCN radical. *J. Mol. Spectrosc.* **1996**, *178* (1), 99–107.

Beaumont, R. C.; Aspin, K. B.; Demas, T. J.; Hoggatt, J. H.; Potter, G. E. Oxidation of the tricyanomethanide ion: the tricyanocarbonium ion. *Inorg. Chim. Acta.* **1984**, *84* (2), 141–147.

Bebarta, V. S.; Pitotti, R. L.; Dixon, P.; Lairet, J. R.; Bush, A.; Tanen, D. A. Hydroxocobalamin versus sodium thiosulfate for the treatment of acute cyanide toxicity in a Swine (*Sus Scrofa*) model. *Ann. Emerg. Med.* **2012**, *59* (6), 532–539.

Bebarta, V. S.; Brittain, M.; Chan, A.; Garrett, N.; Yoon, D.; Burney, T.; Mukai, D.; Babin, M.; Pilz, R. B.; Mahon, S. B.; Brenner, M.; Boss, G. R. Sodium nitrite and sodium thiosulfate are effective against acute cyanide poisoning when administered by intramuscular injection. *Ann. Emerg. Med.* **2017**, *69* (6), 718–725.

Beelitz, J.; Kill, C.; Feldmann, C.; Wulf, H.; Vogt, N.; Veit, F.; Dersch, W. Resuscitation after smoke inhalation with cyanide intoxication: influence of hydroxycobalamin on the change of blood cyanide level during resuscitation. *Resuscitation* **2017**, *118*, e94.

Behera, S.; Jena, P. Stability and spectroscopic properties of singly and doubly charged anions. *J. Phys. Chem.* **2012**, *116* (23), 5604–5617.

Beichert, P.; Pfeiler, D.; Knözinger, E. HCN clusters in molecular beams and cryogenic matrices. *Ber. Bunsenges. Phys. Chem.* **1995**, *99* (12), 1469–1478.

Belbruno, J. J.; Tang, Z.-C.; Smith, R.; Hobday, S. The structure and energetics of carbon-nitrogen clusters. *Mol. Phys.* **2001**, *99* (11), 957–967.

Bell, D. D.; Coombe, R. D. Photodissociation of chlorine isocyanate. *J. Chem. Phys.* **1985**, *82* (3), 1317–1322.

Berger, B. Toxikologie. Eine Einführung Für Naturwissenschaftler und Mediziner. *Angew. Chem.* **1997**, *109* (3), 307.

Bergstrom, F. W. The reaction between mercuric cyanide and certain metals in liquid ammonia. *J. Am. Chem. Soc.* **1924**, *46* (7), 1559–1568.

Berkei, M.; Bernhardt, E.; Schürmann, M.; Mehring, M.; Willner, H. Darstellung, Spektroskopische Charakterisierung und Kristallstrukturen von Quecksilber(II)-Bis(Tetracyanoborat) Hg $[B(CN)_4]_2$ und Diquecksilber(I)-Bis(Tetracyanoborat) $Hg_2[B(CN)_4]_2$. *Z. Anorg. Allg. Chem.* **2002**, *628* (8), 1734.

Berlinerblau, J. Über die Einwirkung von Chlorcyan Auf Ortho- und Auf Para-Amidophenetol. *J. Prakt. Chem.* **1884**, *30* (1), 97–115.

Bernhardt, E.; Henkel, G.; Willner, H. Die Tetracyanoborate $M[B(CN)_4]$, M = $[Bu_4N]^+$, Ag^+, K^+. *Z. Anorg. Allg. Chem.* **2000**, *626* (2), 560–568.

Bernhardt, E.; Henkel, G.; Willner, H.; Pawelke, G.; Bürger, H. Synthesis and properties of the tetrakis(trifluoromethyl)borate anion, $[B(CF_3)_4]^-$: structure determination of $Cs[B(CF_3)_4]$ by single-crystal X-ray diffraction. *Chem. Eur J.* **2001**, *7* (21), 4696–4705.

Bernhardt, E.; Berkei, M.; Willner, H.; Schürmann, M. Die Reaktionen von $M[BF_4]$ (M = Li, K) Und $(C_2H_5)_2O{\cdot}BF_3$ Mit $(CH_3)_3SiCN$. Bildung von $M[BF_x(CN)_{4-x}]$ (M = Li, K; x = 1, 2) Und $(CH_3)_3SiNCBF_x(CN)_{3-x}$, (x = 0, 1). *Z. Anorg. Allg. Chem.* **2003a**, *629* (4), 677–685.

Bernhardt, E.; Finze, M.; Willner, H. Eine Effiziente synthese von Tetracyanoboraten Durch Sinterprozesse. *Z. Anorg. Allg. Chem.* **2003b**, *629* (78), 1229–1234.

Bernhardt, E.; Bernhardt-Pitchougina, V.; Willner, H.; Ignatiev, N. "Umpolung" at boron by reduction of $[B(CN)_4]^-$ and formation of the dianion $[B(CN)_3]^{2-}$. *Angew. Chem. Int. Ed.* **2011a**, *50* (50), 12085–12088.

Bernhardt, E.; Finze, M.; Willner, H. Mechanistic study on the fluorination of $K[B(CN)_4]$ with ClF enabling the high yield and large scale synthesis of $K[B(CF_3)_4]$ and $K[(CF_3)_3BCN]$. *Inorg. Chem.* **2011b**, *50* (20), 10268–10273.

Bernsdorf, A.; Köckerling, M. Chains of alkaline metal cations and tetracyanidoborato anions - syntheses, structures and properties of the new [Al(18-Crown-6)][$B(CN)_4$)] (Al = Cs, Rb). *Eur. J. Inorg. Chem.* **2009**, *2009* (29–30), 4547–4553.

Bernsdorf, A.; Köckerling, M. Crystal structure of tetraphenylphosphonium cyanate, $[P(C_6H_5)_4]OCN$. *Z. Kristallogr. - New Cryst. Struct.* **2012**, *227* (1), 85–86.

Bernsdorf, A.; Brand, H.; Hellmann, R.; Köckerling, M.; Schulz, A.; Villinger, A.; Voss, K. Synthesis, structure, and bonding of weakly coordinating anions based on CN adducts. *J. Am. Chem. Soc.* **2009a**, *131* (25), 8958–8970.

Bernsdorf, A.; Brand, H.; Hellmann, R.; Köckerling, M.; Schulz, A.; Villinger, A.; Voss, K. Synthesis, structure, and bonding of weakly coordinating anions based on CN adducts. *J. Am. Chem. Soc.* **2009b**, *131* (25), 8958–8970.

Berthollet, C.-L. Méthode de Nomenclature Chimique. *Mem. Acad. r. Sci. Paris* **1787**, 148.

Berzelius, J. J. Unterscheidung der Isomerie von Analogen Zuständen. *Ann. Phys.* **1832**, *102* (10), 320–322.

Bessler, E.; Goubeau, J. Darstellung Einiger Cyan-Borverbindungen. *Z. Anorg. Allg. Chem.* **1967**, *352* (1–2), 67–76.

Bessler, E. Darstellung und Eigenschaften von $AgB(CN)_4$ und $CuB(CN)_4$. *Z. Anorg. Allg. Chem.* **1977**, *430* (1), 38–42.

Betts, P. M.; Rinder, D. F.; Fleeker, J. R. Thiocyanate utilization by an arthrobacter. *Can. J. Microbiol.* **1979**, *25* (11), 1277–1282.

Beuermann, G.; Hausmann, A. Elektronenspinresonanz von U_2-Folgezentren in Alkalihalogenid-Kristallen. *Z. Phys.* **1967**, *204* (5), 425–442.

Beyer, H.; Walter, W. *Organische Chemie*; Hirzel Verlag: Stuttgart, **1991**.

Bezsudnova, E. Y.; Sorokin, D. Y.; Tikhonova, T. V.; Popov, V. O. Thiocyanate hydrolase, the primary enzyme initiating

thiocyanate degradation in the novel obligately chemolithoautotrophic halophilic sulfur-oxidizing bacterium thiohalophilus thiocyanoxidans. *Biochim. Biophys. Acta, Proteins Proteomics* **2007**, *1774* (12), 1563–1570.

Bhattacharyya, I.; Bera, N. C.; Das, A. K. Theoretical study of structural properties and dissociation pathways of FCN and ClCN. *Eur. Phys. J. D* **2007a**, *42* (2), 221–226.

Bhattacharyya, I.; Bera, N. C.; Das, A. K. Theoretical study of XCN^- (X=F,Cl) anions. *Int. J. Quantum Chem.* **2007b**, *107* (3), 680–684.

Bhattacharyya, I.; Mondal, B.; Bera, N. C.; Das, A. K. Structure and dissociation of cyanogen halides BrCN and ICN. *Int. J. Quantum Chem.* **2010**, *110*, 1165–1171.

Bhunia, F.; Saha, N. C.; Kaviraj, A. Toxicity of Thiocyanate to fish, Plankton, Worm and Aquatic Ecosystem. *Bull. Environ. Contam. Toxicol.* **2000**, *64* (2), 197–204.

Bijvoet, J. M.; Lely, J. A. Eine Rhombische Modifikation des Kaliumcyanids. Über die lage des Umwandlungspunkts des Natriumcyanids in Abhängigkeit von Beimischungen. *Recl. Trav. Chim. Pays-Bas* **2010**, *59* (9), 908–912.

Biltz, W. Raumchemie der Festen Stoffe. *Ber. Dtsch. Chem. Ges.* **1935**, *68* (7), A91–A108.

Binder, J. F.; Kosnik, S. C.; St Onge, P. B. J.; Macdonald, C. L. B. Synthesis of heavy dicyanamide homologues from air-stable precursors. *Chem. Eur J.* **2018**, *24* (55), 14644–14648.

Binnewies, M.; Finze, M.; Jäckel, M.; Schmidt, P.; Willner, H.; Rayner-Canham, G. *Allgemeine Und Anorganische Chemie*; Springer Berlin Heidelberg: Berlin, Heidelberg, Vol. 58; **2016**.

Binsch, G.; Roberts, J. D. Nitrogen-15 magnetic resonance spectroscopy. Coupling constants in hydrogen cyanide. *J. Phys. Chem.* **1968**, *72* (12), 4310–4311.

Birckenbach, L.; Huttner, K. Über Pseudohalogene, III.: Über Das Pseudohalogen Tricyanmethyl Und Das Mischhalogen Brom-Tricyanmethyl. *Ber. Dtsch. Chem. Ges.* **1929**, *62* (1), 153–163.

Birckenbach, L.; Kellermann, K. Über Pseudohalogene (I). *Ber. Dtsch. Chem. Ges.* **1925a**, *58* (4), 786–794.

Birckenbach, L.; Kellermann, K. Über Pseudohalogene (II.): 1. Der Knallsäure-Rest. 2. Das Gleichgewicht Zwischen Jod, Selenocyan und den Entsprechenden Silbersalzen. 3. Polypseudohalogenide. *Ber. Dtsch. Chem. Ges.* **1925b**, *58* (10), 2377–2386.

Birckenbach, L.; Kellermann, K. Verein Deutscher Chemiker. *Angew. Chem.* **1930**, *43* (31), 700–702.

Birckenbach, L.; Kolb, H. Über Reaktionen und die Tautomerie von Cyanaten (XXIII. Mitteil. Zur Kenntnis der Pseudohalogene). *Ber. Dtsch. Chem. Ges.* **1933**, *66* (10), 1571–1577.

Birckenbach, L.; Linhard, M. Über Pseudohalogene, V.: Über Das Mischhalogen Brom-Oxycyan. *Ber. Dtsch. Chem. Ges.* **1929**, *62* (8), 2261–2277.

Birckenbach, L.; Linhard, M. Über Pseudohalogene, X.: Über Dichlor-Dioxycyan, N^{ω}-Mono- und N^{ω}-Dichlor-Allophansäure-Äthylester und N^{ω}-Chlor-Allophansäure-Chlorid. *Ber. Dtsch. Chem. Ges.* **1930**, *63* (9), 2528–2544.

Birckenbach, L.; Huttner, K.; Stein, W. Über Pseudohalogene, IV.: Die Hydrolysen-Konstanten Des Brom-Tricyanmethyls Und Des Chlor-, Brom- Und Jod-Trinitromethyls. *Ber. Dtsch. Chem. Ges.* **1929a**, *62* (8), 2065–2075.

Birckenbach, L.; Huttner, K.; Stein, W. Über Pseudohalogene, IV.: Die Hydrolysen-Konstanten des Brom-Tricyanmethyls und des Chlor-, Brom- und Jod-Trinitromethyls. *Ber. Dtsch. Chem. Ges.* **1929b**, *62* (8), 2065–2075.

Bither, T. A.; Knoth, W. H.; Lindsey, R. V.; Sharkey, W. H. Trialkyl- and Triaryl(Iso)Cyanosilanes. *J. Am. Chem. Soc.* **1958**, *80* (16), 4151–4153.

Black, J. H.; van Dishoeck, E. F. Electron densities and the excitation of CN in molecular clouds. *Astrophys. J.* **1991**, *369*, 9.

Blanksby, S. J.; Dua, S.; Bowie, J. H.; Schröder, D.; Schwarz, H. Syntheses of NCN and NC_3N from ionic precursors in the gas phase and an unusual rearrangement of neutral NC_3N: a joint experimental and theoretical study. *J. Phys. Chem.* **2000**, *104* (47), 11248–11256.

Bläsing, K.; Ellinger, S.; Harloff, J.; Schulz, A.; Sievert, K.; Täschler, C.; Villinger, A.; Zur Täschler, C. Lewis acid catalyzed synthesis of cyanidoborates. *Eur. J. Inorg. Chem.* **2016a**, *2016* (8), 1175–1183.

Bläsing, K.; Ellinger, S.; Harloff, J.; Schulz, A.; Sievert, K.; Täschler, C.; Villinger, A.; Zur Täschler, C. Lewis acid catalyzed synthesis of cyanidophosphates. *Chem. Eur J.* **2016b**, *22* (12), 4175–4188.

Bläsing, K.; Bresien, J.; Labbow, R.; Schulz, A.; Villinger, A. A dimer of hydrogen cyanide stabilized by a Lewis acid. *Angew. Chem. Int. Ed.* **2018**, *57* (29), 9170–9175.

Bläsing, K.; Harloff, J.; Schulz, A.; Stoffers, A.; Stoer, P.; Villinger, A. Salts of HCN-cyanide aggregates: $[CN(HCN)_2]^-$ and $[CN(HCN)_3]^-$. *Angew. Chem. Int. Ed.* **2020**, *59* (26), 10508–10513.

Blixt, J.; Gyori, B.; Glaser, J. Determination of stability constants for thallium(III) cyanide complexes in aqueous solution by means of carbon-13 and thallium-205 NMR. *J. Am. Chem. Soc.* **1989**, *111* (20), 7784–7791.

Blixt, J.; Glaser, J.; Mink, J.; Persson, I.; Persson, P.; Sandstroem, M. Structure of thallium(III) chloride, bromide, and cyanide complexes in aqueous solution. *J. Am. Chem. Soc.* **1995**, *117* (18), 5089–5104.

Boatright, L. G. Preparation of ammonium cyanate from urea. US2712491, **1954**.

Böhland, H.; Golub, A. M.; Köhler, H.; Lisko, T. P.; Samoilenko, V. M.; Skopenko, V. V.; Cincadze, G. V. *Chemie Der Pseudohalogenide*; DVW: Berlin, **1978**.

Booth, M. R.; Frankiss, S. G. Trimethylsilyl isocyanide. *Chem. Commun. (London)* **1968**, 1347–1348.

Borron, S. W.; Baud, F. J.; Barriot, P.; Imbert, M.; Bismuth, C. Prospective study of hydroxocobalamin for acute cyanide poisoning in smoke inhalation. *Ann. Emerg. Med.* **2007**, *49* (6), 794–801.

Bouchet, L. M.; Peñéñory, A. B.; Argüello, J. E. Synthesis of arylselenide ethers by photoinduced reactions of selenobenzamide, selenourea and selenocyanate anions with aryl halides. *Tetrahedron Lett.* **2011**, *52* (9), 969–972.

Bourson, P.; Ndtoungou, A.; Bouillot, J.; Soubeyroux, J. L.; Durand, D. Phase transition of RbCN. *Phys. B (Amsterdam, Neth.)* **1992**, *180–181*, 351–353.

Bozorth, R. M. The crystal sructure of potassium cyanide. *J. Am. Chem. Soc.* **1922**, *44* (2), 317–323.

Bradforth, S. E.; Kim, E. H.; Arnold, D. W.; Neumark, D. M. Photoelectron spectroscopy of CN–, NCO–, and NCS–. *J. Chem. Phys.* **1993**, *98* (2), 800–810.

Brand, H.; Mayer, P.; Schulz, A.; Weigand, J. J. Nitro(Nitroso) Cyanmethanide. *Angew. Chem.* **2005a**, *117* (25), 3998–4001.

Brand, H.; Mayer, P.; Schulz, A.; Weigand, J. J. Nitro(Nitroso) Cyanomethanides. *Angew. Chem. Int. Ed.* **2005b**, *44* (25), 3929–3932.

Brand, H.; Liebman, J. F.; Schulz, A.; Mayer, P.; Villinger, A. Nonlinear, resonance-stabilized pseudohalides: from alkali methanides to

ionic liquids of methanides. *Eur. J. Inorg. Chem.* **2006**, *2006* (21), 4294–4308.

Brand, H.; Schulz, A.; Villinger, A. Modern aspects of pseudohalogen chemistry: news from CN- and PN-chemistry. *Z. Anorg. Allg. Chem.* **2007**, *633* (1), 22–35.

Brand, H.; Liebman, J. F.; Schulz, A. Cyano-, nitro- and nitrosomethane derivatives: structures and gas-phase acidities. *Eur. J. Org Chem.* **2008**, *2008* (27), 4665–4675.

Brand, H.; Martens, J.; Mayer, P.; Schulz, A.; Seibald, M.; Soller, T. Salts and ionic liquids of resonance stabilized amides. *Chem. Asian J.* **2009**, *4* (10), 1588–1603.

Brazier, C. R.; O'Brien, L. C.; Bernath, P. F. Fourier transform detection of laser-induced fluorescence from the CCN free radical. *J. Chem. Phys.* **1987**, *86* (6), 3078–3081.

Bresien, J.; Ellinger, S.; Harloff, J.; Schulz, A.; Sievert, K.; Stoffers, A.; Täschler, C.; Villinger, A.; Zur Täschler, C. Tetracyanido(difluorido)phosphates $M^+[PF_2(CN)_4]^-$. *Angew. Chem. Int. Ed.* **2015a**, *54* (15), 4474–4477.

Bresien, J.; Ellinger, S.; Harloff, J.; Schulz, A.; Sievert, K.; Stoffers, A.; Täschler, C.; Villinger, A.; Zur Täschler, C. Tetracyanido(difluorido)phosphate $M^+[PF_2(CN)_4]^-$. *Angew. Chem.* **2015b**, *127* (15), 4556–4559.

Britton, D.; Dunitz, J. D. The crystal structure of silver cyanate. *Acta Crystallogr.* **1965a**, *18* (3), 424–428.

Britton, D.; Dunitz, J. D. The crystal structure of silver fulminate. *Acta Crystallogr.* **1965b**, *19* (4), 662–668.

Britton, D. The crystal structure of tetracyanomethane, $C(CN)_4$. *Acta Crystallogr. Sect. B Struct. Crystallogr. Cryst. Chem.* **1974**, *30* (7), 1818–1821.

Brooker, M. H.; Wen, N. Raman studies of cyanate: fermi resonance, hydration and hydrolysis to urea. *Can. J. Chem.* **1993**, *71* (10), 1764–1773.

Brotherton, T. K.; Lynn, J. W. The synthesis and chemistry of cyanogen. *Chem. Rev.* **1959**, *59* (5), 841–883.

Brousseau, L. C.; Williams, D.; Kouvetakis, J.; O'Keeffe, M. Synthetic routes to $Ga(CN)_3$ and $MGa(CN)_4$ (M = Li, Cu) framework structures. *J. Am. Chem. Soc.* **1997**, *119* (27), 6292–6296.

Brown, R. D.; Godfrey, P. D.; Winkler, D. A. The microwave spectrum of HCN dimer. *J. Mol. Spectrosc.* **1981**, *89* (2), 352–355.

Brupbacher, T.; Bohn, R. K.; Jäger, W.; Gerry, M. C. L.; Pasinszki, T.; Westwood, N. P. C. Microwave spectrum and geometry of cyanogen N-oxide, NCCNO. *J. Mol. Spectrosc.* **1997**, *181* (2), 316–322.

Buchholz, C. F. Bemerkungen, Gemacht Bei Gelegenheit Einiger Versuche Über die Reinigung der Blausauren Salze Vom Eisen. In *Beiträge zur Erweiterung und Berichtigung der Chemie*; Erfurt, **1799**; pp. 81–92.

Buljan, A.; Alemany, P.; Ruiz, E. Electronic structure and dynamic properties of solid alkali cyanides. *J. Phys. Chem.* **1997**, *101* (7), 1393–1399.

Bundhun, A.; Abdallah, H. H.; Ramasami, P.; Gaspar, P. P.; Schaefer, H. F. Dicyanogermylenes: a tale of isomers and interconversions. *Inorg. Chem.* **2012**, *51* (22), 12152–12164.

Burchell, C. J.; Aucott, S. M.; Robertson, S. D.; Slawin, A. M. Z.; Woollins, J. D. The chemistry of $(ECN)_2$ (E = S, Se) and related compounds. *Phosphorus, Sulfur Silicon Relat. Elem.* **2004**, *179* (4–5), 865–868.

Burchell, C. J.; Kilian, P.; Slawin, A. M. Z.; Woollins, J. D.; Tersago, K.; Van Alsenoy, C.; Blockhuys, F. $E_2(CN)_2$ (E = S, Se) and related compounds. *Inorg. Chem.* **2006**, *45* (2), 710–716.

Burger, A.; Hornbaker, E. D. Some reactions in the 1,3,5-triazine series. *J. Am. Chem. Soc.* **1953**, *75* (18), 4579–4580.

Burkholder, J. B.; Sinha, A.; Hammer, P. D.; Howard, C. J. High-resolution Fourier transform infrared spectroscopy of the fundamental bands of HNC. *J. Mol. Spectrosc.* **1987**, *126* (1), 72–77.

Burns, W. A.; Leopold, K. R. Unusually large gas–solid structure differences: a crystallographic study of HCN–BF3 [hydrogen cyanide-boron trifluoride]. *J. Am. Chem. Soc.* **1993**, *115* (24), 11622–11623.

Buser, H. J.; Schwarzenbach, D.; Petter, W.; Ludi, A. The crystal structure of prussian blue: $Fe_4[Fe(CN)_6]_3\ xH_2O$. *Inorg. Chem.* **1977**, *16* (11), 2704–2710.

Buxton, L. W.; Campbell, E. J.; Flygare, W. H. The vibrational ground state rotational spectroscopic constants and structure of the HCN dimer. *Chem. Phys.* **1981**, *56* (3), 399–406.

Camargo, S. S.; von der Weid, J. P. Optical absorption of triplet molecular excitons in alkali cyanides. *Solid State Commun.* **1982**, *44* (8), 1227–1229.

Campbell, R.; Davis, M. F.; Fazakerley, M.; Portius, P. Taming Tin(IV) polyazides. *Chem. Eur J.* **2015**, *21* (51), 18690–18698.

Cant, N. W.; Chambers, D. C.; Liu, I. O. Y. The reduction of NO by CO in the presence of water vapour on supported platinum catalysts: formation of isocyanic acid (HNCO) and ammonia. *Appl. Catal. B* **2003**, *46* (3), 551–559.

Cant, N. W.; Chambers, D. C.; Liu, I. O. Y. The formation of isocyanic acid and ammonia during the reduction of NO over supported platinum group metals. *Catal. Today* **2004**, *93–95*, 761–768.

Cant, N. W.; Chambers, D. C.; Liu, I. O. Y. The amplification of ammonia by reaction with NO and CO over dual function platinum and palladium catalyst systems with isocyanic acid as an intermediate. *Appl. Catal. B* **2005a**, *60* (1–2), 57–63.

Cant, N. W.; Chambers, D. C.; Liu, I. O. Y. The formation of isocyanic acid during the reaction of NH_3 with NO and excess CO over silica-supported platinum, palladium, and rhodium. *J. Catal.* **2005b**, *231* (1), 201–212.

Carrasco, N.; Schmitz-Afonso, I.; Bonnet, J.-Y.; Quirico, E.; Thissen, R.; Dutuit, O.; Bagag, A.; Laprévote, O.; Buch, A.; Giulani, A.; Adandé, G.; Ouni, E.; Hadamcik, E.; Szopa, C.; Cernogora, G. Chemical characterization of Titan's tholins: solubility, morphology and molecular structure revisited. *J. Phys. Chem.* **2009**, *113* (42), 11195–11203.

Castanheiro, T.; Suffert, J.; Donnard, M.; Gulea, M. Recent advances in the chemistry of organic thiocyanates. *Chem. Soc. Rev.* **2016**, pp. 494–505.

Cenedella, M. Cyanure de Phosphore. *J. Pharm. (Lahore)* **1835**, *11*, 683.

Cerny, D.; Bacis, R.; Guelachvili, G.; Roux, F. Extensive analysis of the red system of the CN molecule with a high resolution Fourier spectrometer. *J. Mol. Spectrosc.* **1978**, *73* (1), 154–167.

Chacko, S. A.; Krouse, I. H.; Hammad, L. A.; Wenthold, P. G. In situ generation of HCN for mass spectrometric studies. *J. Am. Soc. Mass Spectrom.* **2006**, *17* (1), 51–55.

Chadwick, B. M.; Long, D. A.; Qureshi, S. U. The Raman and infrared spectra of the dicyanoiodate (I) ion. *J. Raman Spectrosc.* **1980**, *9* (1), 1–4.

Challenger, F.; Peters, A. T.; Halévy, J. CCXV.–The introduction of the selenocyano-group into aromatic compounds. *J. Chem. Soc.* **1926**, *129*, 1648–1655.

Chambers, R. D.; Tamura, M. Fluorinated 1,2,3-triazines. *J. Fluor. Chem.* **1985**, *29* (1–2), 127.

Chambers, D. C.; Angove, D. E.; Cant, N. W. The formation and hydrolysis of isocyanic acid during the reaction of NO, CO, and H_2 mixtures on supported platinum, palladium, and rhodium. *J. Catal.* **2001**, *204* (1), 11–22.

Chan, W.-T.; Hamilton, I. P. Geometries and vibrational frequencies for calcium and strontium radical salts of H, F, Cl, Br, I, OH, SH, CN, NC, CCH, NNN, NCO, NCS, NH_2, CH_3, OCH_3, SCH_3, HCOO, CH_3COO, HCONH and $HCONCH_3$. *Chem. Phys. Lett.* **1998**, *297* (3–4), 217–224.

Chandler, J. D.; Day, B. J. Biochemical mechanisms and therapeutic potential of pseudohalide thiocyanate in human health. *Free Radical Res.* **2015**, *49* (6), 695–710.

Chase, M. W.; Curnutt, J. L.; Hu, A. T.; Prophet, H.; Syverud, A. N.; Walker, L. C. JANAF thermochemical tables, 1974 supplement. *J. Phys. Chem. Ref. Data* **1974**, *3* (2), 311–480.

Chau, F. T.; McDowell, C. A.; Tang, Y. W. Determination of geometries and molecular properties of XCN^+ ions (where X is Cl, Br, I) through Franck–Condon analyses on the corresponding photoelectron spectra. *J. Electron Spectrosc.* **1993**, *61* (2), 217–229.

Chadwick, B. M.; Edwards, H. G. M. Vibrational and vibrational-rotational spectroscopy of the cyanide ion, the cyano-radical, the cyanogen molecules, and the triatomic cyanides XCN (X=H, F, Cl, Br, and I). In *Molecular spectroscopy*; Barrow, R. F., Long, D. A., Millen, D. J., Eds.; The Chemical Society: London, **1973**; pp. 516–522.

Chaudhuri, R. K.; Krishnamachari, S. L. N. G. Theoretical Study on the ground and excited states of dicyanocarbene (c_3n_2) and its isomers: a low-temperature matrix emission spectrum attributable to 3-cyano-2h-azirenylidene. *J. Phys. Chem.* **2007**, *111* (22), 4849–4854.

Chavant, C.; Constant, G.; Jeannin, Y.; Morancho, R. Structure Cristalline Du Pentachloroformonitrileniobium(V). *Acta Crystallogr. Sect. B Struct. Crystallogr. Cryst. Chem.* **1975**, *31* (7), 1823–1827.

Chen, Y.; Bai, X. A review on quantum dots modified g-C_3N_4-based photocatalysts with improved photocatalytic activity. *Catalysts* **2020**, *10* (1), 142.

Chen, H.-L.; Zhu, R.; Chen, H.-T.; Li, H.-J.; Ju, S.-P. Ab initio study on mechanisms and kinetics for reaction of NCS with NO. *J. Phys. Chem.* **2008**, *112* (24), 5495–5501.

Chevrier, P. J.; Brownstein, S. Complex fluoroanions in solution – X: complexes of phosphorus and arsenic fluorides with simple anions. *J. Inorg. Nucl. Chem.* **1980**, *42* (10), 1397–1405.

Chizmeshya, A. V. G.; Ritter, C. J.; Groy, T. L.; Tice, J. B.; Kouvetakis, J. Synthesis of molecular adducts of beryllium, boron, and gallium cyanides: theoretical and experimental correlations between solid-state and molecular analogues. *Chem. Mater.* **2007**, *19* (24), 5890–5901.

Chow, Y. M.; Britton, D. Silver dicyanonitrosomethanide, $AgC(CN)_2NO$. *Acta Crystallogr. Sect. B Struct. Crystallogr. Cryst. Chem.* **1974**, *30* (4), 1117–1118.

Christie, A. *Sparkling Cyanide*; Dodd Mead and Company: New York, **1945**.

Cioslowski, J.; Mixon, S. T.; Fleischmann, E. D. Electronic structures of trifluoro-, tricyano-, and trinitromethane and their conjugate bases. *J. Am. Chem. Soc.* **1991**, *113* (13), 4751–4755.

Clementi, E.; Kistenmacher, H.; Popkie, H. Study of the electronic structure of molecules. XVIII. Interaction between a lithium atom and a cyano group as an example of a polytopic bond. *J. Chem. Phys.* **1973**, *58* (6), 2460–2466.

Clifford, E. P.; Wenthold, P. G.; Lineberger, W. C.; Petersson, G. A.; Ellison, G. B. Photoelectron spectroscopy of the NCN^- and $HNCN^-$ ions. *J. Phys. Chem.* **1997**, *101* (24), 4338–4345.

Coates, G. E.; Mukherjee, R. N. Dimethylaluminium cyanide and its gallium, indium, and thallium analogues; beryllium and methylberyllium cyanide. *J. Chem. Soc.* **1963**, *35*, 229–233.

Cochran, E. L.; Adrian, F. J.; Bowers, V. A. ESR detection of the cyanogen and methylene imino free radicals. *J. Chem. Phys.* **1962**, *36* (7), 1938–1942.

Cocksedge, H. E. CCXVII.–Tellurium dicyanide. *J. Chem. Soc. Trans.* **1908**, *93*, 2175–2177.

Coleman, G. H.; Leeper, R. W.; Schulze, C. C.; Scortt, L. D.; Fernelius, W. C. Cyanogen chloride. In *Inorganic synthesis*; McGraw-Hill Book Company, 2, **2007**; pp. 90–94.

Coll, P.; Coscia, D.; Gazeau, M. C.; Guez, L.; Raulin, F. Review and latest results of laboratory investigations of Titan's aerosols. *Origins Life Evol. Biospheres* **1998**, *28* (2), 195–213.

Conrad, M. P.; Schaefer, H. F. Role of different isomers of the H_2CN^+ ion in the formation of interstellar HCN and HNC. *Nature* **1978**, *274* (5670), 456–457.

Coogan, C. K.; Gutowsky, H. S. NMR studies of phase transitions. II. NaCN. *J. Chem. Phys.* **1964**, *40* (11), 3419–3425.

Cook, T. J.; Levy, D. H. Optically detected gas phase magnetic resonance spectrum of the CN radical. *J. Chem. Phys.* **1973**, *58* (9), 3547–3557.

Cook, R. P.; Robinson, P. L. Certain physical properties of cyanogen and its halides. *J. Chem. Soc.* **1935**, 1001–1005.

Corain, B. The coordination chemistry of hydrogen cyanide, cyanogen and cyanogen halides. *Coord. Chem. Rev.* **1982**, *47* (1–2), 165–200.

Cornog, J.; Horrabin, H. W.; Karges, R. A. Iodine monochloride. II. Reactions with salts. *J. Am. Chem. Soc.* **1938**, *60* (2), 429–432.

Cortés, E.; Erben, M. F.; Geronés, M.; Romano, R. M.; Della Védova, C. O. Dissociative photoionization of methyl thiocyanate, CH_3SCN, in the proximity of the sulfur 2p edge. *J. Phys. Chem.* **2009**, *113* (3), 564–572.

Coskran, K. J.; Jones, C. E. Synthesis and spectroscopic properties of some cyanophosphines. *Inorg. Chem.* **1971**, *10* (7), 1536–1537.

Cosslett, V. E. Darstellung und Eigenschaften von Fluorcyan. *Z. Anorg. Allg. Chem.* **1931**, *201* (1), 75–80.

Costain, C. C. Determination of molecular structures from ground state rotational constants. *J. Chem. Phys.* **1958**, *29* (4), 864–874.

Cotton, F. A.; Wilkinson, G.; Fritz, H. P. *Anorganische Chemie*, XIII; DVW: Berlin, **1967**.

Cozzolino, A. F.; Silvia, J. S.; Lopez, N.; Cummins, C. C. Experimental and computational studies on the formation of cyanate from early metal terminal nitrido ligands and carbon monoxide. *Dalton Trans.* **2014**, *43* (12), 4639–4652.

Cravens, T. E.; Robertson, I. P.; Waite, J. H.; Yelle, R. V.; Kasprzak, W. T.; Keller, C. N.; Ledvina, S. A.; Niemann, H. B.; Luhmann, J. G.; McNutt, R. L.; Ip, W.-H.; De La Haye, V.; Mueller-Wodarg, I.; Wahlung, J.-E.; Anicich, V. G.; Vuitton, V. Composition of Titan's ionosphere. *Geophys. Res. Lett.* **2006**, *33* (7), L07105.

Cummins, P. L.; Bacskay, G. B.; Hush, N. S.; Jönsson, B. On the structure, lattice energy and 14N nuclear quadrupole coupling constant of solid HCN. *Chem. Phys. Lett.* **1988**, *145* (5), 399–406.

Cyvin, S. J.; Ratkje, S. K.; Devarajan, V.; Nayar, V. U.; Aruldhas, G. Spectroscopic calculations on phosphorus and arsenic tricyanides: harmonic force fields, mean amplitudes of vibration and vibrational assignments. *J. Mol. Struct.* **1973**, *17* (2), 371–375.

Dagg, I. R.; Anderson, A.; Yan, S.; Smith, W.; Joslin, C. G.; Read, L. A. A. The Quadrupole moment of cyanogen: a comparative study of collision-induced absorption in gaseous C_2N_2, CO_2, and mixtures with argon. *Can. J. Phys.* **1986**, *64* (11), 1475–1481.

Dalla Betta, R. A.; Shelef, M. Isocyanates from the reaction of NO and CO on supported noble-metal catalysts. *J. Mol. Catal.* **1976**, *1* (6), 431–434.

Dammeier, J.; Friedrichs, G. Thermal decomposition of NCN_3 as a high-temperature NCN radical source: singlet–triplet relaxation and absorption cross section of NCN($^3\Sigma$). *J. Phys. Chem.* **2010**, *114* (50), 12963–12971.

Dao, N. Q.; Wilkinson, G. R. Far-infrared and Raman spectra of the crystal KNCS. *J. Chem. Phys.* **1973**, *59* (3), 1319–1324.

Darkwah, W. K.; Ao, Y. Mini review on the structure and properties (photocatalysis), and preparation techniques of graphitic carbon nitride nano-based particle, and its applications. *Nanoscale Res. Lett.* **2018**, *13* (1), 388.

Dash, R. R.; Gaur, A.; Balomajumder, C. Cyanide in industrial wastewaters and its removal: a review on biotreatment. *J. Hazard Mater.* **2009**, *163* (1), 1–11.

Daubert, J.; Knorr, K.; Dultz, W.; Jex, H.; Currat, R. Lattice dynamics of KCN. *J. Phys. C Solid State Phys.* **1976**, *9* (15), L389–L391.

Davies, R. H.; Finch, A.; Gardner, P. J.; Hameed, A.; Stephens, M. The standard enthalpies of hydrolysis and formation of tricyanophosphine. *J. Chem. Soc., Dalton Trans.* **1976**, *6*, 556–558.

Davydova, E. I.; Sevastianova, T. N.; Suvorov, A. V.; Timoshkin, A. Y. Molecular complexes formed by halides of group 4, 5, 13 – 15 elements and the thermodynamic characteristics of their vaporization and dissociation found by the static tensimetric method. *Coord. Chem. Rev.* **2010**, *254* (17–18), 2031–2077.

Decius, J. C.; Jacobson, J. L.; Sherman, W. F.; Wilkinson, G. R. Cyanate ion in alkali halides: new vibrational levels and interpretation of localized lattice modes. *J. Chem. Phys.* **1965**, *43* (7), 2180–2186.

Decker, D. L.; Beyerlein, R. A.; Roult, G.; Worlton, T. G. Neutron diffraction study of KCN III and KCN IV at high pressure. *Phys. Rev. B* **1974**, *10* (8), 3584–3593.

Deflon, V. M.; Lopes, C. C. de S.; Bessler, K. E.; Romualdo, L. L.; Niquet, E. Preparation, characterization and crystal structure of lead(II) tricyanomethanide. *Z. Naturforsch., B: J. Chem. Sci.* **2006**, *61* (1), 33–36.

DeFrees, D. J.; McLean, A. D. Molecular orbital predictions of the vibrational frequencies of some molecular ions. *J. Chem. Phys.* **1985**, *82* (1), 333–341.

Degli Esposti, C.; Favero, P. G.; Serenellini, S.; Cazzoli, G. Rotational spectra of excited vibrational states of $F_{12}C_{15}N$. Equilibrium structure of cyanogen fluoride. *J. Mol. Struct.* **1982**, *82* (3–4), 221–236.

Delbrück, H. Über Das cyan und Paracyan. *J. Prakt. Chem.* **1847**, *41* (1), 161–180.

Delgado, M. S.; Fernandez, V. Die Komplexe von Dioxocyan $(OCN)_2$ Mit $TiCl_4$ und $ZrCl_4$. *Z. Anorg. Allg. Chem.* **1981**, *476* (5), 149–152.

DeLong, M. C.; Rosenberger, F. High purity cyanides: a dying technology revived. *J. Cryst. Growth* **1986**, *75* (1), 164–172.

Deokar, P.; Leitz, D.; Stein, T. H.; Vasiliu, M.; Dixon, D. A.; Christe, K. O.; Haiges, R. Preparation and characterization of antimony and arsenic tricyanide and their 2,2′-bipyridine adducts. *Chem. Eur J.* **2016**, *22* (37), 13251–13257.

Derry, T. K.; Williams, T. I. *A short history of technology: from the earliest times to A.D. 1900*; Dover Publications: New York, **1993**.

Desiderato, R.; Sass, R. L. The crystal structure of ammonium tricyanomethide, $NH_4C(CN)_3$. *Acta Crystallogr.* **1965**, *18* (1), 1–4.

Destro, R.; Merati, F.; Ortoleva, E. An ab initio study of the N–Cl bond. *Chem. Phys. Lett.* **1988**, *145* (3), 193–199.

Dibeler, V. H.; Liston, S. K. Mass-spectrometric study of photoionization. IX. Hydrogen cyanide and acetonitrile. *J. Chem. Phys.* **1968**, *48* (10), 4765–4768.

Diels, O. Zur Kenntnis der Cyanurverbindungen. *Ber. Dtsch. Chem. Ges.* **1899**, *32* (1), 691–702.

Dillard, J. G.; Franklin, J. L. Reactions of negative ions in the gas phase. II. NH_2^-. *J. Chem. Phys.* **1968**, *48* (5), 2353–2358.

Dillon, K. B.; Marshall, A. Tin-119 nuclear magnetic resonance studies of some pseudohalogeno-derivatives of $[SnX_6]^{2-}$ (X = Cl or Br). *J. Chem. Soc., Dalton Trans.* **1987**, No. *2*, 315–317.

Dillon, K. B.; Platt, A. W. G. Cyano- and thiocyanato-derivatives of the hexachlorophosphate ion (PCl_6^-). *J. Chem. Soc. Dalton Trans.* **1982**, No. *7*, 1199–1204.

Dillon, K. B.; Platt, A. W. G. Cyano- and thiocyanato-derivatives of tetrahalophosphonium ions. *Polyhedron* **1983**, *2* (7), 641–643.

Dillon, K. B.; Platt, A. W. G.; Schmidpeter, A.; Zwaschka, F.; Sheldrick, W. S. Tetrachloro- und Tricyanochlorophosphat(III) Strukturbilder Einer Auf Halbem Wege Stehengebliebenen Addition. *Z. Anorg. Allg. Chem.* **1982**, *488* (1), 7–26.

Dixon, D. A.; Calabrese, J. C.; Miller, J. S. Crystal and molecular structure of the charge-transfer salt of decamethylferrocenium and tricyanomethanide, $[Fe(C_5Me_5)_2]^+[C(CN)_3]^-$. The electronic structure and spectra of the tricyanomethanide ion. *J. Am. Chem. Soc.* **1986**, *108* (10), 2582–2588.

Dixon, A. ELIX.–A form of tautomerism occurring amongst the thiocyanates of electronegative radicles. *J. Chem. Soc. Trans.* **1901**, *79*, 541–552.

Dixon, A. E. XVII.–The action of phosphorus trithiocyanate on alcohol. *J. Chem. Soc. Trans.* **1902**, *81* (168), 168–171.

do Carmo, L. C. S.; Lüty, F.; Holstein, T.; Orbach, R. Cooperative stretching vibration absorption in alkali cyanides. *Phys. Rev. B* **1981**, *23* (7), 3186–3196.

Dodonow, J. Bemerkungen Zur Arbeit von E. Zmaczyński: »Über Ein Neues Verfahren Zum Bromieren Und Jodieren von Organischen Verbindungen«. *Ber. Dtsch. Chem. Ges.* **1926**, *59* (9), 2208–2209.

Donald, K. J.; Tawfik, M. The weak helps the strong: sigma-holes and the stability of MF_4·base complexes. *J. Phys. Chem.* **2013**, *117* (51), 14176–14183.

Douay, M.; Bernath, P. F. Laser spectroscopy of CaNC and SrNC. *Chem. Phys. Lett.* **1990**, *174* (3–4), 230–234.

Douglas, A. E.; Sharma, D. Rotation-vibration spectra of diatomic and simple polyatomic molecules with long absorbing paths. IX. The spectra of the HCN and DCN molecules from 2.5 μ to 0.5 μ. *J. Chem. Phys.* **1953**, *21* (3), 448–458.

Downs, A. W. The isolation of a salt of the tellurocyanate anion. *Chem. Commun. (London)* **1968**, 1290–1291.

Du, B.; Zhang, W. Theoretical study on the water-assisted reaction of NCO with HCHO. *J. Phys. Chem.* **2013**, *117* (31), 6883–6892.

Du Plessis, C. A.; Barnard, P.; Muhlbauer, R. M.; Naldrett, K. Empirical model for the autotrophic biodegradation of thiocyanate in an activated sludge reactor. *Lett. Appl. Microbiol.* **2001**, *32* (2), 103–107.

Dua, S.; Blanksby, S. J.; Bowie, J. H. Electron capture of tetracyanoethylene oxide in the gas phase. Rearrangement of the parent radical anion to form $[(NC)_3C]^-$. A joint experimental and ab initio study. *Int. J. Mass Spectrom.* **2000**, *194* (2–3), 165–170.

Duboudin, F.; Cazeau, P.; Babot, O.; Moulines, F. Utilisation en synthese organique de $MeSi(CN)_3$ prepare. *Tetrahedron Lett.* **1983**, *24* (40), 4335–4336.

Dulmage, W. J.; Lipscomb, W. N. The crystal structures of hydrogen cyanide, HCN. *Acta Crystallogr.* **1951**, *4* (4), 330–334.

Dultz, W.; Krause, H. Light-scattering studies of the polymorphism of potassium cyanide under hydrostatic pressure. *Phys. Rev. B* **1978**, *18* (1), 394–400.

Dultz, W.; Otto, H. H.; Krause, H.; Buevoz, J. L. Elastic neutron scattering investigations of new high-pressure phases of KCN. *Phys. Rev. B* **1981**, *24* (3), 1287–1291.

Durand, D.; do Carmo, L. C. S.; Anderson, A.; Lüty, F. Raman and infrared studies of rotational-translational modes in stress-aligned ferroelastic KCN and NaCN. *Phys. Rev. B* **1980**, *22* (8), 4005–4021.

Earnshawb, J. C.; Ireland, N. Infrared spectra of $(HCN)_n$ clusters. *J. Mol. Struct.* **1995**, *348*, 273–276.

Easley, W. C.; Weltner, W. ESR of the CN radical in inert matrices. *J. Chem. Phys.* **1970**, *52* (1), 197–205.

Ebbs, S. Biological degradation of cyanide compounds. *Curr. Opin. Biotechnol.* **2004**, *15* (3), 231–236.

Edwards, H. G. M.; Fawcett, V. Force constants of phosphorus(III) cyanide and arsenic(III) cyanide. *Spectrochim. Acta, Part A* **1987**, *43* (11), 1345–1348.

Edwards, H. G. M.; Ingman, J. S.; Long, D. A. The Raman spectra of phosphorus and arsenic tricyanides, $P(CN)_3$ and $as(CN)_3$. *Spectrochim. Acta, Part A* **1976**, *32* (4), 731–738.

Ehrhardt, K. D.; Press, W.; Lefebvre, J.; Haussühl, S. Lattice dynamics in RbCN. *Solid State Commun.* **1980**, *34* (7), 591–593.

El-Bayoumy, K.; Sinha, R. Mechanisms of mammary cancer chemoprevention by organoselenium compounds. *Mutat. Res. Fundam. Mol. Mech. Mutagen.* **2004**, *551* (1–2), 181–197.

Ellinger, S.; Franke, P.; Harloff, J.; Rijksen, C.; Täschler, C.; Ott, L.; Schulz, A.; Sievert, K.; Stoffers, A.; Zur Täschler, C. *Fluoro and chloro cyano compounds of the 15th group*, **2014**, WO 2014167034 A2, 20141016.

Ellinger, S.; Harloff, J.; Ott, L.; Rijksen, C.; Schulz, A.; Sievert, K. Method for preparation of tricyanidofluoroborates in 2 steps. EP 2772495 A1 20140903: Visp, **2014**.

Elliott, N.; Hastings, J. Neutron diffraction investigation of KCN. *Acta Crystallogr.* **1961**, *14* (10), 1018.

El-Yazal, J.; Martin, J. M. L.; François, J.-P. Structure and vibrations of the C_2P and CNP radicals and their cations using density functional and coupled cluster theories. *J. Phys. Chem.* **1997**, *101* (44), 8319–8326.

Emerson, K.; Britton, D. The crystal and molecular structure of arsenic tricyanide. *Acta Crystallogr.* **1963**, *16* (2), 113–118.

Emerson, K.; Britton, D. The crystal and molecular structure of phosphorus tricyanide. *Acta Crystallogr.* **1964**, *17* (9), 1134–1139.

Emerson, K. The crystal and molecular structure of sulfur dicyanide. *Acta Crystallogr.* **1966**, *21* (6), 970–974.

Emri, J.; Györi, B. On the existence of isocyanotrihydroborate. *Polyhedron* **1994**, *13* (15–16), 2353–2357.

Enders, E. *Process for the production of cyanogen chloride together with cyanuric chloride and tetrameric cyanogen chloride*, **1972**, 3666427.

Epps, G. D. van.; Reid, E. E. Studies in the preparation of nitriles. II. The preparation of aliphatic nitriles. *J. Am. Chem. Soc.* **1916**, *38* (10), 2120–2128.

Ergöçmen, D.; Goicoechea, J. M. Synthesis, structure and reactivity of a cyapho-cyanamide salt. *Angew. Chem. Int. Ed.* **2021**, *60* (48), 25286–25289.

Essers, R.; Tennyson, J.; Wormer, P. E. S. An SCF potential energy surface for lithium cyanide. *Chem. Phys. Lett.* **1982**, *89* (3), 223–227.

Evers, J.; Krumm, B.; Axthammer, Q. J.; Martens, J.; Blaha, P.; Steemann, F. X.; Reith, T.; Mayer, P.; Klapötke, T. M. Molecular structure of isocyanic acid, HNCO, the imide of carbon dioxide. *J. Phys. Chem.* **2018**, *122* (12), 3287–3292.

Eyster, E. H.; Gillette, R. H. The vibration spectra of hydrazoic acid, methyl azide, and methyl isocyanate: the thermodynamic functions of hydrazoic acid. *J. Chem. Phys.* **1940**, *8* (5), 369–377.

Fang, T.; Shimp, D. A. Polycyanate esters: science and applications. *Prog. Polym. Sci.* **1995**, 61–118.

Fauß, R.; Linker, K.-H.; Findeisen, K. *Verfahren Zur Herstellung von Halogencyanen*. **1984**, 3229416.

Fawcett, F. S.; Lipscomb, R. D. Cyanogen fluoride. *J. Am. Chem. Soc.* **1960**, *82* (6), 1509–1510.

Fawcett, F. S.; Lipscomb, R. D. Cyanogen fluoride: synthesis and properties. *J. Am. Chem. Soc.* **1964**, *86* (13), 2576–2579.

Feher, F.; Weber, H. Beiträge Zur Chemie des Schwefels, 49. Über die Homologe Reihe der Cyansulfane $Sn(CN)_2$. *Chem. Ber.* **1958**, *91* (3), 642–650.

Feller, D.; Peterson, K. A.; Dixon, D. A. A survey of factors contributing to accurate theoretical predictions of atomization energies and molecular structures. *J. Chem. Phys.* **2008**, *129* (20), 204105.

Felsing, W. A.; Drake, G. W. The determination of the heat capacities and the heat capacity ratios of gaseous hydrogen cyanide and of hydrogen sulfide. *J. Am. Chem. Soc.* **1936**, *58* (9), 1714–1717.

Ferrario, M.; McDonald, I. R.; Klein, M. L. Anion ordering in alkali cyanide crystals. *J. Chem. Phys.* **1986**, *84* (7), 3975–3985.

Ferus, M.; Kubelík, P.; Kawaguchi, K.; Dryahina, K.; Španěl, P.; Civiš, S. HNC/HCN ratio in acetonitrile, formamide, and BrCN discharge. *J. Phys. Chem.* **2011**, *115* (10), 1885–1899.

Fiacco, D. L.; Hunt, S. W.; Leopold, K. R. Structural change at the onset of microsolvation: rotational spectroscopy of $HCN\cdots HCN–SO_3$. *J. Phys. Chem.* **2000**, *104* (36), 8323–8327.

Fichter, F.; Richard, S. Über Magnesiumcyanid. *Helv. Chim. Acta* **1922**, *5* (3), 396–400.

Fichter, F.; Schölly, C. Das Verhalten von Magnesiumnitrid Gegenüber Kohlenoxid und Kohlendioxid. *Helv. Chim. Acta* **1920**, *3* (1), 298–304.

Fiedler, S. L.; Vaskonen, K.; Ahokas, J.; Kunttu, H.; Eloranta, J.; Apkarian, V. A. Host–guest charge transfer states: CN doped Kr and Xe. *J. Chem. Phys.* **2002**, *117* (19), 8867–8878.

Fieser, L. F.; Fieser, M.; Ho, T. *Fieser and Fieser's reagents for organic synthesis*; Wiley: Hoboken, **2006**.

Finger, L. H.; Sundermeyer, J. Halide-free synthesis of hydrochalcogenide ionic liquids of the type [cation][HE] (E=S, Se, Te). *Chem. Eur J.* **2016**, *22* (12), 4218–4230.

Fitzgerald, M.; Bowie, J. H. The generation of the thiocyanate radical and cation from the thiocyanate anion $[SCN]^-$ in the gas phase. The rearrangements of neutral and cationic SCN. A joint experimental and theoretical study. *J. Phys. Chem.* **2004**, *108* (16), 3668–3674.

Fitzsimmons, A.; Klobukowski, M. Structure and stability of organic molecules containing heavy rare gas atoms. *Theor. Chem. Acc.* **2013**, *132* (2), 1314.

Flemming, A.; Hoffmann, M.; Köckerling, M. Tetracyanidoborates with sterically demanding phosphonium cations – thermally resistant lonic liquids. *Z. Anorg. Allg. Chem.* **2010**, *636* (3–4), 562–568.

Flores, J. R. A. Theoretical study of the excited electronic states of the SiCN system. *Chem. Phys.* **2005**, *310* (1–3), 303–310.

Fluck, E.; Goldmann, F. L.; Rümpler, K.-D. Pseudohalogenide nichtmetallischer elemente. II. Phosphor(III)-isothiocyanat und phosphor(III)-isocyanat die systeme $PCl_3/P(NCS)_3$, $PBr_3/P(NCS)_3$ und $PCl_3/P(NCO)_3$. *Z. Anorg. Allg. Chem.* **1965**, *338* (1–2), 52–57.

Fontaine, D. Structure Du cyanure de Sodium en Phase Ordonnee. *C. R. Seances Acad. Sci., Ser. B* **1975**, *281*, 443–444.

Forney, D.; Thompson, W. E.; Jacox, M. E. The vibrational spectra of molecular ions isolated in solid neon. IX. HCN^+, HNC^+, and CN^-. *J. Chem. Phys.* **1992**, *97* (3), 1664–1674.

Forthomme, D.; McRaven, C. P.; Sears, T. J.; Hall, G. E. Collinear two-color saturation spectroscopy in CN A–X (1–0) and (2–0) bands. *J. Mol. Spectrosc.* **2014**, *296*, 36–42.

Fowler, P. W.; Legon, A. C.; Peebles, S. A. Rotational spectrum of HCN···HI and a comparison of properties in the series HCN···HX (X = F, Cl, Br, I and CN). *Chem. Phys. Lett.* **1994**, *226* (5–6), 501–508.

Fox, J. L.; Yelle, R. V. Hydrocarbon ions in the ionosphere of Titan. *Geophys. Res. Lett.* **1997**, *24* (17), 2179–2182.

Franck, H. H.; Freitag, C. Die Darstellung von Calciumcyanid. *Angew. Chem.* **1926**, *39* (47), 1430–1432.

Franklin, E. C. *The nitrogen system of compounds*; Reinhold Publishing Cooperation: ACS Monograph Series: New York, **1935**.

Freitag, W. O.; Nixon, E. R. Infrared spectra of gaseous and crystalline cyanogen halides. *J. Chem. Phys.* **1956**, *24* (1), 109–114.

Frenking, G.; Schwarz, H. HCN/HNC versus HCN^+/HNC^+ - Zur Ursache der Stabilitätsumkehr Beim Übergang von Den Neutralmolekülen Zu den Radikalkationen. *Sci. Nat.* **1982**, *69* (9), 446–447.

Freudenmann, D.; Wolf, S.; Wolff, M.; Feldmann, C. Ionic liquids: new perspectives for inorganic synthesis? *Angew. Chem. Int. Ed.* **2011**, *50* (47), 11050–11060.

Fridh, C.; Åsbrink, L. Photoelectron and electron impact spectrum of HCN. *J. Electron Spectrosc.* **1975**, *7* (2), 119–138.

Fritz, H. P.; Keller, H. Spektroskopische Untersuchungen an Organometallischen Verbindungen, V. Infrarot-spektren von Organotellurverbindungen. *Chem. Ber.* **1961**, *94* (6), 1524–1533.

Fritz, S.; Lentz, D.; Szwak, M. Synthesis and structure determination of selenium(IV) cyanides. *Eur. J. Inorg. Chem.* **2008**, *2008* (30), 4683–4686.

Frölich, R.; Tebbe, K.-F. Untersuchungen an Polyhalogeniden. 2. Cesiumdicyanotriiodid. *Acta Crystallogr. Sect. B Struct. Crystallogr. Cryst. Chem.* **1982**, *38* (1), 71–75.

Fuith, A. The KSCN family: structural properties and phase transitions of crystals with three-atomic linear anions. *Phase Transitions* **1997**, *62* (1–2), 1–93.

Fukushima, M.; Ishiwata, T. Vibrationally hot bands of the SiCN $\tilde{A}^2\Delta$ – $\tilde{X}^2\Pi$ system. *J. Phys. Chem.* **2013**, *117* (39), 9435–9443.

Fukushima, M. Laser induced fluorescence spectroscopy of AlNC/AlCN in supersonic free expansions. *Chem. Phys. Lett.* **1998**, *283* (5–6), 337–344.

Fulara, J.; Klapstein, D.; Kuhn, R.; Maier, J. P. Emission spectra of supersonically cooled halocyanide cations, XCN^+ (X = Cl, Br, I): $\tilde{A}^2\Sigma^+ \rightarrow \tilde{X}^2\Pi$ and $B^2\Pi \rightarrow \tilde{X}^2\Pi$ band systems. *J. Phys. Chem.* **1985**, *89* (20), 4213–4219.

Gail, E.; Gos, S.; Kulzer, R.; Lorösch, J.; Rubo, A.; Sauer, M. Cyano compounds, inorganic. In *Ullmann's encyclopedia of industrial chemistry*; Wiley-VCH Verlag GmbH & Co. KGaA: Weinheim, Germany, **2004**.

Gall, H.; Schüppen, J. Über die Valenz-Grenze Bei Phosphorcyaniden und Phosphorrhodaniden. *Ber. Dtsch. Chem. Ges.* **1930**, *63* (2), 482–487.

Galliart, A.; Brown, T. M. Ammonium and tetraalkylammonium cyanates. *Synth. React. Inorg. Met.-Org. Chem.* **1972**, *2* (4), 273–275.

Gao, H.; Joo, Y.-H.; Twamley, B.; Zhou, Z.; Shreeve, J. M. Hypergolic ionic liquids with the 2,2-dialkyltriazanium cation. *Angew. Chem. Int. Ed.* **2009**, *48* (15), 2792–2795.

Garand, E.; Yacovitch, T. I.; Neumark, D. M. Slow photoelectron velocity-map imaging spectroscopy of C_2N^-, C_4N^-, and C_6N^-. *J. Chem. Phys.* **2009**, *130* (6), 064304–064310.

Gardner, P. J.; Preston, S. R.; Siertsema, R.; Steele, D. Ab initio molecular orbital studies for compounds of magnesium. *J. Comput. Chem.* **1993**, *14* (12), 1523–1533.

Gauld, J. W.; Eriksson, L. A.; Radom, L. Assessment of procedures for calculating radical hyperfine structures. *J. Phys. Chem.* **1997**, *101* (7), 1352–1359.

Gay-Lussac, L. J. Recherches Sur l'acide Prussique. *Ann. Chim. Phys.* **1815**, *95*, 136–231.

Geier, J.; Willner, H. Tris(trifluoromethyl)borane adducts of cyanogen halides. *Z. Anorg. Allg. Chem.* **2008**, *634* (11), 1863–1866.

Geller, S.; Schawlow, A. L. Crystal structure and quadrupole coupling of cyanogen bromide, BrCN. *J. Chem. Phys.* **1955**, *23* (5), 779–783.

George, J.; Deringer, V. L.; Dronskowski, R. Cooperativity of halogen, chalcogen, and pnictogen bonds in infinite molecular chains by electronic structure theory. *J. Phys. Chem.* **2014**, *118* (17), 3193–3200.

George, J.; Deringer, V. L.; Dronskowski, R. Dimensionality of intermolecular interactions in layered crystals by electronic-structure theory and geometric analysis. *Inorg. Chem.* **2015**, *54* (3), 956–962.

Georgieva, M. K.; Binev, I. G. The computational study on the structural and force field changes, caused by the conversion of dicyanamide into the azanion. *J. Mol. Struct.* **2005**, *752* (1–3), 14–19.

Georgieva, M. K.; Velcheva, E. A. Computational and experimental studies on the IR spectra and structure of the simplest nitriles (C1 and C2), their anions, and radicals. *Int. J. Quantum Chem.* **2006**, *106* (6), 1316–1322.

Gerasimov, I.; Yang, X.; Dagdigian, P. J. Laser fluorescence excitation spectra of the AlNC and AlCN isomers. *J. Chem. Phys.* **1999**, *110* (1), 220–228.

Gettler, A. O.; Baine, J. O. The toxicology of cyanide. *Am. J. Med. Sci.* **1938**, *195* (2), 182–197.

Giauque, W. F.; Ruehrwein, R. A. The entropy of hydrogen cyanide. Heat capacity, heat of vaporization and vapor pressure. hydrogen bond polymerization of the gas in chains of indefinite length. *J. Am. Chem. Soc.* **1939**, *61* (10), 2626–2633.

Glasnov, T. N.; Holbrey, J. D.; Kappe, C. O.; Seddon, K. R.; Yan, T. Methylation using dimethylcarbonate catalysed by ionic liquids under continuous flow conditions. *Green Chem.* **2012**, *14* (11), 3071–3076.

Gleiter, R.; Hyla-Kryspin, I.; Pfeifer, K.-H. On the stability of the tetramers of carbon monoxide, hydrogen isocyanide, and vinylidene. a molecular orbital theoretical rationalization. *J. Org. Chem.* **1995**, *60* (18), 5878–5883.

Glidewell, C.; Thomson, C. Ab initio calculations on the effect of different basis sets and electron correlation on the transition state for the reactions HNC ⇌ HCN and BCN ⇌ BNC. *J. Comput. Chem.* **1984**, *5* (1), 1–10.

Glidewell, C. Jahn-Teller effects in the MNDO approximation: structures of the molecular cations of some simple organosilanes. *J. Organomet. Chem.* **1981**, *217* (1), 11–18.

Glockler, G.; Baker, H. T. Raman line of cyanide ion. *J. Chem. Phys.* **1942**, *10* (5), 305–306.

Glöcklhofer, F.; Lunzer, M.; Fröhlich, J. Facile synthesis of cyanoarenes from quinones by reductive aromatization of cyanohydrin intermediates. *Synlett* **2015**, *26* (07), 950–952.

Goel, R. G.; Prasad, H. S. Organobismuth compounds. V. Preparation, characterization, and properties of triphenylbismuth diazide and dicyanide. *J. Organomet. Chem.* **1973**, *50* (1), 129–134.

Goggin, P. L.; McColm, I. J.; Shore, R. The oxyhalides of indium. *J. Chem. Soc. A* **1966a**, 1004–1008.

Goggin, P. L.; McColm, I. J.; Shore, R. Indium tricyanide and indium trithiocyanate. *J. Chem. Soc. A* **1966b**, 1314–1317.

Goubeau, J.; Jahn, E. L.; Kreutzberger, A.; Grundmann, C., Triazines. X. The infrared and Raman spectra of 1,3,5-triazine. *J. Phys. Chem.* **1954**, *58* (12), 1078–1081.

Gracia, R.; Shepherd, G. Cyanide poisoning and its treatment. *Pharmacotherapy* **2004**, *24* (10), 1358–1365.

Grakauskas, V. *Method for preparation of cyanogen fluoride*. 3532475, **1970**.

Graninger, D. M.; Herbst, E.; Öberg, K. I.; Vasyunin, A. I. The HNC/HCN ratio in star-forming regions. *Astrophys. J.* **2014**, *787* (1), 74.

Grant Hill, J.; Mitrushchenkov, A.; Yousaf, K. E.; Peterson, K. A. Accurate ab initio ro-vibronic spectroscopy of the $\tilde{X}^2\Pi$ CCN radical using explicitly correlated methods. *J. Chem. Phys.* **2011**, *135* (14), 144309–144320.

Greenwood, N. N.; Little, R.; Sprague, M. J. The tellurocyanate ion, $TeCN^-$. *J. Chem. Soc.* **1964**, 1292–1295.

Greenwood, N. N.; Earnshaw, A.; Hückmann, K. *Chemie Der Elemente*, 1st ed.; Wiley VCH: Weinheim, **1988**.

Greetham, G. M.; Ellis, A. M. Ultraviolet laser spectroscopy of jet-cooled CaNC and SrNC free radicals: observation of bent excited electronic states. *J. Chem. Phys.* **2000**, *113* (20), 8945–8952.

Grenier-Loustalot, M. F.; Lartigau, C.; Metras, F.; Grenier, P. Mechanism of thermal polymerization of cyanate ester systems: chromatographic and spectroscopic studies. *J. Polym. Sci., Part A: Polym. Chem.* **1996**, *34* (14), 2955–2966.

Grisley, Jr, D.; Gluesenkamp, E.; Heininger, S. Notes – reactions of nucleophilic reagents with cyanuric fluoride and cyanuric chloride. *J. Org. Chem.* **1958**, *23* (11), 1802–1804.

Gröger, H.; Asano, Y. Cyanide-free enantioselective catalytic strategies for the synthesis of chiral nitriles. *J. Org. Chem.* **2020**, *85* (10), 6243–6251.

Groß, S.; Laabs, S.; Scherrmann, A.; Sudau, A.; Zhang, N.; Nubbemeyer, U. Improved syntheses of cyanuric fluoride and carboxylic acid fluorides. *J. Prakt. Chem.* **2000**, *342* (7), 711–714.

Groutas, W. C. T-butyldimethylsilyl cyanide. *e-EROS Encycl. Reagents Org. Synth.* **2001**, *1* (4), 1–6.

Grundmann, C.; Beyer, E. Triazines. VII. The reaction of cyanuric chloride with lithium aluminum hydride. *J. Am. Chem. Soc.* **1954**, *76* (7), 1948–1949.

Grundmann, C.; Fulton, M. B. Zur Kenntnis des Cyanformaldehyds. *Chem. Ber.* **1964**, *97* (2), 566–574.

Grundmann, C.; Kreutzberger, A. Triazines. IX. 1,3,5-triazine and its formation from hydrocyanic acid. *J. Am. Chem. Soc.* **1954**, *76* (22), 5646–5650.

Grundmann, C.; Kreutzberger, A. Triazines. XIII. The ring cleavage of s-triazine by primary amines. A new method for the synthesis of heterocycles. *J. Am. Chem. Soc.* **1955**, *77* (24), 6559–6562.

Grundmann, C.; Kober, E. Triazines. XVII. s-Triazine from s-triazine-2,4,6-tricarbonic acid. *J. Org. Chem.* **1956**, *21* (12), 1392–1394.

Guélin, M.; Cernicharo, J.; Kahane, C.; Gomez-Gonzalez, J. A new free radical in IRC + 10216. *Astron. Astrophys.* **1986**, *157* (2), 17–20.

Guélin, M.; Muller, S.; Cernicharo, J.; McCarthy, M. C.; Thaddeus, P. Detection of the SiNC radical in IRC+10216. *Astron. Astrophys.* **2004**, *426* (2), 49-L52.

Guenez, M. E. Sur Le Preparation et Les Proprietes Du Cyanure d'arsenic. *C. R. Hebd. Seances Acad. Sci.* **1892**, *114*, 1186–1189.

Guennoun, Z.; Couturier-Tamburelli, I.; Piétri, N.; Aycard, J. P. UV photoisomerisation of cyano and dicyanoacetylene: the first identification of CCNCH and CCCNCN isomers – matrix isolation, infrared and ab initio study. *Chem. Phys. Lett.* **2003**, *368* (5–6), 574–583.

Guernsey, E. W.; Sherman, M. S. The thermal dissociation of sodium cyanide. *J. Am. Chem. Soc.* **1926**, *48* (3), 695–704.

Guerra, M. Role of standard diffuse functions for computing hyperfine splitting constants in radical anions. *J. Phys. Chem.* **1999**, *103* (30), 5983–5988.

Günther, P.; Meyer, R.; Müller-Skjold, F. Zur Thermochemie der Stickstoffwasserstoffsäure. *Z. Phys. Chem.* **1935**, *175* (1), 154–169.

Guo, B.; Pasinszki, T.; Westwood, N. P. C.; Zhang, K.; Bernath, P. F. High resolution infrared spectroscopy of cyanogen N-oxide, NCCNO. *J. Chem. Phys.* **1996**, *105* (11), 4457–4460.

Gutowsky, H. S.; Germann, T. C.; Augspurger, J. D.; Dykstra, C. E. Structure and dynamics of the H_2O–HCN dimer. *J. Chem. Phys.* **1992**, *96* (8), 5808–5816.

Gutsev, G. L.; Boldyrev, A. I. DVM-xα calculations on the ionization potentials of MX_{k+1}^- complex anions and the electron affinities of MX_{k+1} "Superhalogens". *Chem. Phys.* **1981**, *56* (3), 277–283.

Haas, A. Kovalente Kohlenstoffverbindungen. In *Handbuch der präparativen anorganischen Chemie in drei Bänden*; Ferdinand Enke Verlag: Stuttgart, **1978**; pp. 629–630.

Hackspill, L.; Grandadam, R. Contribution to the study of some potassium and sodium salts. *Ann. Chim.* **1925**, *5*, 218–250.

Hagiwara, Y.; Ochi, T.; Ohata, K.; Kasahara, T.; Toba, T.; Mizuta, K.; Katsuyama, H.; Ishida, S.; Nishida, T. *Ionic compound, method for producing the same, and ion-conductive material comprising the same*. US2011150736A1, **2011**.

Haiges, R.; Schneider, S.; Schroer, T.; Christe, K. O. High-energy-density materials: synthesis and characterization of $N_5^+[P(N_3)_6]^-$, $N_5^+[B(N_3)_4]^-$, $N_5^+[HF_2]^-\cdot n$ HF, $N_5^+[BF_4]^-$, N_5^+ $[PF_6]^-$, and $N_5^+[SO_3F]^-$. *Angew. Chem. Int. Ed.* **2004**, *43* (37), 4919–4924.

Hajgató, B.; Flammang, R.; Veszprémi, T.; Nguyen, M. T. Experimental and theoretical study of dicyanocarbene $C(CN)_2$. *Mol. Phys.* **2002**, *100* (11), 1693–1702.

Hakuta, K.; Uehara, H. Laser-induced fluorescence spectrum of the CCN radical with an Ar+ laser. *J. Chem. Phys.* **1983**, *78* (11), 6484–6489.

Halfen, D. T.; Sun, M.; Clouthier, D. J.; Ziurys, L. M. The microwave and millimeter rotational spectra of the PCN radical ($\tilde{X}^3\Sigma^-$). *J. Chem. Phys.* **2012**, *136* (14), 144312.

Hall, A. H.; Dart, R.; Bogdan, G. Sodium thiosulfate or hydroxocobalamin for the empiric treatment of cyanide poisoning? *Ann. Emerg. Med.* **2007**, *49* (6), 806–813.

Hamerton, I.; Hay, J. N. Recent developments in the chemistry of cyanate esters. *Polym. Int.* **1998**, *47* (4), 465–473.

Han, J.; Heaven, M. C.; Schnupf, U.; Alexander, M. H. Experimental and theoretical studies of the CN–Ar van Der Waals complex. *J. Chem. Phys.* **2008a**, *128* (10), 104308.

Han, J.; Heaven, M. C.; Schnupf, U. Spectroscopy, dissociation dynamics, and potential energy surfaces for CN(A)–Ar. *J. Chem. Phys.* **2008b**, *128* (22), 224309.

Hanawalt, J. D.; Rinn, H. W.; Frevel, L. K. Chemical analysis by X-ray diffraction. *Ind. Eng. Chem., Anal. Ed.* **1938**, *10* (9), 457–512.

Hand, C. W.; Hexter, R. M. Flash Photolysis of ozone-cyanogen mixtures. *J. Am. Chem. Soc.* **1970**, *92* (7), 1828–1831.

Hantzsch, A.; Mai, L. Über Imidokohlensäureether und die sogen. normalen Cyansäureether. *Ber. Dtsch. Chem. Ges.* **1895**, *28* (3), 2466–2472.

Hantzsch, A.; Osswald, G. Über cyanoform. *Ber. Dtsch. Chem. Ges.* **1899**, *32* (1), 641–650.

Happold, F. C.; Jones, G. L.; Pratt, D. B. Utilization of thiocyanate by thiobacillus thioparus and t. thiocyanoxidans. *Nature* **1958**, *182* (4630), 266–267.

Harloff, J.; Schulz, A.; Stoer, P.; Villinger, A. Pseudo halide chemistry in ionic liquids with decomposable anions. *Z. Anorg. Allg. Chem.* **2019a**, *645* (12), 835–839.

Harloff, J.; Michalik, D.; Nier, S.; Schulz, A.; Stoer, P.; Villinger, A. Cyanidosilicates – synthesis and structure. *Angew. Chem. Int. Ed.* **2019b**, *58* (16), 5452–5456.

Harloff, J.; Laatz, K. C.; Lerch, S.; Schulz, A.; Stoer, P.; Strassner, T.; Villinger, A. Hexacyanidosilicates with functionalized imidazolium counterions. *Eur. J. Inorg. Chem.* **2020a**, *2020* (25), 2457–2464.

Harloff, J.; Schulz, A.; Stoer, P.; Villinger, A. Pseudohalide HCN aggregate ions: $[N_3(HCN)_3]^-$, $[OCN(HCN)_3]^-$, $[SCN(HCN)_2]^-$ and $[P(CN{\cdot}HCN)_2]^-$. *Dalton Trans.* **2020b**, *49* (38), 13345–13351.

Harrison, P. G.; Stobart, S. R. Derivatives of divalent germanium, tin, and lead. Part I. The protolysis of cyclopentadienyltin(II) compounds by hydroxy-derivatives. Tin(II) Oximes and hydroxylpmines. *J. Chem. Soc., Dalton Trans.* **1973**, *9*, 940–943.

Harrison, P. G. Inorganic tin(II) derivatives. *J. Chem. Soc., Chem. Commun.* **1972**, No. *9*, 544.

Hartman, W. W.; Dreger, E. E. Cyanogen bromide. *Org. Synth.* **1931**, *11*, 30.

Hartwig, A. *Gesundheitsschädliche Arbeitsstoffe - Toxikologisch-Arbeitsmedizinische Begründungen von MAK-Werten*; Wiley VCH: Weinheim, **1972**.

Hauge, S.; Kimmel, E. C.; Holm, B.; Widmark, G.; Koskikallio, J.; Kachi, S. Syntheses and crystal data on salts of the triselenocyanate and seleniumtriselenocyanate ions. *Acta Chem. Scand.* **1971a**, *25*, 3081–3093.

Hauge, S.; Sletten, J.; Rasmussen, S. E.; Svensson, S.; Koskikallio, J.; Kachi, S. The crystal structure of potassium triselenocyanate hemihydrate. *Acta Chem. Scand.* **1971b**, *25*, 3094–3102.

Hauge, S.; Hordvik, A.; Sæthre, L. J.; Andresen, A. F.; Southern, J. T.; Edlund, K.; Eliasen, M.; Herskind, C.; Laursen, T.; Pedersen, P. M. The crystal structure of cesium triselenocyanate. *Acta Chem. Scand.* **1975**, *29a*, 163–169.

Hausmann, A. Elektronenspin-resonanz in Alkalihalogenid-Kristallen Mit Schwefel- und Selenzusätzen. *Z. Phys.* **1966**, *192* (3), 313–328.

Hazell, A. C. The crystal structures of selenium dicyanide and sulphur dicyanide. *Acta Crystallogr.* **1963**, *16* (8), 843–844.

Heaven, M. Spectroscopy and dynamics of open-shell van der Waals molecules. *Annu. Rev. Phys. Chem.* **1992**, *43* (1), 283–310.

Heckathorn, J. W.; Kruger, M. B.; Gerlich, D.; Jeanloz, R. High-pressure behavior of the alkali cyanides KCN and NaCN. *Phys. Rev. B* **1999**, *60* (2), 979–983.

Heiart, R. B.; Carpenter, G. B. The crystal structure of cyanogen chloride. *Acta Crystallogr.* **1956**, *9* (11), 889–895.

Heilos, J.; Heimberger, W.; Lüssling, T.; Weigert, W. *Verfahren Zur Herstellung von Chlorcyan*. 2027957, **1971**.

Heimberger, W.; Schreyer, G. *Process for the production of cyanogen chloride or cyanogen bromide*. 1525343, **1975**.

Hemple, S.; Nixon, E. R. Infrared spectrum of cyanogen iodide vapor. *J. Chem. Phys.* **1967**, *47* (10), 4273–4274.

Henderson, T. J.; Cullinan, D. B. Purity analysis of hydrogen cyanide, cyanogen chloride and phosgene by quantitative ^{13}C NMR spectroscopy. *Magn. Reson. Chem.* **2007**, *45* (11), 954–961.

Hendricks, S. B.; Pauling, L. The crystal structures of sodium and potassium trinitrides and potassium cyanate and the nature of the trinitride group. *J. Am. Chem. Soc.* **1925**, *47* (12), 2904–2920.

Henninger, A. A. Henninger, Aus Paris, 7. **1876**. *Ber. Dtsch. Chem. Ges.* **1876**, *9* (2), 1430–1435.

Hennings, E.; Schmidt, H.; Voigt, W. Structure and thermal properties of lithium cyanate. *Z. Anorg. Allg. Chem.* **2011**, *637* (9), 1199–1202.

Henretig, F. M.; Kirk, M. A.; McKay, C. A. Hazardous chemical emergencies and poisonings. *N. Engl. J. Med.* **2019**, *380* (17), 1638–1655.

Herbst, E.; Klemperer, W. The formation and depletion of molecules in dense interstellar clouds. *Astrophys. J.* **1973**, *185* (9), 505–533.

Henriques, A. B.; von der Weid, J. P. Decay kinetics of triplet molecular excitons in alkali cyanides. *Phys. Status Solidi B* **1985**, *132*(2), 627–633.

Herbst, E. Chemistry in the interstellar medium. *Annu. Rev. Phys. Chem.* **1995**, *46* (1), 27–54.

Hering, C.; von Langermann, J.; Schulz, A. The elusive cyanoformate: an unusual cyanide shuttle. *Angew. Chem. Int. Ed.* **2014**, *53* (32), 8282–8284.

Herz, W.; Neukirch, E. Die Quantitative Bestimmung des Bleis Als Cyanid. *Z. Anorg. Allg. Chem.* **1923**, *130* (1), 343–344.

Hester, R. E.; Lee, K. M.; Mayer, E. Tetracyanomethane as a pseudo-(carbon tetrahalide). *J. Phys. Chem.* **1970**, *74* (18), 3373–3376.

Hinks, D. G.; Price, D. L.; Rowe, J. M.; Susman, S. Single crystal growth of sodium cyanide and potassium cyanide. *J. Cryst. Growth* **1972**, *15* (3), 227–230.

Hipps, K. W.; Aplin, A. T. The tricyanomethanide ion: an infrared, raman, and tunneling spectroscopy study including isotopic substitution. *J. Phys. Chem.* **1985**, *89* (25), 5459–5464.

Ho, W.-C.; Blom, C. E.; Liu, D.-J.; Oka, T. The infrared v_5 band (HNC bend) of protonated hydrogen cyanide, $HCNH^+$. *J. Mol. Spectrosc.* **1987**, *123* (1), 251–253.

Ho, T.-L.; Fieser, M.; Fieser, L.; Danheiser, R.; Roush, W. *Fieser and Fieser's reagents for organic synthesis*; John Wiley & Sons: Hoboken, NJ, USA, **2006**.

Hoffman, R. E.; Hornig, D. F. The infra-red spectrum of solid hydrogen cyanide. *J. Chem. Phys.* **1949**, *17* (11), 1163.

Hoffmann, R.; Zeiss, G. D.; Van Dine, G. W. The electronic structure of methylenes. *J. Am. Chem. Soc.* **1968**, *90* (6), 1485–1499.

Holbrey, J. D.; Rogers, R. D.; Shukla, S. S.; Wilfred, C. D. Optimised microwave-assisted synthesis of methylcarbonate salts: a convenient methodology to prepare intermediates for ionic liquid libraries. *Green Chem.* **2010**, *12* (3), 407–413.

Holland, D. M.; Powis, I.; Karlsson, L.; Trofimov, A.; Schirmer, J.; von Niessen, W. A study of the photoionisation dynamics of the cyanogen halides. *Chem. Phys.* **2004**, *297* (1–3), 55–73.

Hollas, J. M.; Sutherley, T. A. Geometry of cyanogen halide positive ions from photoelectron spectroscopy. *Mol. Phys.* **1971**, *22* (2), 213–223.

Hörst, S. M.; Yelle, R. V.; Buch, A.; Carrasco, N.; Cernogora, G.; Dutuit, O.; Quirico, E.; Sciamma-O'Brien, E.; Smith, M. A.; Somogyi, A.; Szopa, C.; Thissen, R.; Vuitton, V. Formation of amino acids and nucleotide bases in a Titan atmosphere simulation experiment. *Astrobiology* **2012**, *12* (9), 809–817.

Huber, R. E.; Criddle, R. S. Comparison of the chemical properties of selenocysteine and selenocystine with their sulfur analogs. *Arch. Biochem. Biophys.* **1967**, *122* (1), 164–173.

Hübner, H.; Wehrhane, G. Über eine Verbindung des Cyans Mit Phosphor. *Justus Liebigs Ann. Chem.* **1863**, *128* (2), 254–256.

Huthmacher, K.; Most, D. Cyanuric acid and cyanuric chloride. In *Ullmann's encyclopedia of industrial chemistry*; Wiley-VCH Verlag GmbH & Co. KGaA: Weinheim, Germany, **2000**.

Hvastijová, M.; Kohout, J.; Kožíšek, J.; Svoboda, I. X-ray crystallographic evidence for addition of water to nitrosodicyanomethanide in the 3d-metal coordination sphere. *J. Coord. Chem.* **1999**, *47* (4), 573–579.

Ingold, C. K. CVI. The form of the vapour pressure curve at high temperatures. Part II. The curve for sodium cyanide. *J. Chem. Soc. Trans.* **1923**, *123*, 885–891.

Iqbal, Z. Vibrational spectrum of single crystal sodium thiocyanate. *J. Mol. Struct.* **1971**, *7* (1–2), 137–146.

Irran, E.; Jürgens, B.; Schnick, W. Trimerization of alkali dicyanamides $M[N(CN)_2]$ and formation of tricyanomelaminates $M_3[C_6N_9]$ (M = K, Rb) in the melt: crystal structure determination of three polymorphs of $K[N(CN)_2]$, two of $Rb[N(CN)_2]$, and one of $K_3[C_6N_9]$ and $Rb_3[C_6N_9]$ from X-ray powder. *Chem. Eur J.* **2001**, *7* (24), 5372–5381.

Irran, E.; Jürgens, B.; Schnick, W. Synthesis., Crystal structure determination from X-ray powder diffractometry and vibrational spectroscopy of the tricyanomelaminate monohydrates $M_3[C_6N_9]\cdot H_2O$ (M=K, Rb). *Solid State Sci.* **2002**, *4* (10), 1305–1311.

Irvine, W. M.; Schloerb, F. P. Cyanide and isocyanide abundances in the cold, dark cloud TMC-1. *Astrophys. J.* **1984**, *282* (9), 516–521.

Isetti, G.; Neubert, T. J. Light-scattering and color centers in sodium cyanide. *J. Chem. Phys.* **1957**, *26* (2), 337–344.

Ishii, K.; Hirano, T.; Nagashima, U.; Weis, B.; Yamashita, K. An ab initio prediction of the spectroscopic constants of MgNC – the first Mg-bearing molecule in space. *Astrophys. J.* **1993**, *410*, L43–L44.

Ishii, K.; Hirano, T.; Nagashima, U.; Weis, B.; Yamashita, K. Ab initio study on low-lying vibrational states and spectroscopic constants of MgNC ($X^2\Sigma^+$). *J. Mol. Struct.: Theochem.* **1994**, *305* (C), 117–125.

Ishii, K.; Taketsugu, T.; Hirano, T. Theoretical study on the potential energy surfaces of CaNC and CaCN. *Chem. Phys. Lett.* **2003**, *374* (5–6), 506–512.

Ismail, Z. K.; Hauge, R. H.; Margrave, J. L. Infrared study of matrix-isolated lithium isocyanide. *J. Chem. Phys.* **1972**, *57* (12), 5137–5142.

Israël, G.; Szopa, C.; Raulin, F.; Cabane, M.; Niemann, H. B.; Atreya, S. K.; Bauer, S. J.; Brun, J. F.; Chassefière, E.; Coll, P.; Condé, E.; Cascia, D.; Hauchecorne, A.; Millian, P.; Nguyen, M. J.; Owen, T.; Riedler, W.; Samuelson, R. E.; Siguier, J. M.; Steller, M.; Sternberg, R.; Vidal-Madjar, C. Complex organic matter in Titan's atmospheric aerosols from in situ pyrolysis and analysis. *Nature* **2005**, *438* (7069), 796–799.

Jackson, D. A.; Atherton, J. H.; Lennon, M.; Cox, L. C. *Process for the preparation of cyanogen bromide*. WO0142138, **2001**.

Jacobs, K.; Siche, D.; Klimm, D.; Rost, H.-J.; Gogova, D. Pseudohalide vapour growth of thick GaN layers. *J. Cryst. Growth* **2010**, *312* (6), 750–755.

Jacox, M. E.; Thompson, W. E. Infrared spectra of $ClCN^+$, $ClNC^+$, and $BrCN^+$ trapped in solid neon. *J. Chem. Phys.* **2007**, *126* (24), 244311.

Jacox, M. E. Vibrational and electronic energy levels of polyatomic transient molecules: supplement 1. *J. Phys. Chem. Ref. Data* **1990**, *19* (6), 1387–1546.

Jäger, L.; Kretschmann, M.; Köhler, H. Pseudohalogenverbindungen. Darstellung und Reaktionsverhalten von Alkyl- und Arylammoniumdicyanamiden, -Tricyammethaniden und -Dicyanmethanidoacetaten $[RNH_3]X$ (X = $N(CN)_2$, $C(CN)_3$, $C(CN)_2C(O)CH_3$). *Z. Anorg. Allg. Chem.* **1992**, *611* (5), 68–72.

Jana, G.; Pan, S.; Osorio, E.; Zhao, L.; Merino, G.; Chattaraj, P. K. Cyanide–isocyanide isomerization: stability and bonding in noble gas inserted metal cyanides (metal = Cu, Ag, Au). *Phys. Chem. Chem. Phys.* **2018**, *20* (27), 18491–18502.

Jennings, W. L.; Scott, W. B. The preparation of cyanogen chloride. *J. Am. Chem. Soc.* **1919**, *41* (8), 1241–1248.

Jensen, J. N.; Tuan, Y. J. Chemical oxidation of thiocyanate ion by ozone. *Ozone Sci. Eng.* **1993**, *15* (4), 343–360.

Jensen, J. O. Vibrational frequencies and structural determination of phosphorous tricyanide. *Spectrochim. Acta, Part A* **2004a**, *60* (11), 2537–2540.

Jensen, J. O. Vibrational frequencies and structural determination of arsenous tricyanide. *J. Mol. Struct.: Theochem.* **2004b**, *678* (1–3), 195–199.

Jiang, N.; Xu, S.; Ostrikov, K. N.; Tsakadze, E. L.; Long, J. D.; Chai, J. W.; Tsakadze, Z. L. Synthesis and characterization of ternary Al-C-N compound. *Int. J. Mod. Phys. B* **2002**, *16* (06n07), 1132–1137.

Jiang, Z.-Y.; Xu, X.-H.; Wu, H.-S.; Jin, Z.-H. Theoretical study of structures and stabilities of C_mN_2 (M=1–14) Ions. *Int. J. Mass Spectrom.* **2003**, *230* (1), 33–39.

Jin-chai, L.; Xian-feng, L.; Zi-hong, Z.; Huai-xi, G.; Ming-sheng, Y. The preparation and characterization of amorphous SiCN thin films. *Wuhan Univ. J. Nat. Sci.* **2001**, *6* (3), 665–669.

Joannis, A. Cyanure de Sodium et Hydrates. In *Annales de chimie et de physique*; V. Masson: Paris, **1882a**; pp. 484–486.

Joannis, A. Cyanure de Sodium et Hydrates. In *Annales de chimie et de physique*; V. Masson: Paris, **1882b**; pp. 494–496.

Johansson, A.; Kollman, P.; Rothenberg, S. The electronic structure of the HCN dimer and trimer. *Theor. Chim. Acta* **1972**, *26* (1), 97–100.

Johns, I. B.; DiPietro, H. R. Synthesis and reactions of anhydrous lithium cyanide. *J. Org. Chem.* **1964**, *29* (7), 1970–1971.

Jones, C. E.; Coskran, K. J. The synthesis and spectroscopic properties of some cyanophosphines. *Inorg. Chem.* **1971**, *10* (7), 1536–1537.

Jonkers, G.; Mooyman, R.; de Lange, C. A. Ultraviolet photoelectron spectroscopy of the unstable molecules ClSeCN and BrSeCN and the stable $Se(CN)_2$. *Mol. Phys.* **1981**, *43* (3), 655–667.

Jost, M.; Finger, L. H.; Sundermeyer, J.; von Hänisch, C. Simple access to ionic liquids and organic salts containing the phosphaethynolate (PCO^-) and zintl (Sb_{11}^{3-}) Anions. *Chem. Commun.* **2016**, *52* (78), 11646–11648.

Jucks, K. W.; Miller, R. E. Near infrared spectroscopic observation of the linear and cyclic isomers of the hydrogen cyanide trimer. *J. Chem. Phys.* **1988**, *88* (4), 2196–2204.

Jung, S.; Renz, F.; Klein, M.; Menzel, M.; Boča, R.; Stößer, R. Molecular switching in iron complexes bridged via tin-cyanides observed by Mössbauer and ESR spectroscopy. *J. Phys. Conf. Ser.* **2010**, *217* (1), 012027–012032.

Jürgens, B.; Milius, W.; Morys, P.; Schnick, W. Trimerisierung von Dicyanamid-Ionen C_2N^{3-} Im Festkörper – Synthesen, Kristallstrukturen und Eigenschaften von $NaCs_2(C_2N_3)_3$ und $Na_3C_6N_9 \cdot 3\ H_2O$. *Z. Anorg. Allg. Chem.* **1998**, *624* (1), 91–97.

Jürgens, B.; Irran, E.; Schneider, J.; Schnick, W. Trimerization of NaC_2N_3 to $Na_3C_6N_9$ in the solid: ab initio crystal structure determination of two polymorphs of NaC_2N_3 and of $Na_3C_6N_9$ from X-ray powder diffractometry. *Inorg. Chem.* **2000**, *39* (4), 665–670.

Jürgens, B.; Irran, E.; Schnick, W. Syntheses, vibrational spectroscopy, and crystal structure determination from x-ray powder diffraction data of alkaline earth dicyanamides M $[N(CN)_2]_2$ with M = Mg, Ca, Sr, and Ba. *J. Solid State Chem.* **2001**, *157* (2), 241–249.

Jürgens, B.; Höppe, H. A.; Schnick, W. Synthesis., Crystal structure, vibrational spectroscopy, and thermal behaviour of lead dicyanamide $Pb[N(CN)_2]_2$. *Solid State Sci.* **2002**, *4* (6), 821–825.

Jürgens, B.; Irran, E.; Schnick, W. Synthesis and characterization of the rare-earth dicyanamides $L_n[N(CN)_2]_3$ with Ln=La, Ce, Pr, Nd, Sm, and Eu. *J. Solid State Chem.* **2005**, *178* (1), 72–78.

Jursic, B. S. Ab initio and density functional theory studies of the potential energy surface of the LiNC → LiCN isomerization. *J. Mol. Struct.: Theochem.* **1998**, *428* (1–3), 41–47.

Jursic, B. S. Complete basis set ab initio study of potential energy surfaces of the dissociation recombination reaction $HCNH^+ + E^-$. *J. Mol. Struct.: Theochem.* **1999**, *487* (3), 211–220.

Kahlenberg, L.; Steinle, J. V. On the single potential of arsenic and its power to replace other metals in solutions. *Trans. Electrochem. Soc.* **1923**, *44*, 493.

Kaiser, R. I.; Mebel, A. M. On the formation of polyacetylenes and cyanopolyacetylenes in Titan's atmosphere and their role in astrobiology. *Chem. Soc. Rev.* **2012**, *41* (16), 5490–5501.

Kakimoto, M.; Kasuya, T. Doppler-limited dye laser excitation spectroscopy of the CCN radical. *J. Mol. Spectrosc.* **1982**, *94* (2), 380–392.

Kalescky, R.; Kraka, E.; Cremer, D. Identification of the strongest bonds in chemistry. *J. Phys. Chem.* **2013**, *117* (36), 8981–8995.

Kalikhman, I.; Gostevskii, B.; Kertsnus, E.; Botoshansky, M.; Tessier, C. A.; Youngs, W. J.; Deuerlein, S.; Stalke, D.; Kost, D. Competitive molecular rearrangements in hexacoordinate cyanosilicon dichelates. *Organometallics* **2007**, *26* (10), 2652–2658.

Kalmutzki, M.; Ströbele, M.; Meyer, H. J. From cyanate to cyanurate: cyclotrimerization reactions towards the novel family of metal cyanurates. *Dalton Trans.* **2013**, *42* (36), 12934–12939.

Kanamori, H.; Okamoto, H.; Urabe, K. Lattice vibrational modes in potassium thiocyanate. *J. Phys. Chem. Solids* **1981**, *42* (3), 197–202.

Kapp, J.; Schleyer, P. v. R. $M(CN)_2$ species (M = Be, Mg, Ca, Sr, Ba): cyanides, nitriles, or neither? *Inorg. Chem.* **1996**, *35* (8), 2247–2252.

Karpfen, A. Linear and cyclic clusters of hydrogen cyanide and cyanoacetylene: a comparative ab initio and density functional study on cooperative hydrogen bonding. *J. Phys. Chem.* **1996**, *100* (32), 13474–13486.

Kassaee, M. Z.; Musavi, S. M.; Buazar, F.; Ghambarian, M. Novel triplet ground state silylenes: H–N=C=Si, CN–N=C=Si, and MeO–N=C=Si at DFT Levels. *Monatsh. Chem.* **2006**, *137* (11), 1385–1400.

Kauffman, G. B.; Foust, G. E.; Tun, P. Pseudohalogens: a general chemistry laboratory experiment. *J. Chem. Educ.* **1968**, *45* (2), 141–146.

Kaufmann, H. P.; Kögler, F. Blei(4)-Salze der Pseudohalogene. *Ber. Dtsch. Chem. Ges.* **1926**, *59* (2), 178–186.

Kawaguchi, K.; Suzuki, T.; Saito, S.; Hirota, E.; Kasuya, T. Dye Laser Excitation spectroscopy of the CCN radical: the $\tilde{A}\,^2\Delta_i$-$\tilde{X}\,^2\Pi_r$ (0,1,0)-(0,1,0) and (0,2,0)-(0,2,0) Bands. *J. Mol. Spectrosc.* **1984**, *106* (2), 320–329.

Kawaguchi, K.; Kagi, E.; Hirano, T.; Takano, S.; Saito, S. Laboratory spectroscopy of MgNC – the first radioastronomical identification of Mg-bearing molecule. *Astrophys. J.* **1993**, *406*, L39–L42.

Keller, C. N.; Anicich, V. G.; Cravens, T. E. Model of Titans ionosphere with detailed hydrocarbon ion chemistry. *Planet. Space Sci.* **1998**, *46* (9–10), 1157–1174.

Kellö, V.; Sadlej, A. J. Electron correlation and relativistic contributions to molecular electric properties: dipole and quadrupole moments of cyanogen halides. *Mol. Phys.* **1992**, *75* (1), 209–220.

Kelly, D. P.; Baker, S. C. The organosulphur cycle: aerobic and anaerobic processes leading to turnover of C1-sulphur compounds. *FEMS Microbiol. Lett.* **1990**, *87* (3–4), 241–246.

Kempe, R.; Kessenich, E.; Schulz, A. $[Me_3SiN(PPh_3)\cdot ICN]$: a new labile donor–acceptor complex. *Inorg. Chem.* **2001**, *40* (20), 5182–5187.

Kertes, A. S., Ed. *Silver azide, cyanide, cyanamides, cyanate, selenocyanate and thiocyanate*; Elsevier, **1979**.

Ketelaar, J. A. A.; Zwartsenberg, J. W. The crystal structure of the cyanogen halides. I. The structure of cyanogen iodide. *Recl. Trav. Chim. Pays-Bas* **1939**, *58* (5), 448–452.

Khalouf-Rivera, J.; Carvajal, M.; Santos, L. F.; Pérez-Bernal, F. Calculation of transition state energies in the HCN–HNC isomerization with an algebraic model. *J. Phys. Chem.* **2019**, *123* (44), 9544–9551.

Khazaei, M.; Liang, Y.; Bahramy, M. S.; Pichierri, F.; Esfarjani, K.; Kawazoe, Y. High-pressure phases of hydrogen cyanide: formation of hydrogenated carbon nitride polymers and layers and their electronic properties. *J. Phys. Condens. Matter* **2011**, *23* (40), 405403–405414.

Kichigina, G. A.; Mozhaev, P. S.; Kiryukhin, D. P.; Barkalov, I. M. Low-temperature radiation polymerization of cyanogen bromide. *Mendeleev Commun.* **1998**, *8* (4), 159–160.

Kim, S. J.; Katayama, Y. Effect of growth conditions on thiocyanate degradation and emission of carbonyl sulfide by thiobacillus thioparus THI115. *Wat. Res.* **2000**, *34* (11), 2887–2894.

King, B. F.; Weinhold, F. Structure and spectroscopy of $(HCN)_n$ clusters: cooperative and electronic delocalization effects in C–H···N hydrogen bonding. *J. Chem. Phys.* **1995**, *103* (1), 333–347.

Kirk, P. G.; Smith, T. D. The molecular complexity of phosphorus tricyanide in organic solvents. *J. Inorg. Nucl. Chem.* **1968**, *30* (3), 892–893.

Kisiel, Z.; Winnewisser, M.; Winnewisser, B. P.; De Lucia, F. C.; Tokaryk, D. W.; Billinghurst, B. E. Far-infrared spectrum of $S(CN)_2$ measured with synchrotron radiation: global analysis of the available high-resolution spectroscopic data. *J. Phys. Chem.* **2013**, *117* (50), 13815–13824.

Klapötke, T. M.; Schulz, A. Reaction of AgOCN with NO, NO_2, $ClNO_2$, ClNO, and BrNO: evidence of the formation of OCN–NO_2 and OCN–NO. *Inorg. Chem.* **1996**, *35* (26), 7897–7904.

Klapötke, T. M.; McIntyre, G.; Schulz, A. Nitration of hydrogen cyanide with nitryl tetrafluoroborate. *J. Chem. Soc., Dalton Trans.* **1996**, No. *15*, 3237–3241.

Klapötke, T. M.; Krumm, B.; Gálvez-Ruiz, J. C.; Nöth, H.; Schwab, I. Experimental and theoretical studies of homoleptic tellurium cyanides $Te(CN)_X$: crystal structure of $Te(CN)_2$. *Eur. J. Inorg. Chem.* **2004**, *2004* (24), 4764–4769.

Klapötke, T. M.; Krumm, B.; Scherr, M. Homoleptic selenium cyanides: attempted preparation of $Se(CN)_4$ and redetermination of the crystal structure of $Se(CN)_2$. *Inorg. Chem.* **2008**, *47* (15), 7025–7028.

Klapötke, T. M. The $[ICNI]^+$ cation: a combined experimental and theoretical study. Reaction of $[ICNI]^+[AsF_6]^-$ with CsN_3. *J. Chem. Soc. Dalton Trans.* **1997**, *3* (4), 553–558.

Klason, P. Über Das Radical Cyanur und Seine Verbindungen Mit Halogenen. *J. Prakt. Chem.* **1886**, *34* (1), 152–160.

Klein, M. L.; Goddard, J. D.; Bounds, D. G. An ab initio molecular orbital study of NaCN and KCN. *J. Chem. Phys.* **1981**, *75* (8), 3909–3915.

Klemenc, A.; Wagner, G. Bemerkungen Über Das Cyanchlorid. *Z. Anorg. Allg. Chem.* **1938**, *235* (4), 427–430.

Knight, J. S.; Petrie, S. A. H.; Freeman, C. G.; McEwan, M. J.; McLean, A. D.; DeFrees, D. J. Structural Isomers of C_2N^+: a selected-ion flow tube study. *J. Am. Chem. Soc.* **1988**, *110* (16), 5286–5290.

Knopp, G.; Knorr, K.; Loidl, A.; Haussühl, S. On the phase transition in CsCN. *Z. Phys. B: Condens. Matter* **1983**, *51* (3), 259–263.

Knözinger, E. Cluster formation of hydrogen cyanide in solid and liquid CCl_4 matrices. *J. Chem. Phys.* **1986**, *85* (9), 4881.

Kober, E.; Grundmann, C. Triazines. XXII. Fluoro-s-Triazines. *J. Am. Chem. Soc.* **1959**, *81* (14), 3769–3770.

Kober, E.; Schroeder, H.; Ratz, R. F. W.; Ülrich, H.; Gruxdmann, C. Synthesis of polyfluorinated heterocycles by indirect fluorination with silver fluorides. I. Fluoro-s-triazines and reactions of cyanuric fluoride. *J. Org. Chem.* **1962**, *27* (7), 2577–2580.

Kohguchi, H.; Ohshima, Y.; Endo, Y. Laser-induced fluorescence spectroscopy of the $\tilde{C}^2\Sigma^+$–$\tilde{X}^2\Pi_{1/2}$ band system of jet-cooled CCN radical. *J. Chem. Phys.* **1997**, *106* (13), 5429–5438.

Köhler, H.; Lux, G. Zur Kenntnis des Nitrosodicyanmethanid-Ions $[ONC(CN)_2]-$. *Inorg. Nucl. Chem. Lett.* **1968**, *4* (3), 133–136.

Köhler, H.; Seifert, B. Beiträge Zur Chemie des Dicyanamid- und des Tricyanmethanid-Ions XI. Diorganozinn-pseudohalogenide. *J. Organomet. Chem.* **1968**, *12* (1), 253–255.

Köhler, H.; Kolbe, A.; Lux, G. Metall-pseudohalogenide. 27. Zur Struktur der Dicyanamide Zweiwertiger 3d-Metalle $M(N(CN)_2)_2$. *Z. Anorg. Allg. Chem.* **1977**, *428* (1), 103–112.

Köhler, H. Die Fabrikation von Cyanverbindungen aus Tierischen Abfällen und Produkten der Trockenen Destillation. In *Die Industrie der Cyanverbindungen*; Vieweg: Wiesbaden, **1914**; pp. 60–101.

Köhler, H. Beitrage Zur Chemie des Dicyanamid- und des Tricyanmethanidions. I. Die Bildung von Übergangsmetall-Pyridin-Komplexen. *Z. Anorg. Allg. Chem.* **1964**, *331* (5–6), 237–248.

Kohout, J.; Jäger, L.; Hvastijová, M.; Kožíšek, J. Tricyanomethanide and dicyanamide complexes of Cu(II), Ni(II), Co(II), their structures and properties. *J. Coord. Chem.* **2000**, *51* (2), 169–218.

Komornicki, A.; Ishida, K.; Morokuma, K.; Ditchfield, R.; Conrad, M. Efficient determination and characterization of transition states using ab-initio methods. *Chem. Phys. Lett.* **1977**, *45* (3), 595–602.

Kondo, Y.; Schoemaker, D.; Lüty, F. Molecular motion and ordering in rubidium cyanide, studied with dielectric and raman techniques. *Phys. Rev. B* **1979**, *19* (8), 4210–4216.

König, W. Untersuchungen aus Dem Organ.-Chem. Laboratorium der Technischen Hochschule Zu Dresden. XCVII. Über die Umsetzung von Rhodaniden Mit Brom in Wäßriger Lösung. *J. Prakt. Chem.* **1911**, *84* (1), 558–560.

Konnert, J.; Britton, D. The crystal structure of $AgC(CN)_3$. *Inorg. Chem.* **1966**, *5* (7), 1193–1196.

Koppe, K.; Bilir, V.; Frohn, H.-J.; Mercier, H. P. A.; Schrobilgen, G. J. Syntheses., Solution multi-NMR characterization, and reactivities of $[C_6F_5Xe]^+$ salts of weakly coordinating borate anions, $[BY_4]^-$ (Y = CF_3, C_6F_5, CN, or $OTeF_5$). *Inorg. Chem.* **2007**, *46* (22), 9425–9437.

Koppel, I. A.; Burk, P.; Koppel, I.; Leito, I. Generalized principle of designing neutral superstrong brønsted acids. *J. Am. Chem. Soc.* **2002**, *124* (19), 5594–5600.

Koschel, D.; Gmelin, L.; Meyer, R. J.; Pietsch, E. H. E.; Fluck, E. Carbon nitrogen compounds. In *Gmelin handbook of inorganic and organometallic chemistry*; Verl. Chemie: Berlin, **1971**; p. 475.

Kotch, T. G.; Lees, A. J.; Fuerniss, S. J.; Papathomas, K. I. Photocatalyzed polymerization of aromatic dicyanate esters by iron-arene complexes. *Chem. Mater.* **1995**, *7* (4), 801–805.

Kozirovski, Y.; Folman, M. Infra-red spectrum and spectral shifts of HCN adsorbed on evaporated alkali halides. *Trans. Faraday Soc.* **1966**, *62*, 808–820.

Kraemer, W. P.; Bunker, P. R.; Yoshimine, M. A theoretical study of the rotation-vibration energy levels and dipole moment functions of CCN^+, CNC^+, and C_3. *J. Mol. Spectrosc.* **1984**, *107* (1), 191–207.

Kraft, A. "Notitia Caerulei Berolinensis Nuper Inventi" on the 300th anniversary of the first publication on Prussian blue. *Bull. Hist. Chem.* **2011**, *36* (1), 3–9.

Krause, A. Zum Mechanismus der Blausäuresynthese aus Ammoniak, Methan und Luftsauerstoff Am Platinkontakt. *Monatsh. Chem.* **1965**, *96* (4), 1132–1133.

Krauß, N.; Tebbe, K.-F. Polypseudohalogenide des Kaliums. *Z. für Kristallogr. – Cryst. Mater.* **1986**, *174* (1–4), 124–125.

Kreutzberger, A. Die Chemie des S-Triazins. In *Fortschritte der Chemischen Forschung*; Springer-Verlag: Berlin, **2006**; pp. 273–300.

Kroeker, R. M.; Pacansky, J. Observation of electron beam induced chemistry by tunneling spectroscopy. *J. Chem. Phys.* **1982**, *77* (10), 4955–4956.

Krolevets, A. A.; Antipova, V. V.; Martynov, I. V. Organosilicon and organophosphorus compounds with pseudohalide groups. 2. Reactions of alkoxydimethylsilyl cyanides with chlorides of tricoordinated phosphorus. *Bull. Acad. Sci. USSR, Div. Chem. Sci.* **1991**, *40* (12), 2483–2485.

Krüss, G. Über eine Neue darstellungsmethode Für Nitrile. *Ber. Dtsch. Chem. Ges.* **1884**, *17* (2), 1766–1768.

Kuhn, M.; Mecke, R. Die Reaktion von Dirhodan Mit Aliphatischen Aminen. *Chem. Ber.* **1960**, *93* (3), 618–621.

Kuhn, M.; Mecke, R. IR-Spektroskopische Untersuchungen Am Dicyan-amid-Anion, $[N(CN)_2]$. *Chem. Ber.* **1961a**, *94* (11), 3010–3015.

Kuhn, M.; Mecke, R. IR-spektroskopische Untersuchungen Am Dicyan-amid-Anion, $[N(CN)_2]^-$. *Chem. Ber.* **1961b**, *94* (11), 3010–3015.

Kuhnhen, H. B. Notizen: Reaktion von Dirhodan Mit Substituierten Carbonyl(η-Cyclopentadienyl)Iodoeisen-Komplexen/reaction of Thiocyanogen with Substituted Carbonyl(η-Cyclopentadienyl) Iodoiron Complexes. *Z. Naturforsch.* **1977**, *32* (6), 718–720.

Kulsha, A. V.; Sharapa, D. I. Superhalogen and superacid. *J. Comput. Chem.* **2019**, *40* (26), 2293–2300.

Kumar Sau, A.; Currell, D.; Mazumdar, S.; Mitra, S. An NMR and circular dichroism study of the interaction of thiocyanate with human and cross-linked hemoglobin: identification of Lys-α-99 as a possible dissociation linked binding site. *Biophys. Chem.* **2003**, *106* (3), 233–240.

Küppers, T.; Bernhardt, E.; Willner, H.; Rohm, H. W.; Köckerling, M. Tetracyanoborate salts $M[B(CN)_4]$ with M = singly charged cations: properties and structures. *Inorg. Chem.* **2005**, *44* (4), 1015–1022.

Küppers, T.; Bernhardt, E.; Lehmann, C. W.; Willner, H. Die Tetracyanoborsäuren $H[B(CN)_4]_n$ H_2O, n = 0, 1, 2. *Z. Anorg. Allg. Chem.* **2007**, *633* (10), 1666–1672.

Kurnig, I. J.; Lischka, H.; Karpfen, A. Linear versus cyclic $(HCN)_3$: an ab initio study on structure, vibrational spectra, and infrared intensities. *J. Chem. Phys.* **1990**, *92* (4), 2469–2477.

Kwon, H. K.; Woo, S. H.; Park, J. M. Thiocyanate degradation by acremonium strictum and inhibition by secondary toxicants. *Biotechnol. Lett.* **2002**, *24* (16), 1347–1351.

Labbow, R.; Michalik, D.; Reiß, F.; Schulz, A.; Villinger, A. Isolation of labile pseudohalogen NSO species. *Angew. Chem. Int. Ed.* **2016**, *55* (27), 7680–7684.

Ladenburg, A. *Vorträge Über Die Entwicklungsgeschichte Der Chemie Von Lavoirsier Bis Zur Gegenwart*; Friedrich Vieweg & Sohn: Braunschweig, **1907**.

Landmann, J.; Keppner, F.; Hofmann, D. B.; Sprenger, J. A. P.; Häring, M.; Zottnick, S. H.; Müller-Buschbaum, K.; Ignat'ev, N. V.; Finze, M. Deprotonation of a hydridoborate anion. *Angew. Chem. Int. Ed.* **2017**, *56* (10), 2795–2799.

Langel, W.; Kollhoff, H.; Knözinger, E. From isolated HCN molecules to the crystal: inelastic neutron scattering, far infrared spectroscopy, and normal coordinate analysis. *J. Chem. Phys.* **1989**, *90* (7), 3430–3442.

Lanzisera, D. V.; Andrews, L. Reactions of laser-ablated beryllium atoms with hydrogen cyanide in excess argon. FTIR spectra and quantum chemical calculations on BeCN, BeNC, HBeCN, and HBeNC. *J. Am. Chem. Soc.* **1997a**, *119* (27), 6392–6398.

Lanzisera, D. V.; Andrews, L. Reactions of laser-ablated Al, Ga, in, and Tl atoms with hydrogen cyanide in excess argon. Matrix infrared spectra and density functional theory calculations on new cyanide and isocyanide products. *J. Phys. Chem.* **1997b**, *101* (50), 9660–9665.

Lanzisera, D. V.; Andrews, L.; Taylor, P. R. Reactions of laser-ablated boron atoms with HCN during condensation in argon. A comparison of matrix infrared and DFT, CCSD(T), and CASSCF frequencies of BNC, BCN, HBNC, and HBCN. *J. Phys. Chem.* **1997**, *101* (38), 7134–7140.

Largo-Cabrerizo, A.; Barrientos, C. A comparative theoretical study of the C_2N^+ and $SiCN^+$ ions and their formation processes. *Chem. Phys. Lett.* **1988**, *148* (1), 79–85.

Largo, A.; Barrientos, C. Theoretical studies of possible processes for the interstellar production of phosphorus compounds: reaction of phosphorus(1+) with hydrogen cyanide and protonation of cyanogen phosphide compounds. *J. Phys. Chem.* **1991**, *95* (24), 9864–9868.

Largo-Cabrerizo, A. A theoretical study of the SiCN radical. *Chem. Phys. Lett.* **1988**, *147* (1), 95–98.

Larsen, J.; Madsen, D.; Poulsen, J.-A.; Poulsen, T. D.; Keiding, S. R.; Thøgersen, J. The photoisomerization of aqueous ICN studied by subpicosecond transient absorption spectroscopy. *J. Chem. Phys.* **2002**, *116* (18), 7997–8005.

Larson, J. W.; McMahon, T. B. Gas-phase bihalide and pseudobihalide ions. An ion cyclotron resonance determination of hydrogen bond energies in XHY- species (X, Y = F, Cl, Br, CN). *Inorg. Chem.* **1984**, *23* (14), 2029–2033.

Le Bihan, M. Structure Du cyanure de Sodium Hydraté. *Acta Crystallogr.* **1958**, *11* (11), 770–773.

Le Guennec, M.; Wlodarczak, G.; Chen, W. D.; Bocquet, R.; Demaison, J. Rotational spectrum and equilibrium structure of cyanogen bromide. *J. Mol. Spectrosc.* **1992**, *153* (1–2), 117–132.

Lee, T. J.; Racine, S. C. A coupled-cluster study of the molecular structure, vibrational spectrum and relative energies of the XCN and XNC (X = F, Cl) isomers. *Mol. Phys.* **1995**, *84* (4), 717–725.

Lee, T. J.; Schaefer, H. F. Vibrational frequencies and infrared intensities for H_2CN^+, protonated HCN. *J. Chem. Phys.* **1984**, *80* (6), 2977–2978.

Lee, T. J.; Martin, J. M. L.; Dateo, C. E.; Taylor, P. R. Accurate ab initio quartic force fields, vibrational frequencies, and heats of formation for FCN, FNC, ClCN, and ClNC. *J. Phys. Chem.* **1995**, *99* (43), 15858–15863.

Lee, D.; Lee, Y. S.; Hagebaum-Reignier, D.; Jeung, G.-H. First-order correction for bond energy applied to polar molecules: alkali halides, alkali cyanides, $LiCH_3$, and CH_3F. *Chem. Phys.* **2006**, *327* (2–3), 406–414.

Lee, D.; Lim, I. S.; Lee, Y. S.; Hagebaum-Reignier, D.; Jeung, G.-H. Molecular properties and potential energy surfaces of the cyanides of the groups 1 and 11 metal atoms. *J. Chem. Phys.* **2007**, *126* (24), 244313–244321.

Lee, S. Time-dependent hartree approximation applied to the photodissociation of ICN. *J. Chem. Phys.* **1992**, *97* (1), 227–235.

Lee, T. J. Ab initio characterization of triatomic bromine molecules of potential interest in stratospheric chemistry. *J. Phys. Chem.* **1995**, *99* (41), 15074–15080.

Legon, A. C.; Millen, D. J.; Mjöberg, P. J. The hydrogen cyanide dimer: identification and structure from microwave spectroscopy. *Chem. Phys. Lett.* **1977**, *47* (3), 589–591.

Leibovici, C. A. Quantum-mechanical evaluation of the tilt of the cyano group in difluorocyanamide, cyanodifluoro-phosphine and phosphorus tricyanide. *J. Mol. Struct.* **1973**, *18* (2), 343–345.

Lely, J. A.; Bijvoet, J. M. The crystal structure of lithium cyanide. *Recl. Trav. Chim. Pays-Bas* **1942**, *61* (4), 244–252.

Léonard, C.; Gritli, H.; Chambaud, G. Ab initio study of the spectroscopy of the X2Π electronic ground states of CNO and NCO. *J. Mol. Spectrosc.* **2007**, *243* (1), 90–98.

Léonard, C.; Gritli, H.; Chambaud, G. New study of the stability and of the spectroscopy of the molecular anions NCO^- and CNO^-. *J. Chem. Phys.* **2010**, *133* (12), 124318–124327.

Leopold, J. G.; Faraggi, M. Pulse radiolysis of the cyanate anion in aqueous solution. *J. Phys. Chem.* **1977**, *81* (8), 803–806.

LeSar, R.; Gordon, R. G. Density-functional theory for the solid alkali cyanides. *J. Chem. Phys.* **1982**, *77* (7), 3682–3692.

Letts, E. A. Neue Bildungsweisen der Amide und Nitrile. *Ber. Dtsch. Chem. Ges.* **1872**, *5* (2), 669–674.

Li, X.; Sayah, N.; Jackson, W. M. Laser measurements of the effects of vibrational energy on the reactions of CN. *J. Chem. Phys.* **1984**, *81* (2), 833–840.

Li, X.; Zeng, Y.; Zhang, X.; Zheng, S.; Meng, L. Computational studies of σ-type weak interactions between NCO/NCS radicals and XY (X = H, Cl; Y = F, Cl, and Br). *Sci. China Chem.* **2012**, *55* (7), 1395–1404.

Liebig, J.; Gay-Lussac, J. L. Zerlegung des Knallsauren Silberoxids. *Ann. Phys. Chem.* **1824a**, *77*, 117–124.

Liebig, J.; Gay-Lussac, J. L. Analyse Du Fulminate. *Ann. Chim. Phys.* **1824b**, *25*, 285–311.

Liebig, J.; Wöhler, F. Untersuchungen Über die Cyansäure. *Ann. Phys.* **1830**, *96* (11), 369–400.

Lin, Y.; Heaven, M. C. Observation and analysis of the CN–Ne B–X transition. *J. Chem. Phys.* **1991**, *94* (8), 5765–5768.

Lin, H.-S.; Erickson, M. G.; Lin, Y.; Basinger, W. H.; Lawrence, W. G.; Heaven, M. C. Vibronic relaxation dynamics of CN in Ar matrices and clusters. *Chem. Phys.* **1994**, *189* (2), 235–243.

Linke, K.-H.; Lemmer, F. Röntgenographische Kristallstrukturanalyse von Schwefeldicyanid. *Z. Anorg. Allg. Chem.* **1966a**, *345* (3–4), 203–210.

Linke, K.-H.; Lemmer, F. Röntgenographische Kristallstrukturanalyse von Selendicyanid. *Z. Anorg. Allg. Chem.* **1966b**, *345* (3–4), 211–216.

Linnemann, F. Untersuchung Über Das Cyansulfid. *Justus Liebigs Ann. Chem.* **1861**, *120* (1), 36–47.

Lipscomb, R. D.; Smith, W. C. *Preparation of cyanogen fluoride*. 3008, **1961**.

Liszt, H.; Lucas, R. Comparative chemistry of diffuse clouds. *Astron. Astrophys.* **2001**, *370* (2), 576–585.

Liu, R.; Chen, Z.; Yao, Y.; Li, Y.; Cheema, W. A.; Wang, D.; Zhu, S. Recent advancements in g-C_3N_4-based photocatalysts for photocatalytic CO_2 reduction: a mini review. *RSC Adv.* **2020**, *10* (49), 29408–29418.

Livinghouse, T. Trimethylsilyl cyanide: cyanosilation of p-benzoquinone. *Org. Synth.* **1981**, *60*, 126.

Löber, M.; Dolabdjian, K.; Ströbele, M.; Romao, C. P.; Meyer, H.-J. Synthesis, structure, and electronic properties of $Sn(CN_2)$ and $Sn_4Cl_2(CN_2)_3$. *Inorg. Chem.* **2019**, *58* (12), 7845–7851.

Loew, G. H.; Chang, S. Quantum chemical Study of HCN dimer and its role in chemical evolution. *Tetrahedron* **1971**, *27* (13), 2989–3001.

Loew, G. H. Conformation of hydrogen cyanide dimer and its role in chemical evolution. *J. Theor. Biol.* **1971**, *33* (1), 121–130.

Loewenschuss, A.; Marcus, Y. Standard thermodynamic functions of some isolated ions at 100–1000 K. *J. Phys. Chem. Ref. Data* **1996**, *25* (6), 1495–1507.

Loidl, A.; Knorr, K.; Daubert, J.; Dultz, W.; Fitzgerald, W. J. Inelastic neutron scattering by coupled rotational and translational modes in KCN. *Z. Phys. B: Condens. Matter* **1980a**, *38* (2), 153–163.

Loidl, A.; Knorr, K.; Kjems, J. I.; Haussuhl, S. Inelastic neutron scattering by coupled rotational and translational modes in CsCN. *J. Phys. C Solid State Phys.* **1980b**, *13* (14), L349–L355.

Loidl, A.; Haussühl, S.; Kjems, J. K. Elastic properties of CsCN. *Z. Phys. B: Condens. Matter* **1983**, *50* (3), 187–192.

Long, D. A.; Steele, D. Spectroscopic studies of compounds containing the —CN group—II: vibrational spectra, assignments and configuration of sulphur dicyanide $S(CN_2)$. *Spectrochim. Acta* **1963**, *19* (11), 1731–1737.

Long, D. A.; Carrington, R. A. G.; Gravenor, R. B. Vibrational spectra and structure of the tricyanomethanide ion $C(CN)^-_3$. *Nature* **1962**, *196*, 371–372.

Lord, G.; Woolf, A. A. The cyanogen halides. Part III. Their heats of formation and free energies. *J. Chem. Soc.* **1954**, 2546.

Lössner, L.; Kretzschmar, A.; Peitzsch, B.; Salomon, F. Einwirkung von Phosphorchlorid und von Benzoylchlorid Auf Rhodankalium. *J. Prakt. Chem.* **1873**, *7* (1), 474–480.

Lotsch, B. V.; Senker, J.; Schnick, W. Characterization of the thermally induced topochemical solid-state transformation of $NH_4[N(CN)_2]$ into NCN[double bond]$C(NH_2)_2$ by means of X-ray and neutron diffraction as well as Raman and solid-state NMR spectroscopy. *Inorg. Chem.* **2004**, *43* (3), 895–904.

Loupy, A.; Corset, J. Infrared spectral studies of ion association in nonaqueous solutions of cyanide salts with consequences for their nucleophilic reactivity. *J. Solution Chem.* **1976**, *5* (12), 817–831.

Lovallo, C. C.; Klobukowski, M. Improved model core potentials: application to the thermochemistry of organoxenon complexes. *Int. J. Quantum Chem.* **2002**, *90* (3), 1099–1107.

Lu, Y.; Wang, H.; Xie, Y.; Liu, H.; Schaefer, H. F. The cyanate and 2-phosphaethynolate anion congeners ECO^- (E = N, P, as, Sb, Bi): prelude to experimental characterization. *Inorg. Chem.* **2014**, *53* (12), 6252–6256.

Lucchese, R. R.; Schaefer, H. F. Dicyanocarbene. Triplet and singlet structures and energetics. *J. Am. Chem. Soc.* **1977**, *99* (1), 13–14.

Ma, B.; Yamaguchi, Y.; Schaefer, H. F. Spectroscopic constants and potential energy surfaces for the possible interstellar molecules AlNC and AlCN. *Mol. Phys.* **1995**, *86* (6), 1331–1337.

MacLean, E. J.; Harris, K. D. M.; Kariuki, B. M.; Kitchin, S. J.; Tykwinski, R. R.; Swainson, I. P.; Dunitz, J. D. Ammonium cyanate shows N–H···N hydrogen bonding, not N–H···O. *J. Am. Chem. Soc.* **2003**, *125* (47), 14449–14451.

Madelung, W.; Kern, E. Über Dicyanamid. *Justus Liebigs Ann. Chem.* **1922a**, *427* (1), 1–26.

Madelung, W.; Kern, E. Über Tricyanmelamin. *Justus Liebigs Ann. Chem.* **1922b**, *427* (1), 26–34.

Maeda, A.; Habara, H.; Amano, T. Submillimetre-wave spectrum of NCS. *Mol. Phys.* **2007**, *105* (5–7), 477–495.

Magnusson, E. The electronic structures of P(III) compounds with P–C bonds. *Phosphorous Sulfur Relat. Elem.* **1986**, *28* (3), 379–394.

Mai, K.; Patil, G. Alkylsilyl cyanides as silylating agents. *J. Org. Chem.* **1986**, *51* (18), 3545–3548.

Maier, G.; Reisenauer, H. P. Reactions of silicon atoms with cyanogen: generation and matrix-spectroscopic identification of five C_2N_2Si isomers. *Eur. J. Org Chem.* **2005**, *2005* (10), 2015–2021.

Maier, G.; Teles, J. H. Isolierung und Photoisomerisierung von Einfach Substituierten Nitriloxiden. *Angew. Chem.* **1987a**, *99* (2), 152–153.

Maier, G.; Teles, J. H. Isolation and photoisomerization of simply substituted nitrile oxides. *Angew. Chem. Int. Ed.* **1987b**, *26* (2), 155–156.

Maier, G.; Naumann, M.; Reisenauer, H. P.; Eckwert, J. Diisocyanate. *Angew. Chem. Int. Ed.* **1996a**, *35* (15), 1696–1697.

Maier, G.; Naumann, M.; Reisenauer, H. P.; Eckwert, J. Diisocyanat. *Angew. Chem.* **1996b**, *108* (15), 1800–1801.

Maier, G.; Reisenauer, H. P.; Eckwert, J.; Naumann, M.; De Marco, M. Isomers of the elemental composition CN_2O. *Angew. Chem. Int. Ed.* **1997a**, *36* (16), 1707–1709.

Maier, G.; Reisenauer, H.; Eckwert, J.; Naumann, M.; Marco, M. Isomere der Elementarzusammensetzung CN_2O. *Angew. Chem.* **1997b**, *109* (16), 1785–1787.

Maier, G.; Reisenauer, H. P.; Egenolf, H.; Glatthaar, J. Reaction of silicon atoms with hydrogen cyanide: generation and matrix-spectroscopic identification of CHNSi and CNSi isomers. *Eur. J. Org Chem.* **1998**, *1998* (7), 1307–1311.

Maier, G.; Reisenauer, H. P.; Ruppel, R. Dicyanocarbene and its isomers: a matrix spectroscopic study. *Eur. J. Org Chem.* **2003**, *2003* (14), 2695–2701.

Maier, L. Organische Phosphorverbindungen. IX. Über Einige Reaktionen des Methyldibromphosphins [CH_3PBr_2]. *Helv. Chim. Acta* **1963**, *46* (7), 2667–2676.

Maillard, J.; Schmitz-Afonso, I.; Gautier, T.; Afonso, C.; Carrasco, N. Suggested plausible structures for Titan's haze analogs using tandem mass spectrometry. *Icarus* **2021**, *358*, 114181.

Makarewicz, J.; Ha, T.-K. Vibrational states of LiCN calculated from an ab initio potential energy surface. *Chem. Phys. Lett.* **1995**, *232* (5–6), 497–502.

Maki, A.; Decius, J. C. Infrared spectrum of cyanate ion as a solid solution in a potassium iodide lattice. *J. Chem. Phys.* **1958**, *28* (5), 1003–1004.

Maki, A.; Decius, J. C. Vibrational spectrum of cyanate ion in various alkali halide lattices. *J. Chem. Phys.* **1959**, *31* (3), 772–782.

Maki, A. G.; Sams, R. L. High temperature, high resolution infrared spectral measurements on the HNC–HCN equilibrium system. *J. Chem. Phys.* **1981**, *75* (9), 4178–4182.

Mamajanov, I.; Herzfeld, J. HCN polymers characterized by solid state NMR: chains and sheets formed in the neat liquid. *J. Chem. Phys.* **2009**, *130* (13), 1–6.

Mandal, S. K.; Roesky, H. W. Interstellar molecules: guides for new chemistry. *Chem. Commun. (London)* **2010**, *46* (33), 6016–6041.

Marcos-Fernández, A.; Posadas, P.; Rodríguez, A.; González, L. Synthesis and characterization of new dicyanate monomers. A way to obtain fully aromatic crosslinked poly(ether ketone)S. *J. Polym. Sci. Part A: Polym. Chem.* **1999**, *37* (16), 3155–3168.

Marín-Yaseli, M. R.; Cid, C.; Yagüe, A. I.; Ruiz-Bermejo, M. Detection of macromolecular fractions in HCN polymers using electrophoretic and ultrafiltration techniques. *Chem. Biodiversity* **2017**, *14* (2), e1600241.

Markley, T. J.; Toby, B. H.; Pearlstein, R. M.; Ramprasad, D. New synthesis routes to lithium and cesium cyanide salts. *Inorg. Chem.* **1997**, *36* (15), 3376–3378.

Marszalek, M.; Fei, Z.; Zhu, D.-R.; Scopelliti, R.; Dyson, P. J.; Zakeeruddin, S. M.; Grätzel, M. Application of ionic liquids containing tricyanomethanide $[C(CN)_3]^-$ or tetracyanoborate $[B(CN)_4]^-$ anions in dye-sensitized solar cells. *Inorg. Chem.* **2011**, *50* (22), 11561–11567.

Martin, G.; Barbour, W. *The cyanide and Prussiate Industry*; Crosby Lockwood and Son: London, **1915**; Vol. Chapter VI.

Martin, J. M. L.; Taylor, P. R. Ab initio study of the isoelectronic molecules BCN, BNC, and C3 including anharmonicity. *J. Phys. Chem.* **1994**, *98* (24), 6105–6109.

Martin, J. M. L.; Taylor, P. R.; François, J. P.; Gijbels, R. Ab initio study of the spectroscopy and thermochemistry of the C_2N and CN_2 molecules. *Chem. Phys. Lett.* **1994**, *226* (5–6), 475–483.

Matsuo, T.; Suga, H.; Seki, S. Thermodynamic properties and phase transitions of sodium cyanide crystal. *Bull. Chem. Soc. Jpn.* **1968**, *41* (3), 583–593.

Maxwell, A. F.; Fry, J. S.; Bigelow, L. A. The indirect fluorination of cyanuric chloride. *J. Am. Chem. Soc.* **1958**, *80* (3), 548–549.

Maya, L. Paracyanogen reexamined. *J. Polym. Sci. Part A: Polym. Chem.* **1993**, *31* (10), 2595–2600.

Mayer, E. Einfache Darstellung von Cyanfluorid. *Angew. Chem.* **1969a**, *81* (16), 627.

Mayer, E. Darstellung und Eigenschaften von Tetracyanmethan. *Monatsh. Chem.* **1969b**, *100* (2), 462–468.

Mayer, E. Simple preparation of cyanogen fluoride. *Angew. Chem. Int. Ed.* **1969c**, *8* (8), 601.

McCarthy, M. C.; Apponi, A. J.; Gottlieb, C. A.; Thaddeus, P. Rotational spectra of SiCN, SiNC, and the SiC_nH (N = 2, 4–6) radicals. *J. Chem. Phys.* **2001**, *115* (2), 870–877.

McCoy, A. B. Potential energy surfaces and properties of ICN^- and ICN. *Int. J. Quantum Chem.* **2013**, *113* (3), 366–374.

McDonald, J. R.; Scherr, V. M.; McGlynn, S. P. Lower-energy electronic states of HNCS, NCS^-, and thiocyanate salts. *J. Chem. Phys.* **1969**, *51* (5), 1723–1731.

McEwan, M. J.; Anicich, V. G.; Huntress, W. T.; Kemper, P. R.; Bowers, M. T. Reactions of CN^+ and C_2N^+ ions. *Int. J. Mass Spectrom. Ion Phys.* **1983**, *50* (1–2), 179–187.

McGibbon, G. A.; Kingsmill, C. A.; Terlouw, J. K.; Burgers, P. C. The isomeric C_2NO+ ions NCCO+, CNCO+, CCNO+ and their neutral counterparts are stable species in the gas phase. *Int. J. Mass Spectrom. Ion Processes* **1992**, *121* (1–2), R11–R18.

Meloni, G.; Gingerich, K. A. Thermodynamic investigation of the AlNC and AlCN Isomers by Knudsen cell mass spectrometry. *J. Chem. Phys.* **1999**, *111* (3), 969–972.

Menzer, W. Zur Kenntnis des Germaniumtetracyanids. *Angew. Chem.* **1958**, *70* (21), 656.

Meot-Ner, M.; Speller, C. V. Multicomponent cluster ions. 2. Comparative stabilities of cationic and anionic hydrogen-bonded networks. Mixed clusters of water and hydrogen cyanide. *J. Phys. Chem.* **1989**, *93* (9), 3663–3666.

Meot-Ner, M.; Cybulski, S. M.; Scheiner, S.; Liebman, J. F. Is cyanide significantly anisotropic? Comparison of cyanide vs chloride: clustering with hydrogen cyanide and condensed-phase thermochemistry. *J. Phys. Chem.* **1988**, *92* (10), 2738–2745.

Meot-Ner, M. Solvation of the proton by hydrogen cyanide and acetonitrile. Condensation of hydrogen cyanide with ions in the gas phase. *J. Am. Chem. Soc.* **1978**, *100* (15), 4694–4699.

Meredith, T. J.; Jacobsen, D.; Haines, J. A.; Berger, J. C.; Heijst, A. N. P. *Antidotes for poisoning by cyanide*, 2nd ed.; Cambridge University Press: Cambridge, **1993**.

Merer, A. J.; Travis, D. N. Absorption spectrum of the CCN radical. *Can. J. Phys.* **1965**, *43* (10), 1795–1830.

Merer, A. J.; Travis, D. N. The absorption spectrum of CNC. *Can. J. Phys.* **1966**, *44* (2), 353–372.

Messer, C. E.; Ziegler, W. T. III. Rotation of groups in ionic lattices. The heat capacities of sodium and potassium cyanides. *J. Am. Chem. Soc.* **1941**, *63* (10), 2703–2708.

Metzger, F. J. Calcium cyanide – "powdered hydrocyanic acid". *Ind. Eng. Chem.* **1926**, *18* (2), 161–163.

Meyer, R. E. Zur Kenntnis des Indiums. *Justus Liebigs Ann. Chem.* **1869**, *150* (2), 137–160.

Meyer, J. Zur Kenntnis Der Alkalicyanide. *Z. Anorg. Allg. Chem.* **1921**, *115* (1), 203–217.

Middleton, W. J.; Little, E. L.; Coffman, D. D.; Engelhardt, V. A. Cyanocarbon chemistry. V. Cyanocarbon acids and their salts. *J. Am. Chem. Soc.* **1958**, *80* (11), 2795–2806.

Mihrin, D.; Jakobsen, P. W.; Voute, A.; Manceron, L.; Wugt Larsen, R. High-resolution synchrotron terahertz investigation of the large-amplitude hydrogen bond librational band of $(HCN)_2$. *Phys. Chem. Chem. Phys.* **2018**, *20* (12), 8241–8246.

Mikhailov, V.; Wheeler, M. D.; Ellis, A. M. Laser-induced fluorescence spectroscopy of the BaNC free radical in a supersonic jet. *J. Phys. Chem.* **2003**, *107* (22), 4367–4372.

Miller, F. A.; Wilkins, C. H. Infrared spectra and characteristic frequencies of inorganic ions. *Anal. Chem.* **1952**, *24* (8), 1253–1294.

Miller, F. A.; Carlson, G. L.; Bentley, F. F.; Jones, W. H. Infrared spectra of inorganic ions in the cesium bromide region (700–300 cm^{-1}). *Spectrochim. Acta* **1960**, *16* (1–2), 135–235.

Miller, F. A.; Frankiss, S. G.; Sala, O. Infrared and Raman spectra of $P(CN)_3$ and $as(CN)_3$. *Spectrochim. Acta* **1965**, *21* (4), 775–781.

Miller, E. M.; Sheps, L.; Lu, Y.-J.; Case, A. S.; McCoy, A. B.; Carl Lineberger, W. New view of the ICN A continuum using photoelectron spectroscopy of ICN^-. *J. Chem. Phys.* **2012**, *136* (4), 044313.

Milligan, D. E.; Jacox, M. E. Matrix-isolation study of the photolysis of cyanogen azide. II. The symmetric stretching fundamental of the free radical NCN. *J. Chem. Phys.* **1966**, *45* (5), 1387–1391.

Milligan, D. E.; Jacox, M. E. Matrix-isolation study of the infrared and ultraviolet spectra of the free radical NCO. *J. Chem. Phys.* **1967a**, *47* (12), 5157–5168.

Milligan, D. E.; Jacox, M. E. Spectroscopic study of the vacuum-ultraviolet photolysis of matrix-isolated HCN and halogen cyanides. Infrared spectra of the species CN and XNC. *J. Chem. Phys.* **1967b**, *47* (1), 278–285.

Milligan, D. E.; Jacox, M. E.; Bass, A. M. Matrix isolation study of the photolysis of cyanogen azide. The infrared and ultraviolet spectra of the free radical NCN. *J. Chem. Phys.* **1965**, *43* (9), 3149–3160.

Minkwitz, R.; Gerhard, V. Preparation and spectroscopic characterization of cyansulfonium salts. $S(CN)_3^+AsF_6^-$ and $(CH_3)_2SCN^+MF_6^-$. *Z. Naturforsch.* **1991**, *46b* (3), 265–269.

Minkwitz, R.; Hertel, T. Formation of cyanoiodine dinitrate $NCI(ONO_2)_2$. *Z. Naturforsch. B: J. Chem. Sci.* **1997**, *52* (10), 1191–1193.

Minkwitz, R.; Nowicki, J.; Jahnkow, B.; Koch, M. Darstellung von Cyanhalogenmethyl- Und Dicyanhalogensulfoniumsalzen $CH_3(CN)SHal^+MF_6^-$ und $(CN)_2SHal^+MF_6^-$ (Hal = F, Cl, Br, I; M = As, Sb) sowie von Methylthionitrillium- und (μ-Thio) bisnitriliumhexafluorometallaten $CH_3SCNX^+MF_6^-$ und $S(CNH)_2^{2+}(MF_6^-)_2$ (X = H, D). *Z. Anorg. Allg. Chem.* **1991**, *596* (1), 77–88.

Mishra, S.; Vallet, V.; Poluyanov, L. V.; Domcke, W. Calculation of the vibronic structure of the $\tilde{X}^2\Pi$ photoelectron spectra of XCN, X = F, Cl, and Br. *J. Chem. Phys.* **2006**, *124* (4), 044317.

Moffat, J. B.; Tang, K. F. A theoretical study of the reactive dimerization of HCN. *J. Theor. Biol.* **1976**, *58* (1), 83–95.

Moffat, J. B. A quantum-chemical Study of BCN. *J. Mol. Struct.* **1971**, *7* (3–4), 474–477.

Moffat, J. B. Cyanide-isocyanide isomerization in the structural isomers of cyanogen isocyanate. *Int. J. Quantum Chem.* **1979**, *15* (5), 547–557.

Mokross, B. J.; Pirc, R. Elastic interaction of tunneling impurities in solids. *J. Chem. Phys.* **1978**, *68* (11), 4823–4831.

Moreno, M. A.; Maté, B.; Rodríguez-Lazcano, Y.; Gálvez, O.; Gómez, P. C.; Herrero, V. J.; Escribano, R. The structure and spectroscopy of cyanate and bicarbonate ions. Astrophysical implications. *J. Phys. Chem.* **2013**, *117* (39), 9564–9573.

Morris, S.; Wyller, A. A. Molecular dissociative equilibria in carbon stars. *Astrophys. J.* **1967**, *150*, 877–907.

Morris, D. F. C. Crystal radius of the cyanide ion. *Acta Crystallogr.* **1961**, *14* (5), 547–548.

Mowry, D. T. The preparation of nitriles. *Chem. Rev.* **1948**, *42* (2), 189–283.

Mudder, T.; Botz, M.; Smith, A. *Chemistry and treatment of cyanidation wastes*, 2nd ed.; Mining Journal Books Ltd: London, **1991**.

Müller, P.; Müller-Dolezal, H.; Stoltz, R.; Söll, H. Peroxides, carbonic acid derivatives, carboxylic acids, carboxylic acid derivatives. In *Methods of organic chemistry*; Thieme - Houben Weyl: Stuttgart, **2014**; p. 775.

Müller, U. Darstellung, Eigenschaften Und Schwingungsspektren von $K[SbCl_5N_3]$, $K[SbCl_5NCO]$ Und $K[SbCl_5CN]$. *Z. Anorg. Allg. Chem.* **1973**, *396* (2), 187–198.

Murray, J. S.; Lane, P.; Politzer, P. A predicted new type of directional noncovalent interaction. *Int. J. Quantum Chem.* **2007a**, *107* (12), 2286–2292.

Murray, J. S.; Lane, P.; Clark, T.; Politzer, P. σ-Hole bonding: molecules containing group VI atoms. *J. Mol. Model.* **2007b**, *13* (10), 1033–1038.

Murrell, J. N.; Derzi, A. A. Calculations on the ground states of HCN^+ and HNC^+. *J. Chem. Soc., Faraday Trans. 2* **1980**, *76* (3), 319–323.

Muthmann, W.; Schröder, E. Einige Beobachtungen Über Cyanselenverbindungen. *Ber. Dtsch. Chem. Ges.* **1900**, *33* (2), 1765–1769.

Nagarajan, G. Potential field and force constants of phosphorus and arsenic tricyanides. *Proc. Int. Conf. Cosmic Rays, 11th* **1966**, *20* (4), 323–329.

Nagy, P.; Fischer, A.; Glaser, J.; Ilyukhin, A.; Maliarik, M.; Tóth, I. Solubility, complex formation, and redox reactions in the Tl_2O_3–HCN/CN^-–H_2O system. Crystal structures of the cyano compounds $Tl(CN)_3{\cdot}H_2O$, $Na[Tl(CN)_4]{\cdot}3H_2O$, $K[Tl(CN)_4]$, and $Tl^I[Tl^{III}(CN)_4]$ and of $Tl^I{}_2C_2O_4$. *Inorg. Chem.* **2005**, *44* (7), 2347–2357.

Nambu, H. X-ray diffraction study of KOCN at room temperature. *J. Phys. Chem. Solids* **2003**, *64* (11), 2269–2272.

Nauta, K.; Miller, R. E.; Series, N.; Mar, N. Nonequilibrium self-assembly of long chains of polar molecules in superfluid helium. *Science* **1999**, *283* (5409), 1895–1897.

Nauth, A. M.; Opatz, T. Non-toxic cyanide sources and cyanating agents. *Org. Biomol. Chem.* **2019**, *17* (1), 11–23.

Nenajdenko, V. *Fluorine in heterocyclic chemistry*, Vol. 2; Nenajdenko, V., Ed.; Springer International Publishing: Cham, **2014**.

Neubert, T. J.; Susman, S. Purification and single-crystal growth of potassium cyanide. *J. Chem. Phys.* **1964**, *41* (3), 722–729.

Neubner, R. Die Umwandlungsgleichung $Ba(CN)_2 \rightarrow BaCN_2 + C$ Im Temperaturgebiet von 500 Bis 1000 °C. *Z. Elektrochem. Angew. Phys. Chem.* **1934**, *40* (10), 693–698.

Neukirch, M.; Tragl, S.; Meyer, H.-J.; Küppers, T.; Willner, H. M $[B(CN)_4]_2$: Zwei Neue Tetracyanoborate Mit Zweiwertigen Kationen (M = Zn, Cu). *Z. Anorg. Allg. Chem.* **2006**, *632* (6), 939–944.

Newhouse, K.; Chiu, N. *Toxicological review of hydrogen cyanide and cyanide salts*; EPA - United States Environmental Protection Agency: Washington D.C., **2010**.

Ng, V. M.; Xu, M.; Huang, S. Y.; Long, J. D.; Xu, S. Assembly and photoluminescence of SiCN nanoparticles. *Thin Solid Films* **2006**, *506–507*, 283–287.

Ngassam, V.; Orel, A. E.; Suzor-Weiner, A. Ab initio study of the dissociative recombination of $HCNH^+$. *J. Phys. Conf. Ser.* **2005**, *4*, 224–228.

Nitschke, C.; Köckerling, M. A new transition metal tetracyanidoborate: synthesis, structure and properties of Co $[B(CN)_4]_2{\cdot}2H_2O$. *Z. Anorg. Allg. Chem.* **2009**, *635* (3), 503–507.

Nitschke, C.; Köckerling, M. Iron salts with the tetracyanidoborate anion: $[Fe^{III}(H_2O)_6][B(CN)_4]_3$, coordination polymer $[Fe^{II}(H_2O)_2\{\kappa^2N[B(CN)_4]\}_2]$, and $[Fe^{II}(DMF)_6][B(CN)_4]_2$. *Inorg. Chem.* **2011**, *50* (10), 4313–4321.

Nitschke, C.; Köckerling, M.; Bernhardt, E.; Küppers, T.; Willner, H. Structural diversity and spectral and thermal properties of the first alkaline earth metal tetracyanidoborates: $[Mg(H_2O)_6][B(CN)_4]_2$, $[Mg(H_2O)_2][B(CN)_4]_2$, $[Mg(DMF)_6][B(CN)_4]_2$, $[Ca(H_2O)_3][B(CN)_4]_2$, and $[Ca(H_2O)_2(CH_3CN)][B(CN)_4]_2$. *Dalton Trans.* **2014**, *43* (19), 7128–7138.

Nolan, M. F.; Pendlebury, J. N.; Smith, R. H. Kinetics of the reactions Br_2 + HCN, BrCN + I^-, $S(CN)_2$ + I^- in aqueous acid solution. *Int. J. Chem. Kinet.* **1975**, *7* (2), 205–214.

Norbury, A. H.; Thompson, M.; Songstad, J. X-ray photoelectron spectroscopy of the cynate, thiocyanate, selenocyanate and tellurocyanate ions. *Inorg. Nucl. Chem. Lett.* **1973**, *9* (3), 347–350.

North, M.; Omedes-Pujol, M.; Young, C. Kinetics and mechanism of the racemic addition of trimethylsilyl cyanide to aldehydes catalysed by Lewis bases. *Org. Biomol. Chem.* **2012**, *10* (21), 4289–4298.

Northrup, F. J.; Sears, T. J. Laser-induced fluorescence spectroscopy of NCS in a free jet expansion. *J. Chem. Phys.* **1989**, *91* (2), 762–774.

Northrup, F. J.; Sears, T. J. Renner–Teller Spin-orbit and Fermi-resonance interactions in $X^2\Pi$ NCS Investigated by LIF spectroscopy. *Mol. Phys.* **1990**, *71* (1), 45–64.

Noshita, T.; Kidachi, Y.; Funayama, H.; Kiyota, H.; Yamaguchi, H.; Ryoyama, K. Anti-nitric oxide production activity of isothiocyanates correlates with their polar surface area rather than their lipophilicity. *Eur. J. Med. Chem.* **2009**, *44* (12), 4931–4936.

Oberhammer, H. Die Molekülstruktur des Tetracyanmethans. *Z. Naturforsch., A: Phys. Sci.* **1971**, *26a* (12), 2043–2046.

Oberhauser, F. Das Verhalten des Bromcyans Gegenüber Metallsalzen. *Ber. Dtsch. Chem. Ges.* **1927**, *60* (6), 1434–1439.

Ohshima, Y.; Endo, Y. Fourier-transform microwave spectroscopy of CCN ($X\ ^2\Pi_{1/2}$). *J. Mol. Spectrosc.* **1995**, *172* (1), 225–232.

Ohtoshi, H.; Tsukiyama, K.; Yanagibori, A.; Shibuya, K.; Obi, K.; Tanaka, K. Laser induced fluorescence of NCS in the gas phase. *Chem. Phys. Lett.* **1984**, *111* (1–2), 136–140.

Okabayashi, T.; Tanimoto, M. Millimeter and submillimeter wave spectroscopy of HNC and DNC in the vibrationally excited states. *J. Chem. Phys.* **1993**, *99* (5), 3268–3271.

Okabe, H.; Mele, A. Photodissociation of NCN_3 in the vacuum-ultraviolet production of CN $B^2\Sigma$ and NCN $A^3\Pi$. *J. Chem. Phys.* **1969**, *51* (5), 2100–2106.

Okabe, H. Photodissociation of HNCO in the vacuum ultraviolet; production of NCO $A^2\Sigma$ and NH($A^3\pi$, πc^1). *J. Chem. Phys.* **1970**, *53* (9), 3507–3515.

Okubo, T.; Ise, N. Catalysis of the ammonium cyanate-urea conversion by polyelectrolytes. *Proc. R. Soc. London, Ser. A* **1972**, *327* (1570), 413–424.

Olah, G. A.; Kiovsky, T. E. Stable carbonium ions. LXV. Protonation of hydrogen cyanide and alkyl nitriles in FSO_3H-SbF_5-SO_2 solution. Comparative study of Meerwein's N-alkylnitrilium ions. *J. Am. Chem. Soc.* **1968**, *90* (17), 4666–4672.

Olah, G. A.; White, A. M. Stable carbonium ions. XCI. Carbon-13 nuclear magnetic resonance spectroscopic study of carbonium ions. *J. Am. Chem. Soc.* **1969**, *91* (21), 5801–5810.

Oliphant, N.; Lee, A.; Bernath, P. F.; Brazier, C. R. Fourier transform emission spectroscopy of the jet-cooled CCN free radical. *J. Chem. Phys.* **1990**, *92* (4), 2244–2247.

Olsson, L.; Ottosson, C.-H.; Cremer, D. Properties of R_3SiX compounds and R_3Si^+ ions: do silylium ions exist in solution? *J. Am. Chem. Soc.* **1995**, *117* (28), 7460–7479.

Ong, W.-J.; Tan, L.-L.; Ng, Y. H.; Yong, S.-T.; Chai, S.-P. Graphitic carbon nitride (g-C_3N_4)-based photocatalysts for artificial photosynthesis and environmental remediation: are we a step closer to achieving sustainability? *Chem. Rev.* **2016**, *116* (12), 7159–7329.

Onyszchuk, M.; Castel, A.; Riviere, P.; Satge, J. Germanium(II) pseudohalides: $Ge(CN)_2$, $Ge(NCO)_2$ and $Ge(NCS)_2$; syntheses and reactivities. *J. Organomet. Chem.* **1986**, *317* (3), C35–C37.

Ortiz-Lopez, J.; Luty, F. Optical studies of thermal cycling and hysteresis effects in elastic order-disorder phase transformations. I. Pure alkali-metal cyanide crystals. *Phys. Rev. B* **1988**, *37* (10), 5452–5460.

Osei Owusu, A.; Martin, G. C.; Gotro, J. T. Triazine formation in cyanate-based resin systems at room temperature conditions. *Polymer.* **1996**, *37* (21), 4869–4872.

Ott, L.; Rijksen, C.; Ellinger, S.; Sievert, K.; Harloff, J.; Schulz, A. Method for the preparation of tetraalkylammonium tetracyanidoborates. WO 2014029834 A1 20140227, **2014a**.

Ott, L.; Rijksen, C.; Ellinger, S.; Sievert, K.; Harloff, J.; Schulz, A. Method for the preparation of tetraalkylammonium or tetraalkylphosphonium tricyanidofluoroborates. WO 2014029833 A1 20140227, **2014b**.

Pacansky, J.; Dalal, N. S.; Bagus, P. S. SCF ab-initio ground state potential energy surfaces for HCN and HCN^-. *Chem. Phys.* **1978**, *32* (2), 183–187.

Pacansky, J. The infrared spectrum of a molecular aggregate. The hydrocyanic acid dimer isolated in an argon matrix. *J. Phys. Chem.* **1977**, *81* (24), 2240–2243.

Palatinszky, M.; Herbold, C.; Jehmlich, N.; Pogoda, M.; Han, P.; Von Bergen, M.; Lagkouvardos, I.; Karst, S. M.; Galushko, A.; Koch, H.; Berry, D.; Daims, H.; Wagner, M. Cyanate as an energy source for nitrifiers. *Nature* **2015**, *524* (7563), 105–108.

Pan, S.; Gupta, A.; Saha, R.; Merino, G.; Chattaraj, P. K. A coupled-cluster study on the noble gas binding ability of metal cyanides versus metal halides (metal = Cu, Ag, Au). *J. Comput. Chem.* **2015**, *36* (29), 2168–2176.

Panas, I. A self-consistent crystal field approach to the structures of molecular crystals applied to solid HCN. *Chem. Phys. Lett.* **1992**, *194* (3), 239–246.

Panas, I. Two hypothetical structures of solid FCN. *Theor. Chim. Acta* **1994**, *87* (4–5), 335–342.

Parent, D. C. Reactions of the carbene ions C_nN^+ with labeled methane: mechanistic interpretation. *J. Am. Chem. Soc.* **1990**, *112* (16), 5966–5973.

Park, D. J.; Stern, A. G.; Wilier, R. L. A convenient laboratory preparation of cyanogen. *Synth. Commun.* **1990**, *20* (18), 2901–2906.

Park, J. *The cyanide process of gold extraction*; Nabu Press: London, **2014**.

Parry, G. S. Studies in domain crystallography. II. A new low-temperature crystal structure of potassium cyanide. *Acta Crystallogr.* **1962**, *15* (6), 601–607.

Pascoli, G.; Lavendy, H. Are C_nN^- clusters really bent? *Chem. Phys. Lett.* **1999**, *312* (2–4), 333–340.

Pasinszki, T. Quantum-chemical study of the structure and stability of pseudohalogens: OCN–NCO and its isomers. *Phys. Chem. Chem. Phys.* **2008**, *10* (10), 1411.

Pasternack, L.; Dagdigian, P. J. Laser-fluorescence study of the reactions of alkaline earth atoms with BrCN: spectroscopic observation of the alkaline earth monocyanides. *J. Chem. Phys.* **1976**, *65* (4), 1320–1326.

Pau, C. F.; Hehre, W. J. Heat of formation of hydrogen isocyanide by ion cyclotron double resonance spectroscopy. *J. Phys. Chem.* **1982**, *86* (3), 321–322.

Paul, D. E.; Dalby, F. W. Kinetics of disappearance of the CN radical formed from C_2N_2. *J. Chem. Phys.* **1962**, *37* (3), 592–598.

Pauling, L.; Springall, H. D.; Palmer, K. J. The electron diffraction investigation of methylacetylene, dimethylacetylene, dimethyldiacetylene, methyl cyanide, diacetylene, and cyanogen. *J. Am. Chem. Soc.* **1939**, *61* (4), 927–937.

Pauling, L. The rotational motion of molecules in crystals. *Phys. Rev.* **1930**, *36* (3), 430–443.

Pauling, L. *Die Natur Der Chemischen Bindung*, 3. Aufl.; Verl. Chemie: Weinheim/Bergstr., **1968**.

Pearson, P. K.; Schaefer, H. F. Some properties of H_2CN^+: a potentially important interstellar species. *Astron. J.* **1974**, *192* (2), 33–36.

Pearson, P. K.; Schaefer, H. F.; Wahlgren, U. Potential energy surface for the model unimolecular reaction HNC → HCN. *J. Chem. Phys.* **1975**, *62* (2), 350–354.

Pearson, R. G. Hard and soft acids and bases, HSAB, Part 1: fundamental principles. *J. Chem. Educ.* **1968**, *45* (9), 581–587.

Pedersen, L. The structure of the triatomic free radicals HCO, HCN^-, and FCO. *J. Mol. Struct.* **1970**, *5* (1–2), 21–26.

Penna-Franca, E.; Dodson, R. W. The effect of cyanide on the rate of the Thallous-Thallic exchange reaction. *J. Am. Chem. Soc.* **1955**, *77* (9), 2651–2653.

Penneman, R. A.; Staritzky, E. Infra-red and crystallographic investigation of the TlCN–KCN–H_2O system; the lack of Tl(I)-cyanide complexes. *J. Inorg. Nucl. Chem.* **1958**, *6* (2), 112–118.

Penzias, A. A.; Wilson, R. W.; Jefferts, K. B. Hyperfine structure of the CN radical determined from astronomical observations. *Phys. Rev. Lett.* **1974**, *32* (13), 701–703.

Perry, J. H.; Bardwell, D. C. The vapor pressures of solid and liquid cyanogen. *J. Am. Chem. Soc.* **1925**, *47* (11), 2629–2632.

Petersen, G.; Franck, H. H. Beiträge Zur Kenntnis des Calciumcyanides, Insbesondere Zur Umwandlung Calciumcyanid ⇄ Calciumcyanamid. *Z. Anorg. Allg. Chem.* **1938**, *237* (1), 1–37.

Peterson, P. E.; Abu-Omar, M.; Johnson, T. W.; Parham, R.; Goldin, D.; Henry, C.; Cook, A.; Dunn, K. M. Ab initio predictions of vibrational frequencies for cationic species. *J. Phys. Chem.* **1995**, *99* (16), 5927–5933.

Petrie, S.; Freeman, C. G.; Meot-Ner, M.; McEwan, M. J.; Ferguson, E. E. Experimental study of HCN^+ and HNC^+ ion chemistry. *J. Am. Chem. Soc.* **1990**, *112* (20), 7121–7126.

Petrie, S. Structural trends in the monocyanides of the second-row metal ions Na^+, Mg^{m+} (m = 1, 2), and Al^n+ (n = 1–3). *J. Phys. Chem.* **1996**, *100* (28), 11581–11588.

Petrie, S. Trends in M(CN) isomerism: a computational study of monocyanides of the main-group third row atoms. *Phys. Chem. Chem. Phys.* **1999a**, *1* (12), 2897–2905.

Petrie, S. Magnesium dicyanide: three isomers or seven? *J. Phys. Chem.* **1999b**, *103* (13), 2107–2116.

Petrov, P. K.; Charters, J. W.; Wallschläger, D. Identification and determination of selenosulfate and selenocyanate in flue gas desulfurization waters. *Environ. Sci. Technol.* **2012**, *46* (3), 1716–1723.

Pettersson, M.; Lundell, J.; Khriachtchev, L.; Räsänen, M. Neutral rare-gas containing charge-transfer molecules in solid matrices. III. HXeCN, HXeNC, and HKrCN in Kr and Xe. *J. Chem. Phys.* **1998**, *109* (2), 618–625.

Pézolet, M.; Savoie, R. Raman spectra of liquid and crystalline HCN and DCN. *Can. J. Chem.* **1969**, *47* (16), 3041–3048.

Pézolet, M.; Savoie, R. Raman spectra of liquid and crystalline ClCN and BrCN. *J. Chem. Phys.* **1971**, *54* (12), 5266–5270.

Pham, T. A.; Kim, D.-P.; Lim, T.-W.; Park, S.-H.; Yang, D.-Y.; Lee, K.-S. Three-dimensional SiCN ceramic microstructures via nano-stereolithography of inorganic polymer photoresists. *Adv. Funct. Mater.* **2006**, *16* (9), 1235–1241.

Pham-Tran, N.-N.; Hou, X. J.; Nguyen, M. T. On the nature of the CP group adjacent to a valence-deficient atom: phosphaethynyl substituent vs. phosphorus center. *J. Phys. Org. Chem.* **2006**, *19* (3), 167–172.

Plumet, J.; Roscales, S. Mini-review: organic catalysts in the 1,3-dipolar cycloaddition reactions of nitrile oxides. *Heterocycles* **2019**, *99* (2), 725.

Poletto, G.; Rigutti, M. The $A^2\Pi$ and $X^2\Sigma$ states of the CN molecule from the Berkeley analysis of the CN red system. *Nuovo Cimento* **1965**, *39* (2), 519–530.

Politzer, P.; Murray, J. S.; Lane, P. σ-Hole bonding and hydrogen bonding: competitive interactions. *Int. J. Quantum Chem.* **2007**, *107* (15), 3046–3052.

Pople, J. A.; Krishnan, R.; Schlegel, H. B.; Binkley, J. S. Electron correlation theories and their application to the study of simple reaction potential surfaces. *Int. J. Quantum Chem.* **1978**, *14* (5), 545–560.

Poppinger, D.; Radom, L. A. Theoretical study of substituted CHNO isomers. *J. Am. Chem. Soc.* **1978**, *100* (12), 3674–3685.

Price, C. J.; Chen, H.-Y.; Launer, L. M.; Miller, S. A. Weakly coordinating cations as alternatives to weakly coordinating anions. *Angew. Chem. Int. Ed.* **2009**, *48* (5), 956–959.

Provasi, P. F.; Aucar, G. A.; Sanchez, M.; Alkorta, I.; Elguero, J.; Sauer, S. P. A. Interaction energies and NMR indirect nuclear spin-spin coupling constants in linear NCH and CNH complexes. *J. Phys. Chem.* **2005**, *109*, 6555–6564.

Purdy, A. P.; Houser, E.; George, C. F. Lithium dicyanamide, its reactions with cyanuric chloride, and the crystal structures of

$LiN(CN)_2(MeCN)_2$ and $LiCN(C_5H_5N)_2$. *Polyhedron* **1997**, *16* (20), 3671–3679.

Pyykkö, P.; Atsumi, M. Molecular double-bond covalent radii for elements Li-E112. *Chem. Eur J.* **2009**, *15* (46), 12770–12779.

Pyykkö, P.; Runeberg, N. Ab initio studies of bonding trends. *J. Mol. Struct.: Theochem.* **1991**, *234* (C), 269–277.

Pyykko, P.; Zhao, Y. Ab initio study of bonding trends. 4. The 22-electron A=B=C series: possible new anions down to NCB^{4-} and possible new cations up to FNF^{3+}. *J. Phys. Chem.* **1990**, *94* (20), 7753–7759.

Qin, L.; Yu, J.; Kuang, S.; Xiao, C.; Bai, X. Few-atomic-layered boron carbonitride nanosheets prepared by chemical vapor deposition. *Nanoscale* **2012**, *4* (1), 120–123.

Rabalais, J. W.; McDonald, J. R.; McGlynn, S. P. Electronic states of HNCO, cyanate salts, and organic isocyanates. II. Absorption studies. *J. Chem. Phys.* **1969a**, *51* (11), 5112–5117.

Rabalais, J. W.; McDonald, J. R.; McGlynn, S. P. Electronic states of HNCO, cyanate salts, and organic isocyanates. I. Luminescence studies. *J. Chem. Phys.* **1969b**, *51* (11), 5095–5102.

Radford, H. E.; Broida, H. P. Rotational perturbations in CN. Zero-field theory, optical zeeman effect, and microwave transition probabilities. *Phys. Rev.* **1962**, *128* (1), 231–242.

Raksit, A. B.; Bohme, D. K. Flow tube studies of reactions of cyanogen with ions selected from cyanogen. *Int. J. Mass Spectrom. Ion Processes* **1985**, *63* (2–3), 217–229.

Ramos, M. N.; Taft, C. A.; Tostes, J. G. R.; Lester, W. A. An spectroscopic study of the HCN…HCN and HCN…HNC linear complexes. *J. Mol. Struct.* **1988**, *175*, 303–306.

Rao, V. S.; Vijay, A.; Chandra, A. K. A comparative study of the energetics, structures, and mechanisms of the HCN ↔ HNC and LiCN ↔ LiNC isomerizations. *Can. J. Chem.* **1996**, *74* (6), 1072–1077.

Raschig, F. Zur Kenntniss des Jodstickstoffs. *Justus Liebigs Ann. Chem.* **1885**, *230* (2), 212–221.

Rastogi, M. K. Synthesis and characterization of some cyclopentadienylantimony(III) pseudohalides. *Synth. React. Inorg. Met.-Org. Chem.* **1987**, *17* (5), 525–537.

Reckeweg, O.; Schulz, A.; Leonard, B.; DiSalvo, F. J. Single-crystal X-ray diffraction study of Na[OCN] at 170 K and its vibrational spectra. *Z. Naturforsch. B* **2010**, *65* (4), 528–532.

Reddy, P. N.; Srikanth, R.; Bhanuprakash, K.; Srinivas, R. Generation and characterization of ionic and neutral methylene isothiocyanate by a combined tandem mass spectrometry and computational study. *Rapid Commun. Mass Spectrom.* **2004**, *18* (17), 1939–1946.

Redmon, L. T.; Purvis, G. D.; Bartlett, R. J. Correlation effects in the isomeric cyanides: HNC ↔ HCN, LiNC ↔ gLiCN, and BNC ↔ gBCN. *J. Chem. Phys.* **1980**, *72* (2), 986–991.

Reeve, S. W.; Burns, W. A.; Lovas, F. J.; Suenram, R. D.; Leopold, K. R. Microwave spectra and structure of hydrogen cyanide-boron trifluoride: an almost weakly bound complex. *J. Phys. Chem.* **1993**, *97* (41), 10630–10637.

Reghunadhan Nair, C. P.; Mathew, D.; Ninan, K. N. *Cyanate ester resins, recent developments. Advances in polymer science*. Springer, Berlin, Heidelberg **2001**, pp. 1–99.

Rehwald, W.; Sandercock, J. R.; Rossinelli, M. Elastic properties of KCN and $K(CN)_{1-x}Cl_x$. *Phys. Status Solidi* **1977**, *42* (2), 699–705.

Reifsig, T. Über Einige Rubidiumverbindungen. *Justus Liebigs Ann. Chem.* **1863**, *127* (1), 33–37.

Renz, F.; Jung, S.; Klein, M.; Menzel, M.; Thünemann, A. F. Molecular switching complexes with iron and tin as central atom. *Polyhedron* **2009a**, *28* (9–10), 1818–1821.

Renz, F.; Zaba, C.; Roßberg, L.; Jung, S.; Klein, M.; Klingelhöfer, G.; Wünsche, A.; Reinhardt, S.; Menzel, M. Spin transition in heptanuclear star-shaped iron(III)–antimony(V) NCS- and CN-bridged compounds. *Polyhedron* **2009b**, *28* (9–10), 2036–2038.

Rhimi, B.; Wang, C.; Bahnemann, D. W. Latest progress in g-C_3N_4 based heterojunctions for hydrogen production via photocatalytic water splitting: a mini review. *J. Phys. Energy* **2020**, *2* (4), 042003.

Richardson, N. A.; Yamaguchi, Y.; Schaefer, H. F. Isomerization of the interstellar molecule silicon cyanide to silicon isocyanide through two transition states. *J. Chem. Phys.* **2003**, *119* (24), 12946–12955.

Riemenschneider, W. Neue Einstufen-Synthese von Dicyan Oder Oxamid aus Blausäure. *Chem. Ing. Tech.* **1978**, *50* (1), 55.

Riggs, N.; Radom, L. Ab initio studies on amides: cyanamide, dicyanamide and tricyanamide. *Aust. J. Chem.* **1985**, *38* (6), 835.

Robles, N. L.; Flores Antognini, A.; Romano, R. M. Formation of XNCO species (X=F, Cl) through matrix-isolation photochemistry of XSO_2NCO molecules. *J. Photochem. Photobiol., A* **2011**, *223* (2–3), 194–201.

Roesky, H. W.; Dhathathreyan, K. S. Insertion of $P(CN)_3$ and $as(CN)_3$ as their isonitrile forms into the dimer of hexafluorothioacetone. *J. Chem. Soc., Chem. Commun.* **1984**, 1053–1054.

Roesky, H. W.; Dhathathreyan, K. S.; Noltemeyer, M.; Sheldrick, G. M. Reactions of the hexafluorothioacetone dimer with cyanides of phosphorus, arsenic and germanium. *Z. Naturforsch., B: J. Chem. Sci.* **1985**, *40* (2), 240–246.

Roesky, H. W. Preparation of tetrachlorodicyanophosphates and the existence of tetrachlorodifluorophosphates. *Angew. Chem. Int. Ed.* **1967**, *6* (4), 363.

Rogers, M. T.; Gross, K. J. The electric moments of some sulfur and selenium compounds. *J. Am. Chem. Soc.* **1952**, *74* (21), 5294–5296.

Romano, J. A.; Lukey, B. J.; Salem, H. *Chemical warfare agents chemistry, pharmacology, toxicology, and therapeutics*; CRC Press: Boca Raton, **2007**.

Root, K. D. J.; Symons, M. C. R.; Weatherley, B. C. Electron spin resonance spectrum of HCN^- in alkali halide matrices. *Mol. Phys.* **1966**, *11* (2), 161–164.

Rösslein, M.; Hanratty, M. A.; Maier, J. P. The r_s-structure of bromocyanogen cation: $BrCN^+$ [Xtilde]$^2\Pi$. *Mol. Phys.* **1989**, *68* (4), 823–833.

Rossmanith, K. Neue Wege Zur Herstellung von Reinem Lithiumcyanid und Lithiumcyanoargentat. *Monatsh. Chem.* **1965**, *96* (6), 1690–1694.

Roth, K. Berliner Blau: Alte Farbe in Neuem Glanz. *Chem. Unserer Zeit* **2003**, *37* (2), 150–151.

Rowe, J. M.; Rush, J. J.; Prince, E.; Chesser, N. J. Neutron scattering studies of crystal dynamics and order-disorder phase transitions in alkali cyanides. *Ferroelectrics* **1977a**, *16* (1), 107–109.

Rowe, J. M.; Rush, J. J.; Prince, E. Neutron diffraction study of the structure and phase transitions of alkali cyanide crystals. *J. Chem. Phys.* **1977b**, *66* (11), 5147–5149.

Rowe, J. M.; Rush, J. J.; Susman, S. Neutron powder diffraction study of phase transitions and structures of $(KCN)_x(KBr)_{1-x}$ mixed crystals. *Phys. Rev. B* **1983**, *28* (6), 3506–3511.

Rowe, J. M.; Rush, J. J.; Lüty, F. Crystal structure of rubidium cyanide at 4 K determined by neutron powder diffraction. *Phys. Rev. B* **1984**, *29* (4), 2168–2170.

Rubo, A.; Kellens, R.; Reddy, J.; Steier, N.; Hasenpusch, W. Alkali metal cyanides. In *Ullmann's encyclopedia of industrial chemistry*; Wiley-VCH Verlag GmbH & Co. KGaA: Weinheim, Germany, **2006**; pp. 1–16.

Rüger, C. P.; Maillard, J.; Le Maître, J.; Ridgeway, M.; Thompson, C. J.; Schmitz-Afonso, I.; Gautier, T.; Carrasco, N.; Park, M. A.; Giusti, P.; Afonso, C. Structural study of analogues of Titan's haze by trapped ion mobility coupled with a fourier transform ion cyclotron mass spectrometer. *J. Am. Soc. Mass Spectrom.* **2019**, *30* (7), 1169–1173.

Ruiz-Bermejo, M.; Zorzano, M.-P.; Osuna-Esteban, S. Simple organics and biomonomers identified in HCN polymers: an overview. *Life* **2013**, *3* (3), 421–448.

Ruoff, R. S.; Emilsson, T.; Klots, T. D.; Chuang, C.; Gutowsky, H. S. Rotational spectrum and structure of the linear HCN trimer. *J. Chem. Phys.* **1988**, *89* (1), 138–148.

Ruoff, A. Die Kraftkonstanten der Moleküle FCN, ClCN, BrCN und ICN. *Spectrochim. Acta, Part A* **1970**, *26* (3), 545–556.

Ruscic, B.; Berkowitz, J. The H–NCS bond energy, ΔH^{O}_{f} (HNCS), ΔH^{O}_{f} (NCS), and IP(NCS) from photoionization mass spectrometric studies of HNCS, NCS, and $(NCS)_2$. *J. Chem. Phys.* **1994**, *101* (9), 7975–7989.

Rusinov, V. L.; Nosova, E. V.; Charushin, V. N. Fluorinated triazines. In *Fluorine in heterocyclic chemistry*, Vol. 2; Springer International Publishing: Cham, **2014**; 673–716.

Ryu, I.; Murai, S.; Shinonaga, A.; Horiike, T.; Sonoda, N. Dimethyldicyanosilane: a reagent for concurrent silylation and cyanosilylation of β-diketones. *J. Org. Chem.* **1978**, *43* (4), 780–782.

Ryu, B. G.; Kim, W.; Nam, K.; Kim, S.; Lee, B.; Park, M. S.; Yang, J. W. A comprehensive study on algal-bacterial communities shift during thiocyanate degradation in a microalga-mediated process. *Bioresour. Technol.* **2015**, *191*, 496–504.

Ryu, I. Dicyanodimethylsilane. *e-EROS Encycl. Reagents Org. Synth.* **2001**, *2* (8), 5–6.

Saal, T.; Christe, K. O.; Haiges, R. Lewis adduct formation of hydrogen cyanide and nitriles with arsenic and antimony pentafluoride. *Dalton Trans.* **2019**, *48* (1), 99–106.

Sagan, C.; Khare, B. N. Tholins: organic chemistry of interstellar grains and gas. *Nature* **1979**, *277* (5692), 102–107.

Sakai, S.; Inagaki, S. Abnormally narrow carbon-metal-carbon bond angle in M(L1)L2 complexes (M = silicon, aluminum, magnesium, sodium; L1 and L2 = CO, CN). *J. Am. Chem. Soc.* **1990**, *112* (22), 7961–7964.

Salud, C.; Feher, M.; Amano, T. Infrared diode laser detection of the v_1 fundamental band of $BrCN^+$. *J. Mol. Spectrosc.* **1993**, *162* (1), 172–177.

Salzner, U.; von Raguè Schleyer, P. $CH_{4-n}X_n$: a comparison between the stabilized X=F series and the destabilized X=CN series. *Chem. Phys. Lett.* **1992**, *190* (5), 401–406.

Samuni, U.; Kahana, S.; Fraenkel, R.; Haas, Y.; Danovich, D.; Shaik, S. The ICN-INC system: experiment and quantum chemical calculations. *Chem. Phys. Lett.* **1994**, *225* (4–6), 391–397.

Sato, T.; Narazaki, A.; Kawaguchi, Y.; Niino, H.; Bucher, G. Dicyanocarbodiimide and trinitreno-s-triazine generated by consecutive photolysis of triazido-s-triazine in a low-temperature nitrogen matrix. *Angew. Chem. Int. Ed.* **2003**, *42* (42), 5206–5209.

Sato, T.; Narazaki, A.; Kawaguchi, Y.; Niino, H.; Bucher, G.; Grote, D.; Wolff, J. J.; Wenk, H. H.; Sander, W. Generation and photoreactions of 2,4,6-trinitreno-1,3,5-triazine, a septet trinitrene. *J. Am. Chem. Soc.* **2004**, *126* (25), 7846–7852.

Schalke, P. M. Cyanates, inorganic salts. In *Ullmann's encyclopedia of industrial chemistry*; Wiley-VCH Verlag GmbH & Co. KGaA: Weinheim, Germany, **2006**.

Schalley, C. A.; Hornung, G.; Schrdder, D.; Schwarz, H. Mass spectrometry as a tool to probe the gas-phase reactivity of neutral molecules. *Int. J. Mass Spectrom. Ion Processes* **1998**, *172* (3), 181–208.

Scheers, J.; Lim, D.-H.; Kim, J.-K.; Paillard, E.; Henderson, W. A.; Johansson, P.; Ahn, J.-H.; Jacobsson, P. All fluorine-free lithium battery electrolytes. *J. Power Sources* **2014**, *251*, 451–458.

Schiavon, R. P.; Caldwell, N.; Morrison, H.; Harding, P.; Courteau, S.; MacArthur, L. A.; Graves, G. J. Star clusters in M31. IV. A comparative analysis of absorption line indices in old M31 and milky way clusters. *Astron. J.* **2012**, *143* (1), 14–32.

Schilke, P.; Walmsley, C. M.; Pineau Des Forets, G.; Roueff, E.; Flower, D. R.; Guilloteau, S. A study of HCN, HNC and their isotopometers in OMC-1. I. Abundances and chemistry. *Astron. Astrophys.* **1992**, *256*, 595–612.

Schmidpeter, A.; Zwaschka, F. Dicyanphosphid. *Angew. Chem.* **1977a**, *89* (10), 747.

Schmidpeter, A.; Zwaschka, F. Dicyanophosphide. *Angew. Chem. Int. Ed.* **1977b**, *16* (10), 704–705.

Schmidpeter, A.; Zwaschka, F. Cyanohalophosphates(III) – hypervalent anions containing lamdba5-phosphorus(III). *Angew. Chem. Int. Ed.* **1979**, *18* (5), 411–412.

Schmidpeter, A.; Burget, G.; Zwaschka, F.; Sheldrick, W. S. Cyanphosphorverbindungen. IX. Cyanidabbau von Weißem Phosphor Zu Dicyanphosphiden und die Dicyanphosphid-Struktur. *Z. Anorg. Allg. Chem.* **1985a**, *527* (8), 17–32.

Schmidpeter, A.; Zwaschka, F.; Sheldrick, W. S. Cyanphosphorverbindungen, 8. Das Ungewöhnliche anion $P_2C_{10}N_{10}^{2-}$. *Chem. Ber.* **1985b**, *118* (3), 1078–1085.

Schmidt, H.; Meinert, H. Elektrolysen von Cyaniden. III. Elektrolysen von Cyaniden in Wasserfreiem Pyridin. *Z. Anorg. Allg. Chem.* **1958**, *295* (3–4), 173–184.

Schmidt, F.; Gruber, L.; Knorr, K. Effects of pressure and of thermal history on the structural phase transition of KCN. *Z. Phys. B: Condens. Matter* **1992**, *87* (1), 127–131.

Schmidt, B.; Schröder, B.; Sonnenberg, K.; Steinhauer, S.; Riedel, S. From polyhalides to polypseudohalides: chemistry based on cyanogen bromide. *Angew. Chem. Int. Ed.* **2019**, *58* (30), 10340–10344.

Schmidtmann, H. Über Einige derivate des Malonitrils. *Ber. Dtsch. Chem. Ges.* **1896**, *29* (2), 1168–1175.

Schmiedekamp, A.; Bock, C. W.; George, P. An ab initio study of the structures and the harmonic and anharmonic stretching force constants of the cyanides HCN, LiCN, FCN, ClCN and isocyanides HNC, LiNC, FNC, ClNC. *J. Mol. Struct.* **1980**, *67*, 107–119.

Schneider, R. Über Das Verhalten des Cyansilbers Zum Schwefelchlorür. *J. Prakt. Chem.* **1885**, *32* (1), 187–210.

Schulz, A.; Klapötke, T. M. Zum Koordinationsverhalten Der Lewis-Basen HCN Und DCN Gegenüber $Cp_2Ti(AsF_6)_2$. *J. Organomet. Chem.* **1992**, *436* (2), 179–183.

Scholl, R. Zur Darstellung des Bromcyans sowie des Mono- und Dibromnitromethans. *Ber. Dtsch. Chem. Ges.* **1896**, *29* (2), 1822–1825.

Schoneshofer, M.; Beck, G.; Henglein, A. Pulsradiolytische Untersuchung der Hydrolyse des Dirhodans. *Chem. Ber.* **1970**, *74*, 1011–1015.

Schrems, O.; Huth, M.; Kollhoff, H.; Wittenbeck, R.; Knözinger, E. FTIR-spectroscopy of molecular clusters in liquid solutions and cryogenic solids. *Ber. Bunsenges. Phys. Chem.* **1987**, *91* (11), 1261–1266.

Schröder, H. Zur Darstellung von Cyanchlorid. *Z. Anorg. Allg. Chem.* **1958**, *297* (5–6), 296–299.

Schultz, P. W. Ab initio calculations of ionic and hydrogen bonding interactions with the OCN^-, SCN^- and $SeCN^-$ anions. *Mol. Phys.* **1996**, *88* (1), 217–246.

Schulz, A.; Klapötke, T. M. Does Diisooxocyan (OCN–NCO) exist? *Inorg. Chem.* **1996**, *35* (16), 4791–4793.

Schulz, A.; Villinger, A. Pseudohalonium ions: $[Me_3Si\text{-}X\text{-}SiMe_3]+$ (X=CN, OCN, SCN, and NNN). *Chem. Eur J.* **2010**, *16* (24), 7276–7281.

Schulz, A.; Surkau, J.; Zander, E. Synthesis of $Pb(CN)_2$. *Priv. Commun.* **2021**.

Schulz, O. *No title*, Göttingen, **1856a**.

Schulz, C. Verbindungen des Cyans Mit den Metallen der Alkalischen Erden. *J. Prakt. Chem.* **1856b**, *68* (1), 257–279.

Schulz, A. Computed spectroscopic data of some basic CN species. *Priv. Commun.* **2021**.

Seel, F.; Wesemann, D. Eine Neue Darstellungsweise Für Dirhodan. *Chem. Ber.* **1953**, *86* (9), 1107–1110.

Seifer, G. B. Cyanuric acid and cyanurates. *Koord. Khim.* **2002**, *28* (5), 301–324.

Selliez, L.; Maillard, J.; Cherville, B.; Gautier, T.; Thirkell, L.; Gaubicher, B.; Schmitz-Afonso, I.; Afonso, C.; Briois, C.; Carrasco, N. High-resolution mass spectrometry for future space missions: comparative analysis of complex organic matter with LAb-CosmOrbitrap and laser desorption/ionization Fourier transform ion cyclotron resonance. *Rapid Commun. Mass Spectrom.* **2020**, *34* (10), 8645.

Sequeira, A. On the detection of cyanide-ion rotation in potassium cyanide by neutron diffraction. *Acta Crystallogr.* **1965**, *18* (2), 291–292.

Shannon, M. S.; Tedstone, J. M.; Danielsen, S. P. O.; Hindman, M. S.; Irvin, A. C.; Bara, J. E. Free volume as the basis of gas solubility and selectivity in imidazolium-based ionic liquids. *Ind. Eng. Chem. Res.* **2012**, *51* (15), 5565–5576.

Shapiro, H.; Hnizda, V. F.; Calingaert, G. *Manufacture of lead cyanide*. US2674519, **1954**.

Sheldrick, W. S.; Kroner, J.; Zwaschka, F.; Schmidpeter, A. Struktur des Dicyanphosphid-Ions Im Kronenether-Natriumsalz. *Angew. Chem.* **1979**, *91* (12), 998–1000.

Sheldrick, W. S.; Schmidpeter, A.; Zwaschka, F.; Dillon, K. B.; Platt, A. W. G.; Waddington, T. C. The structures of hypervalent phosphorus(III) anions $P(CN)_{4-n}Br_n^-$. Transition from ψ-trigonal-bipyramidal to ψ-octahedral co-ordination and deviation from valence shell electron pair repulsion theory. *J. Chem. Soc., Dalton Trans.* **1981**, No. *2*, 413–418.

Sheridan, J.; Tyler, J. K.; Aynsley, E. E.; Dodd, R. E.; Little, R. Microwave spectrum of fluorine cyanide. *Nature* **1960**, *185* (4706), 96.

Shi, D.; Li, W.; Sun, J.; Zhu, Z. MRCI study on spectroscopic and molecular properties of several low-lying electronic states of the CN radical. *J. Quant. Spectrosc. Radiat. Transfer* **2011**, *112* (14), 2335–2346.

Shimada, T.; Matsuo, T.; Suga, H.; Luty, F. Phase transition and glass transition in rubidium cyanide. *J. Chem. Phys.* **1986**, *85* (6), 3530–3536.

Shimada, Y.; Chikamatsu, K.; Kimura, C.; Aoki, H.; Sugino, T. Effect of plasma treatment on interface property of BCN/GaN structure. *Appl. Surf. Sci.* **2006**, *253* (3), 1459–1463.

Shlyaykher, A.; Ehmann, M.; Karttunen, A. J.; Tambornino, F. A comprehensive study on the full series of alkali-metal selenocyanates $A^I[SeCN]$ (A^I = Li–Cs). *Chem. Eur J.* **2021**, *27* (54), 13552–13557.

Shmel'kova, T. K.; Ignatenko, A. V.; Krukovskii, S. P.; Ponomarenko, V. A. Synthesis of fluoro-containing substituted 1,3,5-triazines. *Bull. Acad. Sci. USSR Div. Chem. Sci.* **1989**, *38* (4), 836–840.

Shorter, J. The conversion of ammonium cyanate into urea – a saga in reaction mechanisms. *Chem. Soc. Rev.* **1978**, 1–14.

Shrift, A.; Virupaksha, T. K. Biosynthesis of Se-methylselenocysteine from selenite in selenium-accumulating plants. *Biochim. Biophys. Acta* **1963**, *71*, 483–485.

Sidorov, L. N. Mass spectrometric investigation into inorganic complex molecules and stability of BeF_3, AlF_4, FeF_4. *Koord. Khim.* **1977**, *3* (8), 1128–1139.

Sievert, K.; Schulz, A.; Harloff, J.; Ellinger, St.; Täschler, C. Method for preparation of fluoro cyano compounds of the 15th group with a Lewis acid. WO 2015067404, **2015**.

Simmons, J. W.; Anderson, W. E.; Gordy, W. Microwave spectrum and molecular constants of hydrogen cyanide. *Phys. Rev.* **1950**, *77* (1), 77–79.

Simpson, J. B.; Smith, J. G.; Whiffen, D. H. Microwave spectrum of ICN including $IC^{15}N$. *J. Mol. Spectrosc.* **1972**, *44* (3), 558–570.

Singh, P. Bimetallic tetrathiocyanates and selenocyanates as Lewis acids. *Coord. Chem. Rev.* **1980**, *32* (1), 33–65.

Sinosaki, H.; Hara, R. Unknown. *Technol. Rep. Tohoku Univ.* **1929**, *8* (297).

Šišak, D.; McCusker, L. B.; Buckl, A.; Wuitschik, G.; Wu, Y.-L.; Schweizer, W. B.; Dunitz, J. D. The search for tricyanomethane (cyanoform). *Chem. Eur J.* **2010**, *16* (24), 7224–7230.

Skatrud, D. D.; De Lucia, F. C.; Blake, G. A.; Sastry, K. V. L. N. The millimeter and submillimeter spectrum of CN in its first four vibrational states. *J. Mol. Spectrosc.* **1983**, *99* (1), 35–46.

Slotta, K. H. Bromcyan Und Wasserfreie Blausäure. *Ber. Dtsch. Chem. Ges.* **1934**, *67* (6), 1028–1030.

Smallwood, Z. M.; Davis, M. F.; Hill, J. G.; James, L. J. R.; Portius, P. Syntheses, structures, and infrared spectra of the hexa(cyanido) complexes of silicon, germanium, and tin. *Inorg. Chem.* **2019**, *58* (7), 4583–4591.

Smith, A. G.; Ring, H.; Smith, W. V.; Gordy, W. Interatomic distances and nuclear quadrupole couplings in ClCN, BrCN, and ICN. *Phys. Rev.* **1948**, *74* (4), 370–372.

Smith-Gicklhorn, A. M.; Frankowski, M.; Bondybey, V. E. Tetracyanoethylene, its ions and ionic fragments. *Phys. Chem. Chem. Phys.* **2002**, *4* (8), 1425–1431.

Smolin, E. M.; Rapoport, L. *S-Triazines and derivatives*; Interscience Publishers INC.: New York, **1959**.

Smuczyńska, S.; Skurski, P. Halogenoids as ligands in superhalogen anions. *Inorg. Chem.* **2009**, *48* (21), 10231–10238.

Söderbäck, E. Studien Über Das Freie Rhodan. *Justus Liebigs Ann. Chem.* **1919**, *419* (3), 217–322.

Sommerfeld, T.; Bhattarai, B. $Al(CN)^{3-}{}_6$ and $Al(NC)^{3-}{}_6$ trianions. *Phys. Chem. Chem. Phys.* **2011**, *13* (41), 18393.

Sommerfeld, T. FCN^- and FNC^- radical anions. *Phys. Chem. Chem. Phys.* **2001**, *3* (12), 2394–2399.

Somogyi, Á.; Thissen, R.; Orthous-Daunay, F. R.; Vuitton, V. The role of ultrahigh resolution Fourier transform mass spectrometry (FT-MS) in astrobiology-related research: analysis of meteorites and tholins. *Int. J. Mol. Sci.* **2016**, *17*(4), 439–453.

Sorensen, T. E.; England, W. B. Valence states of the cyano radical Feynman's way. *Int. J. Quantum Chem.* **2002**, *90* (2), 516–533.

Sorokin, D. Y.; Tourova, T. P.; Lysenko, A. M.; Kuenen, J. G. Microbial thiocyanate utilization under highly alkaline conditions. *Appl. Environ. Microbiol.* **2001**, *67* (2), 528–538.

Soto-Blanco, B. *Cyanide: occurrence, characteristics and applications*; Nova Science Publishers: New York, **2013**.

Spencer, H. K.; Lakshmikantham, M. V.; Cava, M. P. Organotellurium chemistry. 1. Benzyl tellurocyanate: a stable alkyl tellurocyanate. *J. Am. Chem. Soc.* **1977**, *99* (5), 1470–1473.

Spencer, E. S.; Dale, E. J.; Gommans, A. L.; Rutledge, M. T.; Vo, C. T.; Nakatani, Y.; Gamble, A. B.; Smith, R. A. J.; Wilbanks, S. M.; Hampton, M. B.; Tyndall, J. D. A. Multiple binding modes of isothiocyanates that inhibit macrophage migration inhibitory factor. *Eur. J. Med. Chem.* **2015**, *93*, 501–510.

Sprenger, J. A. P.; Landmann, J.; Drisch, M.; Ignat'ev, N.; Finze, M. Syntheses of tricyanofluoroborates $M[BF(CN)_3]$ (M = Na, K): $(CH_3)_3SiCl$ catalysis, countercation effect, and reaction intermediates. *Inorg. Chem.* **2015**, *54* (7), 3403–3412.

Stafford, D. A.; Callely, A. G. The utilization of thiocyanate by a heterotrophic bacterium. *J. Gen. Microbiol.* **1969**, *55* (2), 285–289.

Staib, C.; Lant, P. Thiocyanate degradation during activated sludge treatment of Coke–Ovens wastewater. *Biochem. Eng. J.* **2007**, *34* (2), 122–130.

Starynowicz, P. Structure of caesium dicyanamide. *Acta Crystallogr. Sect. C Cryst. Struct. Commun.* **1991**, *47* (10), 2198–2199.

Steimle, T. C.; Fletcher, D. A.; Jung, K. Y.; Scurlock, C. T. Molecular beam optical stark spectroscopy of calcium monocyanide. *J. Chem. Phys.* **1992**, *97* (5), 2909–2919.

Steimle, T. C.; Fletcher, D. A.; Jung, K. Y.; Scurlock, C. T. Erratum: Molecular beam optical stark spectroscopy of calcium monocyanide [J. Chem. Phys. 97, 2909 (1992)]. *J. Chem. Phys.* **1994**, *100* (5), 4025–4026.

Steinkopf, W. Apparatives aus Dem Laboratorium. *J. Prakt. Chem.* **1925**, *109* (1), 347–351.

Støgard, Å. Ab initio calculations on CICN and ONCI. *Chem. Phys. Lett.* **1976**, *40* (3), 429–432.

Stokes, H. T.; Decker, D. L.; Nelson, H. M.; Jorgensen, J. D. Structure of potassium cyanide at low temperature and high pressure determined by neutron diffraction. *Phys. Rev. B* **1993**, *47* (17), 11082–11092.

Stopenko, V. V.; Golub, A. M.; Köhler, H. *Chemistry of pseudohalides*; Elsevier: Amsterdam, **1986**.

Stott, M. B.; Franzmann, P. D.; Zappia, L. R.; Watling, H. R.; Quan, L. P.; Clark, B. J.; Houchin, M. R.; Miller, P. C.; Williams, T. L. Thiocyanate removal from saline CIP process water by a rotating biological contactor, with reuse of the water for bioleaching. *Hydrometallurgy* **2001**, *62* (2), 93–105.

Stratford, J.; Dias, A. E. X. O.; Knowles, C. J. The utilization of thiocyanate as a nitrogen source by a heterotrophic bacterium: the degradative pathway involves formation of ammonia and tetrathionate. *Microbiology* **1994**, *140* (10), 2657–2662.

Strössner, K.; Hochheimer, H. D.; Hönle, W.; Werner, A. High-pressure Raman and X-ray studies of the alkali cyanides up to 27 GPa. *J. Chem. Phys.* **1985**, *83* (5), 2435–2440.

Suga, H.; Matsuo, T.; Seki, S. Thermodynamic properties and order-disorder phase transitions of the potassium cyanide crystal. *Bull. Chem. Soc. Jpn.* **1965**, *38* (7), 1115–1124.

Sugino, T.; Etou, Y.; Tai, T.; Mori, H. Dielectric constant of boron carbon nitride films synthesized by plasma-assisted chemical-vapor deposition. *Appl. Phys. Lett.* **2002**, *80* (4), 649–651.

Sugisaki, M.; Matsuo, T.; Suga, H.; Seki, S. Phase transitions and thermodynamic properties of rubidium and cesium cyanides. *Bull. Chem. Soc. Jpn.* **1968**, *41* (8), 1747–1756.

Sulzer, H. Verfahren Zur Darstellung von Ammoniak und Ameisensäure aus Kalkstickstoff. *Angew. Chem.* **1912**, *25* (25), 1268–1273.

Sun, Y.; Metz, M. V.; Stern, C. L.; Marks, T. J. Al-, Nb-, and Ta-based perfluoroaryloxide anions as cocatalysts for metallocene-mediated Ziegler–Natta olefin polymerization. *Organometallics* **2000**, *19* (11), 1625–1627.

Sundermeyer, W. Salzschmelzen und Ihre Verwendung Als Reaktionsmedien. *Angew. Chem.* **1965**, *77* (6), 241–258.

Swank, D. D.; Willett, R. D. The crystal structure of potassium selenocyanate. *Inorg. Chem.* **1965**, *4* (4), 499–501.

Swanson, H.; Tatge, E. *Standard X-ray diffraction powder patterns*; Washington D.C.: Washington D.C., I, **1953**.

Swenson, J. S.; Renaud, D. J. Dicyanocarbene. *J. Am. Chem. Soc.* **1965**, *87* (6), 1394.

Szopa, C.; Cernogora, G.; Boufendi, L.; Correia, J. J.; Coll, P. PAMPRE: a dusty plasma experiment for Titan's tholins production and study. *Planet. Space Sci.* **2006**, *54* (4), 394–404.

Talbi, D.; Ellinger, Y. Potential energy surfaces for the electronic dissociative recombination of $HCNH^+$: astrophysical implications on the HCN/HNC abundance ratio. *Chem. Phys. Lett.* **1998**, *288* (1), 155–164.

Talbi, D.; Herbst, E. An extensive ab initio study of the $C^+ + NH_3$ reaction and its relation to the HNC/HCN abundance ratio in interstellar clouds. *Astron. Astrophys.* **1998**, *333* (3), 1007–1015.

Talbi, D. An extensive ab initio study of a process of astrophysical interest: the $N^+(N) + CH_3(CH_3^+)$ reaction. *Chem. Phys. Lett.* **1999**, *312* (2–4), 291–298.

Tang, T. B.; Swallowe, G. M.; Mohan, V. K. Application of continuously recorded time-resolved mass spectrometry to the study of thermal explosions. *J. Solid State Chem.* **1984**, *55* (2), 239–242.

Tao, Y.; Ding, Y.; Liu, J.; Li, Z.; Huang, X.; Sun, C.-C. Theoretical mechanistic study on the ion–molecule reactions of CCN^+/CNC^+ with H_2O and HCO^+/HOC^+ with HCN/HNC. *J. Chem. Phys.* **2002a**, *116* (5), 1892–1910.

Tao, Y.; Ding, Y.; Liu, J.; Li, Z.; Huang, X.; Sun, C.-C. Theoretical mechanistic study on the ion–molecule reactions of CCN^+/NC^+ with H_2S. *J. Phys. Chem.* **2002b**, *106* (12), 2949–2962.

Tatsumi, R.; Aoki, Y.; Maeda, S.; Hori, M.; Hayakawa, S. Ionic liquid, electrolyte, lithium secondary battery comprising same, and process for producing ionic liquid. EP 2410601 A1: Osaka-shi, **2012**.

Tattershall, B. W. Phosphorus-carbon nuclear magnetic coupling constants in phosphorus(III) cyanides. *Polyhedron* **1990**, *9* (4), 553–555.

Tautz, H.; Blumberg, W. *Verfahren Zur Herstellung von Chlorcyan*; DE102007052538A1: Essen, **2007**.

Taylor, E. C.; Andrade, J. G.; John, K. C.; McKillop, A. Thallium in organic synthesis. 50. A convenient synthesis of thallium(I) cyanide, a useful reagent in organic synthesis. *J. Org. Chem.* **1978**, *43* (11), 2280–2282.

Tebbe, K.-F.; Fröhlich, R. Untersuchungen an Polypseudohalogeniden. 4. Darstellung und Kristallstrukur von Kalium(0,6)Rubidium(0,4) Dicyanoiodat(I)-Diiminooxalsäurediethylester (2/1) $K_xRb_{1-x}[I(CN)_2]$ x 1/2 $C_6H_{12}N_2O_2$ (x = 0,6). *Z. Anorg. Allg. Chem.* **1983a**, *505* (10), 19–31.

Tebbe, K.-F.; Fröhlich, R. Untersuchungen an Polypseudohalogeniden. 3. Darstellung und Kristallstruktur von Kaliumdicyanoiodat(I)-Diiminooxalsäurediethylester (1/1), $K[I(CN)_2]$ x $C_6H_{12}N_2O_2$. *Z. Anorg. Allg. Chem.* **1983b**, *505* (10), 7–18.

Tebbe, K.; Fröhlich, R. Studies on the polypseudohalides, II. Preparation and crystal structure of $Rb[I(ICN)_2]$. *Z. Naturforsch. B: J. Chem. Sci.* **1983c**, *38* (5), 549–553.

Tebbe, K.; Gräfe-Kavoosian, A. Studies on polypseudohalides, VII preparation and crystal structure of $[K(Crypt\text{-}2.2.2)]\ I(ICN)_2$. *Z. Naturforsch. B: J. Chem. Sci.* **1996**, *51* (7), 1007–1010.

Tebbe, K.; Krauß, N. Studies on the polypseudohalides, V preparation and crystal structure of $K[I(CN)_2]$. *Z. Naturforsch. B* **1988**, *43* (2), 149–152.

Thalhammer, F.; Trautz, H. *Verfahren Zur Herstellung von Natrium-Dicyanamid*; DE19904877A1: Trostberg, **2000**.

Thaulow, H. Über die Einwirkung der Schwefelsäure Auf Ferrocyankalium und Über die Medizinische Blausäure. *J. Prakt. Chem.* **1844**, *31* (1), 234–256.

Thielemann, G.; Spange, S. Polarity of tetraalkylammonium-based ionic liquids and related low temperature molten salts. *New J. Chem.* **2017**, *41* (16), 8561–8567.

Thoma, A.; Schallmoser, G.; Smith, A. M.; Wurfel, B. E.; Bondybey, V. E. Visible absorption and infrared emission of CN–Xe in an argon Matrix. *J. Chem. Phys.* **1994**, *100* (7), 5387–5389.

Thomas, B. H.; Orville-Thomas, W. J. Molecular parameters and bond structure. *J. Mol. Struct.* **1969**, *3* (3), 191–206.

Thompson, J. P.; Marrs, T. C. Hydroxocobalamin in cyanide poisoning. *Clin. Toxicol.* **2012**, *50* (10), 875–885.

Thompson, W. R.; McDonald, G. D.; Sagan, C. The Titan haze revisited: magnetospheric energy sources and quantitative tholin yields. *Icarus* **1994**, *112* (2), 376–381.

Thompson, M. R. Purification and analysis of alkali cyanides. *Bur. Stand. J. Res.* **1931**, *6* (6), 1051–1059.

Thomson, C.; Wishart, B. J. Electronic structure of unstable intermediates. *Theor. Chim. Acta* **1974**, *35* (3), 261–265.

Thomson, C. An INDO investigation of the electronic structure and hyperfine coupling constants of the radicals HBO^-, HCO and HCN^-. *Theor. Chim. Acta* **1970**, *17* (4), 320–322.

Timoshkin, A. Y.; Schaefer, H. F. Ab initio and DFT investigations of Al, Ga, and in tricyanides and triisocyanides. *J. Struct. Chem.* **2000**, *41* (1), 35–40.

Tokue, I.; Nanbu, S. Theoretical transition probabilities for the $\tilde{A}^1\Pi$-$\tilde{X}^1\Sigma^+$ system of AlNC and AlCN isomers based on global potential energy surfaces. *J. Chem. Phys.* **2006**, *124* (22), 224301.

Tokue, I.; Nanbu, S. Isomerization reaction between linear AlNC and AlCN including the $\tilde{X}^1\Sigma^+$ and $\tilde{A}^1\Pi$ states studied by three-dimensional wave packet propagation. *J. Chem. Phys.* **2011**, *135* (2), 024305.

Tornieporth-Oetting, I.; Klapötke, T. Synthese Und Charakterisierung von (Iodcyan)Iodonium-Hexafluoroarsenat, $[ICNI]^+[AsF6]^-$. *Chem. Ber.* **1990**, *123* (6), 1343–1344.

Tornieporth-Oetting, I.; Klapötke, T. Untersuchung Zum Reaktionsverhalten von Nitrilen RCN Gegenüber $[I_3]^+[AsF_6]^-$ (R = CH_3, CF_3, Br, I, H). *Chem. Ber.* **1991**, *124* (7), 1571–1573.

Tornieporth-Oetting, I. C.; Gowik, P.; Klapötke, T. M. $[FCNF]^+[AsF_6]^-$, Ein Salz des Linearen 22-Valenzelektronen-Kations $[FCNF]^+$. *Angew. Chem.* **1991**, *103* (11), 1490–1492.

Tornieporth-Oetting, I. C.; Klapötke, T. M.; Cameron, T. S.; Valkonen, J. ; Rademacher, P.; Kowski, K. Reactivity of Lewis acids towards nitriles; crystal structure and electron deformation density of $C_2N_2{\cdot}SbF_5$ and photoelectron spectrum of AsF_5. *J. Chem. Soc. Dalton Trans.* **1992**, *2* (4), 537–543.

Torrie, B. H.; Powell, B. M. Cyanogen: structure, dynamics and intermolecular potentials. *J. Phys. Condens. Matter* **1989**, *1* (34), 5827–5835.

Townes, C. H.; Holden, A. N.; Merritt, F. R. Rotational spectra of some linear molecules near 1-cm wave-length. *Phys. Rev.* **1947**, *71* (1), 64.

Townes, C. H.; Holden, A. N.; Merritt, F. R. Microwave spectra of some linear XYZ molecules. *Phys. Rev.* **1948**, *74* (9), 1113–1133.

Trofimenko, S.; Little, E. L.; Mower, H. F. Tricyanomethane (cyanoform), carbamyldicyanomethane, and their derivatives. *J. Org. Chem.* **1962**, *27* (2), 433–438.

Tsuda, S.; Yokohata, A.; Umaba, T. Measurement of negative ions formed by electron impact. VIII. Ionization efficiency curves of negative ions from methyl and ethyl cyanides. *Bull. Chem. Soc. Jpn.* **1971**, *44* (6), 1486–1491.

Tyler, J. K.; Sheridan, J. Structural studies of linear molecules by microwave spectroscopy. *Trans. Faraday Soc.* **1963**, *59*, 2661.

Tyuzyo, K. Stoichiometric investigations of the liquid state IV. Viscosity of associated liquid. *Bull. Chem. Soc. Jpn.* **1957**, *30* (7), 782–789.

Tzialla, O.; Veziri, C.; Papatryfon, X.; Beltsios, K. G.; Labropoulos, A.; Iliev, B.; Adamova, G.; Schubert, T. J. S.; Kroon, M. C.; Francisco, M.; Zubeir, L. F.; Romanos, G. E.; Karanikolos, G. N. Zeolite imidazolate framework–ionic liquid hybrid membranes for highly selective CO_2 separation. *J. Phys. Chem. C* **2013**, *117* (36), 18434–18440.

Ugarov, M.; Ageev, V.; Karabutov, A.; Loubnin, E.; Pimenov, S.; Konov, V.; Bensaoula, A. UV laser induced interfacial synthesis of CN–BCN layers on diamond films in borazine and ammonia. *Appl. Surf. Sci.* **1999**, *138–139* (1–4), 359–363.

Unknown. Notitia Caerulei Berolinensis Nuper Inventi. *Miscnea. Berol. Soc. Sci.* **1710**, *1*, 377–378.

Unland, M. L. Isocyanate intermediates in the reaction of NO and CO over noble metal catalysts. *J. Catal.* **1973**, *31* (3), 459–465.

Vadhanavikit, S.; Ganther, H. E. Nutritional availability and chronic toxicity of selenocyanate in the rat. *J. Nutr.* **1988**, *118* (6), 718–722.

Vaes, J.; Chabanel, M.; Martin, M. L. Ionic interactions in lithium thiocyanate solutions. Nitrogen-15 and lithium-7 nuclear magnetic resonance studies. *J. Phys. Chem.* **1978**, *82* (22), 2420–2423.

van de Burgt, L. J.; Nicolai, J.; Heaven, M. Laser induced fluorescence Study of the $HeBr_2$ van Der Waals Complex. *J. Chem. Phys.* **1984**, *81* (12), 5514–5520.

van Rooyen, P. H.; Boeyens, J. C. A. Sodium thiocyanate. *Acta Crystallogr. Sect. B Struct. Crystallogr. Cryst. Chem.* **1975**, *31* (12), 2933–2934.

van Vaals, J. J.; Meerts, W. L.; Dymanus, A. Rotational spectrum, hyperfine spectrum and structure of lithium isocyanide. *Chem. Phys.* **1983**, *82* (3), 385–393.

van Vaals, J. J.; Meerts, W. L.; Dymanus, A. High-resolution molecular-beam spectroscopy of NaCN and $Na^{13}CN$. *Chem. Phys.* **1984a**, *86* (1–2), 147–159.

van Vaals, J. J.; Leo Meerts, W.; Dymanus, A. Molecular beam electric resonance study of KCN, $K^{13}CN$ and $KC^{15}N$. *J. Mol. Spectrosc.* **1984b**, *106* (2), 280–298.

Varma, R.; Signorelli, A. J. A new synthesis of cyanogen chloride. *Inorg. Nucl. Chem. Lett.* **1969**, *5* (12), 1017–1019.

Vazquez, G. J.; Gouyet, J.-F. SCF CI potential energy surfaces for the HCN α HCN isomerisation reaction. *Chem. Phys. Lett.* **1981**, *77* (2), 233–238.

Verneuil, A. Recherches Sur Quelques Combinaisons Azotees Du Selenium. *Ann. Chim. Phys.* **1886**, *9*, 289.

Verweel, H. J.; Bijvoet, J. M. Die Kristallstruktur von NaCN. *Z. für Kristallogr. Cryst. Mater.* **1939**, *100* (1–6), 201–207.

Vichietti, R. M.; Haiduke, R. L. A. Kinetic study of the isomerization reaction $HC_nN \rightarrow HC_{n-1}NC$ (n = 1, 3 and 5). *Mon. Not. R. Astron. Soc.* **2014**, *437* (3), 2351–2360.

Völker, T. Polymere Blausäure. *Angew. Chem.* **1960**, *72* (11), 379–384.

von der Weid, J. P.; do Carmo, L. C. S.; Ribeiro, S. C. Substitutional HCN^- molecular ions in KCN crystals: a paramagnetic probe in a ferroelastic material. *J. Phys. C: Solid State Phys.* **1979**, *12* (22), 4927–4938.

von Ittner, F. *Beiträge Zur Geschichte Der Blausäure Mit Versuchen Über Ihre Verbindungen Und Wirkungen Auf Den Tierischen Organismus*; Universität Freiburg: Freiburg, **1809**.

von Meyer, E. Zur Kenntniss der Blausäure und des Jodcyans. *J. Prakt. Chem.* **1887**, *36* (1), 292–299.

von Ragué Schleyer, P.; Sawaryn, A.; Reed, A. E.; Hobza, P. The remarkable structure of lithium cyanide/isocyanide. *J. Comput. Chem.* **1986**, *7*(5), 666–672.

Voorhoeve, R. J. H.; Thimble, L. E. Synthesis of ammonium cyanate and urea from NO over Pt, Os, Ru, and CuNi catalysts. *J. Catal.* **1978**, *53* (2), 251–259.

Vörös, T.; Bazsó, G.; Tarczay, G.; Pasinszki, T. Matrix-isolation spectroscopic and computational study of [2C, 2N, 2S] isomers: photochemical generation of SCNNCS and NCSNCS from NCSSCN. *J. Mol. Struct.* **2012**, *1025*, 117–123.

Vörös, T.; Pacsai, B.; Magyarfalvi, G.; Tarczay, G. Generation and spectroscopic identification of NCXNC and NCNCX (X = S, Se) in low-temperature inert matrices. *J. Mol. Spectrosc.* **2015**, *316*, 95–104.

Voss, K.; Becker, M.; Villinger, A.; Emel'yanenko, V. N.; Hellmann, R.; Kirchner, B.; Uhlig, F.; Verevkin, S. P.; Schulz, A. Ionic liquids containing the triply negatively charged tricyanomelaminate anion and a $B(C_6F_5)_3$ adduct anion. *Chem. Eur J.* **2011**, *17* (48), 13526–13537.

Vuitton, V.; Bonnet, J. Y.; Frisari, M.; Thissen, R.; Quirico, E.; Dutuit, O.; Schmitt, B.; Le Roy, L.; Fray, N.; Cottin, H.; Sciamma-O'Brien, E.; Carrasco, N.; Szopa, C. Very high resolution mass spectrometry of HCN polymers and tholins. *Faraday Discuss.* **2010**, *147*, 495–508.

Wald, M. H.; Lindberg, H. A.; Barker, M. H. The toxic manifestations of the thiocyanates. *JAMA J. Am. Med. Assoc.* **1939**, *112* (12), 1120.

Walden, P. C. W. S. Ein Gedenkblatt Zu Seinem 200. Geburtstage. *Z. Anorg. Allg. Chem.* **1943**, *250* (3–4), 230–235.

Walker, K. A.; Evans, C. J.; Suh, S.-H. K.; Gerry, M. C. L.; Watson, J. K. G. Fourier transform microwave spectroscopy of cyanides and isocyanides of Al, Ga, and in. *J. Mol. Spectrosc.* **2001**, *209* (2), 178–191.

Walsh, B.; Barnes, A. J.; Suzuki, S.; Orville-Thomas, W. J. Studies of intermolecular interactions by matrix isolation vibrational spectroscopy and normal coordinate analysis. *J. Mol. Spectrosc.* **1978**, *72* (1), 44–56.

Wang, C.-R.; Huang, R.-B.; Liu, Z.-Y.; Zheng, L.-S. Laser generation and ab initio studies of C_nN^- clusters. *Chem. Phys. Lett.* **1995**, *237* (5–6), 463–467.

Wang, D.-C.; Chau, F.-T.; Lee, E. P. F.; Leung, A. K.-M.; Dyke, J. M. The $X^2\Pi$ and $A^2\Sigma$ states of FCN^+ and $ClCN^+$: ab initio calculations and simulation of the HeI photoelectron spectra of FCN and ClCN. *Mol. Phys.* **1998**, *93* (6), 995–1005.

Wang, Q.; Ding, Y.; Sun, C. Theoretical study on germanium cyanide radical GeCN and its ions. *J. Chem. Phys.* **2005**, *122* (20), 204305–204312.

Wang, J.; Ding, Y.; Sun, C. Cyanomethylidyne: a reactive carbyne radical. *ChemPhysChem* **2006**, *7* (3), 710–722.

Wang, Z.; Zhang, J.; Wu, J.; Cao, W. Theoretical investigation on intermolecular interactions between HCN and HNC: the nature and thermodynamic properties. *J. Mol. Struct.: Theochem.* **2007**, *806* (1–3), 239–246.

Wasserman, E.; Barash, L.; Yager, W. A. The electron paramagnetic resonance of triplet CNN, NCN, and NCCCN. *J. Am. Chem. Soc.* **1965**, *87* (9), 2075–2076.

Wasylishen, R. E.; Jeffrey, K. R. Nitrogen-14 NMR study of molecular motion in rubidium and cesium cyanide. *J. Chem. Phys.* **1983**, *78* (2), 1000–1002.

Watts, M. P.; Moreau, J. W. *New insights into the genetic and metabolic diversity of thiocyanate-degrading microbial consortia. Applied microbiology and biotechnology*, 3rd ed.; Springer-Verlag, 100, **2016**; pp. 1101–1108.

Wehrhane, G.; Hübner, H. Über Den Cyanphosphor. *Justus Liebigs Ann. Chem.* **1864**, *132* (3), 277–289.

Weidinger, D.; Houchins, C.; Owrutsky, J. C. Vibrational dynamics of tricyanomethanide. *Chem. Phys. Lett.* **2012**, *525–526*, 60–63.

Weinberg, J. M.; Fishburne, E. S.; Narahari Rao, K. Infrared bands of the CN red system ($A^2\Pi$-$X^2\Sigma$). *J. Mol. Spectrosc.* **1967**, *22* (1–4), 406–418.

Wen, J.; Xie, J.; Chen, X.; Li, X. A review on g-C_3N_4-based photocatalysts. *Appl. Surf. Sci.* **2017**, *391*, 72–123.

Werner, H.; Follmeg, B.; Alexander, M. H. Adiabatic and diabatic potential energy surfaces for collisions of CN($X^2\Sigma^+$, $A^2\Pi$) with He. *J. Chem. Phys.* **1988**, *89* (5), 3139–3151.

Whitham, C. J.; Soep, B.; Visticot, J.; Keller, A. Observation and spectroscopy of metallic free radicals produced by reactive collisions during a supersonic expansion. *J. Chem. Phys.* **1990**, *93* (2), 991–1000.

Wiberg, K. B.; Rablen, P. R. Origin of the stability of carbon tetrafluoride: negative hyperconjugation reexamined. *J. Am. Chem. Soc.* **1993**, *115* (2), 614–625.

Wijeyasinghe, N.; Anthopoulos, T. D. Copper(I) thiocyanate (CuSCN) as a hole-transport material for large-area opto/electronics. *Semicond. Sci. Technol.* **2015**, *30* (10), 104002.

Wilcox, D. E.; Bromley, L. A. Computer estimation of heat and free energy of formation for simple inorganic compounds. *Ind. Eng. Chem.* **1963**, *55* (7), 32–39.

Wilkie, C. A.; Parry, R. W. Halocyanophosphines, $P(CN)_YX_{3-y}$, and related cyanophosphine derivatives. *Inorg. Chem.* **1980**, *19* (6), 1499–1502.

Willemin, M.-E.; Lumen, A. Thiocyanate: a review and evaluation of the kinetics and the modes of action for thyroid hormone perturbations. *Crit. Rev. Toxicol.* **2017**, *47* (7), 543–569.

Williams, D. R.; Damrauer, R. Molecular orbital calculations on substituted carbodiimides. *Theor. Chim. Acta* **1971**, *23* (2), 195–202.

Williams, D.; Kouvetakis, J.; O'Keeffe, M. Synthesis of nanoporous cubic $in(CN)_3$ and $In_{1-x}Ga_x(CN)_3$ and corresponding inclusion compounds. *Inorg. Chem.* **1998**, *37* (18), 4617–4620.

Williams, D.; Pleune, B.; Kouvetakis, J.; Williams, M. D.; Andersen, R. A. Synthesis of $LiBC_4N_4$, BC_3N_3, and related C–N compounds of boron: new precursors to light element ceramics. *J. Am. Chem. Soc.* **2000**, *122* (32), 7735–7741.

Williams, D.; Pleune, B.; Leinenweber, K.; Kouvetakis, J. Synthesis and structural properties of the binary framework C–N compounds of Be, Mg, Al, and Tl. *J. Solid State Chem.* **2001**, *159* (1), 244–250.

Williams, H. E. *The chemistry of cynanogen compounds*; J. & A. Churchill: London, **1915**.

Williams, H. E. *Cyanogen compounds: their chemistry, detection and estimation*, 2nd ed.; Edward Arnold: London, **1948**.

Wilson, I. R.; Harris, G. M. The oxidation of thiocyanate ion by hydrogen peroxide. II. The acid-catalyzed reaction. *J. Am. Chem. Soc.* **1961**, *83* (2), 286–289.

Wilson, I. R.; Harris, G. M.; Wilson, I. R.; Harris, G. M. The oxidation of thiocyanate ion by hydrogen peroxide. I. The PH-independent reaction. *J. Am. Chem. Soc.* **1960**, *82* (17), 4515–4517.

Wittig, G.; Bille, H. Notizen: Über aluminium-tricyanid und lithium-aluminium-tetracyanid. *Z. Naturforsch. B: J. Chem. Sci.* **1951**, *6* (4), 226.

Wittig, G.; Raff, P. Notizen: Darstellung von Lithium-Monocyano-Borhydrid. *Z. Naturforsch. B: J. Chem. Sci.* **1951**, *6* (4), 225.

Wizemann, T.; Müller, H.; Seybold, D.; Dehnicke, K. Reaktionen von Rirhodan Mit Einigen Organometall-Verbindungen. *J. Organomet. Chem.* **1969**, *20* (1), 211–217.

Wofford, B. A.; Bevan, J. W.; Olson, W. B.; Lafferty, W. J. Rotational analysis and vibrational predissociation in the N_2 band of HCN dimer. *J. Chem. Phys.* **1986**, *85* (1), 105–108.

Wöhler, F. Über Einige Verbindungen des Cyans (Blaustoffs). *Ann. Phys.* **1821**, *69* (11), 271–282.

Wöhler, F. Analytische Versuche Über die Cyansäure. *Ann. Phys.* **1824**, *77* (5), 117–124.

Wöhler, F. Über Cyan Verbindungen. *Ann. Phys.* **1825a**, *79* (2), 177–182.

Wöhler, F. Über die Zusammensetzung der Cyansäure. *Ann. Phys.* **1825b**, *81* (11), 386–388.

Wöhler, F. Ueber Künstliche Bildung des Harnstoffs. *Ann. Phys.* **1828**, *88* (2), 253–256.

Wootten, A.; Lichten, S. M.; Sahai, R.; Wannier, P. G. CN abundance variations in the shell of IRC + 10216. *Astrophys. J.* **1982**, *257*, 151.

Wormer, P. E. S.; Tennyson, J. Ab initio SCF calculations on the potential energy surface of potassium cyanide (KCN). *J. Chem. Phys.* **1981**, *75* (3), 1245–1252.

Wu, W. W.; Chadik, P. A.; Schmidt, C. J. An in situ synthesis of cyanogen chloride as a safe and economical aqueous standard. *Wat. Res.* **1998**, *32* (9), 2865–2869.

Wu, C.; Xiong, Y.; Gao, Z.; Kong, F.; Lu, H.; Yang, X.; Xu, Z. Ionization and dissociation of acetonitrile by intense femtosecond laser pulse. *Chin. Sci. Bull.* **2000**, *45* (21), 1953–1955.

Yamamoto, J.; Okabe, Y. Ab initio molecular dynamics simulation on SiN + CH and SiC + NH reactions. *Comput. Theor. Chem.* **2011**, *963* (1), 24–33.

Yan, G.; Zhang, Y.; Wang, J. Recent advances in the synthesis of aryl nitrile compounds. *Adv. Synth. Catal.* **2017**, *359* (23), 4068–4105.

Yang, Z.; Luty, F. Theoretical investigation of ferroelastic phase transition of pure and mixed alkali cyanide systems by the elastic dipole model. II. The cubic-monoclinic phase transition of pure rubidium cyanide. *Phys. Status Solidi B* **1989**, *154* (1), 181–194.

Yang, D. L.; Yu, T.; Lin, M. C.; Melius, C. F. CN radical reactions with hydrogen cyanide and cyanogen: comparison of theory and experiment. *J. Chem. Phys.* **1992**, *97* (1), 222–226.

Yang, Z.; Cole, C. A.; Martinez, Jr., O.; Carpenter, M. Y.; Snow, T. P.; Bierbaum, V. M. Experimental and theoretical studies of reactions between h atoms and nitrogen-containing carbanions. *Astrophys. J.* **2011**, *739* (1), 19–28.

Yoshimura, Y.; Shinohara, S.; Tsuda, N.; Iwasaki, H. X-ray diffraction study of the low temperature phase of rubidium cyanide. *J. Phys. Soc. Jpn.* **1996**, *65* (7), 2099–2105.

Yoshimura, Y. Stucture determination of the monoclinic form of KCN. *J. Phys. Soc. Jpn.* **1989**, *58* (11), 3993–3998.

Yost, D. M.; Stone, W. E. The complex ions formed by iodine cyanide with cyanide and iodide ions. The vapor pressure, free energy and dissociation of iodine cyanide. *J. Am. Chem. Soc.* **1933**, *55* (5), 1889–1895.

Youatt, J. B. Studies on the metabolism of thiobacillus thiocyanoxidans. *J. Gen. Microbiol.* **1954**, *11* (2), 139–149.

Yu, D.; Rauk, A.; Armstrong, D. A. Electron affinities and thermodynamic properties of some triatomic species. *J. Phys. Chem.* **1992**, *96* (14), 6031–6038.

Yu, J.-T.; Teng, F.; Cheng, J. The construction of X-CN (X = N, S, O) bonds. *Adv. Synth. Catal.* **2017**, *359* (1), 26–38.

Zarges, W.; Marsch, M.; Harms, K.; Boche, G. $[\{Li_2(Me_3SiCCN)\}_{12}(Et_2O)_6(C_6H_{14})]$, Kristallstruktur Mit Dem Trimethylsilylacetonitril-Dianion. *Chem. Ber.* **1989**, *122* (7), 1307–1311.

Zhan, C.; Iwata, S. Ab initio studies on the structures, vertical electron detachment energies, and fragmentation energies of C_nN^- clusters. *J. Chem. Phys.* **1996**, *104* (22), 9058–9064.

Zhang, L.-Y.; Shi, L.-X.; Chen, Z.-N. Syntheses, structures, and electronic interactions of dicyanamide/tricyanomethanide-bridged binuclear organometallic complexes. *Inorg. Chem.* **2003**, *42* (2), 633–640.

Zhang, M.; Gong, J.; Ma, A.; Rice, S. A. Infrared multiphoton induced isomerization and dissociation of FCN, ClCN, and BrCN in liquid Ar: a classical simulation study. *J. Chem. Phys.* **2007**, *127* (14), 144501.

Zhang, C.; Li, Y.; Shuai, D.; Shen, Y.; Xiong, W.; Wang, L. Graphitic carbon nitride ($g\text{-}C_3N_4$)-based photocatalysts for water disinfection and microbial control: a review. *Chemosphere* **2019**, *214*, 462–479.

Zhao, W.; Pan, J.; Huang, F. Nonaqueous synthesis of metal cyanamide semiconductor nanocrystals for photocatalytic water oxidation. *Chem. Commun. (London)* **2018**, *54* (13), 1575–1578.

Zheng, Z. Q.; Wang, J.; Wu, T. H.; Zhou, X. P. Alkylation of ammonium salts catalyzed by imidazolium-based ionic liquid catalysts. *Adv. Synth. Catal.* **2007**, *349* (7), 1095–1101.
Zhu, Z.; Zhang, Z.; Huang, C.; Pei, L.; Chen, C.; Chen, Y. Kinetics of CCN radical reactions with a series of normal alkanes. *J. Phys. Chem.* **2003**, *107* (48), 10288–10291.
Zhu, C.; Räsänen, M.; Khriachtchev, L. Fluorinated noble-gas cyanides FKrCN, FXeCN, and FXeNC. *J. Chem. Phys.* **2015**, *143* (7), 074306.
Ziegler, K. Über die Darstellung Wasserfreier Blausäure. *Ber. Dtsch. Chem. Ges.* **1921**, *54* (1), 110–112.
Zúñiga, J.; Picón, J. A. G.; Bastida, A.; Requena, A. A spectroscopic potential energy surface for FCN. *J. Quant. Spectrosc. Radiat. Transfer* **2012**, *113* (11), 1155–1169.

Bionotes

Axel Schulz
Chemie, Universität Rostock, Albert-Einstein-Straße 3a, 18059 Rostock, Mecklenburg-Vorpommern, Germany
axel.schulz@uni-rostock.de
https://orcid.org/0000-0001-9060-7065

Axel Schulz studied chemistry at the Humboldt-University and Technical University of Berlin (1987–1992), with a diploma thesis (1993) in inorganic chemistry and a doctoral thesis (1993–1994) in inorganic chemistry (Thomas M. Klapötke, nitrogen chemistry). Thereafter he was a research associate at the university of Glasgow (1995–1997) and a postdoctoral fellow at the ANU in Canberra with Leo Radom (computational chemistry). In 1997, he went to the LMU Munich where he received his second PhD (Dr. Habil.) in 2001 (elementorganic and theoretical chemistry). In 2006 he was appointed full professor for inorganic chemistry at the University of Rostock. Research in the Schulz group largely focuses on fundamental main group element chemistry and the quantum mechanical description of chemical bonding. The group's more applied interests include the synthesis of new hydrogen acids of pseudohalogens, their stabilization using Lewis acids, the study of their chemical properties and their application in noval reaction pathways.

Jonas Surkau
Chemie, Universität Rostock, Albert-Einstein-Straße 3a, 18059 Rostock, Mecklenburg-Vorpommern, Germany
https://orcid.org/0000-0001-8729-9807

In 2019, Jonas Surkau joined the group of Axel Schulz at the University of Rostock to work on his BSc thesis on the topic of pseudohalogen chemistry. For his MSc (2021) and PhD he set his focus on the stabilization of hydrogen acids by Lewis acids, the influence of adduct formation on the tautomeric equilibrium and their reaction behavior towards hydrocarbons.